TABLE OF CONTENTS

LIST OF FIGURES

CHAPTER 2

CHAPTER 3

CHAPTER 4

CHAPTER 5

LIST OF TABLES

CHAPTER 1

DEFINITION OF THE PROBLEM

CHAPTER 1

DEFINITION OF THE PROBLEM

1.1. INTRODUCTION

The increasing demand for weight reduction and low fuel consumption in the automotive industry has had a marked effect on the judicious selection of materials. Historically, the most common engine material has been grey cast iron because of its high temperature strength, machinability and cost. However, cast iron with its high density is not a material of choice for light weight design. Weight reduction objectives of the engine designers has lead to efforts to replace grey cast iron blocks with lightweight materials such as compacted graphite iron, magnesium alloys and aluminum alloys. The high strength to weight ratio, high fluidity, low thermal expansion coefficient, and high corrosion resistance of aluminum-silicon foundry alloys, typically B319.2 and A356.2, make them materials of choice for the manufacture of automobiles especially when it concerns engine construction. The microstructure and mechanical properties attainable in these alloys are strongly influenced by the alloy composition, impurity elements, melt treatments, solidification characteristics, casting defects, and heat treatment. [1, 2, 3]

Heat treatment is the most common process used to alter the mechanical properties of cast aluminum alloys. The heat treatment helps to obtain a desired combination of

strength and ductility values. Traditional heat treatment technology applies circulating air convection furnaces for solution heat treating and aging for the purposes of obtaining a T6 or T7 temper. This treatment is applied with the intention of improving the mechanical properties, microstructure, and residual stress states of Al-Si-(Cu/Mg) cast alloys through a process known as precipitation hardening which consists of a solution heat treatment, quenching (water, air or sand), and artificial aging. The solution heat treatment increases the ultimate tensile strength and ductility as well as the quality of such Al-Si-(Cu/Mg) cast alloys as A356 and B319.2 alloys, whereas aging increases the yield strength at the expense of ductility. With regard to subsequent aging, the precipitation of Mg_2Si and $CuAl_2$ phases occurs in alloys 356 and 319, respectively, through a series of stages, starting with the formation of Guinier Preston (GP) zones which are enriched in solute. A further increase in the duration time of the aging treatment results in the formation of coherent and semi-coherent precipitates at the sites of the GP zones. [4, 5, 6]

With conventional heat treating systems, however, prolonged solution heat treatment and aging times of over 20 hrs are required for heat treatment of aluminum casting alloys, entailing high energy costs. [7, 8] Commonly used air circulation furnaces offer greater operational flexibility in operating temperatures, but their relatively slow heating rates result in long heat treat cycles. The long cycle times required for heat treating with conventional systems go contrary to industry requirements where the goal is to improve the performance of the part and to reduce the time of manufacturing. The fluidized bed (FB) heat-treating process makes it possible to reduce the time required for heat treating

significantly, while at the same time increasing the uniformity of the heat treatment process. [9, 10]

Over the last several years, fluidized beds have made a dramatic impact as furnaces for the heat treatment of metals; this technique is energy efficient, versatile and non-polluting. For the foundry industry, fluidized beds are used for several applications such as preheating for burning and welding, stress relieving on small and large castings and weldments, normalizing and hardening under protective atmospheres and tempering. The fluidized bed exhibits remarkable liquid-like behavior, where fluidization is obtained by transformation of solid particles into fluid-like state through suspension in a gas or an air. The fluid like nature of the bed allows parts to be easily immersed and conveyed through the media. The most desirable characteristic of a fluidized bed is that the rate of heat transfer between a fluidized bed and immersed objects is high. [11, 12]

The use of fluidized beds is considered to be an innovative technology for the heat treatment process of Al-Si cast alloys and appears to be more effective than conventional furnace techniques. The beds can be used for solutionizing, quenching and aging heat treatments. With the use of fluidized sand bed furnaces, the solution heat treatment time required to obtain optimum mechanical properties may be reduced to six times less than required in a conventional convection furnace. [13] Quenching with the fluidized bed is considered as an alternative well suited for parts requiring low residual stresses and for reducing susceptibility for part distortion compared to water quenching. The high heating rate in a fluidized bed also plays an important role in increasing the kinetics of the aging process by having an effect on the aging characteristics of Al-Si-(Cu/Mg) alloys. The high

heating rate of a fluidized sand bed heat treatment medium is known to produce premium strength and optimum quality in Al-Si casting alloys. [14]

The quality of Al-Si castings plays a vital role in determining specific metallurgical conditions for an alloy casting required to fulfill particular engineering applications. There are several parameters affecting the quality of Al-Si castings such as alloy composition, melt treatment, and heat treatment steps. [15] For specific engineering applications, good alloy quality is achieved by reaching a suitable compromise between several parameters involving maximum performance, minimum risk, and taking into consideration the cost efficiency. It is possible to define the quality of aluminum-silicon castings using specific mathematical equations, where tensile properties can be combined to express the alloy quality using a single quality index value Q. [16] Two models of quality indices were used in this study to correlate the quality of the Al-Si-(Cu/Mg) alloys investigated to the mechanical properties of these alloys, as will be discussed later. Quality charts generated using these equations are useful in deciding upon the optimum heat treatment conditions required to obtain specific properties and/or quality in a particular casting.

An improvement in the performance of Al-Si-Cu/Mg alloys and an understanding of its relationship to heat treatment parameters may be accomplished by applying statistical techniques to the design of experiments (DOE). The selection of an experimental design involves a detailed study of the process aiming at finding the variables affecting the properties. Design of experiments (DOE) is a powerful approach for discovering a set of process or design variables which are most important to the process and then determine at what levels these variables must be kept to optimize the response or quality characteristic of

interest. The effect of the independent variable (the factor), namely factor, on the dependent variable (the response), namely response, is determined through applying an efficient experimentaion technique (DOE), where the relation between these variables is illustrated by means of a regression model using the experimental data. Some of the previously developed DOE techniques were the random blocks, the Latin squares, the Greco-Latin squares and the Hyper-Greco-Latin squares, limited to investigating a small number of variables. [17] Another DOE, called Factorial design, was introduced with the aim of increasing the number of variables to all possible levels of combinations. This DOE has the advantage of investigating the interactions between the variables involved, but it requires a large number of experimental trial runs as the number of variables increases. The interactions may be investigated with only a fraction of the total number of runs by using the Fractional Factorial design. Its construction is carried out by fractioning the Factorial design using some high order interactions as a basis. Newly reported developments have been the Mixture designs and Response surface designs, devoted to defining a mathematical model applicable to the problem under investigation. [18]

In this study, the statistical design of experiments approach has been used to examine and control the performance of the A356.2 and B319.2 aluminum cast alloys and also to develop regression equations between the metallurgical parameters studied (factors) and the tensile results as well as the quality indices (responses).

1.2. OBJECTIVES

Due to the fact that the heat treatment process is the most important means for improving the mechanical properties of Al-Si alloys, there is an emerging need to develop novel heat treatment technologies and to establish a relevant comparison between these techniques and the traditional ones. The present study was therefore undertaken to arrive at a better understanding of the effects of melt treatment as well as solution heat treatment time, quenching media, namely water, air and sand, and multi-temperature aging treatments on the microstructure, tensile properties and quality of T6-tempered A356.2 and B319.2 cast alloys heat treated using a fluidized sand bed furnace (FB) as opposed to a conventional convection furnace (CF). The main objectives of this study may be summarized as follows:

1. Studying the influence of metallurgical parameters on the tensile properties as well as the quality indices of A356.2 and B319.2 aluminum castings including:
    a) The effect of heating and cooling rates using two different heat treatment techniques (FB vs CF).
    b) The effects of strontium (Sr)-modification and (TiB)-grain refinement.
    c) The effects of solution heat treatment time, quenching media, aging temperature, and aging time.
2. Developing a fundamental knowledge base for the heat-treating of Al-Si-(Cu/Mg) castings by using the new fluidized bed technology and comparing it with that obtained with conventional furnaces.

3. Establishing a microstructure-property relationship of FB heat-treated castings using optical microscopy, scanning electron microscopy (SEM), and field emission gun scanning electron microscopy (FEGSEM).
4. Generating quality index maps of the tensile data as a tool for evaluating the tensile properties and quality indices of the alloys investigated and for selecting the optimum metallurgical conditions to be applied practically in A356.2 and B319.2 type casting alloys.
5. Using a statistical design of experiments (DOE) for the purposes of identification of heat treatment parameters, optimization of selected levels, and establishing regression equations by carrying out a mathematical analysis of the tensile and quality data obtained for the two alloy types.

CHAPTER 2

SURVEY OF THE LITURATURE

CHAPTER 2

SURVEY OF THE LITURATURE

2.1. INTRODUCTION

Aluminum and its alloys have become competitive materials in engineering applications from an economical point of view due to such advantageous features as their light weight, attractive appearance; castability, physical and mechanical properties; and excellent corrosion resistance in most environments. With the purpose of reducing vehicle weight in the automotive industry, lightweight parts made of aluminum casting alloys have virtually replaced iron and steel in several automotive parts including engine blocks, pistons, transmission housings and cylinder heads. [19, 20, 21, 22, 23, 24]

Aluminum alloys containing silicon as a major alloying element find widespread application including the military, automobile, aerospace, and general engineering sectors because of a number of distinct benefits. Such benefits include low specific gravity; excellent cast-ability and fluidity; high resistance to wear; reduced thermal expansion because of the presence of silicon; good wear and corrosion resistance; and adequate physical and mechanical properties at elevated temperatures. [6, 25, 26] The presence of silicon imparts good castability and resistance to hot tearing. Also, since silicon increases in volume during solidification, the susceptibility of the casting to shrinkage defects is reduced. Consequently, alloys containing silicon are ideally suited for high volume

production in aluminum foundries; Al-Si castings represent as much as 90% of the total aluminum cast parts produced. [5, 7, 27, 28, 29, 30, 31] According to their level of silicon content, aluminum-silicon casting alloys are subdivided into hypoeutectic alloys (5-10% Si), eutectic alloys (11-13% Si), and hypereutectic alloys (14-20% Si); Figure 2.1 shows the phase diagram of the Al-Si binary system. [5, 6, 32, 33] Hypoeutectic and near eutectic Al-Si alloys are more common commercially than the hypereutectic ones; the addition of copper and magnesium greatly improves the strength of these alloys by improving their response to heat treatment. In hypoeutectic alloys, the dendritic network α-aluminum are formed and followed by the formation of eutectic Al-Si in the interdendritic regions. The eutectic silicon phase in the alloy consists of brittle acicular flakes and plates, which affect the mechanical properties of the alloy, namely its strength and ductility. Small additions of Na or Sr can "modify" the morphology of the eutectic silicon from its acicular form to a fine fibrous form which improves the mechanical properties. [34, 35, 36] Magnesium and copper are the other major alloying elements that may be present in cast aluminum-silicon alloys. Magnesium combines with silicon to from Mg_2Si and provides the ability to heat-treat the Al-Si-Mg family of alloys to high strength levels. Copper in aluminum-silicon alloys such as 319 improves their as-cast and high temperature strength properties.

Two hypoeutectic A356.2 and B319.2 Al-Si casting alloys were investigated in the current study to obtain a correlation between the metallurgical and processing parameters with the resulting tensile properties and quality index values. Apart from solidification conditions and the chemical composition of the alloy, heat treatment is also an important means by which the mechanical properties and quality of the alloys may be improved.

Thus, with respect to the latter, an extensive investigation was carried out covering the heat treatment of these alloys using a range of heat treatment conditions, as well as employing conventional (furnace) versus more recent (fluidized sand bed) techniques for comparison purposes.

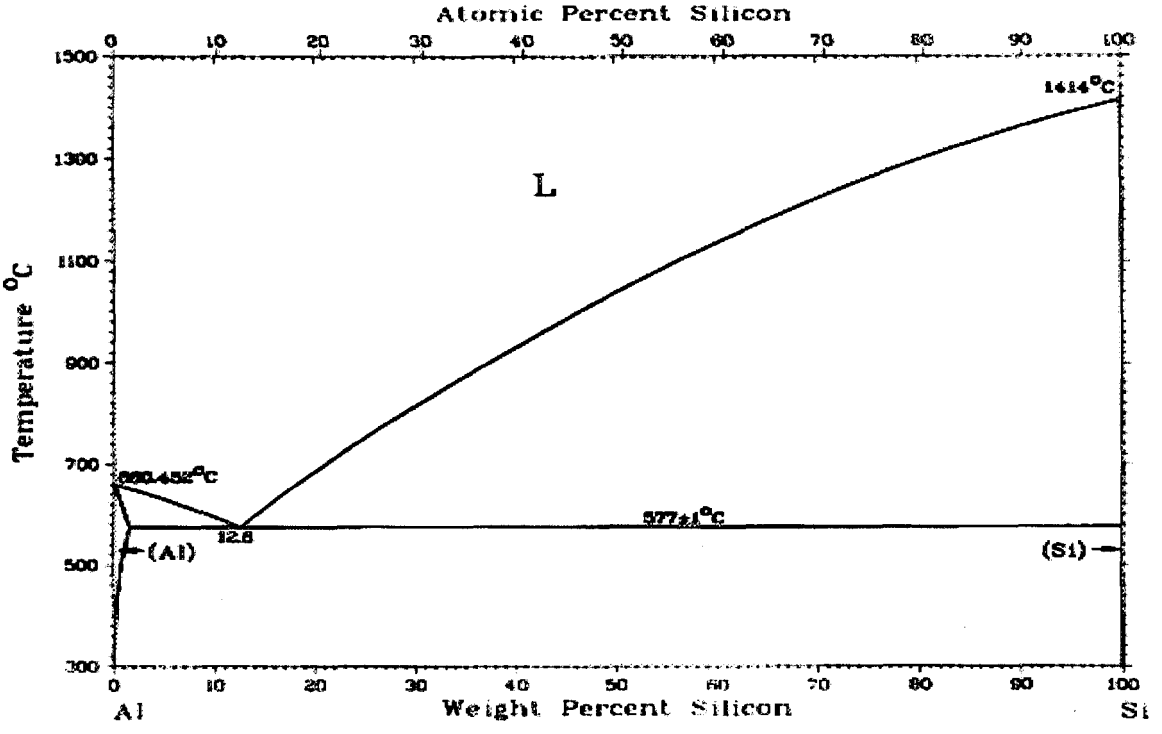

Figure 2.1. Aluminum-silicon binary phase diagram. [32]

The current chapter will therefore concentrate on reviewing the heat treatment regimes and techniques used for A356.2 and B319.2 aluminum-silicon casting alloys, focusing on the fluidized sand bed heat treatment technique. In covering the heat treatments, the metallurgical and microstructural aspects involved in the different heat treatment stages of solutionizing, quenching and aging of such alloys will be presented, together with their effects on the resulting alloy properties. The mathematical concept of

quality indices and the usefulness of quality charts in selecting specific alloy conditions/properties for practical applications will be also reviewed.

2.2. HEAT TREATMENT SYSTEMS

The main goal of the heat treatment of aluminum casting alloys is to obtain the best possible mechanical properties for meeting the standards required for specific industrial applications. The mechanical properties are enhanced through a number of microstructural changes which take place as a function of the applied heat treatment regime and the designated thermal treatment parameters, namely temperature and time. Precise control of the time-temperature profile, tight temperature uniformity, and compliance with industry-wide specifications are required in order to achieve repeatable results and produce a high-quality, functional product. In addition, heating and cooling rates of the heat treatment media are also significant parameters that may affect the heat treatment performance of the alloys.

2.2.1. Conventional Heat Treatment procedures

Heat treatment of Al-Si-(Cu/Mg) castings has the advantage of microstructural homogenization; of residual stress relief; and of improved dimensional stability, machinability and corrosion resistance. There are several steps involved in a conventional heat treatment process. Table 2.1 details the most commonly applied heat treatments. Among these, the T6 temper is commonly applied to Al-Si (Cu/Mg) alloys which necessitates setting in motion a specific sequence of steps, namely, solution heat treatment, rapid cooling in water (or quenching), and artificial aging. [37, 38, 39] The T6 treatment refers

to a phase transformation process known as precipitation hardening since the small particles of the new phase which are formed may be termed precipitates. The highest possible increase in mechanical properties for a given alloy is accomplished in two distinct stages, namely solution heat treatment and age hardening. Age hardening is also used to designate precipitation hardening since the strength develops with the passage of time. The basic requirement for an alloy to be amenable to age hardening is a decrease in the solid solubility of one or more of the alloying elements with decreasing temperature. [40, 41, 42, 43] Applying the appropriate heat treatment parameters (including control of the heating and cooling rates) to Al-Si casting alloys may enhance the mechanical properties and quality of these alloys as a result of their influence on the microstructure of Al-Si casting alloys.

Table 2.1. Common Al-Si-(Cu/Mg) heat treatments. [37, 38, 39, 40, 41, 42, 43]

Temper	Solution Treatment	Quenching	Aging Treatment
T_4	8-12 hours at 495°C for 319 alloys 5-8 hours at 530°C for 356 alloys	Applied	At room temperature for 24-48 hours
T_6	8-12 hours at 495°C for 319 alloys 5-8 hours at 530°C for 356 alloys	Applied	180°C for 319 alloys 155°C for 356 alloys
T_7	8-12 hours at 495°C for 319 alloys 5-8 hours at 530°C for 356 alloys	Applied	240°C for 5 hours

2.2.1.1. Solution Heat Treatment

Solution heat treatment is carried out to dissolve a high amount of certain elements present in the alloy such as Cu and Mg in the α-aluminum solid solution. The dissolution of these elements will enhance the precipitation hardening during the artificial aging treatment. Solution heat treatment includes the exposure of the casting to high temperature, just below the solidus temperature of heat treated alloys, for a certain length of time to

obtain a homogeneous supersaturated structure; holding time at a specific temperature depends on the solubility of the various phases involved in the aluminum cast alloys. Since the structures of aluminum-silicon casting alloys are relatively heterogeneous, much longer solution treatment times will be required. The temperature of solution treatment should be restricted to a range below the solidification point expected for the phases in the cast structure so as to avoid the incipient melting of these soluble phases. [44, 45] The solution heat treatment time represents a compromise between the mechanical properties achieved, alloy quality, and economic efficiency; shorter solution heat treatment times are required in permanent mold castings than in investment or sand mold castings.[46,47]

The roles of solution heat treatment in Al-Si-(Cu/Mg) casting alloys are to obtain a maximum dissolution of the hardening precipitates Al_2Cu and Mg_2Si into aluminum matrix, so as to homogenize the as-cast structure, and to cause a morphological change in the eutectic silicon particles through coarsening and spheroidization. The soluble phases and precipitates which form earlier during solidification are dissolved into the matrix by a diffusion-controlled process. Maximum dissolution of these hardening elements, namely Cu and Mg, in the aluminum matrix will enhance the precipitation hardening during the artificial aging treatment. Figure 2.2 shows the solution heat treatment temperature, T_{SHT}, at which a supersaturated solid solution of α-Al is obtained, for a hypothetical alloy Al-Cu with a composition Cx. The solute elements tend to segregate into networks of eutectic constituents during dendritic solidification in the as-cast alloy; this segregation of alloying and impurity elements may have an adverse effect on mechanical properties. The solution heat treatment may cause a redistribution of the elements in the constituent phases when

they dissolve and segregation is minimized. The dissolution of some constituent phases such as iron-rich intermetallics which contain insoluble elements may change little by solution heat treatment; however, the temperature and time of solution treatment may determine the susceptibility of these iron-intermetallics to be fragmented and dissolved.[6, 7, 8]

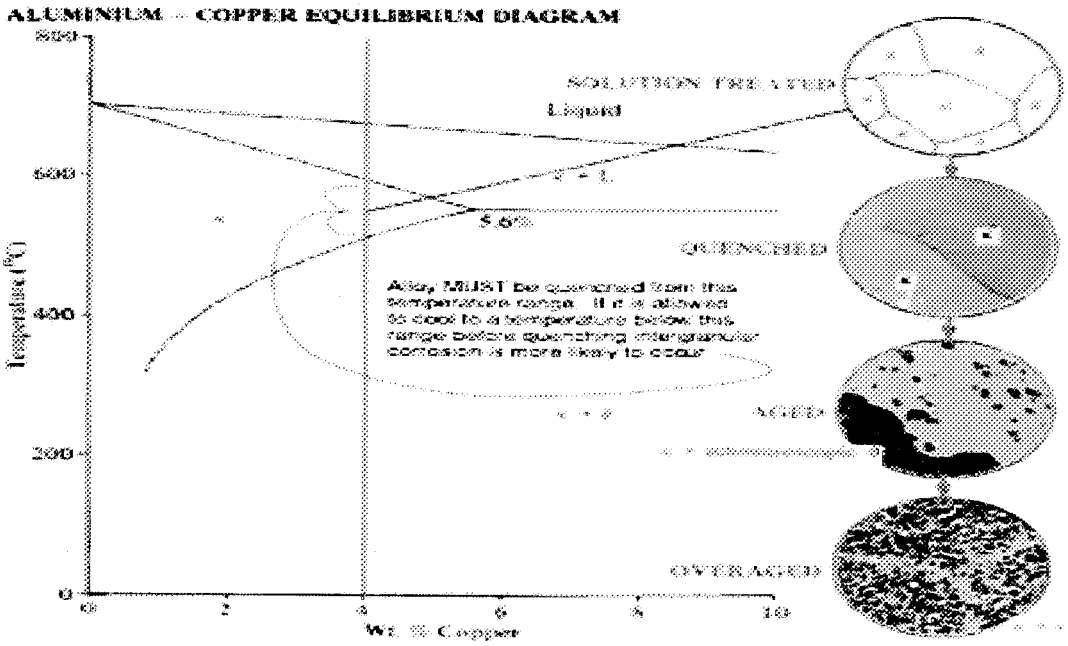

Figure 2.2. Hypothetical phase diagram.[6]

The morphology of the eutectic silicon plays a significant effect on the mechanical properties of aluminum cast alloys; the eutectic silicon particles are present in the form of coarse needles, acicular structure, under normal cooling conditions. These needles act as stress raisers and crack initiators which may have a negative effect on the mechanical properties; fibrous Si particles may be obtained by using Sr-modifiers. The solution heat treatment tends to spheroidize the silicon particles reducing the surface energy through

fragmentation or dissolution of the eutectic silicon branches and spheroidization of these fragmented particles. The change in the size and morphology of eutectic silicon takes place through several stages during solution heat treatment; the acicular eutectic silicon platelets undergo necking and separate into segments during the initial stage. Following this, the average particle size decreases and the fragmented segments gradually spheroidize. [48, 49, 50, 51] Depending on the solution heat treatment parameters, in particular, the heating rate to attain the specified solution temperature, the spheroidization and the coarsening of the eutectic silicon can occur during this stage. In modified structures, the fibrous eutectic silicon particles undergo spheroidization at an early stage of solution heat treatment; modification facilitates fragmentation of these acicular particles since it promotes eutectic silicon branching. Li *et al.* [52] reported that the eutectic silicon particles in modified Al-Si cast alloys are completely spheroidized after 1 hour of solution heat treatment, while in unmodified alloys even after 12 hours some coarse needles of Si may be shown in the microstructure. Figure 2.3 shows a schematic of the spheroidization and coarsening process. [53] The globularization and coarsening process of the silicon particles is due to the growth of larger particles at the expense of smaller ones and is known as *Ostwald ripening* which explains why during the solution heat treatment, the number of silicon particles decreases as their average size increases. The driving force for this process results from the fact that the surface energy is higher in smaller particles due to their smaller radius compared to larger particles, so that a concentration gradient exists from larger to smaller particles; this difference in concentration gradient may cause the preferential dissolution of smaller particles. [54]

Solution heat treatment applied to Al-Si casting alloys at high heating rate (temperature and time) may result in improving microstructural characteristics, as well as enhancing mechanical properties and quality indices. The solution heat treatment increases ultimate tensile strength and ductility (*i.e.* quality), while aging increases yield strength at the expense of ductility. A quenching step is required in order to maintain the desirable conditions, supersaturated solid solution, for obtaining precipitation hardening; solution heat treatment followed by quenching may increase the strength through the solute solid solution strengthing mechanism.

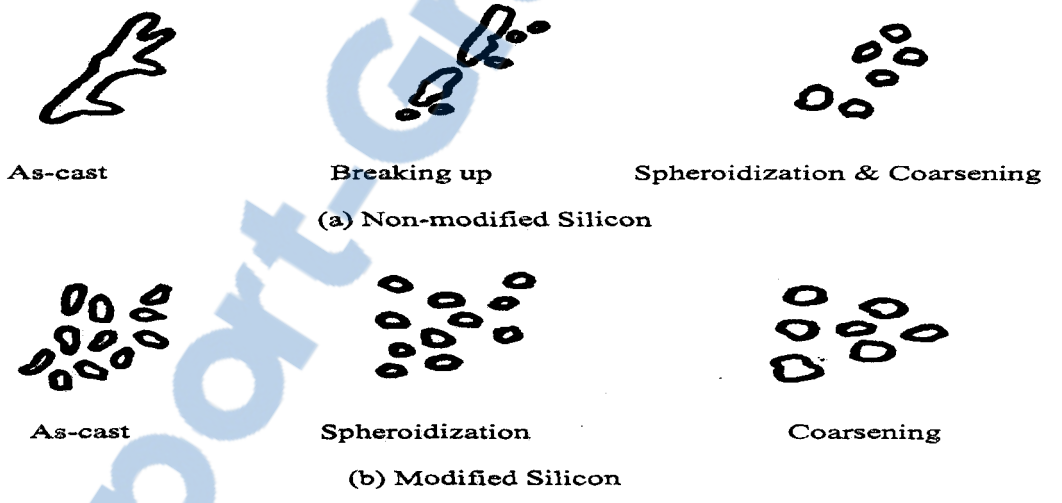

Figure 2.3. Schematic diagram showing behavior of eutectic Si particles during solution heat treatment in the case of: (a) non-modified and (b) modified Al-Si cast alloys. [53]

2.2.1.2. Quenching

The objectives of quenching are (a) to retain the maximum amount of the precipitating alloying elements in solution to form a supersaturated solid solution at low temperatures; and to (b) obtain as many vacancies as possible within the atomic lattice

which will act as initial potential sites for formation of precipitates during artificial aging treatment. The cooling rate during quenching step may affect the optimum conditions required for a successful precipitation process during the subsequent aging treatment. The casting alloys may be quenched by cooling to lower temperature in water, hot air using an air forced convection furnace (CF), or any other suitable quenching medium such as hot sand using the fluidized sand bed technique (FB). The quenching step using any of the different quenching media mentioned above aims mainly at preventing the precipitation of equilibrium phases dissolved in the aluminum matrix such as Al_2Cu and Mg_2Si as well as reducing the residual stresses and distortions of alloys which might accompany the fast cooling rate. The lowest level of induced residual stresses and the least distortion possible at room temperature are suitable conditions for avoiding a decrease in the mechanical properties of the final heat treated product. [55, 56, 57]

In the quenching heat treatment step, the time delay in quenching and the quenching rate parameters have a significant effect on the mechanical properties of Al-Si cast alloys. It is recommended that the quenching step should be performed directly after solutionizing heat treatment at high temperature for the purpose of minimizing the time delay in quenching. [43, 58, 59] An excessive delay in quenching may result in a temperature drop and rapid formation of coarse precipitates in a temperature range at which the effects of precipitation are ineffective for hardening purposes. For casting alloys, the delay in quenching should not exceed 45 sec and a maximum quenching delay of 10 sec is usually acceptable, as specified by ASTM standards. [43, 60]

Rapid quenching increase response to age hardening, but it also creates residual stresses and distortion; while slow quenching rates result in precipitation during quenching, localized over-aging, loss of corrosion resistance at grain boundaries and lower response to age hardening. Several studies [43, 61] suggests that most commercial quenching is accomplished in water near the boiling point to avoid premature precipitation that is detrimental to tensile properties and corrosion resistance. Cooling rates should be selected to obtain the desired microstructure and to reduce the duration time over certain critical temperature ranges during quenching in the regions where diffusion of smaller atoms can lead to the precipitation of potential defects. [62] The quenchants used for quenching aluminum alloys include water, hot air, and sand in a fluidized bed; the effectiveness of the quench is dependent upon the quench media and the quench interval. To quench parts quickly, the industry has traditionally employed water as a quenchant. Regardless of the type of quenchant being used, cooling generally occurs in three distinct stages, namely vapor stage, boiling stage and convection phase as shown in Figure 2.4. The vapor stage is known by its slow cooling rate, where the heat transfer occurs by radiation and conduction through the vapor blanket. In the boiling stage period, high heat extraction rates are observed while in the final stage of cooling, the convection stage, heat is removed very slowly. [63, 64]

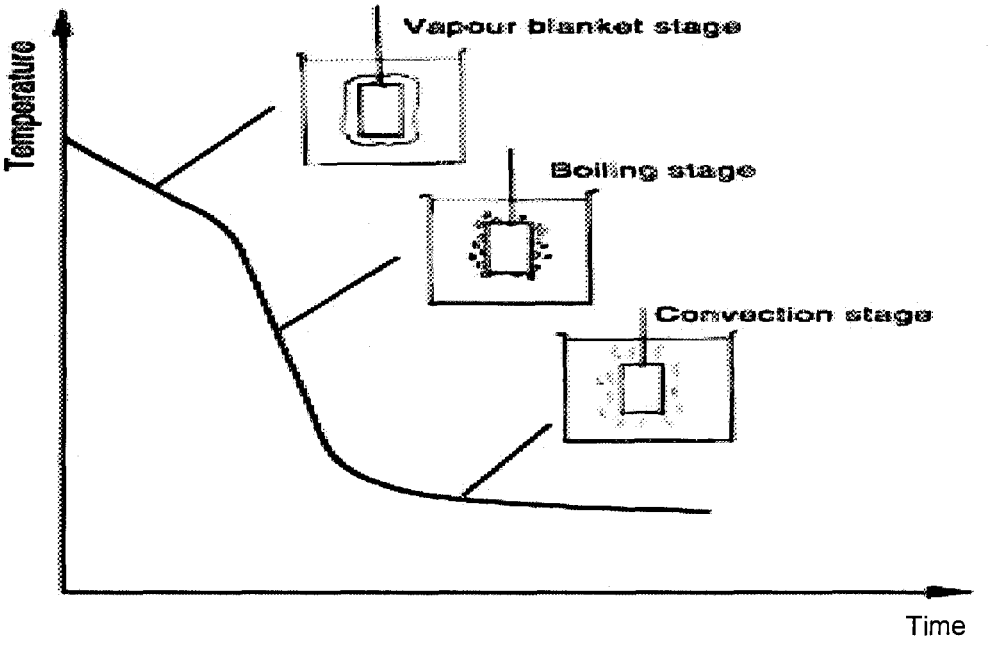

Figure 2.4. Formation of the three stages of cooling process during quenching. [63, 64]

Water exhibits an excellent heat-transfer coefficient and is relatively simple to add to the heat-treating process; for applications requiring high strength results, quenching with water would be most advisable. It was reported, however, that the quenching capacity of water is higher than necessary to obtain optimum properties, where the high internal stresses resulting from rapid quenching are undesirable. [63] The cooling rates of water as a quenchant can be measured using probes instrumented with thermocouples; the mechanism of water quenching can be explained using a graph of temperature against time as shown in Figure 2.5, where the water quenching is considered as a three-phase process. Initially, as the part is immersed in water, a vapor blanket envelops the heat-treated part; this vapor blanket acts as an insulator resulting in a relatively slow cooling rate for the quenched alloy as depicted by the phase I stage in Figure 2.5. As the quench process continues and the

surface of the part begins to cool down, the vapor blanket starts to collapse and the quenchant comes in direct contact with the part's surface. Thus, the Phase II or boiling stage exhibits a dramatic increase in the cooling rate of the part; the final phase begins where convection finishes the quenching process, where the surface temperature of the part falls below the boiling temperature for the quenchant. [64] This complicated nature of water quenching is responsible for such problems as part deformation and high residual stresses. The disadvantage of water quenching is that for large parts and parts with complicated geometries, the various phases which may precipitate may do so at different times, resulting in large temperature gradients within the part. These gradients may manifest as high residual stresses, part distortion, and cracking. In comparison, quenching in a fluidized sand bed is an alternative well suited for parts requiring low residual stresses and for reducing susceptibility of the part to distortion.

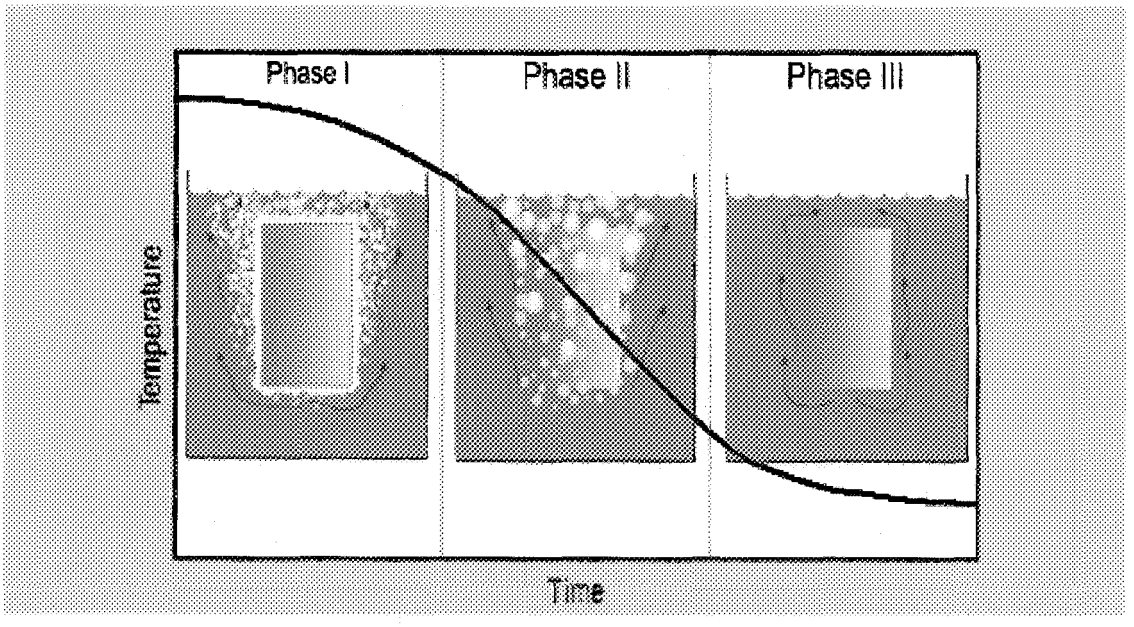

Figure 2.5. A typical cooling profile (S-curve) of a heat-treated part quenched in water.[64]

2.2.1.3. Aging

Ageing is the controlled decomposition of the supersaturated solid solution to form finely dispersed precipitates in heat-treatable alloys, usually by soaking for convenient times at one or sometimes two temperature levels. The decomposition is normally complicated and occurs through several precipitate stages. These finely dispersed precipitates have a dominant effect in raising yield and tensile strengths, and may also affect other properties such as corrosion resistance and dimensional stability. Aging temperature and aging time are the main parameters controlling the characteristics of the phases precipitated during aging treatment as well as the mechanical properties of these alloys. The precipitation process can occur at room temperature after direct quenching from a high solution treatment temperature, namely T4 temper, or may be accelerated by artificial aging at temperatures ranging from 90 to 260^0C, namely T6 and T7 tempers, so as to allow the diffusion of solute atoms and precipitation of secondary phases. [65, 66, 67]

During the initial stages of artificial aging at low temperatures, a redistribution of solute atoms within the lattice takes place to form ordered clusters or GP (Guinier-Preston) zones which are enriched in solute atoms. GP zones may precipitate in different shapes: rods, needles, spherical clusters; their form depends to a high degree on the specific alloy system. There are several alloying elements that exhibit GP zones in Al alloys and their formation requires the movement of solute atoms such as silver, copper, magnesium and zinc, over relatively short distances so that they are finely dispersed in the matrix. The rate of nucleation is influenced by the presence of excess concentrations of vacant lattice sites, or vacancies, which are formed from the solution stage by quenching. These vacancies

facilitate the transport of the solute atoms. [68] Figure 2.6 shows a schematic illustration of coherent, semi-coherent and non-coherent precipitates; where high strength will be obtained in the transition (coherent and semi coherent) zones. [69]

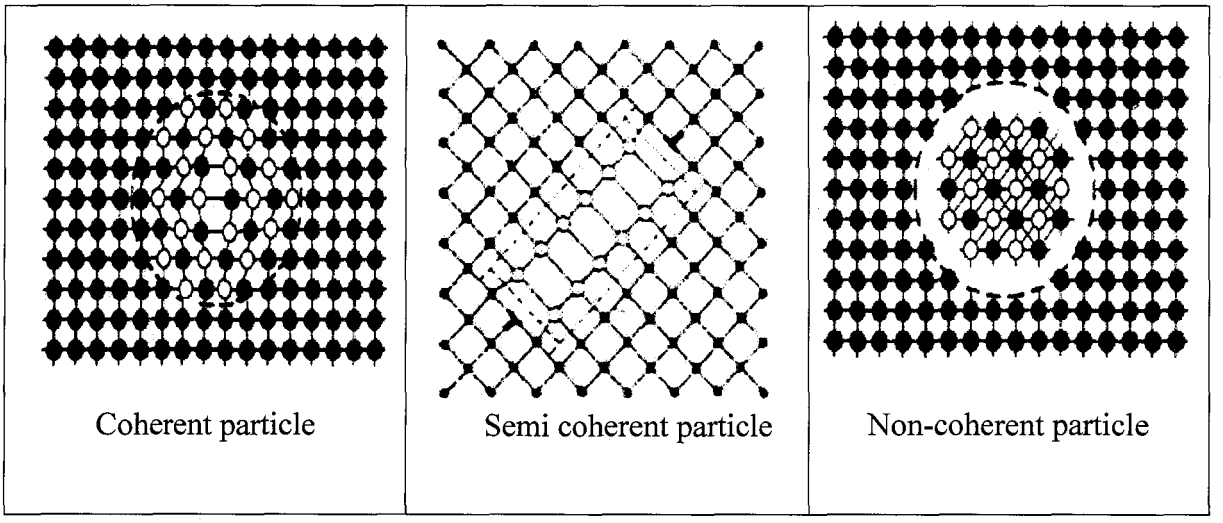

Figure 2.6. Schematic representation of precipitate coherency.[69]

The strength mechanism resulting from age hardening process can be explained by two basic concepts which depend on the interaction between the moving dislocations and the precipitated phases as well as the number and size of the precipitating particles. [69] An increased number, or high volume fraction, of GP zones in the matrix increases the distortion and thus also the stress required to move dislocations, since a single GP zone on its own has only a minimal effect on impeding dislocation gliding. The strengthing effect increases as the size of the precipitates increases, as long as the dislocations continue to cut through the precipitates. This stage is regarded as the peak aging condition, i.e. where the highest strength is achieved. As aging progresses, these particles grow, thereby increasing

coherency strains, until the interfacial bond is exceeded and coherency disappears. As precipitates grow and become more widely spaced, they can be readily bypassed by dislocations forming loops around them, a phenomenon known as the Orowan mechanism for dispersion hardening, and causing the strengthing to decrease, as shown in Figure 2.7. [69, 70] This stage is called overaging, which may occur by treatment at a higher temperature and/or longer time than that used for a T6 temper, as in case of a T7 temper which is applied at 240°C. [70] Hard particles provide maximum hardening levels for the age-hardened alloys while soft phases provide lower strength values. The strengthing effect which results from hard particles depends on the volume fraction and size of these precipitates. The level of hardening obtained also depends on the inter-particle spacing.

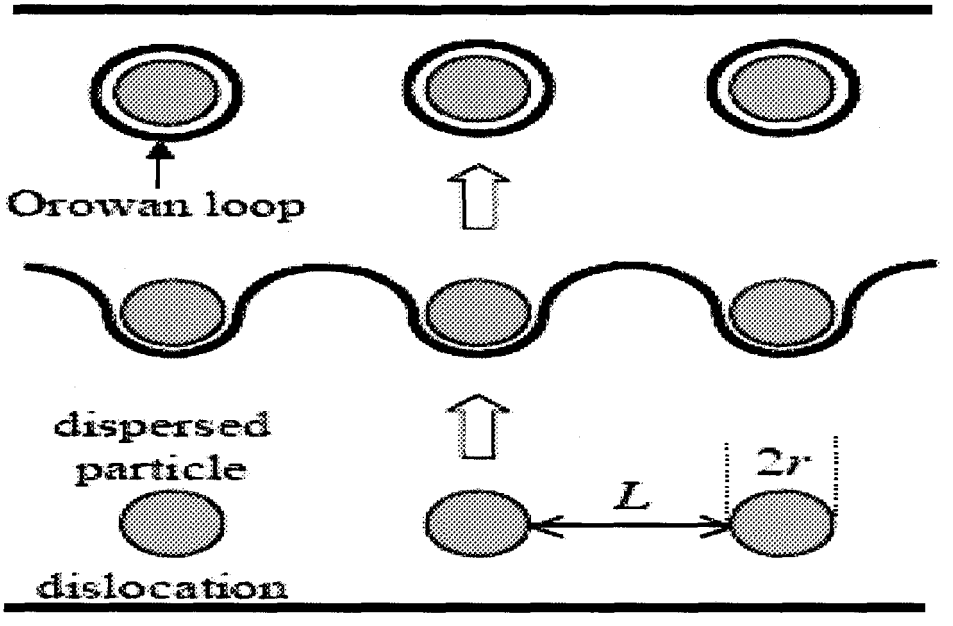

Figure 2.7. Orowan mechanism for dispersion hardening. [69, 70]

The Al-Si-(Mg/Cu) alloy system can be naturally aged at room temperature, where the longer the natural aging stage, the more adversely affected the mechanical properties will be. It should be noted, however, that the natural aging has a significant effect on the tensile results obtained after subsequent artificial aging. Several studies [55, 71, 72] on Al-Si-Mg alloys have found that it is beneficial to use a pre-aging holding time of 24 h before applying artificial aging, whereas another study reports that this is not effective except for a slight increase in elongation; small additions of elements such as Cd, Sn, and Cu are employed to inhibit natural aging in these cast alloys. [73] The aging rate can be accelerated by heat treating the product at higher temperatures of 150-200°C for specific times ranging from 2-12 hrs to facilitate the diffusion of solute atoms and precipitation of secondary phases; this process is known as artificial aging. A number of studies carried out on Al-Si-(Mg/Cu) alloys using TEM revealed that besides the θ-$CuAl_2$ and β-Mg_2Si phases, certain other precipitates exist such as the W (Al Cu_4 Mg_5 Si_4) and S (Cu Al_2 Mg) phases. [73, 74, 75]

In the context of the current study, several parameters may affect the mechanical performance of Al-Si-(Cu/Mg) cast alloys during aging treatment: (i) the various solution heat treatment times as well as heating rates depending on the heating techniques used (CF or FB); (ii) the quenching medium used such as water, or hot forced air using either a CF or an FB; and (iii) the aging parameters. The heating rate plays an important role in increasing the kinetics of the aging process by having an effect on the aging characteristics of Al-Si-(Cu/Mg) alloys.

2.2.2. Precipitation Hardening of Al-Si-(Cu/Mg) Castings

With respect to the precipitation hardening of Al-Si-(Cu/Mg) alloys, for each of the Al-Si-Mg and Al-Si-Cu-Mg alloy systems, there exist optimum time and temperature parameters to maximize the alloy strength and hardness. For Al-Si-(Cu/Mg) casting alloys, the optimum temperature for solution heat treatment ranges from 495°C to 540°C and from 150°C to 200°C for aging temperature; the optimum time for all T6-heat treatment steps may range from 15 to 20 hours when using a conventional convection furnace. [76, 77]

2.2.2.1. B319.2-Type Aluminum-Silicon Casting Alloys

The cast B319.2 type (Al-Si-Cu-Mg) cast alloys display high strength values at the expense of somewhat reduced ductility after the application of heat treatment; this improvement in the strength may be related to the presence of the hardening elements such as copper and magnesium. Based on the Al-Si system, the alloy contains 3-4 % copper and 0.4% magnesium as the main alloying elements. During the solidification of 319 alloys, the first reaction observed is the formation of the dendritic network of α-aluminum; the Al-Si eutectic reaction occurs next, followed by the precipitation of secondary eutectic phases like $CuAl_2$. The α-Al_{15} $(Mn,Fe)_3Si_2$ and β-Al_5FeSi iron intermetallics phases normally formed after the α-Al dendrites have formed but before the appearance of the Al-Si eutectic, i.e., in a pre-eutectic reaction. [78, 79, 80] The sequence of reactions during solidification and the phases observed in both alloys are listed in Table 2.2. The characteristics and compositions of these phases are provided in Table 2.3. The intermetallic phases that Cu forms with Al during solidification are the block-like Al_2Cu

and/or fine eutectic form as (Al + Al2Cu) which depends on the levels of Cu, Fe, and Sr in the alloy. It was noted that precipitation of the Cu phase is strongly dependent on the possible sites available for nucleation of the phase, which is determined by the amount and nature of the β-iron phase precipitation and the cooling rate. [81] In magnesium containing B319.2 type alloys, the increased level of magnesium does not change the solidification process significantly, except that an increased amount of the Q-$Al_5Mg_8Cu_2Si_6$ phase is observed. Figure 2.8 shows the optical micrograph of an Al-Si-Cu-Mg ingot sample, showing the most common phases in this alloy.

Table 2.2. Sequence of phase precipitation during solidification of Al-Si-Cu-Mg cast alloys. [79]

Isothermal reactions	**Reaction type / T °C**
Aluminum dendrites	Dendritic Reaction / 609°C
Aluminum dendrites and $Al_{15}Mn_3Si_2$ and/or Al_5FeSi	Dendritic Post-dendritic / 590°C Pre-eutectic
Eutectic Al + Si , Al_5FeSi and Mg_2Si	Eutectic Co-eutectic / 575°C
Al + $CuAl_2$ + Si + Al_5FeSi	Post-eutectic / 525°C
Al+$CuAl_2$+Si+$Al_5Mg_8Cu_2Si_6$	Post-eutectic / 507°C

Table 2.3. Phases observed by optical microscopy, SEM, EDX in A319.2 alloys. [79]

Phase	α-Al	Si	$CuAl_2$	Al_5FeSi	$Al_{15}Mn_3Si_2$	$Al_5Mg_8Cu_2Si_6$
Characterization	Dendrite	gray	Pink particles	needle	Brown Chinese script	Brown bulk

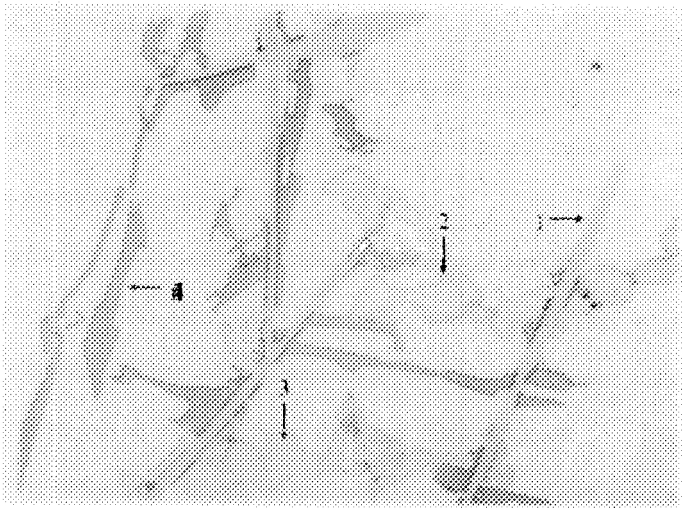

Figure 2.8. The most common phases formed in Al-Si-Cu-Mg cast alloys: (1) β-Al_5FeSi, (2) blocky Al_2Cu phase, (3) $Al_5Mg_8Cu_2Si_6$ phase, (4) acicular Si phase. [81, 82]

The presence of magnesium with copper improves the strength after precipitation hardening heat treatment due to the formation of several hardening phases such as β-Mg_2Si and Q-$Al_5Mg_8Cu_2Si_6$ in addition to the Cu-based phase, θ-$CuAl_2$ phase. [81, 82] Figure 2.9 shows a schematic skeletal phase diagram presenting four phases in equilibrium formed in the Al-Si-Cu-Mg system, where the coexisting equilibrium three-phase fields expand into three tetrahedral composition spaces. [83]

Most of the recommended heat treatments of Al-Si cast alloys that contain copper restrict the solutionizing temperature below the final solidification point in order to avoid the melting of the copper-containing phases. Solution heat treatment is usually carried out at a temperature of 500°C to 505°C, and held for 8-12 hours at this temperature; quenching is accomplished in water at 65° to 100°C. Aging (for T6 temper) is done at 150° to 155°C, for times ranging from 2 to 5 hours. For solution heat treatment of 319 alloys, it was observed that raising the temperature from 490 °C to 510°C results in a considerable

improvement in the tensile properties which are related to the microstructural changes occurring when increasing the temperature. [84, 85, 86, 87] These improvements are due to spheroidization of the eutectic silicon; the fragmentation and dissolution of β-iron platelets; and the reduction in the amount of block like Al_2Cu phase; Figure 2.10 shows the difference between the microstructures of an as-cast Al-Si-Cu-Mg alloys and a solution heat treated one.

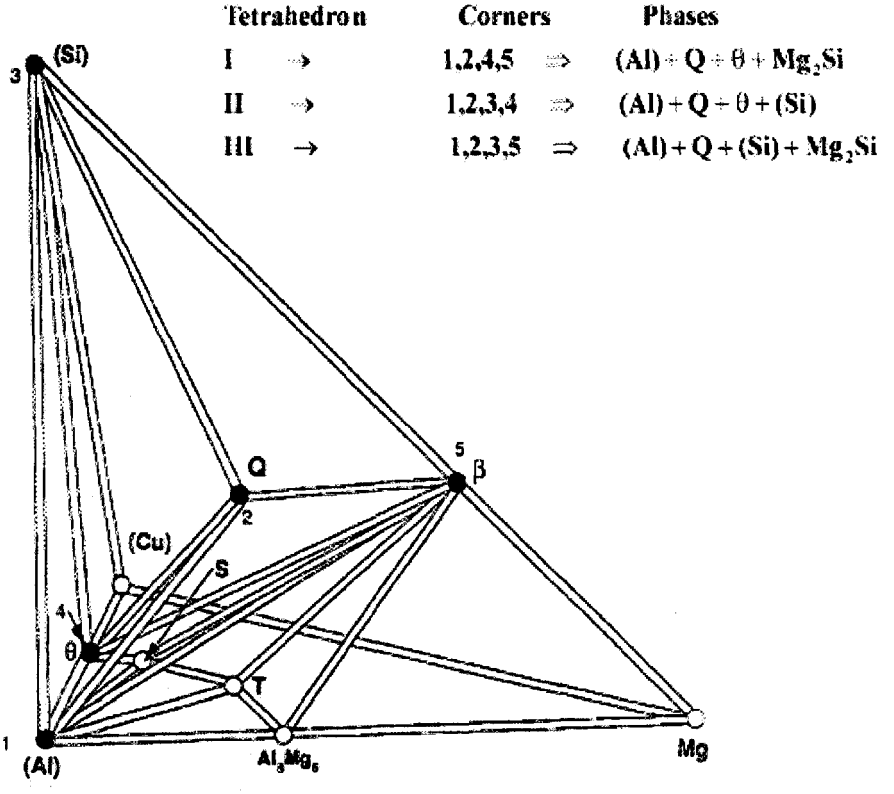

Figure 2.9. Line diagram of stable equilibrium phase fields in Al–Mg–Si–Cu system at room temperature. [83]

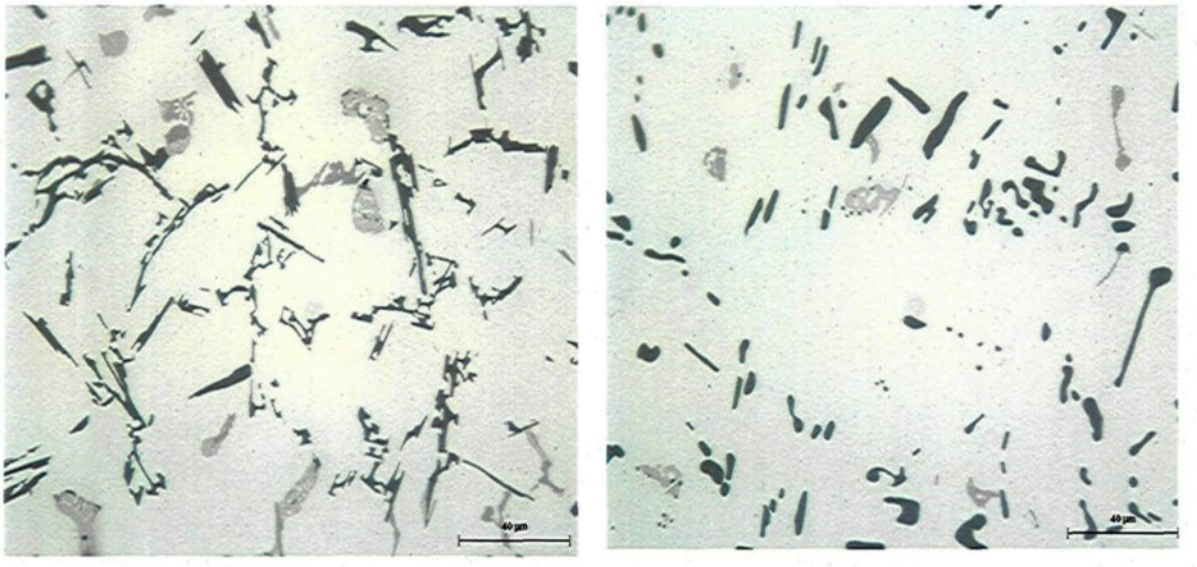

Figure 2.10. Optical micrographs of (a) As-cast and (b) Solution heat treated samples of an Al-Si-Cu-Mg. [86, 87]

Samuel *et al.* [88] reported that solution treatment at 500°C for 8 to 10 hours using a conventional furnace appeared to be the best solution heat treatment recommended for high Mg-content 319 alloys. It has been reported also that increasing the solution temperature in the range of 480°C to 515°C for 2-24 hours may improve the ultimate tensile strength and elongation values since this provides safe temperature range limits for dissolution of the $CuAl_2$. The dissolution of $CuAl_2$ is accelerated with increasing solution temperature from 505°C to 515°C as well as with increasing solution heat treatment time as shown in Figure 2.11. [88, 89] Upon increasing the amount of dissolved Al_2Cu, an enrichment of the supersaturated solid solution structure in Cu may be observed; this leads to an enhancement of the driving force for Al_2Cu precipitation during aging treatment, thereby multiplying the tensile properties. [89] Crowell *et al.*[90] stated that the blocky Cu phase in B319 alloys may be partially dissolved with increasing solution heat treatment time at the recommended

solution temperature of 495°C. From most of the previous studies applied on 319 cast alloys, it may be noted that high temperature and/or long time of solution heat treatment may be required to achieve standard mechanical properties needed for a particular engineering applications. The high temperature and/or long time of solutionizing process is required for the purposes of fragmentation and dissolution of acicular eutectic Si particles; and dissolution of β-Mg_2Si, θ-$CuAl_2$ and Q-$Al_5Mg_8Cu_2Si_6$ hardening phases in the aluminum matrix.

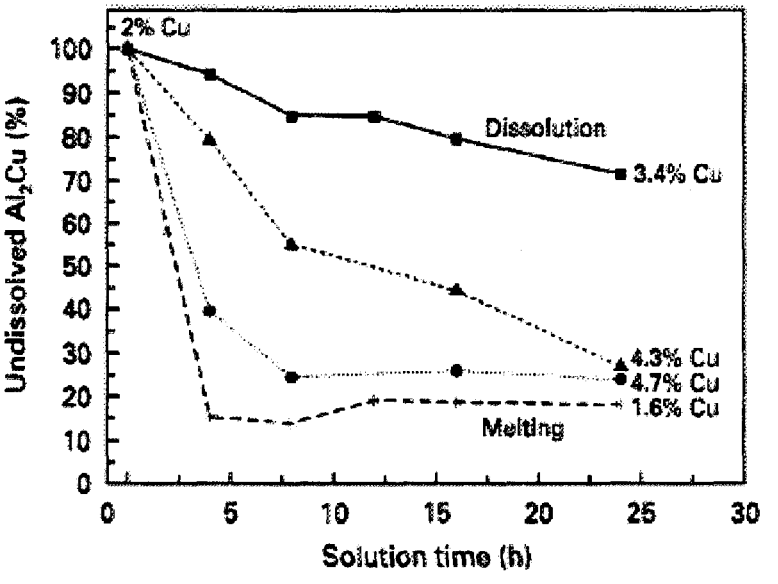

Figure 2.11. Effect of solution heat treatment on the amount of dissolved $CuAl_2$ in 319 alloy. [89]

The solution heat treatment should be followed by quenching from high temperature to either the room temperature, using a fast cooling rate medium such as water, or the aging temperature using direct quenching-aging media with lower cooling rates than water, such as those of the CF and FB techniques. Byczynski *et al.* [91] studied the effect of the quench

rate on the mechanical properties of 319-type alloys and determined that quenching in water at 65°C may be beneficial to the mechanical properties analyzed.

The aging treatment of Al-Si-Cu cast alloys results in the formation of various forms of $CuAl_2$ precipitates; the $CuAl_2$ precipitation sequence is generally described as follows: [92, 93, 94]

$$\alpha_{(SSS)} \rightarrow GP_{(1)}\text{ zones} \rightarrow GP_{(2)}\ (\theta''\ (Al_2Cu)) \rightarrow \text{Transition phase, } \theta'\ (Al_2Cu) \rightarrow$$

$$\text{Incoherent equilibrium phase } \theta\ (Al_2Cu)$$

The sequence begins with the decomposition of the supersaturated solid solution and the clustering of Cu atoms which lead to the formation of coherent disk-shaped GP (Guinier–Preston) zones. GP zones provide an increase in the strength properties but reduction in ductility. [68, 95] Increasing the aging temperature above 100°C and/or the aging time leads to the GP zones being replaced by θ'' and θ' precipitates, which probably nucleate and grow within fcc α-Al-matrix; the θ' precipitates germinate on fcc matrix dislocations. [95] Figure 2.12 shows the SEM and TEM micrographs of θ' semi-coherent precipitates obtained after aging treatment. [96, 97] The coherent and semi-coherent phases, θ'' and θ' respectively, contribute to increasing the strength of the alloys. At high aging temperature and/or after a long aging time, the incoherent equilibrium precipitate θ ($CuAl_2$) is formed in the aluminum matrix; this type of equilibrium precipitates results in diminishing the hardening effect observed in the alloys due the θ'' and θ' phases, as the coherency between the stable phases and the metal matrix is lost. A high degree of coherency causes extensive coherency-strain fields to arise, conferring peak strength the alloys at the corresponding aging time. [92, 96]

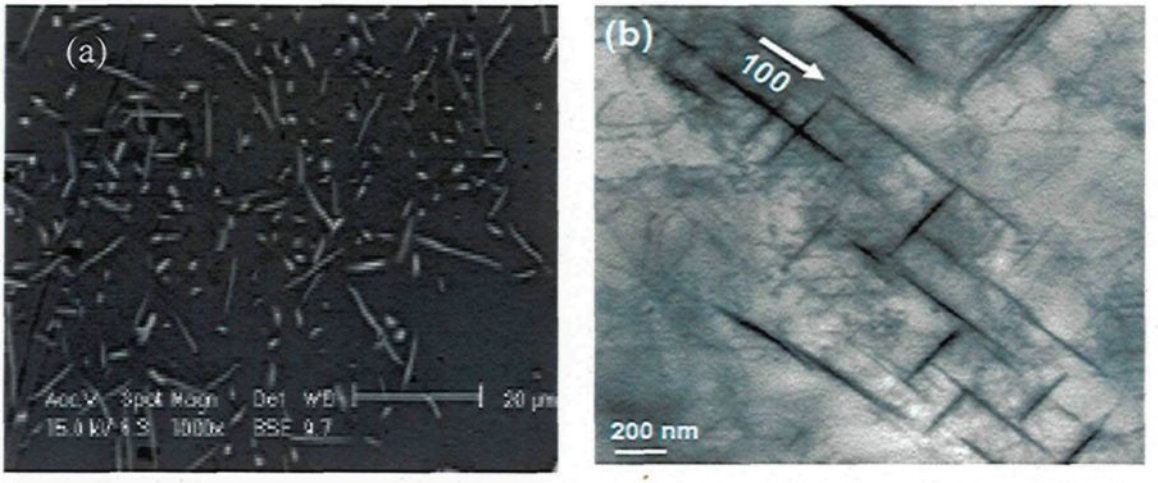

Figure 2.12. (a) SEM and (b) TEM micrographs of meta stable θ' precipitates. [96, 97]

The effect of Mg additions, specifically on the aging behavior of 319-type alloys, was studied by Apelian *et al.* [55], Ouellet and Samuel [98] and Wang *et al.* [99] A Mg level of 0.6 wt pct leads to an increase in strength compared to the strength obtained in alloys with only 0.2 wt pct Mg. This is due to the increase in the formation of the β'-Mg_2Si hardening precipitates, with the increased amount of Mg in solid solution. It was also determined that additions of 0.45% Mg enhance the response of the alloy to heat treatment, particularly in the T6 condition where improvements of more than 40% in strength were obtained in samples that contained 0.45% Mg, in comparison with samples treated at the same temperature and time (8h at 180°C) containing very low levels of Mg, about 0.06%. [55, 98, 99, 100] Typical mechanical properties for cast test bars of alloy 319.0 are summarized in Table 2.4. Regarding the age hardening of B319.2-type Al-Si-Cu-Mg cast alloys, it was reported that a quaternary Q-phase is formed in addition to other hardening phases such as $CuAl_2$ and Mg_2Si. [101] This Q-$Al_5Mg_8Cu_2Si_6$ phase, in addition to the latter phases, is also responsible for the strengthening of B319.2 cast alloys. It has been reported, however, that

the dissolution of this phase during solution heat treatment is much more difficult than that of $CuAl_2$. [89, 102] In such cases, the high heating rate (to attain the solution temperature) may be considered as an important factor affecting the dissolution of the phase, where the morphology nature of such phases would also play a role in its dissolution.

Table 2.4. Typical mechanical properties of cast test bars of alloy 319. [5, 6, 7, 100]

Mechanical property	**Permanent mold cast**	
	As cast	**T6**
Tensile strength, MPa	235	280
Yield strength, MPa	130	185
Elongation, %	2.5	3.0
Hardness, HB	85	95

2.2.2.2. A356.2-Type Aluminum-Silicon Casting Alloys

As mentioned previously, A356.2 type alloys constitute an important series of Al-Si alloys, which are age hardenable due to the presence of magnesium. Aluminum-silicon alloys that do not contain copper additions are used when good castability and good corrosion resistance are needed; magnesium can act as a substitute for copper. Magnesium and silicon form the intermetallic hardening phase Mg_2Si which precipitates in the α-aluminum matrix and increases the yield strength. Suitable distribution of Mg_2Si precipitatesd can be obtained through a solution heat treatment, quenching and aging procedure. The chemical composition of alloys with increased Mg content is given in Table 2.5.

Table 2.5. Chemical composition of A356, A357 and AlSi7Mg0.8 alloys in wt%. [103]

Alloy	Si	Mg	Fe	Mn	Cu	Ti	Be	Sr
AlSi7Mg0.3 (A356)	7.15	0.32	0.15	0.017	0.004	0.086	0.002	0.031
AlSi7Mg0.5 (A357)	6.88	0.53	0.16	0.009	0.005	0.064	0.002	0.031
AlSi7Mg0.8	7.1	0.79	0.15	0.010	0.005	0.08	0.001	0.028

The hardening phase Mg_2Si has a solubility limit corresponding to approximately 0.45% to 0.7% Mg in the heat-treated condition at 555°C, so that no further strengthening will occur beyond this limit. [103, 104] The strengthening mechanism depends on the microstructural morphology of the precipitates, which are generated by the interfacial and strain energies of the precipitate/matrix system. The main isothermal reaction of Mg_2Si phase precipitation during solidification occurs at 555°C. The black particles of the secondary eutectic phase, Mg_2Si, appear in the microstructure on account of the high Mg content of the alloy, 0.3%-0.7% Mg; Figure 2.13 shows the optical micrograph typically obtained from an as-cast 356 alloy. [105]

Figure 2.13. Optical micrograph of as-cast Al-7% Si-0.4% Mg alloy. [105]

The main sequence of phase precipitation during solidification is listed in Table 2.6. The corresponding phases and their characteristics are given in Table 2.7. [79]

Table 2.6. Sequence of phase precipitation during solidification of Al-Si-Mg castings. [79]

Isothermal reactions	Reaction type / T °C
Aluminum dendrites	Dendritic Reaction / 615°C
Aluminum-Silicon Al + Al_5FeSi	Eutectic / 575 °C
Eutectic (Al + Si) +Al_5FeSi +$Al_8Mg_3FeSi_6$	Eutectic / 575 °C Pretectic / 567 °C
Al + Mg_2Si + Si	Post-eutectic / 555 °C
Al+Si+Mg_2Si+$Al_8Mg_3FeSi_6$	Post-eutectic / 554 °C

Table 2.7. Phases observed by optical microscopy, SEM, EDX in A356.2 alloys. [79]

Phase	α-Al	Si	$Al_8Mg_3FeSi_6$	Mg_2Si	Al_5FeSi
Characteristics	Dendrite	Gray	Brown Script	Black	Needle

Figure 2.14 illustrates a pseudo-binary section through the system AlSiMg0.3; it may be observed the formation of Mg2Si phase in addition to the α-Al matrix and Si phases. The temperature interval of solidification is about 60°C and the semi-solid forming temperature, TSS, at a liquid and solid fraction of 50% can be detected to ~580°C. [106] Compared to B319.2 alloys, A356 alloys have a good control over amount of impurities, especially iron, which is detrimental to the mechanical properties of the alloy.

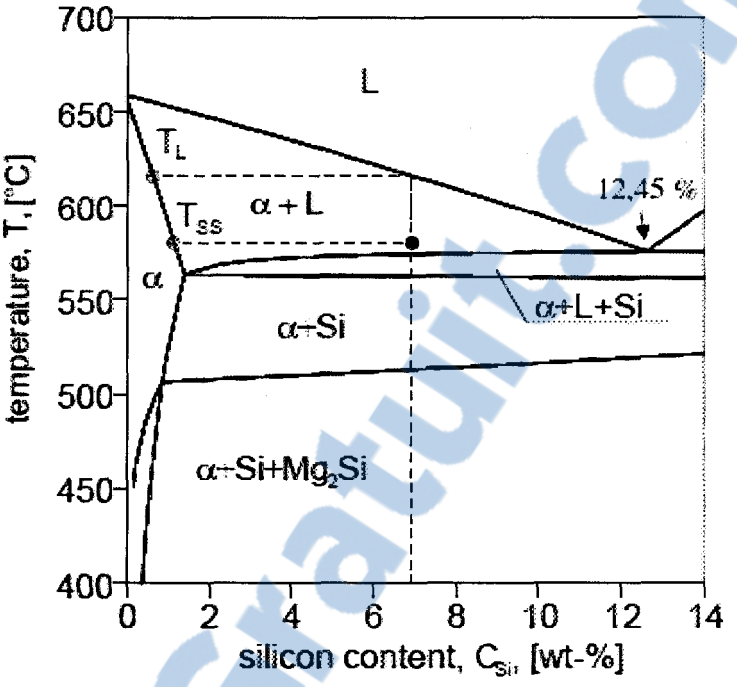

Figure 2.14. Pseudo-binary section of the system Al-Si-0.3%Mg. [106]

For the T6-conventional heat traetment of A356.2 type aluminum–silicon cast alloys, the solution heat treatment is applied within a temperature range of 535° to 540 °C for 8 hours while the aging treatment is applied at 150°C to 155°C for 3 to 5 hours. [55, 56, 107] Taylor *et al.* [108] and Tiryakioglu [109] studied the influence of solution heat treatment paramters on the microstructural characteristics of Al-Si-Mg cast alloys; it was observed that homogenization of the cast structure is achieved after 6 hours solution heat treatment at 540°C. The content of Mg in the aluminum matrix was observed to increase from 0.44wt% to 0.75wt% upon increasing the solution heat treatment temperature up to 555°C for 6 hours. [55, 110] Magnesium which cannot be dissolved in the matrix is available for the

formation of undesired intermetallics compounds. Figure 2.15 shows the solubility of Mg and Si in the α-Al matrix after solution heat treatment at 555°C. [55]

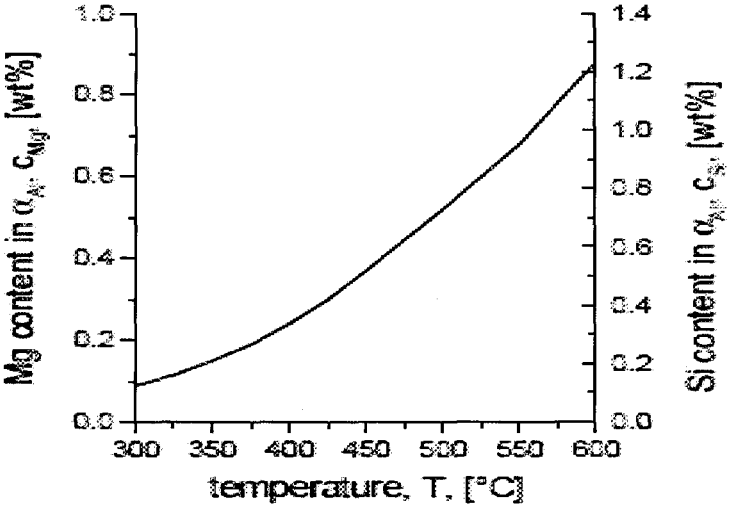

Figure 2.15. Solubility of Mg and Si in α-Al with concurrent presence of Mg_2Si and Si in equilibrium. [55, 110]

It was observed that upon increasing the solution treatment time, the Si particles become gradually rounded and coarsened. [110] Li *et al.* [52] reported that spheroidization of eutectic Si particles in Al-Si-Mg cast alloys was complete after 1 hr of solution treatment in modified alloys, while in non-modified alloys, even after 12 hours, some coarse needles of Si were still visible. It was reported that the optimum parameters affecting the microstructural features and mechanical properties were 1-2 hours of solution heat treatment time at a solution temperature of 540°C, however, a shorter solution heat treatment time may be enough for complete dissolution of the Mg_2Si phase in the aluminum matrix. [52, 56, 111] Nevertheless, a long solution treatment time may be required for fragmentation and/or

spheroidization of the eutectic Si particles. Figure 2.16 shows typical microstructures of A356.2 cast alloy samples in the as cast condition and after solution heat treatment at 540°C for 5 hours. A further increase in the solutionizing temperature, 560°C, is not recommended to avoid incipient melting of the microstructural constituents; the heating rate of the applied solution heat treatment may also have a significant effect on the fragmentation and/or spheroidization of the Si particles. [46, 112]

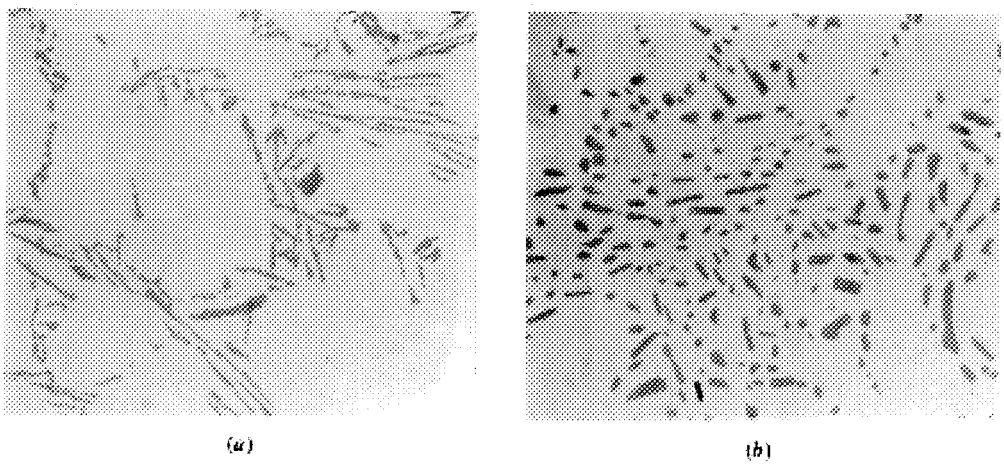

Figure 2.16. Effect of solution heat treatment on the non-modified eutectic Si at magnification of 270x: (a) before heat treatment, (b) After solution heat treatment at 540°C for 5 h. [111]

Quenching is the next critical step after solutionizing treatment at high temperature; it has been reported that the water temperature affects significantly the mechanical properties of 356 type alloys once the quenching takes place in hot water in a temperature range of 60°-70°C. [113] Zhang *et al.* [114] studied the effect of quenching rates on the tensile properties of A356.2 cast alloys; it was reported that increasing the quenching rate from 0.5°C/s to 250°C/s, using different quenching media and quenching temperatures, results in an improvement in the tensile properties of the alloys investigated. Aging may occur if the

alloys are kept in the quenched state for a long time; this type of treatment is called natural aging, T4, produces an increase in the mechanical properties of 356 alloys with increasing time, due to the formation of co-clusters and/or precipitates of Mg-Si as illustrated in Figure 2.17. [113]

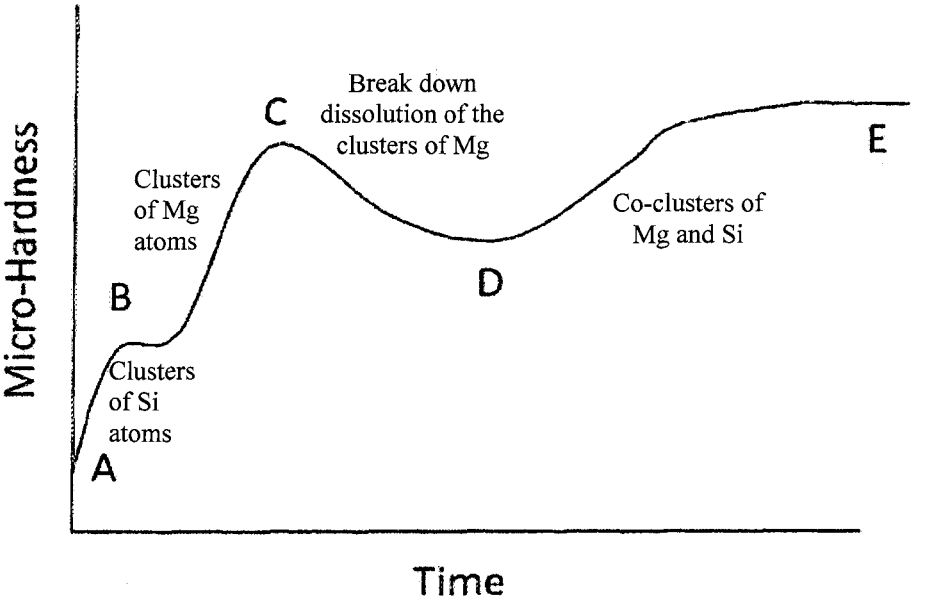

Figure 2.17. Schematic of a typical variation of the micro-hardness data with time during the natural ageing of an A356.2 alloy sample at room temperature showing the various critical stages in the precipitation reaction process. [113]

The strengthening of Al-Si-Mg cast alloys can also occur through the application of an artificial aging treatment at elevated temperatures, where the precipitation of Mg_2Si hardening phases takes place in a sequence of phase transformations. The phase transformation sequence is related to the variation in the aging parameters of temperature and time, applied during the aging treatment. Shivkumar *et al.* [110] reported that the improvement in strength of 356 cast alloys has been attributed to the precipitation of Mg-Si

containing phases from a supersaturated matrix; the precipitation sequence in T6 heat-treated and aged 356 alloys may be described as follows:

$\alpha_{(SSS)}$ → GP Zones → intermediate phase β''(Mg_2Si) together with a homogenous precipitation → intermediate phase β' (Mg_2Si) together with a heterogeneous precipitation→ equilibrium phase β(Mg_2Si).

The GP zones appear in the form of ~10 nm long needles , while the β (Mg_2Si) phase appears in the form of rods or plates (0.1 μm x 1 μm in size). [115, 116] During the initial period of artificial aging at a specific temperature, the main change is a redistribution of solute atoms within the solid-solution lattice to form clusters or GP zones that are much richer in solute. The strengthening effect of the zones results from the additional interference with the motion of dislocations when they cut the GP zones. At higher temperatures and/or longer times the formation of intermediate phases takes place. In the Al-Si-Mg system mentioned above, the GP zones are reported to be of spherical shape which convert to needle-like forms near the maximum strength inflections of the aging curves. Further aging converts the zones to rod-shaped particles. At higher temperatures, this transition phase undergoes diffusionless transformation to the equilibrium Mg_2Si phase. Strength continues to increase as the size of these precipitates increases, as long as the dislocations continue to cut the precipitates. [117, 118] The maximum alloy strength is achieved just before the precipitaion of the incoherent β- Mg_2Si platelets; the strength of Al-Si-Mg is related to the amount of Mg_2Si present in the alloy . The YS, after T6 tempers, increases almost linearly with the level of Mg_2Si content in the Al-Mg-Si cast alloys during aging at 180°C; the

significant increase in YS values occurs after 5 hours of aging as illustrated in Figure 2.18. [118]

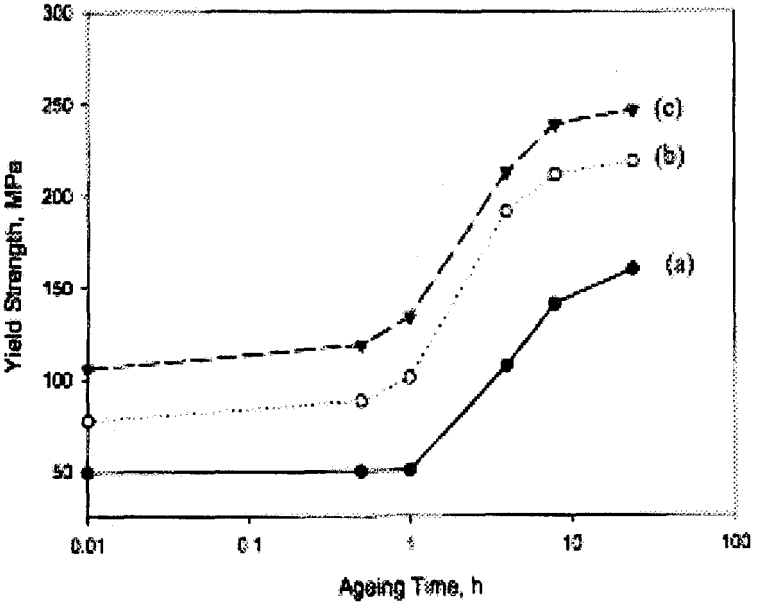

Figure 2.18. Effect of wt.% Mg_2Si on aging behavior of T6-heat treated Al-Mg-Si alloys aged at 180°C: (a) 0.63 wt.%; (b) 0.95 wt.%; (c) 1.26 wt.%. [118]

Apelian *et al.* [55] studied the aging behavior of Al-Si-Mg cast alloys and observed that the precipitation of very fine β′-Mg_2Si during aging leads to a pronounced improvement in strength properties. Both aging temperature and time affect the final properties; increasing the aging temperature by 10°C is equivalent to increasing the aging time by a factor of two. [55] The high heating rate of aging treatment may have a significant role in activating the precipitaion kinetics of hardening phases to form at an early stage of aging and with high density.

2.2.3. Heat Treatment Media

The majority of heat treating system depends on the the equipment required for heat treatment operations such as heating furnaces, quenching systems, and atmosphere and temperature control systems. In this subsection, modes of heat transmission in heating furnaces will be covered since it significantly affects the performance of the heat-treated Al-Si cast alloys.

Heat transfer during the heat tratment process may occur by three basic modes; these modes of heat transmision are by conduction, convection and radiation. Conduction is the most significant means of heat transfer within a solid or between solid objects in thermal contact under the influence of a temperature gradient, and without appreciable displacement of the material particles. The rate of heat transfer by conduction within the material/alloy is relativly fast; the required time for continus heat flow until equilibrium is reached will depend on the conductivity of the heat-treated alloys. The conduction mode of heat transfer during heating in a fluidized bed (FB) plays an important role since the hot medium is in direct contact with the heat-treated part. The convection mode refers to transfer of heat from one point to another by the movement of fluids, and is usually the dominant form of heat transfer in liquids and gases. This mode of heating would occur in a forced air convection furnace (CF), where hot air is forced through the heating chamber. In the case of heat transfer by radiation, the heating rate of the part being heat-treated would depend on the surface of material, where a highly reflective materials would absorb heat at lower rate compared to a part with a dark surface. Most heat treating furnaces used for heating to a temperatures higher than 595°C are heated by radiation, whether they are

heated by electrical resistance elements, or directly by means of radiation, or indirectly by radiant tubes. In a fluidized bed, heating may occur by all three modes of heat transmission. [119, 120] The solid particles of sand in direct contact with the heat-treated part would provide conduction heating, the use of air or gas for transferring heat from the electrical elements beneath the sand bed would provide convection heating, as well as increase the heating efficiency and temperature uniformity of the bed and workpieces.

The success of heat treatment depends on proper choice of heat treating furnace and the type of atmosphere maintained in the furnace. The heat transfer media could be gaseous as (air or vacuum), liquid- as in molten salt bath, or solid as with a fluidized sand bed furnace. Two characteristics of heat processing furnaces that are of great importance are heating rate and temperature uniformity, where the furnace user and the furnace manufacturer strive to continuously improve these characteristics. Improved heating rate reduces cycle time; improved temperature uniformity improves product quality and product yield rate. Short cycle heat treatment of aluminum castings has been shown to be possible in laboratory environments while the industry requires a production furnace that looks like and operates like a conventional mass flow convection furnace; however, the higher heating rate, heating rate uniformity and temperature uniformity of such furnaces render short heat treatment cycles possible. [120] Energy efficiency and cost of heat-treating operations are substantially affected by the method of converting stored energy into molecular kinetic energy (temperature) of the work-piece. For electric furnaces, high relative efficiencies between 85 and 100% are feasible, but the cost of electric energy is substantially higher than that of fuels such as natural gas. Consequently, gas-fired furnaces are often more

economical than electrically heated ones, even though their efficiencies are generally lower than the latter. [120]

Heat treatment of aluminum casting alloys may be carried out using salt baths, air convection furnaces, induction heaters and fluidized bed furnaces, where each technique has its advantages and limitations. The most commonly used air convection furnace (CF) offers greater flexibility in operating temperatures and has no hazardous effects except that its relatively slow heating rates results in long heat treatment cycles. Heating using molten salt baths is comparatively faster and uniform with minimum distortion, but this technique may be potentially hazardous and require special precautions. Induction heating is not used in the case of aluminum, as the efficiency and power factors of the technique are significantly low. A fluidized sand bed may be considered an efficient technique with lower equipment costs than electrical and gas-fired furnaces; it may be also well suited to heat treating of aluminum cast alloys and appears to be more effective than conventional convection furnace technique since it has a higher heating rate. [120, 121, 122] Figure 2.19 shows the relative heat transfer rates of different heating media. The fluidized sand bed can be used for solution heat treatment, quenching and aging of Al-Si-(Cu/Mg) cast alloys, saving time, energy and equipment that would be otherwise required for full heat treatment of such alloys using conventional techniques.

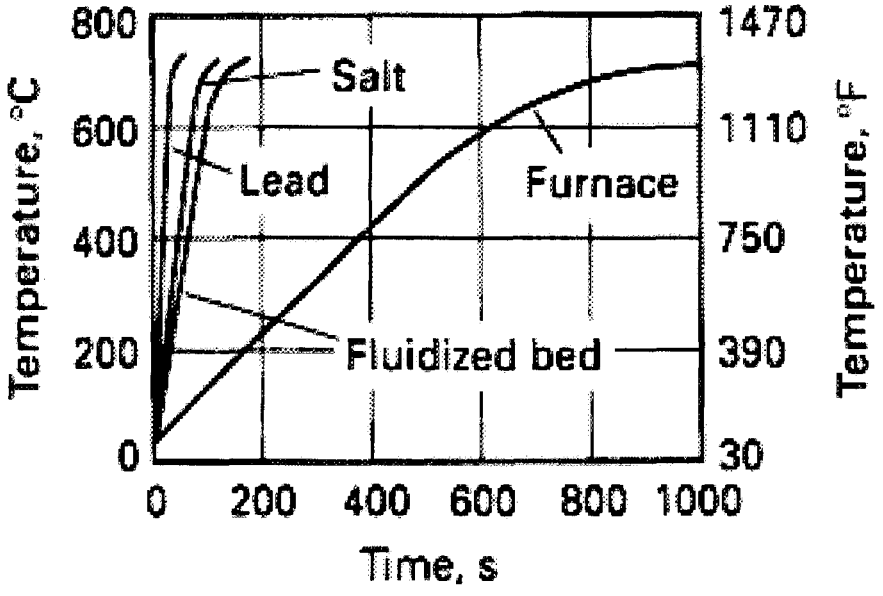

Figure 2.19. Relative heat transfer rates of different heating media. [122]

2.3. FLUIDIZED BED TECHNOLOGY

As has been discussed in the previous section, the fluidized bed furnace has the capability of replacing some of the traditional types of heat treating furnaces; it is capable of improving both operating efficiency and process quality in various engineering applications. The environmental and safety advantages as well as flexibility, simplicity, low cost and economy of the fluidized bed technique make it one of the most useful techniques avaialable for metallurgical processes such as those involved in the different stages of a heat treatment procedure or temper. The use of fluidized beds is considered to be an innovative technology for the heat treatment of Al-Si-(Cu/Mg) cast alloys in that the fluidized bed heat treating process significantly reduces the time required for heat treating and increases the uniformity of the heat treating process.

2.3.1. Fluidization Phenomenon and Modern Fluidized Sand Bed

The fluidization process essentially consists of the transformation of solid particles into a fluid-like state through suspension in a moving gas or an air that is fed upward through a diffuser or distributor into the bed. The most desirable characteristic of a fluidized bed is that the rate of heat transfer between a fluidized bed and the objects immersed in it is high. The fluidized bed itself consists of a medium of dry and finely divided solid particles (aluminum oxide, olivine sand, etc.) that is made to behave like a fluid by a fluidizing gas (nitrogen based atmosphere and/or air). The air or gas is passed through the media from orifices beneath the bed, where the moving air/gas separates the particles enough to slide freely past each other as can be shown in Figure 2.20. [122, 123, 124]

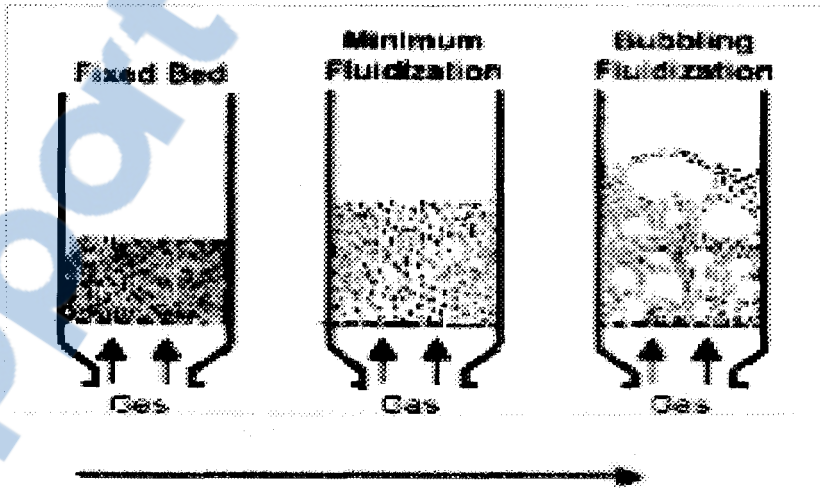

Figure 2.20. Schematic drawing of the fluidized bed principle. The horizontal arrow refers to direction of increasing gas flow rate. [124]

At a sufficiently high air-flow rate, the terminal velocity of the solids is exceeded, the bed goes into motion, and the upper surface of the bed disappears. The fluid like nature of the bed allows parts to be easily immersed and conveyed through the media. [123, 124] The properties of solid and fluid alone determine the quality of fluidization, although other factors such as bed geometry and gas-flow rate influence the rate of solid mixing in the bed. In gas-solid systems, fluidized bed motion can be observed by using a dense gas at high pressure with fine light particles; Figure 2.21 presents a schematic representation of the principle of fluidization. [124]

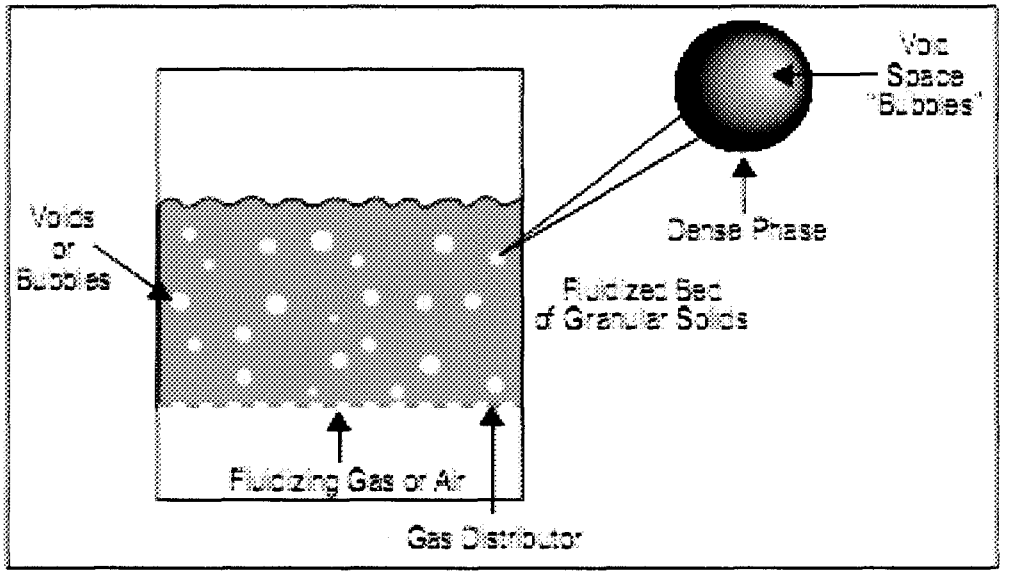

Figure 2.21. The fluidization principle. [123]

With increasing flow rate of air or gas, large instabilities with bubbling are observed and the movement of the solid particles becomes more vital; such a bed is called a bubbling fluidized bed. The fluid-like behavior of solid particles with their easy movement and direct contact with the gas is often the most important property recommending its use for

industrial operations. The fluid-like flow produces close to isothermal conditions throughout the reactor, thereby controlling the operations simply and reliably. Heat and mass transfer rates between gas and particles are high and, consequently, between the fluidized bed and immersed objects. [124, 125] High-efficiency heat transfer is an important characteristic of fluidized bed which affects its performance. Actually, there are several factors affecting the performance of a fluidized bed furnace including particle (sand) diameter, bed material, fluidization velocity of gas/air and heating rates. The diameter of the fluidized bed particles has the greatest effect; where the particles should be as small as possible to increase the contact area between particles and the samples. On the other hand, dense particle materials produce lower heat transfer coefficients. In the design of heat-treating furnaces, the effect of temperature must also be considered. Figure 2.22 shows that the flow of gas required for fluidization decreases rapidly with increases in temperature. [122]

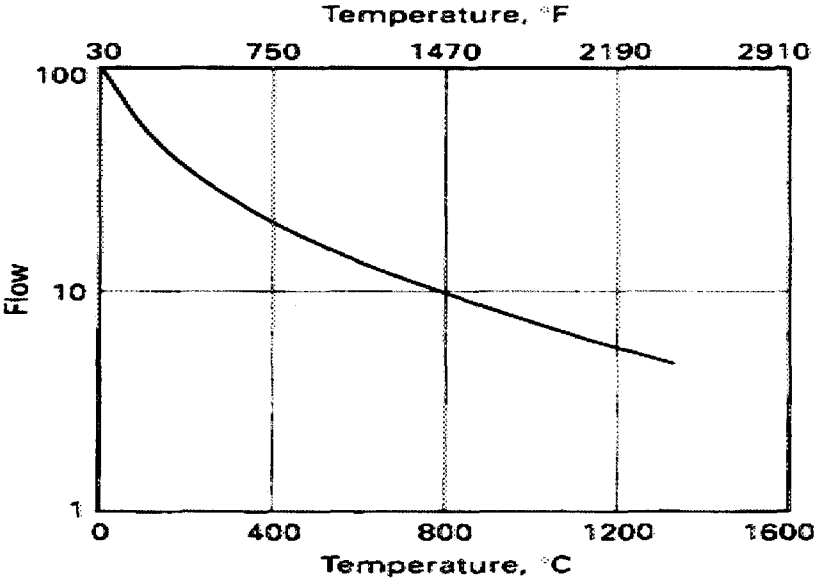

Figure 2.22. Effect of temperature on the flow corresponding to minimum fluidization for particles 0.1 mm in diameter having an apparent density of 2. [122]

The gas flow rate should be used to provide maximum heat transfer, where too high a flow rate leads to particle entrainment, high gas consumption and poor heat transfer. On the other hand, a flow rate that is too low leads to poor heat transfer and lack of temperature uniformity of the bed.

Generally, the sand bed material has a negligible role on heat transfer. [126] For the type of sand used in a fluidized bed, any type of sand can be used as bed material since the thermo-physical properties of the sand have no significant role on heat transfer except that, the use of silica sand is not recommended due to the toxicity of silica dust at high temperature. In addition to staurolite sand, $Fe_2Al_9Si_4O_{22}(OH)_2$, the bed materials that may be used in a fluidized bed furnace are olivine sand and aluminum oxide; these materials remain inert upon heating and will not break down or melt even at elevated temperatures since the materials are physically and chemically stable. The heat transfer coefficient as well as heating rate of FBs using staurolite sand bed, $Fe_2Al_9Si_4O_{22}(OH)_2$, are affected by the average particle size of the fluidized particles (80-120μm), and the gas flow rate. [122, 123, 126]

In using the conventional fluidized bed for heat treating operations, two major drawbacks are: (i) the inefficient heat transfer from the heat source to the fluidized bed due to the use of a single hot air system to provide both heating and fluidization, and (ii) the inefficient recovery of the temperature drop in the fluidized bed upon part loading. To overcome these drawbacks, Girrell [126] and Fainshmidt [127] have modified the system to a modern one. The modified modern fluidized bed is different in that the fluidizing air is made to flow over heating elements before entering the furnace. The problem of the

inefficient transfer of heat to the fluidizing medium was solved by using radiant heaters which were immersed in the medium just downstream of the fluidizing air entrance to allow this medium to be heated directly via conduction, radiation, and convection. The use of immersed heaters makes it possible for very fast temperature recovery to occur as a direct result of the efficient heat transfer to the specific medium. The faster heat transfer rates in such FBs will simplify direct heat treatment thereby making energy savings possible. Cast parts may also be submitted to heat treatment before they have fully cooled down from the casting process, [127, 128] which will ensure minimum heat loss from the bed and excellent temperature uniformity.

The modern fluidized bed has been developed to continuously heat-treat via in line solutionizing, quenching, and aging beds, which eliminates the traditional method of batch processing. The heat treating unit is coupled with a robotic unit which is used for loading the parts and continuously for in-line heat treating operations. The technique offers clean and safe operations for each of the heat treatment stages involved, as well as low maintenance costs. This type of fluidized bed was used for the heat treatment of the A356.2 and B319.2 type cast alloys investigated in this study; this technique offers clean and safe operations during solutionizing, quenching and aging processes as well as low maintenance cost. Alloys that respond particularly well to fluidized-bed solution treating, aging and fluid-bed quenching are aluminum alloys with various amounts of silicon, copper, and magnesium. The modern fluidized-bed furnace displays a uniformity of ±1.5°C and does not generally overheat by more than ±1°C. The density of the fluidized bed supporting the

aluminum casting minimizes the distortion which can occur at the high temperatures associated with a typical heat treatment process such as the T6 or T7 tempers. [128]

Figure 2.23 shows a schematic of FB reactor, [128] while figure 2.24 compares the temperature profile of a part heated using a conventional furnace with that of a part heated in a fluidized bed. The fluidized bed offers excellent heat transfer of 120-1200 $W/m^2°C$ which is higher than the 80-90 $W/m^2°C$ attained with the convection furnace. Besides a high heat-transfer rate, fluidized beds offer precise temperature control to the cast part. [129] The high heating rates obtained by fluidized beds are a result of the high heat transfer inherent in the system.

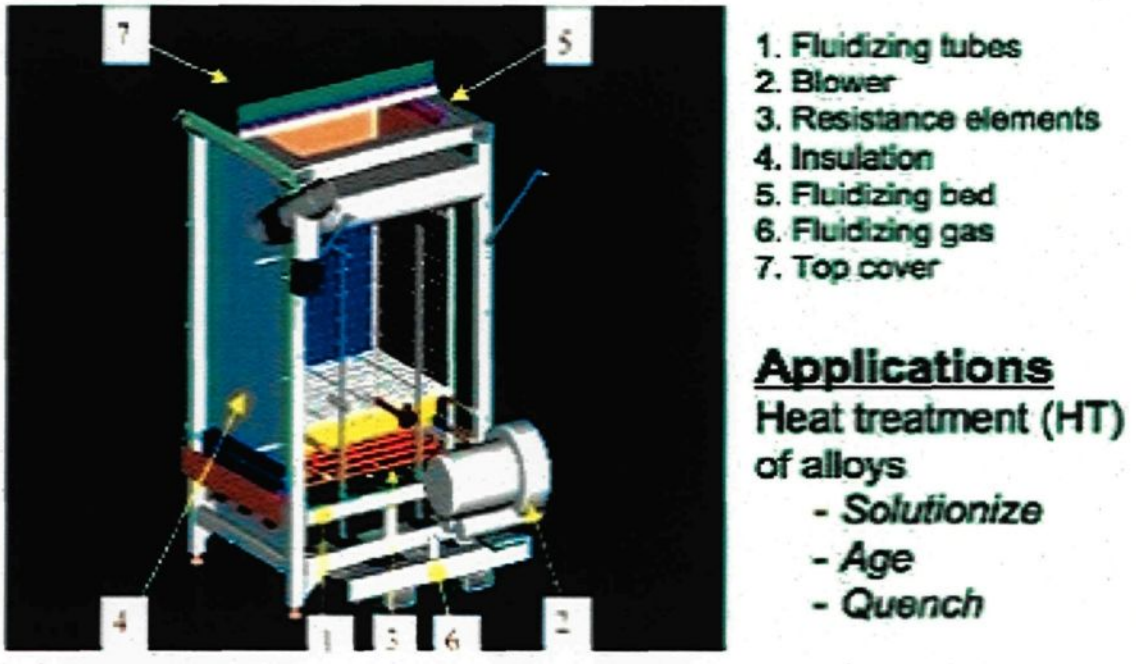

Figure 2.23. Schematic drawing for a fluidized bed technique. [128]

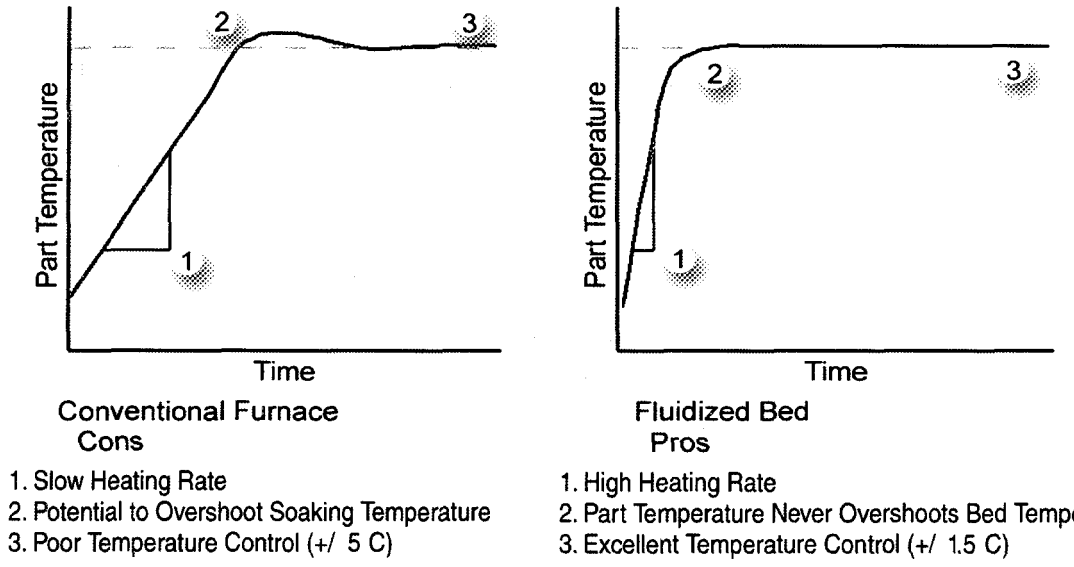

Figure 2.24. Comparison of temperature profiles for a part heated in a conventional furnace to one heated in a fluidized bed. [129]

The excellent temperature uniformity and temperature control offered by the fluidized bed reduces part distortion during heating. One of the most important fluidized bed parameters is the minimum fluidization velocity, $\mu_{mf,}$ which is a function of the particle diameter (d) and particle mass (p) as shown in Equation 1. [122, 124]

$$\mu_{mf} = d^2 p \qquad \textit{Equation 1}$$

The effect of the temperature on the flow of the gas required for fluidization is also an important consideration, where the gas flow decreases rapidly with increase in temperature. The global heat transfer coefficient of a fluidized sand bed is related to the temperature of the heat-treated part in the bed through the following heat transfer and energy balance equations:

$$Q(t) = h\,A\,(T_{FB} - T_p(t)) = mc_p\,dTp/dt \qquad \textit{Equation 2}$$

$$T_p\,(t) = T_{FB} + (T_p(0) - T_{FB})\exp(-\,hAt/mc_p) \qquad \textit{Equation 3}$$

where Q(t) is the heat flow rate, h is the heat transfer coefficient, A is the surface area of the part, Tp(t) is the part temperature as a function of time, T_{FB} is the bulk fluidized bed temperature, m is the mass of the part, c_p is the specific heat of the part, and $T_p(0)$ is the initial temperature of the part. [119, 122, 126, 130]

2.3.2. Development of Fluidized Sand Bed for Heat Treatment of Aluminum Alloys

Using fluidized beds is a relatively old technology which has, so far, had limited use in manufacturing. Fluidized bed technology was once used in the steel industry primarily for the hardening of tool steels over fifty years ago, although the process goes back even further for more than 100 years, when, in 1879, a first patent demonstrated the excellent temperature uniformity of the fluidized bed for roasting minerals. [121, 122, 123] Previously, the solutionizing, quenching and ageing steps in a heat treatment process would take long times to achieve the required properties in total over 20 hours. With the advent of fluidized bed reactors (FB), heat treatment processing time has been reduced. For example, instead of long solutionizing time in a conventional furnace (CF), the time required in an FB is less than an hour. The rate of heat transfer in the fluidized bed is higher than in standard furnaces, which permits the heating time to be shortened. [128, 129] Chaudhury *et al.* [131] observed that a sample heated in the fluidized bed reached the solution temperature six times faster than one that was heated in a conventional furnace. The high heating rate in a FB enhances both solutionizing, and precipitation kinetics; fluidized bed technique can be used for direct quenching to the aging temperature using the same furnace/medium as that used for quenching (termed quenching-aging medium). Quenching in a fluidized bed

ensures minimal warping and internal stresses as compared to quenching in water, where high internal stresses which occur during quenching are undesirable. [64, 130] The advantages of this fluidized-bed quench include a cooling rate sufficient to achieve the required strength and ductility, but slow enough to minimize any risk of distortion or cracking; a buoyancy factor to further minimize distortion; and the elimination of a wet quench. Compared with water quenching, it was reported that FB quenching reduces residual stresses by 70% in alloy A356 casting, where the residual stresses is quantified as von Misses stresses. [132]

The main goal of aging using a fluidized bed is to activate the precipitation process, in which the precipitates may be formed in less time in stable and high density conditions through the rapid heating rates obtained with the system. As well as effectuating solution treatment, fluidized beds have the capacity to reach aging temperatures which are four to six times faster than conventional furnaces. It should also be noted that a 10°C increase in aging temperature makes it possible to decrease the aging time by a factor of two. [55, 9, 121, 131] The use of fluidized beds is considered to be an innovative technology for the heat treatment of Al-Si cast alloys and appears to be more effective than conventional furnace techniques.

2.3.2.1. FB vs CF Heat Treatment Techniques for Al-Si Cast Alloys

With regard to solution heat treating, it has long been held in the industry that several hours are required for adequate treatment using a convection furnace. Gauthier *et al.* [133] and Samuel *et al.* [89] reported that the best solution heat-treatment time for high Mg-

containing 319.2 cast alloys at 500°C is 8–10 hours using a convection furnace. Also, due to the presence of the low melting point (515°–540°C) Al_2Cu phase, it is recommended that fluctuations in solution temperature should be controlled to within a very narrow range. A fluidized bed, on the other hand, provides excellent temperature uniformity with satisfactory temperature control thereby reducing the allowance made for part distortion during heating. Also, with the use of fluidized bed furnaces, the solution treatment time required to obtain optimum mechanical properties is reduced to less than 1 hour instead of the customary 8–10 hours necessary in a convection furnace.

Keist [129], Apelian and Chaudhury [134] and Van Wert et al. [13] have reported that the fluidized bed heat treatment technique reduces the time required for heat treating. Acoording to Bergman [12] for alloy A356, a solution heat treatment temperature of 554°C, which is just 1.7°C below the solidus temperature, may be applied using a fluidized bed because of its tight temperature control which would not have been possible with a conventional convection furnace. Kiest and Bergman [135] observed that using the fluidized bed technology for the heat treatment of 356 casting alloys results in a significant increase in strength values after only 15 min of solution heat treatment at 540°C and 550°C. Chaudhury and Apelian [136, 137] reported that the optimum solution heat-treatment times required for modified and non-modified Al–Si–Mg alloys are 30 min and 60 min, respectively, when using the fluidized bed technique, to achieve complete dissolution of Mg_2Si in the matrix as well as that of the greater part of the intermetallics present in the microstructure. [136] In the case of 354 alloys, the optimum solution heat-treatment time using the fluidized bed technique is 45 min at 527°C, for the complete dissolution of Mg_2Si

and Q-$Al_5Cu_2Mg_8Si_6$ phases. [137] There have been some reported cases of incomplete dissolution for other formed phases such as Al_2Cu and Fe-rich intermetallics after solution heat treatment using FB and CF techniques. A number of studies, such as those carried out by Apelian *et al.* [55] and Shivkumar *et al.*, [110] have reported on the kinetics of the rapid dissolution of Mg and Si in 356-type cast alloys. At temperatures of 530–540°C, dissolution of these two elements is complete after solution heat treatment for 30 min and 60 min, using FB and CF techniques, respectively.

Several studies have shown that short solution treatment times at the specified solution treatment temperature using a conventional furnace may provide adequate mechanical properties. [131, 135, 138] For example, alloy 356 attained 90% of its peak tensile strength after undergoing a solutionizing treatment for only 10 min at 540°C, but achieved peak tensile properties after 50 min of solution treatment at 550°C. The reason for longer solution times required in a CF may be attributed to the thermal modification of the acicular Si phase which can occur over a period of up to 12 hours. [138, 139, 140, 141] Shorter solution heat-treatment times of 3–4 hours can be used with Sr-modified 356 cast alloys with a CF, while the thermal modification of the Si phase during solution heat treatment is more rapid in a fluidized bed furnace, i.e. 30–60 min. [52, 136, 142] The Si flakes start to fragment into finer Si particles within 15 minutes of solution heat treating using an FB; also the coarsening of the eutectic Si particles takes place through the Ostwald ripening effect after 120 minutes of solutionizing. In addition to the high heating rate of an FB, modification has a strong influence on the spheroidization and coarsening kinetics of Si particles as reported by Druge and Pantya. [143] The high heating rate during fluidized bed solution heat treatment

causes faster fragmentation and spheroidization of the eutectic Si particles compared to that obtained with conventional air convection furnaces.

The heating rate also plays an important role in increasing the kinetics of the aging process by having an effect on the aging characteristics of Al-Si-(Cu/Mg) alloys. The main goal of aging with a fluidized bed is to accelerate the precipitation process so that a high density of precipitates may be formed in less time through the rapid heating rates obtained with the application of this particular technique. As well as effectuating solution treatment, fluidized beds have the capacity to reach aging temperatures which are four to six times faster than conventional furnaces. [144, 145, 146] It was reported by Chaudhury *et al.* [145, 146] that the precipitation rate for hardening phases in both 357 and 354 cast alloys is greater in fluidized bed furnaces due to the formation of a greater weight fraction and number density of Mg_2Si, $CuAl_2$, and $Al_5Cu_2Mg_8Si_6$ precipitates than that obtained with a conventional furnace. The aging of solutionized samples of Al-Si-Mg cast alloys using an FB results in small spherical Mg_2Si precipitates in the 30-100 nm size range; on the other hand, CF solutionized samples exhibit coarse Mg_2Si needle-like precipitates with sizes in the range of the 1000nm-2000 nm upon subsequent aging. [146]

With regard to fluidized bed heat treatments, it was reported that the high heating rate of the FB increases the kinetics of the precipitation rate of such phases as $Al_5Cu_2Mg_8Si_6$ and Al_2Cu during aging of Al-Si-Cu-Mg cast alloys. [147] From thermal analysis of samples heated up to the aging temperature, no phase transformation or dissolution of precipitates was observed when using the fluidized bed. It was reported that the high heating rate in an FB leads to the formation of more stable clusters, or GP zones,

compared to a CF during the heating up stage to reach the aging temperature. [147] The correlation between the heating rate and the radius of the formed clusters is given by Equation 4. [147] These clusters can act as suitable sites for the heterogeneous nucleation of further precipitates.

$$\frac{dT}{dt} = \frac{2\gamma\Omega}{k^2 D X_p \ln S} \times \frac{r^2 r_m}{r - r_m} \qquad \textit{Equation 4}$$

2.3.2.2. Fluidized Sand Bed Quenching Medium

Quenching is considered to be the critical step in the heat treatment process to obtain a supersaturated solid solution as well as to achieve optimum mechanical properties and alloy quality. The cooling rate during quenching determines the amount of strengthening elements that remain in the solutionized matrix. Furthermore, the cooling rate also has an important effect on the resulting vacancy concentration and phase formation in the metal matrix. The resulting vacancies formed after quenching have an important role in the diffusion process necessary for forming hardening phases in the subsequent age hardening stage. Several studies, such as those carried out by Abubakre *et al.* [148] and Bycznski *et al.* [91], have reported that a lower vacancy concentration leads to slower aging kinetics and to higher temperatures of phase transformation into GP zones during the aging process. In addition, the vacancy concentration influences the precipitates size and distribution in the matrix; clusters containing solute and vacancies act as effective nucleation sites for GP zones, where these clusters also affect the distribution of GP zones. Pedersen *et al.* [149] reported that a decrease in the quenching rate lowers the strength and

increases the ductility of Al-Si-Mg alloys; low quenching rate leads to the precipitation of Si within the aluminum metal matrix. The slow cooling rate associated with forced air quenching reduces the peak strength due to the low rate of heat transfer as compared to that obtained with water quenching. Water quenching medium displays an excellent heat-transfer coefficient especially for applications requiring high strength values, although this step involves a number of complex stages as well as high residual stresses when compared to an FB quenching medium. It has been reported that the quenching capacity of water is higher than necessary to obtain optimum properties, where the high internal stresses generated from the rapid quenching are undesirable. [60, 61, 63, 64] One of the main concerns with water quenching is the transition from the vapor blanket stage to the boiling one, where temperature gradients are created along the surface resulting in part distortion. The large thermal gradients are related to the vapor blanket that envelopes the part when it is immersed in the water and acts as an insulator leading to a relatively slow cooling rate for that particular part. [63, 64]

As reported by Keist and Bergman, [150] a fluidized bed as a quenching medium lacks any vapor barrier which is in nature predicted by water quenching. When the part is immersed in the fluidized bed, the medium will come into direct contact with that part. The same cooling conditions from one section of the sample to another will reduce temperature gradients within the part resulting in a reduction in both residual stresses and in the susceptibility to part distortion, as shown in Figure 2.25. [129] Thus, the fluidized bed is an attractive alternative to forced air and water as quenching media; the internal stresses and

resulting distortion of samples associated with water quenching can be minimized/avoided by quenching in a fluidized bed.

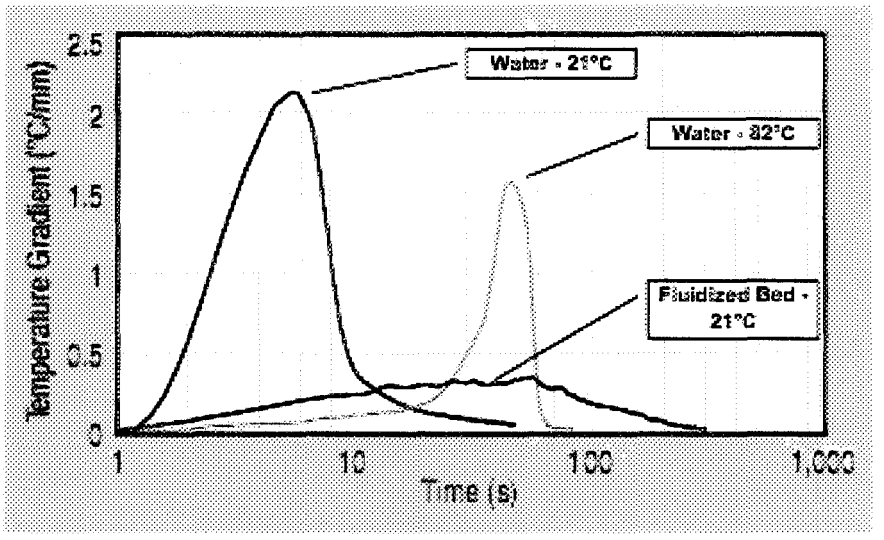

Figure 2.25. Temperature gradients versus quenching time obtained from cooling curves for A356.2. [129]

In another study [151] that investigated the quench sensitivity of Al-Si-(Cu/Mg) cast alloys using fluidized bed quenching, it was reported that the change in the cooling rate during water quenching was more drastic as compared to FB quenching, where the cooling rate varied from 0 to -80 KS^{-1} in less than 8 seconds, whereas with FB quenching, the cooling rate varied from 0 to -14 KS^{-1} in 18 seconds. [151] In addition, the FB quenching resulted in the formation of metastable phases in Al-Si-Cu-Mg alloys which was not observed with water quenching. The different cooling rates would affect the mechanical and quality performance of Al-Si cast alloys.

2.4. QUALITY INDICES

The quality of Al-Si alloy castings plays a vital role in determining specific metallurgical conditions for an alloy required to fulfill particular engineering application specifications. There are several parameters affecting the quality of Al-Si castings such as alloy composition, melt treatment, and the applied heat treatment conditions. It is possible to determine the quality of an alloy using specific mathematical equations, where both UTS and elongation values can be combined to express the quality of alloys using a single quality index value, Q. [152, 153, 154] Quality charts generated using these equations are useful in deciding upon the optimum heat treatment conditions required to obtain specific properties or qualities in a particular casting. Such quality charts have often been used in conjunction with heat treatment studies of aluminum alloys for the same reasons.

In the present study, an attempt was made to elucidate the effects of quenching-aging media using FB versus CF heat treatment techniques on the quality results obtained by means of quality index charts. The effects of cooling rate as well as heating rate - in these heat treatment techniques - on the quality of the alloys studied will be investigated employing a T6 heat treatment regime, using several heat treatment conditions. The results will be evaluated using quality charts derived from two models of quality indices, namely, those of Drouzy *et al.* [155] and Cáceres. [160]

Drouzy *et al.* [155] first introduced the concept of quality index, Q, to better express the tensile properties of the Al-Si-Mg alloys they examined, by means of which the "quality" of an alloy could be determined using specific mathematical equations to generate

iso-Q and *iso-YS* lines and subsequently to construct a quality index chart. The *iso-Q* lines and *iso-YS* lines were generated using the following equations:

$$Q = P_{UTS} + d \log (S_f) \qquad \textit{Equation 5}$$

$$P_{YS} = a\, P_{UTS} - b \log (S_f) + C \qquad \textit{Equation 6}$$

where Q is the quality index in MPa; P_{UTS} is the ultimate tensile strength in MPa; S_f is the elongation to fracture in pct; and d is a material constant (d = 150 in the case of the Al-Si-Mg 356 type alloys used by the researchers). The coefficients *a*, *b*, and *c* are alloy-dependent parameters; for Al-Si-Mg, the coefficients *a*, *b*, and *c* were determined as 1, 60, and -13, respectively.

The quality chart generated using Equations 5 and 6 is shown in Figure 2.26. Such charts are very useful in determining the best possible compromise between tensile properties and quality of alloys investigated. The properties that may be obtained from the quality charts constructed using the Drouzy quality index model are UTS, YS, and elongation to fracture, and the quality index value, Q. In the quality chart shown in Figure 2.26, the dashed lines represent the iso-Q and iso-YS lines as determined using Equations 5 and 6 in which the iso-YS lines are identified by the yield stress value, while the iso-Q lines are identified by the Q-value. [155, 156]

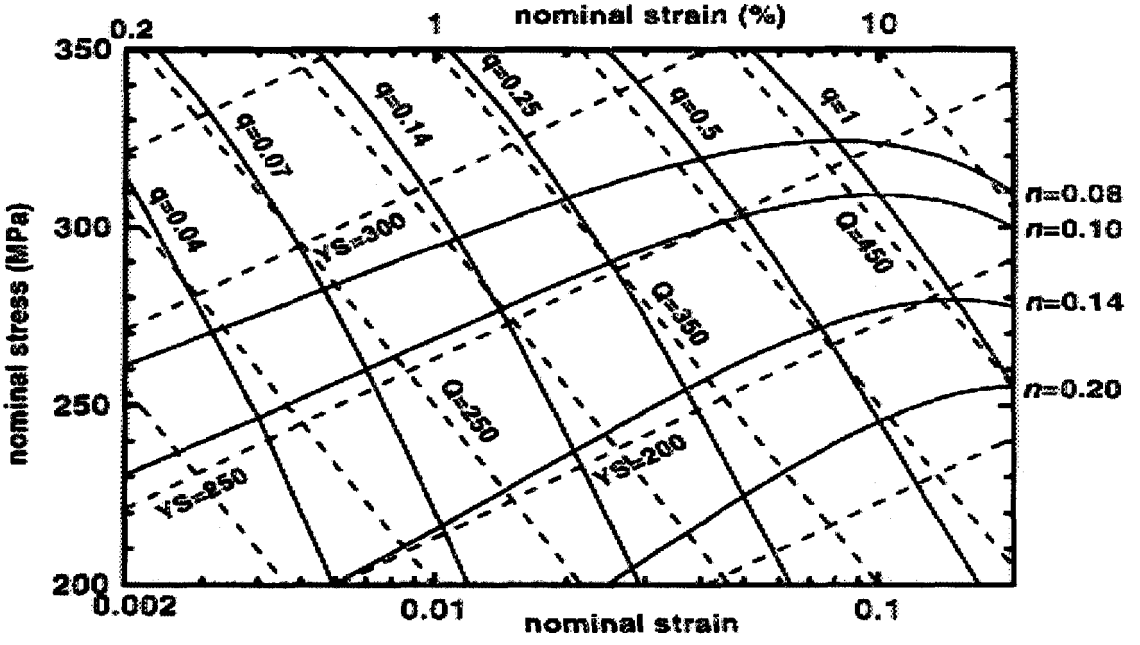

Figure 2.26. A quality index chart for alloy 356; the dashed lines are generated using Equations 5 and 6. [155, 156]

Although the concept of quality index was developed specifically for alloys 356 and 357, it has occasionally been applied to other alloy systems as well.[157, 158] A number of studies on Al-Cu-Mg-Ag alloys, however, showed that in contrast with the linear behavior of alloy 356, a plot of UTS *vs* S_f describes a curvilinear contour if the material has undergone aging, as was observed to be the case for alloy 201. [159, 160] Furthermore, the parameters involved in Equations 5 and 6 displayed different numerical values and varied with the prevailing aging conditions. The curvilinear contour in the plots which is present in the aluminum alloys containing copper implies that extending the quality index concept to systems other than the Al-Si-Mg casting alloys requires determining the behavior of the strength-ductility relationship as the material undergoes the aging process. These behaviors

suggest that the curvilinear pattern may be a characteristic of Cu-containing aluminum alloys. [161]

The quality index, *Q*, proposed by Cáceres [156, 162, 163] is the most widely used to predict the quality of Al-Si cast alloys. In this more recent model, Cáceres has developed a theoretical approach which explains the physical significance of the quality index. The analytical model for the quality index proposed by him assumes that the deformation curves of the material can be described using the Holloman equation as follows:

$$\delta = K\varepsilon^n \qquad \textit{Equation 7}$$

where δ is the true flow stress, ε is the true strain, K is the strength coefficient of the material, and n is the strain-hardening exponent. The values of *n* and *K* may be calculated from a *log-log* plot of true stress versus true strain, as shown in Figure 2.27. This strain-hardening exponent value varies from n = 0 for perfect plastic material to n = 1 for elastic material; most materials are known to have n values lying between 0.1 and 0.5. [164] The strain-hardening exponent n correlates to the rate of strain hardening rate, $d\sigma/d\varepsilon$, through the following equation: [164, 165]

$$n = \varepsilon/\sigma \times d\sigma/d\varepsilon \qquad \textit{Equation 8}$$

The tensile test samples may produce a certain amount of necking till fracture according to their ductility; necking usually starts at the point of tensile instability when the strain hardening rate and the true stress are equal. It may be considered that the necking will begin when the strain hardening exponent (n) equals the true uniform plastic strain (ε).

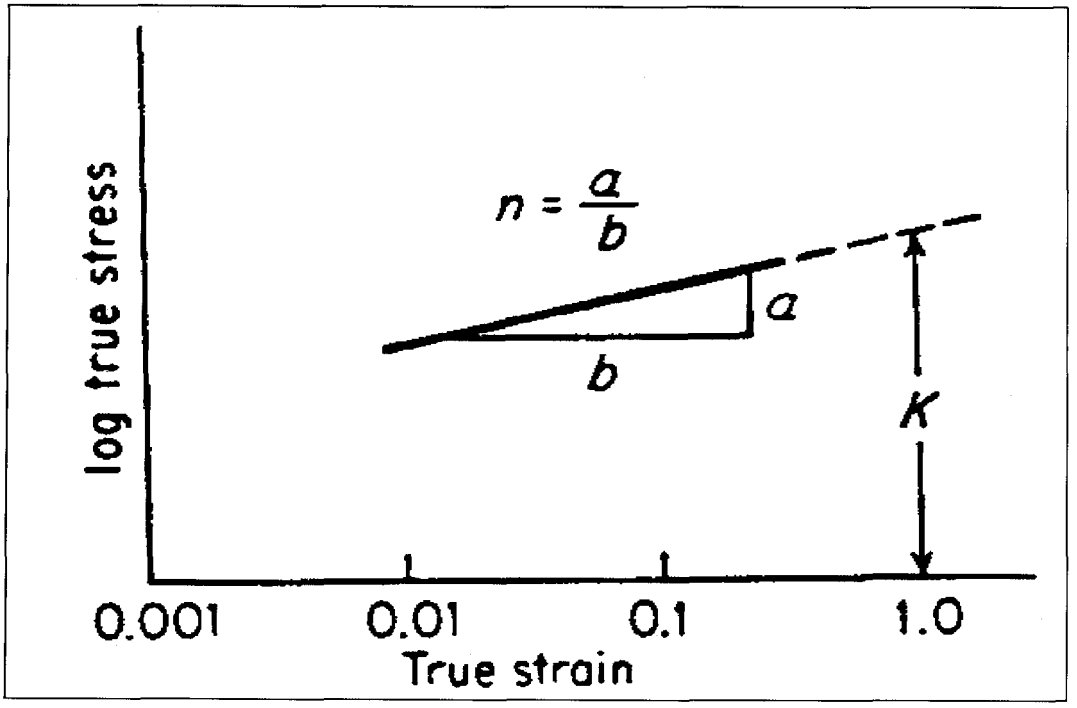

Figure 2.27. A log-log plot of true stress versus true strain for calculating n and K values in Equation 7. [164]

Cáceres defined the ratio of nominal strain at fracture to the nominal strain at necking as the relative quality index, q, which may be presented by *iso-q* lines. The proposed relative quality index has the following form:

$$q = S_f / S_u = S_f / n \qquad \textit{Equation 9}$$

The true stress-strain curve may be obtained from Equation 7 by relating the true values of the stress and strain, σ and ε, and the corresponding engineering values, P and s, by $\varepsilon = ln(1+s)$ and $P = \sigma/(1+s)$, respectively. [157, 160, 166] If the elastic component of the strain is disregarded and assuming that true and nominal strain are equivalent, which is a reasonable assumption for casting alloys due to their limited ductility, then the nominal stress-strain

curve can be approximated by Equation 10. The *iso-q* lines in quality maps are generated using Equation 10 as follows:

$$P = K\, S^{(s/q)}\, e^{-S} \qquad \textit{Equation 10}$$

where P is the nominal stress and S is the nominal plastic strain. The iso-flow lines, n, in the quality charts are determined by the following equation:

$$P = K\, S^{n}\, e^{-S} \qquad \textit{Equation 11}$$

where the relative quality index q may be expressed in terms of engineering stress and strain by Equation 11 which results from Equations 9 and 10. In Figure 2.26, the solid lines are flow curves identified by the n-value and iso-q lines are those identified by the q-value, having been calculated using Equations 10 and 11, respectively, assuming K = 430 MPa and the n values are varying between 0.08 and 0.2 for the different aging conditions. Cáceres assumed that the iso-q lines generated using Equation 10 are roughly equivalent to the iso-Q lines generated by Drouzy *et al.*; by correlating the relative quality index q with the quality index Q, the slope of the iso-q lines is considered to be equivalent to the parameter d in Equation 5. This slope of the iso-q lines may be determined by differentiating Equation 10 with respect to the strain S when the q-value tends to 1, resulting in the following correlation: [161, 162, 163, 167]

$$d = -\,dP / dS \sim 0.4\, K \qquad \textit{Equation 12}$$

The Q-value is obtained by correlating Equations 9, 11 and 12 with Equation 5, and may be calculated using Equation 13 as follows:

$$Q = K\,[1.12 + 0.22 \ln (q)] \qquad \textit{Equation 13}$$

The quality index charts, proposed by Casers, may be considered as an important tool that provides several significant properties obtained from tensile test data. For each point located in the chart, the tensile strength, plastic elongation to fracture, yield strength, relative quality index (q) and quality index value (Q) may be obtained from the one chart or plot.

CHAPTER 3

METHODOLOGY AND EXPERIMENTAL PROCEDURES

CHAPTER 3

METHODOLOGY AND EXPERIMENTAL PROCEDURES

3.1. INTRODUCTION

The experimental procedure designed for this specific work aimed at investigating the influence of various metallurgical parameters on the tensile properties and quality indices of B319.2 type Al-8%Si-3%Cu-0.25%Mg and A356.2 type Al-8%Si-0.35%Mg casting alloys used in the automotive industry. The metallurgical parameters investigated include heating rate; cooling rate; solution heat treatment time; aging time; and aging temperature. The performance of these alloys has been studied after applying conventional continuous T6-aging treatments and non-conventional ones including different heat treatment media as well as multi-temperature aging cycles. In the present study, the fluidized sand bed technique was employed to investigate its effect, as a heating and/or quenching medium, on the heat treatment characteristics of the alloys studied. A relevant comparison of the fluidized sand bed as the heat treatment medium was made with that of conventional furnace heat treatment by using an air forced convection furnace for heating and quenching; water was also used for quenching, in order to obtain different cooling rates.

The relevant details concerning the alloys studied, heat treatment cycles applied and the heat treatment technique used in this work are provided in the following subsections

together with a description of the general melting and casting procedures applied. The various techniques employed for microstructural characterization, namely, optical microscopy, scanning electron microscopy, and field emission gun scanning electron microscopy, and details of the tensile testing procedures applied for evaluating the mechanical properties of the alloys investigated are also provided.

3.2. CASTING PROCEDURES

The 356 and 319 alloys received in the form of ingots were melted in a silicon carbide crucible of 150-kg capacity, using an electrical resistance furnace; the melting temperature was held at 740° ± 5°C. The molten metal was degassed for 30 minutes using pure dry argon injected into the molten metal (at a flow rate of 30 $ft^3\ h^{-1}$) by means of a rotary graphite degassing impeller, rotating at a speed of 150 rpm for 30 minutes, in order to minimize the hydrogen level of the melt, and to eliminate inclusions and oxides via flotation. After degassing, the melt surface was carefully skimmed to remove the oxide layers and prevent it from entering the casting mold during pouring.

Melt treatments *viz.*, modification and grain refining were applied to half of the molten metal used, to study the performance of modified and grain refined cast alloys, coded K3 and K4, and compare them with their non-modified counterparts, namely K1 and K2 alloys, following heat treatment using the FB *vs* the CF technique. For modification purposes, 200 ppm Sr was added to the melt, in the form of rods of Al-10%Sr master alloy; the melts of the modified alloys were then grain refined using Al-5%Ti-1%B master alloy, added to the degassed melt prior to casting.

Samplings for chemical analysis were taken from each alloy melt. The chemical analysis was carried out using arc spark spectrometry at GM facilities in New Hampshire. Figure 3.1 shows the Spectrolab Jr CCD Spark Analyzer that was employed for this purpose. With respect to the alloy codes, K1 and K3 represent the non-modified and Sr-modified A356.2 alloys, respectively, while K2 and K4 correspond to the non-modified and modified B319.2 alloys.

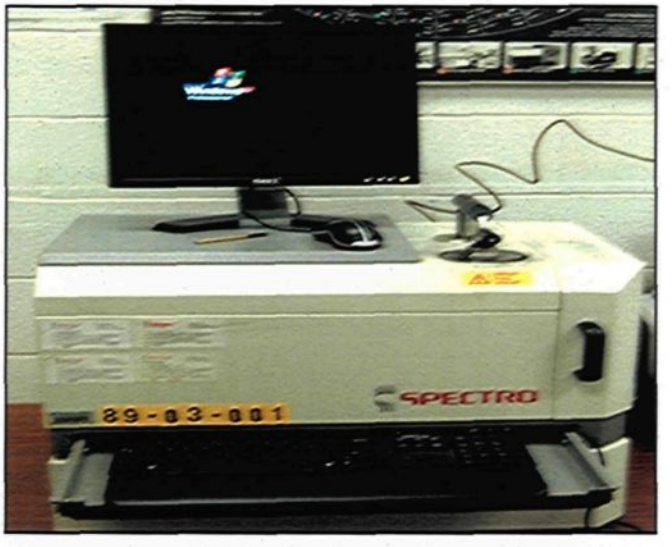

Figure 3.1. Spectrolab Jr CCD Spark Analyzer used in the current study.

The actual chemical compositions of the alloys used in this study are shown in Table 3.1, and represent the average composition of three readings taken per sample. The degassed melt in each case was carefully poured into an ASTM B-108 type permanent mold preheated to 500°C, to prepare tensile test castings; each casting provided two test bars. The melt pouring temperature was 740± 5°C, with humidity in the range of 11-15%, and a melt hydrogen level of 0.1 ml/100g. Five tensile test bars were used for each alloy/heat treatment condition studied. Figures 3.2 (a), (b) and (c) show the actual standard mold used

for casting and the corresponding casting, with the dimensions of the tensile test specimens, respectively.

Table 3.1. Actual chemical composition of the 356 and 319 alloys investigated.

Alloys Type		Chemical Analysis, wt%								
		Si	Cu	Mg	Mn	Fe	Sr	Ti	B	Al
Alloys Code	K1 356/(Al-Si-Mg)	7.52	0.0186	0.364	0.004	0.075	-	0.121	0.0002	Bal
	K2 319/(Al-Si-Cu-Mg)	7.97	3.323	0.266	0.245	0.418	-	0.131	0.0002	Bal
	K3 356/(Al-Si-Mg)+ Sr	7.55	0.042	0.329	0.004	0.088	0.013	0.205	0.006	Bal
	K4 319/(Al-Si-Cu-Mg)+Sr	8.41	3.193	0.218	0.256	0.347	0.007	0.216	0.019	Bal

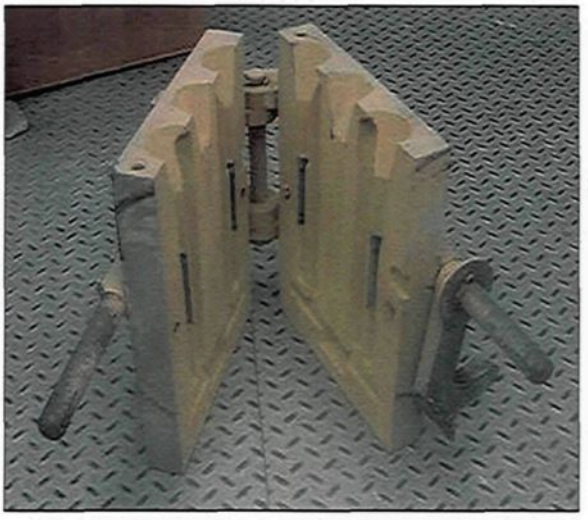

(a)

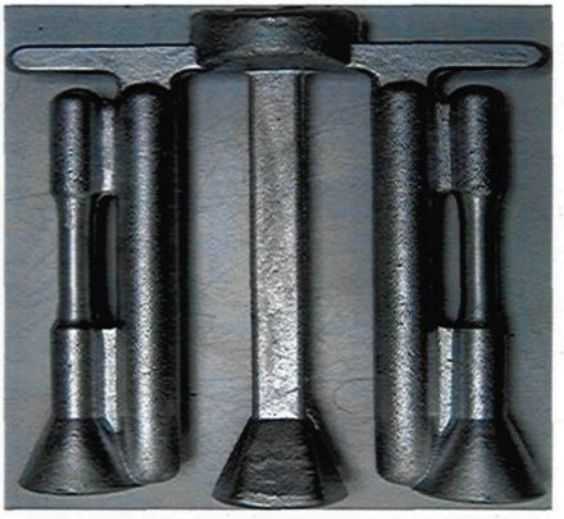

(b)

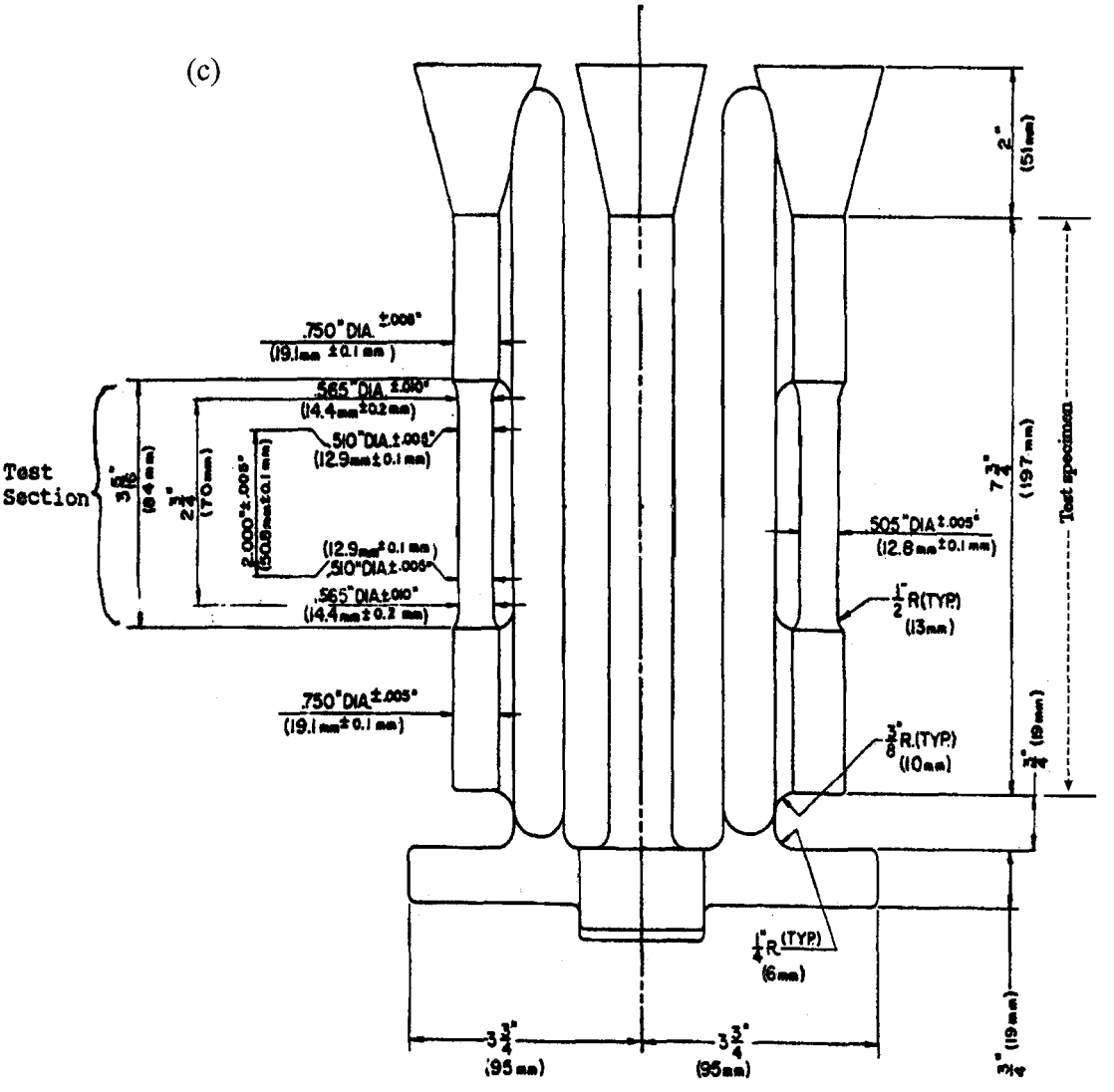

Figure 3.2. (a) ASTM B-108 permanent mold used for casting; (b) actual casting; and (c) schematic drawing showing the dimensions of the tensile test specimens.[103]

3.3. HEAT TREATMENT PROCEDURES

The samples obtained from the cast alloys K1-K4 were first solution heat-treated and then quenched in different media, whether water or sand; the artificial aging treatment was subsequently carried out by applying either T6 continuous or T7/T6 multi-temperature cycles in the same furnace. A conventional forced air furnace (CF) as well as a fluidized

bed furnace (FB), both shown in Figure 3.3, were used for heat treatment purposes to establish a relevant comparison between the two heat treatment techniques. The convection furnace used for conventional heat treatment is a Lindberg/Blue M electric resistance air-forced furnace where the temperature may be controlled to within ±1 °C.

The heat treatment process using a Fluidized Bed Technique (FBT) was carried out at General Motors (GM) facilities. The fluidized bed used in this study consists of finely divided particles, usually sand, which are made to behave like a fluid. The sand bed material is olivine sand which is free from silica. The fluidization gas is air drawn in from the atmosphere and blown in through pipes beneath the electric heater tubes to be found at the bottom of the fluidized bed. The main heat transfer mechanism, to transfer heat energy into the sand bed, is the presence of indirect electric elements which heat the bed. This method of energy transfer by radiation to the sand using the electric elements is efficient, in addition to that utilizing the fluidization air to transfer the heat by convection. Heat-treated samples submerged into an isothermal sand bed have complete free surface contact with the sand, where the transfer of heat energy to the samples takes place by conduction, convection and radiation modes through all contact surfaces. This fluidized bed technique, as indicated in the literature, facilitates rapid energy transfer into the part, resulting in faster times of less than 10-15 minutes to process solution treatment temperatures of 495-530°C, compared to 30 minutes to process aging temperatures of 155-180°C using a convection furnace as illustrated in Figure3.4.

(a)

(b)

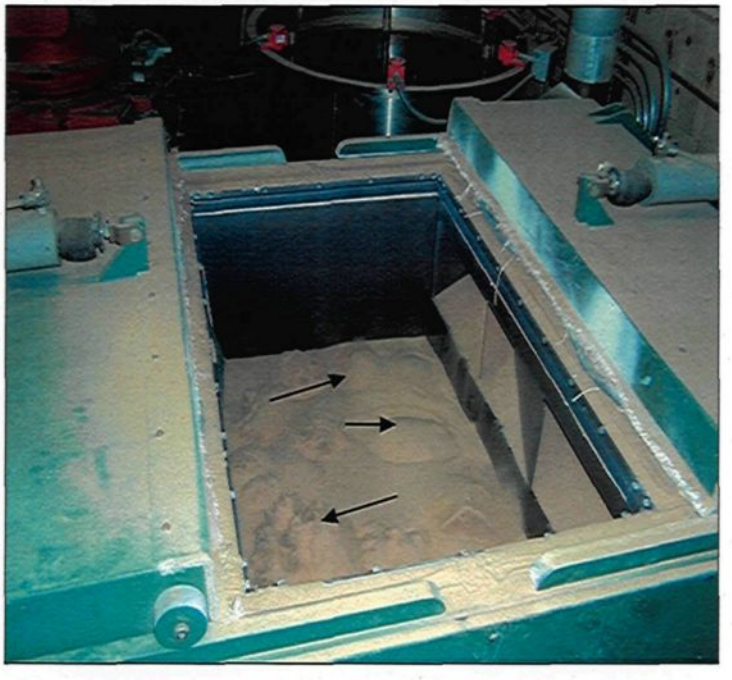

Figure 3.3. (a) Air forced convection furnace (CF); (b) fluidized sand bed furnace (FB). Arrows point to bubbles in the fluidized sand bed.

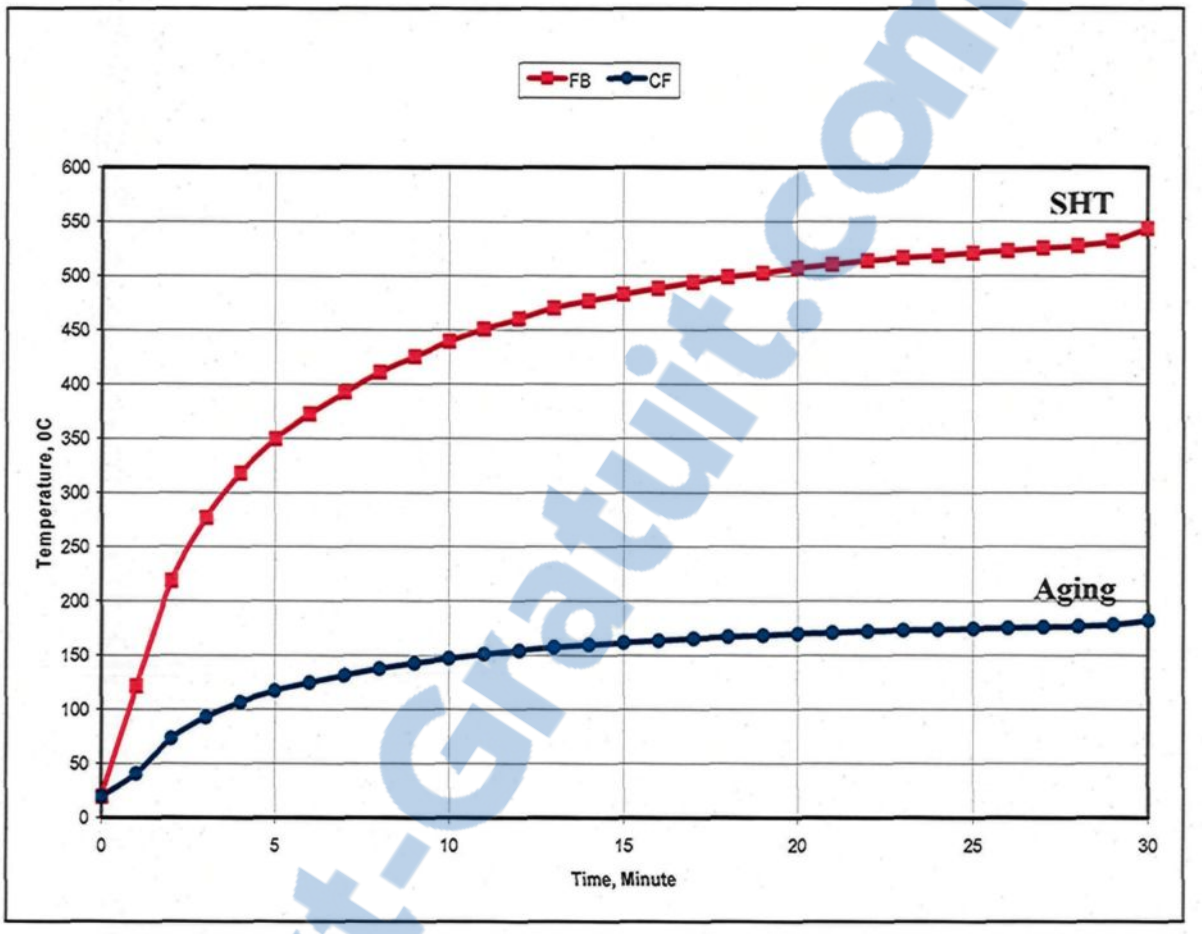

Figure 3.4. Temperature-time record of heat treated samples during heating using a CF and an FB.

In the present study, three heat treatment cycles were applied to cover most of the metallurgical parameters affecting the selected B319.2 and A356.2 type cast alloys. These heat treatment cycles aimed at investigating the following variables: (i) solution heat treatment time, (ii) quenching medium and (iii) multi-aging temperatures, as well as the heat treatment technique type (CF *vs* FB), in relation to the tensile properties and the quality indices of the alloys studied. Corresponding to the three sets of variables, the heat treatment cycles were coded I, II, and III, respectively, and are described below in detail. It is worth mentioning here that it was considered important to include the fourth variable,

namely the heat treatment technique *type*, in this study, based on the fact that a comparison between the results obtained with the more recently introduced fluidized bed technique (for the heat treatment of aluminum casting alloys) with those of the conventional convection furnace technique (used since decades for these same alloys) would provide a concrete basis for, and put into proper perspective, the claims of the fluidized bed technique reported in the literature.

(A) Heat Treatment Cycle I - Influence of Solution Treatment Time

This heat treatment cycle was applied to investigate the influence of solution heat treatment time on the tensile properties and quality indices of T6-tempered B319.2 and a356.2 type aluminum-silicon cast alloys using both CF and FB heat treatment techniques. The tensile test bars obtained from the cast alloys K1–K4 (see Table 3.1) were heat-treated to a T6 temper as follows: Solution heat treatment was carried out in both CF and FB furnaces for various times, namely 0.5, 1, 5, 8, 12, and 24 h, then quenched in warm water at 60°C, followed by aging in both CF and FB furnaces for several durations of time, namely 0.5, 1, 5, 8 and 12 h. The 356 (K1 and K3) alloys were solutionized at 530°C then quenched in warm water at 60°C; after that they were pre-aged at room temperature for 24 h, followed by artificial aging at 155°C for the five aging times mentioned above. The 319 (K2 and K4) alloys were solutionized at 495°C, quenched in warm water at 60°C, and then aged directly at 180°C for the same five aging times.

(B) Heat Treatment Cycle II - Influence of Quenching Media

In this heat treatment cycles, the influences of quenching media, namely water, CF (hot air) and FB (hot fluidized sand), on the mechanical properties and quality indices of the K1-K4 alloys were investigated. Heat treatment was applied using several heat treatment conditions in both CF and FB furnaces. Specifically, two fluidized bed furnaces were used, for solution heat treatment, and for direct quenching-aging, respectively. These heat treatment conditions were divided into three groups, namely B, C and D; group B refers to the water quenched-T6 tempered alloys; group C refers to the alloys subjected to direct quenching-aging either in hot sand using an FB or in hot air using a CF; and group D corresponds to the alloys that were subjected to water quenching, followed by multi-temperature aging, using both CF and FB. Accordingly, the results corresponding to this part are expected to reveal how the tensile properties as well as the quality of the alloys investigated, K1-K4, respond to (i) the effects of the different quenching media, whether water, air or sand, (ii) the effects of direct quenching to the artificial aging temperature after solution treatment, and (iii) the effects of multi-stage aging temperatures, using an incubation time of 24 h between the two aging stages in the case of the 356 alloys. Table 3.2 shows in detail the various heat treatment conditions that were applied to the 356 and 319 alloys within the heat treatment cycle II, using both CF and FB techniques.

Table 3.2. Heat treatment conditions/codes applied to A356.2 and B319.2 cast alloys within Heat Treatment Cycle II.

HT Code	Solutionizing Temp-time*	Quenching Media	delay	Age 1 T,^{0}C –time, h	delay	Age 2 T, ^{0}C– time, h
A	As-cast	-	-	-	-	-
B1	495(530)°C -5 h	32°C water	24 hr	170°C -4 h	-	-
B2	495(530)°C -5 h	32°C water	24 hr	170°C -8 h	-	-
B3	495(530)°C -5 h	32°C water	24 hr	170°C -12 h	-	-
C1	495(530)°C -5 h	170°C sand/(air)**	0	170°C -4 h	-	-
C2	495(530)°C -5 h	190°C sand/(air)**	0	190°C -4 h	-	-
C3	495(530)°C -5 h	210°C sand/(air)**	0	210°C -4 h	-	-
D1	495(530)°C -5 h	32°C water	24 hr	240°C -1 h	24 hr	170°C -1 h
D2	495(530)°C -5 h	32°C water	24 hr	240°C -1 h	24 hr	170°C -4 h
D3	495(530)°C -5 h	32°C water	24 hr	240°C -1 h	24 hr	170°C -8 h

*Alloys 319 and 356 were solutionized at 495°C and 530°C respectively.
** Alloys 319 and 356 were quenched-aged in sand using an FB; and in air using a CF.

(C) Heat Treatment Cycle III - Influence of Multi-Temperature Aging

In this case, the alloy samples were solution heat-treated at specific temperatures, corresponding to the alloy type, using both CF and FB techniques, then quenched immediately in warm water at 60 °C; after that, the artificial aging treatment was carried out using T7/T6 multi-temperature aging treatments, employing both CF and FB heat treatment techniques. The conventional continuous T6-standard aging was also applied to the alloys investigated to establish a comparison with the alloys that were subjected to non-conventional multi-temperature aging cycles. Details of the multi-temperature aging cycles are summarized in Table 3.3. These aging cycles were designed using temperatures typically employed in several foundries as well as in industrial applications.

Table 3.3. Multi-temperature aging cycles employed in Heat Treatment Cycle III.

Heat Treatment Regimes				
HT ID	**Solution**	**Quench**	**Age 1**	**Age 2**
SA32	495 (530) °C	60°C water	230°C -2h	180°C-0h
	495 (530) °C	60°C water		180°C-2h
	495 (530) °C	60°C water		180°C-4h
	495 (530) °C	60°C water		180°C-8h
SA34	495 (530) °C	60°C water	230°C -4h	180°C-0h
	495 (530) °C	60°C water		180°C-2h
	495 (530) °C	60°C water		180°C-4h
	495 (530) °C	60°C water		180°C-8h
SA51	495 (530) °C	60°C water	249°C -1h	180°C-0h
	495 (530) °C	60°C water		180°C-2h
	495 (530) °C	60°C water		180°C-4h
	495 (530) °C	60°C water		180°C-8h
SA52	495 (530) °C	60°C water	249°C -2h	180°C-0h
	495 (530) °C	60°C water		180°C-2h
	495 (530) °C	60°C water		180°C-4h
	495 (530) °C	60°C water		180°C-8h
SA54	495 (530) °C	60°C water	249°C -4h	180°C-0h
	495 (530) °C	60°C water		180°C-2h
	495 (530) °C	60°C water		180°C-4h
	495 (530) °C	60°C water		180°C-8h
SA71	495 (530) °C	60°C water	270°C -1h	180°C-0h
	495 (530) °C	60°C water		180°C-2h
	495 (530) °C	60°C water		180°C-4h
	495 (530) °C	60°C water		180°C-8h
T6	495 (530) °C	60°C water	180°C -8h	none

Greater hardening may be achieved if more uniform dispersions of one or more type of precipitates are obtained, where this may have been one of the objectives of the multi-stage aging treatments of Cycle III. In this subsection, six multi-aging treatment cycles were applied in both CF and FB furnaces for the purposes of investigating the effects, on the tensile properties and quality indices of the B319.2 and A365.2 types Al-Si

cast alloys, of multi-temperatures aging without applying an incubation time between aging stages.

3.4. MECHANICAL TESTING

Two tensile test bar castings were prepared from the non-modified and modified A356.2 and B319.2 alloys using the standard ASTM B-108 permanent mold. Each casting provided two test bars, each having a length of 197 mm, 70 mm gauge length and a cross-sectional diameter of 12.8 mm; five test bars were prepared for each alloy/heat treatment condition. All samples, whether as-cast, solution heat-treated, or aged, were pulled to fracture at room temperature at a strain rate of 1×10^{-4}/s using a Servohydraulic MTS Mechanical Testing machine, as shown in Figure 3.5. A strain gauge extensometer attached to the test bar gauge section measured the percentage elongation as the load was applied. A data acquisition system attached to the MTS machine recorded the tensile test data using software program to control the test, from which the tensile properties, namely ultimate tensile strength (UTS), yield strength (YS) and elongation, were determined. The corresponding stress-strain curve obtained illustrates the mechanical behavior of each specimen under the applied load. The average UTS, YS, and $\%E_f$ values obtained from the five test bars used per alloy/heat treatment condition were considered as the values representing that condition. A large number of test bars, approximately 3000 bars, were cast in order to obtain a reliable evaluation of the influence of metallurgical parameters on the tensile properties and the quality indices of the A356.2 and B319.2 casting alloys.

Figure 3.5. The MTS Servohydraulic Mechanical Testing Machine.

3.5. MICROSTRUCTURAL CHARACTERIZATION

The microstructures of selected A356.2 and B319.2 tensile samples were examined for the purpose of correlating their microstructural features with their mechanical properties in (a) the as-cast condition, and (b) after various heat treatment cycles where both FB and CF technique were employed for executing the heat treatment. Qualitative and quantitative analysis of the microstructural features, namely porosity, eutectic silicon particles, grain size and hardening precipitates, were carried out using an optical microscope-image

analysis system, as well as scanning electron microscopy (SEM), and field emission gun scanning electron microscopy (FEGSEM) for following the precipitation hardening behavior during heat treatment.

For microstructural examination, metallographic samples of 10 mm height were sectioned from the tensile-tested bars at a distance of 10 mm below the fracture surface, individually mounted in bakelite using a Struers LaboPress-3 machine, followed by grinding and polishing, using a Struers TegraForce-35 machine, to obtain the desired fine finish. The grinding procedures were applied using a silicon carbide (SiC) wear papers of various fineness numbers for abrasive materials, 120 grit to 1200 grit size, from more abrasive papers to soft ones. The water was used as a lubricant in this stage of grinding. Subsequently the first step of the polishing process was carried out using Struers diamond-suspension, which contains a diamond particle size of 6 μm; further polishing was applied through the application of the same suspension containing a smaller diamond particle size of 3 μm. The lubricant used for this polishing stage is a Struers DP-lubricant. Mastermet colloidal silica suspension, SiO_2, having a particle size of 0.6 μm was used for the final stage of polishing, where water was used as lubricant. By the final stage of polishing, a mirror-like surface samples was obtained to be ready for the microstructural examination.

The eutectic Si-particle characteristics as well as porosity percentage and grain size were measured and quantified using an Olympus PMG3 optical microscope linked to a Clemex image analysis system, for the samples subjected to first heat treatment cycles. The set-up is shown in Figure 3.6.

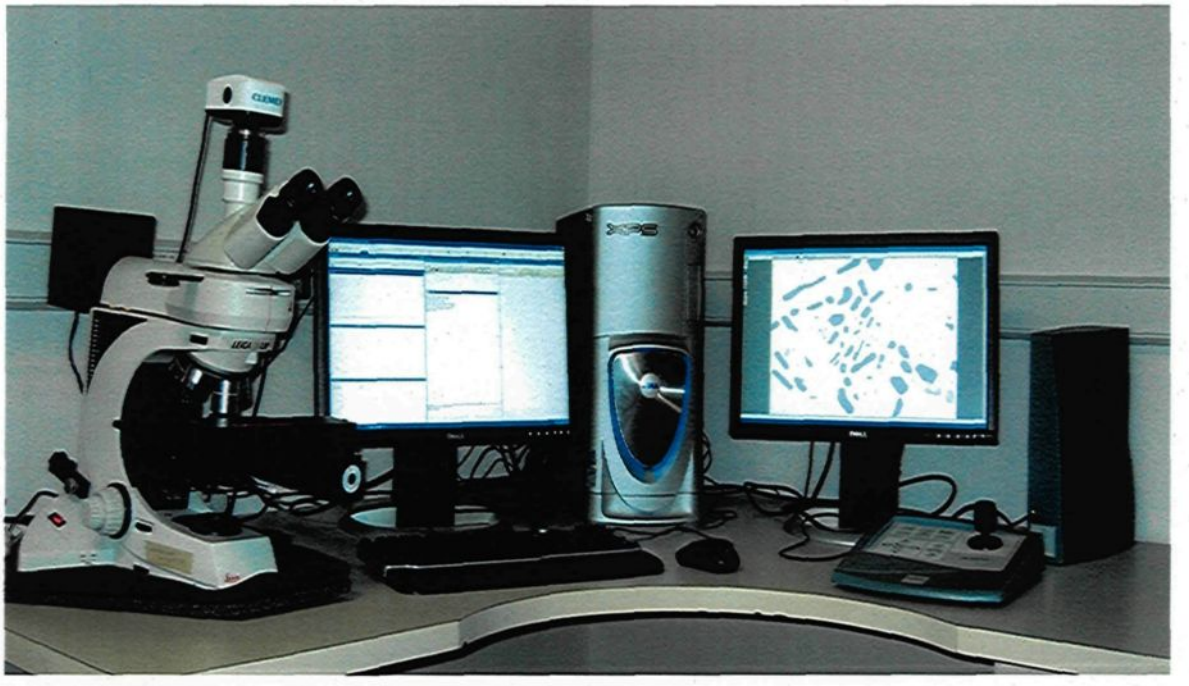

Figure 3.6. Clemex Vision PE4 image analysis system.

Quantitative measurements of the eutectic Si particle characteristics, *viz*, area, length and aspect ratio, were carried out for as-cast and solution heat-treated samples of modified and non-modified alloys. For each sample, fifty fields were examined over the entire surface of the sample, by traversing it in a regular and systematic manner; the Si particle characteristics were recorded for each field. Measurements were carried out at a magnification of 500X and 1000X for the non-modified and Sr-modified alloy samples, respectively. With regard to the A356.2 alloys, the eutectic silicon particles was carried out K1 (non-modified) and K3 (modified) alloy samples after solution heat treatment using both CF and FB techniques for 0.5, 5 and 12 h solutionizing times. Likewise, for the B319.2 alloys, the measurements were carried out for K2 (non-modified) and K4

(modified) alloy samples after solution heat treatment using both CF and FB techniques for 0.5, 5, 12 and 24h solutionizing times. These measurements, applied for A356 and B319 alloys, were carried out to investigate the influences of Sr-modification and the high heating rate involved in the FB technique on the fragmentation, dissolution and spheroidization of the eutectic Si particles after various solution treatment times.

For samples of A356 and B319.2 alloys subjected to first heat treatment cycles, grain size measurements were carried out employing the optical microscope-image analysis system, and using the line intercept method. The samples investigated were prepared from the as-cast and solution heat-treated test bars corresponding to specific solution treatment times. For grain size measurements, the polished samples were etched using a solution containing 12.5 gm CrO_3, 2.5 ml HF, 30 ml HCl, 40 ml HNO_3, and 42.5 ml distillated water for 3 minutes. The polished surface was swabbed until the contrast in revealed grains was high enough. To better highlight the grain structure, filtered lights at different incident angles were used; a combination of red, green, blue and yellow light gave an enhanced contrast to the grain structure. At least 5 measurements were taken from each sample and averaged; micrographs were also obtained from the polished samples using optical microscopy. Porosity measurements were made using the same procedures as those used to measure the Si particles characteristics. The average values of pore area, pore length, and area percentage porosity were obtained for the samples of K1, K2, K3 and K4 alloys in the as-cast condition.

The precipitate characteristics were examined after various heat treatment cycles of the A356.2 and B319.2 alloys using scanning electron microscopy (SEM) and field-

emission gun scanning electron microscopy (FEGSEM). The aim of using electron microscopy in this case was to examine the density and distribution of the hardening precipitates formed under various aging treatment parameters/heat treatment cycles applied in this study with the intention of comparing the influence of high heating rate as obtained in an FB heat treatment technique with that obtained with a CF. A JEOL 840A scanning electron microscope (SEM) attached to an EDAX Phoenix system designed for image acquisition and energy dispersive X-ray (EDX) analysis was employed for this purpose, using an accelerating voltage of 15 KeV for imaging, an emission current of 60 μm, and a beam diameter of less than 0.5 μm. Figure 3.7 shows a photograph of this SEM.

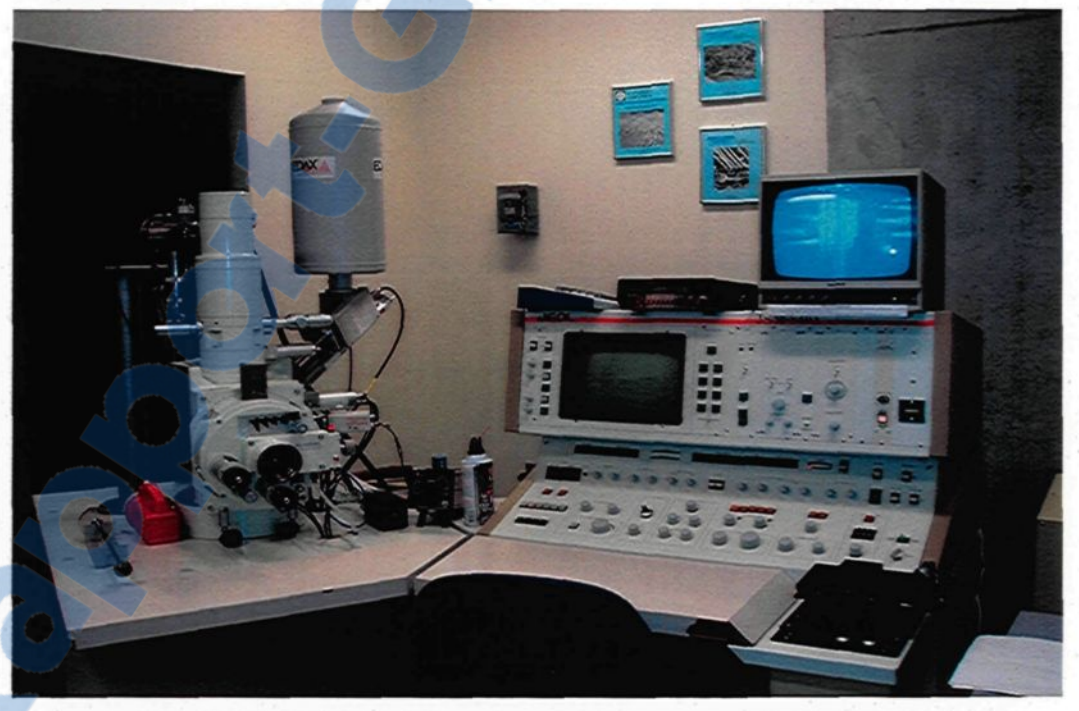

Figure 3.7. The JEOL 840A scanning electron microscope.

Compared to an SEM, an FEGSEM provides clear high-resolution images and good contrast even at low voltages and very high magnifications. The FESEM used in this study was the Hitachi S-4700 FEGSEM shown in Figure 3.8, which was sufficient to identify the smaller size and grey color of the Mg_2Si precipitates observed in the 356 alloy after aging treatment using a fluidized bed. The FEGSEM produces images of 2.1 nm resolution at 1 kV and of 1.5 nm resolution at 15 kV. For precipitate characterization, polished samples prepared from the gauge length of the tensile-tested specimens were subjected to a chemical micro-etching process using a specific solution composed of 1 ml HF (48%) + 200 ml distilled water. The micro-etching process was applied to the heat-treated samples at room temperature for 30 seconds and 90 seconds for the B319.2 and A356.2 alloys respectively.

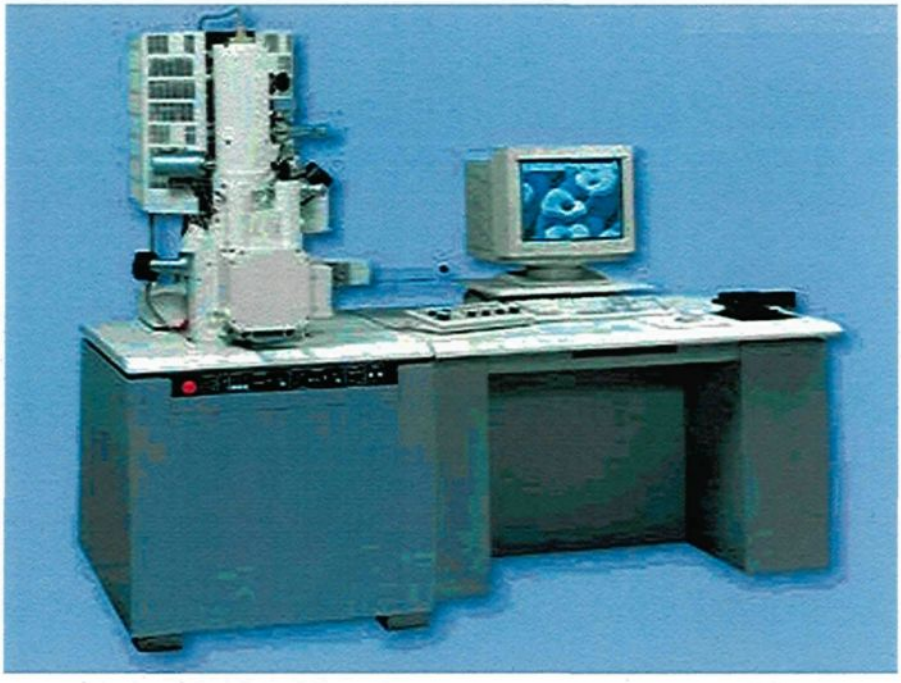

Figure 3.8. The Hitachi S-4700 field emission gun scanning electron microscope.

CHAPTER 4

INFLUENCES OF MELT AND SOLUTION HEAT TREATMENTS ON ALLOY PERFORMANCE

CHAPTER 4

INFLUENCES OF MELT AND SOLUTION HEAT TREATMENTS ON ALLOY PERFORMANCE

4.1. INTRODUCTION

The current chapter presents results and discussion to arrive at a better understanding of the influences of several metallurgical parameters on the tensile properties and quality indices of T6-tempered A356.2 and B319.2 cast alloys using a fluidized sand bed furnace (FB) for the heat treatment, as opposed to a conventional convection furnace (CF). The metallurgical parameters studied are the effects of solution heat-treatment time, aging time and melt treatment process using chemical modifiers. Modification and grain refinement are commonly employed in producing aluminum castings in order to improve their mechanical properties. Modification is carried out using Sr in the form of Al-10%Sr master alloy whereas Al-Ti-B grain refiners are used for refining the grain size. In this chapter, the tensile results and the quality index values of the alloy castings investigated are correlated to the microstructural constituents and features resulting from the specific heat treatment conditions investigated, with the aim of interpreting the results obtained. Statistical analysis of the data will also be presented.

4.2. CHARACTERIZATION OF THE MICROSTRUCTURE

The characteristics of the eutectic silicon particles, the grain size, porosity; and the hardening precipitates observed under specific heat treatment conditions in the alloys investigated are discussed in detail in the subsections that follow.

4.2.1. Characteristics of Eutectic Silicon Particles

The eutectic Si morphology plays a vital role in determining the mechanical properties of Al-Si alloys, where the particle size and shape of the silicon particles are the factors which greatly influence the alloy performance. In the present case, quantitative measurements of the eutectic silicon particles were carried out on samples sectioned from the B319.2 and A356.2 alloy castings obtained in the as-cast and solution heat-treated conditions. Table 4.1 summarizes the silicon particle characteristics obtained for the alloys solution heat treated for 0.5 h, 5 h, 12 h and 24 h, using FB and CF heat treatment techniques. Both solution heat treatment conditions as well as Sr-modification result in transforming the morphology of the eutectic silicon particles from acicular particles into fibrous ones; increasing the duration of the solution treatment time produces further improvement in the eutectic silicon morphology. [168, 169] As may be seen from Table 4.1, the smallest particle size was obtained after solution heat treatment using a fluidized sand-bed, for which the optimum solution heat treatment time was 0.5 h for modified alloys and up to 5 h for non-modified alloys.

Table 4.1. Average silicon particle characteristics.

Alloy Code	ST, hr // HT Medium	Average Si Particle Characteristics					
		Area, μm^2		Length, μm		Aspect Ratio%	
		Av.	SD	Av.	SD	Av.	SD
K1 (356 non-modified)	**As-Cast**	**13.81**	**17.7**	**9.13**	**9.1**	**3.1**	**1.82**
	0.5 // CF	11.1	15	6.61	6.53	2.65	1.05
	0.5 // FB	6.96	8.22	4.42	3.34	2.01	1.22
	5 // CF	8.48	8.74	5.55	4.08	2.29	1.27
	5 // FB	8.16	9.42	5.03	4.54	2.06	1.13
	12 // CF	12.42	13.9	7.77	6.22	2.97	1.24
	12 // FB	12.13	13.5	7.48	5.6	2.8	1.27
K3 (356 modified)	**As-Cast**	**2.9**	**3.42**	**2.55**	**2.3**	**1.71**	**0.635**
	0.5 // CF	2.2	3.16	1.64	1.25	1.31	0.457
	0.5 // FB	1.95	2.45	1.27	1.13	1.14	0.615
	5 // CF	4.39	4.76	2.77	1.71	1.75	0.582
	5 // FB	4.22	4.49	2.74	1.8	1.61	0.584
	12 // CF	6.21	6.41	3.21	1.98	1.79	0.534
	12 // FB	5.67	6.1	3.13	2.03	1.72	0.654
K2 (319 non-modified)	**As-Cast**	**26.5**	**35.3**	**10.83**	**10.9**	**4**	**2.8**
	0.5 // CF	23	27.2	9.25	8.56	3.57	1.83
	0.5 // FB	13.85	16.9	8	7.58	2.96	1.85
	5 // CF	17.1	20.2	8.89	6.84	3.57	1.98
	5 // FB	15.85	16.84	8.47	6.19	3.15	2.78
	12 // CF	23.35	30.14	10.22	9.78	3.51	2.17
	12 // FB	22.86	24.6	10.04	8.71	3.45	2.34
	24 // CF	26.79	30.25	10.89	9.24	3.87	2.42
	24 // FB	27	29.22	11.3	9.56	3.93	2.66
K4 (319 modified)	**As-Cast**	**19.1**	**33.6**	**9.73**	**10.2**	**3.58**	**2.15**
	0.5 // CF	14.87	19.25	8.87	8.93	2.97	1.21
	0.5 // FB	11.04	15.23	7.76	7.32	2.87	1.31
	5 // CF	10.03	11.32	7.61	6.14	2.77	1.15
	5 // FB	13.16	14.25	8.11	6.33	3.07	2.01
	12 // CF	14.87	17.31	9	7.26	3.13	2.1
	12 // FB	17.14	19.75	9.43	8.44	3.23	2.03
	24 // CF	19.8	20.6	9.78	8.18	3.63	2.61
	24 // FB	20	19.7	9.88	7.1	3.83	2.42

*Aspect ratio: Ratio of maximum to minimum dimensions of a Si particle; ST: Solution treatment time

The average silicon particle length and area obtained after 0.5 h solution heat treatment in an FB are smaller by 33-37% and 14-40% than the values obtained using a CF for the non-modified 356 and 319 alloys, respectively, as shown in Table 4.1. In relation to the modified condition, it may be noted that after a 0.5 h solution heat treatment using an FB, the particle size is lowered by 23% and 12% for alloys 356 and 319, respectively, compared to the values obtained using a CF, indicating that in comparison to the latter, the fluidized bed has a greater effect in refining the Si particle size, since the particle size is reduced by more than half after 0.5 h solution heat treatment compared to the as-cast condition. Upon increasing the solution heat treatment time to 5 h in an FB, however, a coarsening of the eutectic Si occurs which may be ascribed to the Ostwald ripening phenomenon. [170]

In general, the FB treatment produces smaller Si particle sizes than does the CF through solution heat treatment time cycles of up to 12 h for non-modified 356 and 319 alloys. It should also be noted that, with the conventional furnace, the smallest Si particle size for non-modified alloys was obtained after 5 h of solution heat treatment compared to 0.5 h with the fluidized bed. The high heating rate in fluidized beds promotes the fragmentation and spheroidization kinetics of the eutectic Si particles. A longer solution heat treatment time leads to a coarsening of the Si particles where the driving forces for the coarsening have been related to the reduction of strain energy and surface energy of the Si particles.

Modification has the strongest influence on the spheroidization and coarsening kinetics of Si particles in Al-Si alloys. The silicon represents the hard phase of the alloy which causes a discontinuity of the soft and ductile matrix of aluminum. Because α-Al is

the softer phase and Si is the harder and less ductile one, stresses cause anisotropic distribution of the plastic deformation, which is greater in the softer phase. The local plastic constraint in the softer phase leads to a rapid strengthening of the alloy, with dislocations piling up at the α-Al/Si interfaces. This can lead to the formation of cleavage microcracks at these ductile-brittle sites. On such a basis, it is to be expected that differences between the mechanical properties of the five tensile bars will be higher for the unmodified alloy. As may be seen from Table 4.1, the Si particles are present in the form of coarse acicular plates in the as-cast condition, with an aspect ratio of 3.1 and 4 for 356 and 319-type alloys respectively. The addition of 150 ppm Sr reduces the aspect ratios to 1.71 and 3.58, respectively, in the as-cast modified alloys. For alloy 356, the average particle area is reduced from 13.81μm^2 to 2.9μm^2, *i.e.* by about 78%, and the average particle length from 9.13μm to 2.55μm, *i.e.* by about 75%, with respect to the as-cast condition. The strontium was observed to have a significant effect by changing the coarse, acicular eutectic silicon into a fine, fibrous form thereby enhancing both the strength and the ductility of the alloys investigated. [77, 170] For the alloys investigated in the as-cast condition, the variations existing between the particles were estimated by means of the standard deviation, which is used to assess the accuracy of the measurements under the same experimental conditions. For the purposes of this examination of microstructures, the standard deviation was considered to assess the structural uniformity of the silicon phase within the microstructure. In the presence of strontium, the degree of modification was appreciable, and one of the aspects of this was reflected by a narrowing of the deviations. The standard deviation between the Si particle area decreased from ± 17.7 to ± 3.42 and from ± 35.3 to ± 23.2 for

the 356 and 319 alloys, respectively, thereby showing the increase in the uniformity of the microstructure associated with modification. Table 4.1 shows that the Si particles size decreases with increasing solution heat treatment time of up to 5 h, irrespective of whether the treatment is carried out in an FB or CF, indicating the effect of solutionizing time on the mass transfer of silicon. This mass transfer causes the fragmentation and spheroidization of eutectic silicon, both of which are dependent on the diffusion of solute and matrix atoms. In the modified alloys, a high degree of spheroidization followed by coarsening occurs during solutionizing at 5 h, 12 h and 24 h. The microstructural changes resulting from solution heat-treatment originate from the instability of the interface between two phases. Plate-like eutectics are more resistant to interfacial instabilities and subsequent spheroidization than the fibrous kind. Thus, the rate of spheroidization is extremely rapid in modified alloys. Spheroidization and coarsening of the discontinuous phase occurs at elevated temperatures,[171] because the interfacial energy of a system decreases with the reduction in interfacial surface area per unit volume of the discontinuous phase. The reduction in interfacial energy is the driving force for the spheroidization and the coarsening processes which are also diffusion-controlled.[172] It may be noted from Table 4.1 that the average Si particles size values for the A356.2 modified alloys are smaller as compared to those obtained for the B319.2 modified alloys; this difference in Si particle sizes may be related to the presence of more Cu and Mg in the composition of B319.2 alloys. It may be noted that increasing the level of Cu and Mg leads to an increase in the average length and area of Si particles, due to the fact that both Mg and Cu react with the Si and Sr in the alloy to form $Mg_2Sr(Si,Al)$ and Al-Cu-Sr compounds, respectively. [170, 171, 172] Thus, there is less Sr

available to achieve the same level of modification in the eutectic Si particles than would be expected with the amount added. Also the presence of $Al_{15}Mn_3Si_2$ and Al_5FeSi, phases formed in pre-eutectic reactions, as well as $CuAl_2$ during solidification of B319.2 cast alloys may hinder the diffusion of Si to the matrix leading to the presence of Si particles with larger size after solidification as compared to the A356 alloys.

Figures 4.1 and 4.2 show the effects of the heating rate on the number of cracked Si particles observed beneath the fracture surface of 356 and 319 alloy samples after 0.5h solution heat treatment using fluidized bed and convection furnace techniques. It should be noted that the high heating rate of the fluidized bed results in a greater number of fractured Si particles after only 0.5 h of solution heat treatment than that obtained at the comparatively lower heating rate of the convection furnace. For the 356 non-modified alloy, the cracked Si particles may be seen clearly as indicated by the arrows and encircled areas in Figure 4.1(a) and (b); on the other hand, the fibrous morphology of the Si particles in the modified alloy resists the fracture process, resulting in fewer cracked particles, Figure 4.1(c) and (d). For alloy 319, after 0.5 h of solution heat treatment, there is no significant difference to be observed in the density of the cracked particles between those treated in the fluidized bed and those obtained from the conventional furnace. The high heating rate of the FB enhances the fragmentation kinetics of the eutectic Si particles through the generation of high thermal stresses owing to the thermal expansion mismatch between the eutectic Si and the Al matrix. This thermal mismatch occurs as a result of the thermal expansion coefficient of Si being much lower than that of Al. Generating thermal stresses through the eutectic Si induces thermal elastic strains on the Si particles as well as

the Al matrix; the brittle fracture of the particles will occur when the thermal strain exerted on the Si exceeds its fracture strain. [55, 136, 137]

Table 4.2 lists the number of cracked Si particles, total particles, and the area density of cracked particles observed beneath the fracture surface of the non-modified 356 and 319 alloy samples after 0.5 h solution treatment using FB and CF heat treatment techniques. The quantitative measurements were made over 50 fields at a magnification of 500X on the polished surface of samples sectioned perpendicular to the fracture surface of the tensile-tested samples, using an optical microscope linked to a Clemex image analysis system. It will be noted that the number of fragmented particles as well as the area density of broken particles obtained for samples heat treated using an FB are greater than those to be observed when using a CF for both 356 and 319 alloys. The overall percentage of cracked Si particles beneath the fracture surface, however, shows no difference between the fluidized bed and the convection furnace heat treatment techniques for the two alloys. The difference in the actual overall percentage values of fragmented Si particles (22% for 356 alloys *vs.* 14% for 319 alloys) may be related to the difference in ductility between the two alloys, namely, 12% for the 356 alloys *vs.* 3% elongation for the 319 alloys.

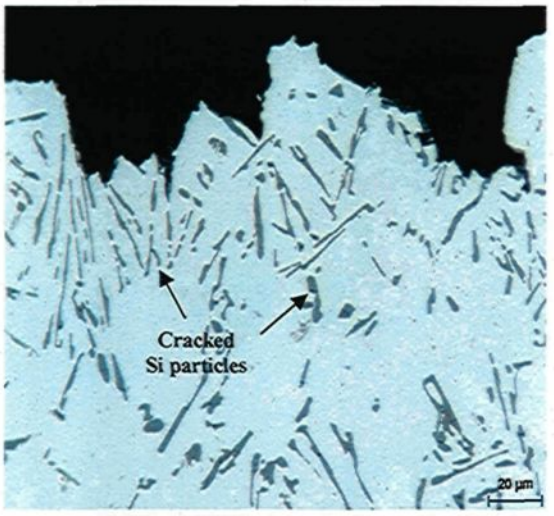

356 Non-Modified -0.5 hr SHT-CF

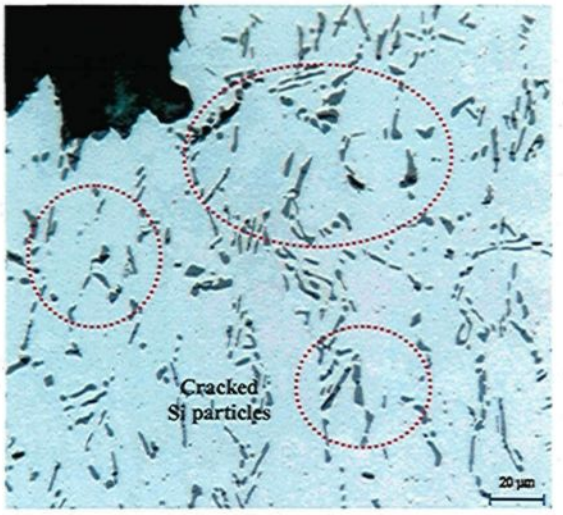

356 Non-Modified -0.5 hr SHT-FB

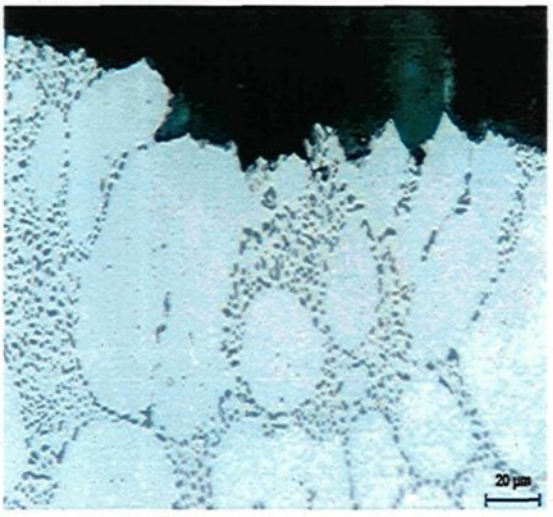

356 Modified -0.5 hr SHT-CF

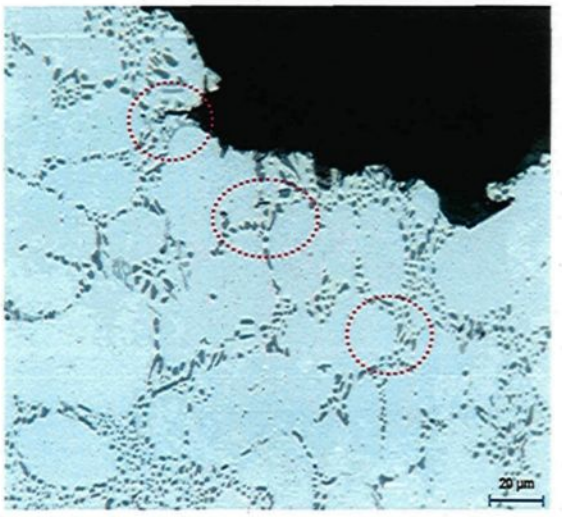

356 Modified -0.5 hr SHT-FB

Figure 4.1. Fractured Si particles beneath the fracture surface in samples obtained from 356 non-modified and modified alloys after 0.5hr solution heat treatment (SHT): FB *vs* CF techniques.

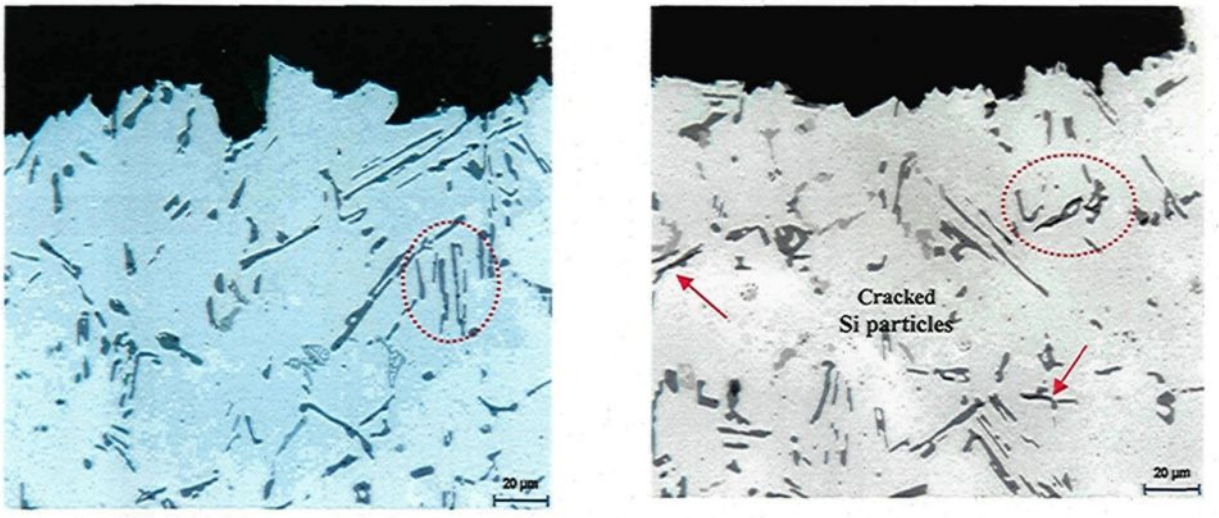

Figure 4.2. Fractured Si particles beneath the fracture surface in samples obtained from 319 non-modified alloys after 0.5 hr solution heat treatment (SHT) using (a) CF, and (b) FB techniques.

Table 4.2. Effects of heating rate on Si particles beneath fracture surface of alloys 356 and 319 after 0.5 hr solution heat treatment using CF vs. FB techniques.

Alloy	**356 non-modified (K1)**		**319 non-modified (K2)**	
Heat Tmt Technique	**CF**	**FB**	**CF**	**FB**
No. of cracked Si particles	700	1056	290	425
Total No. of Si particles	3256	4890	2045	3040
% of cracked Si particles	22%	22%	14%	14%
Area density of fragmented Si particles/mm^2	1321	1992	547	800

Figures 4.3 and 4.4 show the effects of solution heat treatment on the morphology of eutectic Si for alloys 319 and 356, respectively, using CF *vs* FB techniques. Under normal cooling conditions, eutectic silicon forms a network of interconnected irregular flakes. As was observed, the eutectic Si may be chemically modified to a fine fibrous structure. High temperature treatments and/or long time can also alter Si particle characteristics. In recent years, both chemical and thermal modifications have been used in conjunction with each other to produce the desired properties of the casting.

The figures show the observable effects of the high heating rate of the fluidized bed on the fragmentation and spheroidization of Si particles. The Si particles start to become fragmented into finer particles within 30 minutes of solution heat treatment in the fluidized bed. It can be seen from Figure 4.3(b, c) that the high heating rate in the fluidized bed results in an increased density of broken and more fibrous Si particles than occurs in a convection furnace after a 0.5h solution heat treatment of the non-modified 319 alloys. Van Wert *et al.* [13] reported that the solution heat treatment procedure using an FB results in faster fragmentation and spheroidization of the eutectic Si particles. After 12 h of solution heat treatment in a fluidized bed, the Si particles in modified 319 alloys display coarser spheroidized particles than those obtained in a conventional furnace, as may be seen from Figure 4.3. The increased spheroidization and coarsening of eutectic Si in the fluidized bed heat-treated alloy is closely related to the high heat transfer rate which has an observable effect on the diffusion rate of the Si particles. It has been reported that the reduction of strain energy as well as the reduction in surface energy are the driving forces for the coarsening of eutectic Si during solution heat treatment.

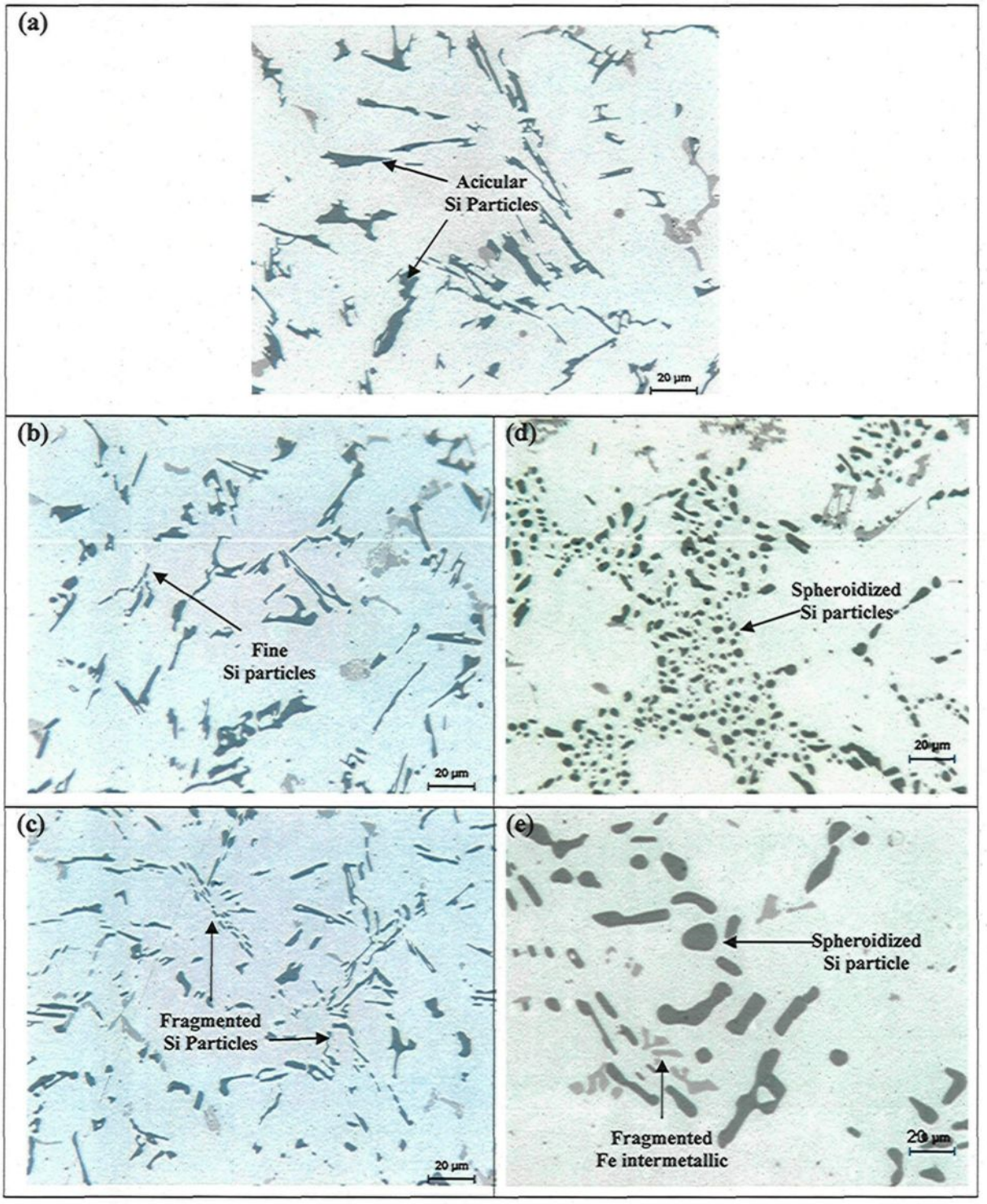

Figure 4.3. Optical micrographs of (a-c) non-modified 319 alloy: (a) as-cast, (b) SHT-0.5hr in CF, (c) SHT-0.5hr in FB; and (d-e) modified 319 alloy: (d) SHT-12hrs in CF, (e) SHT-12hrs in FB.

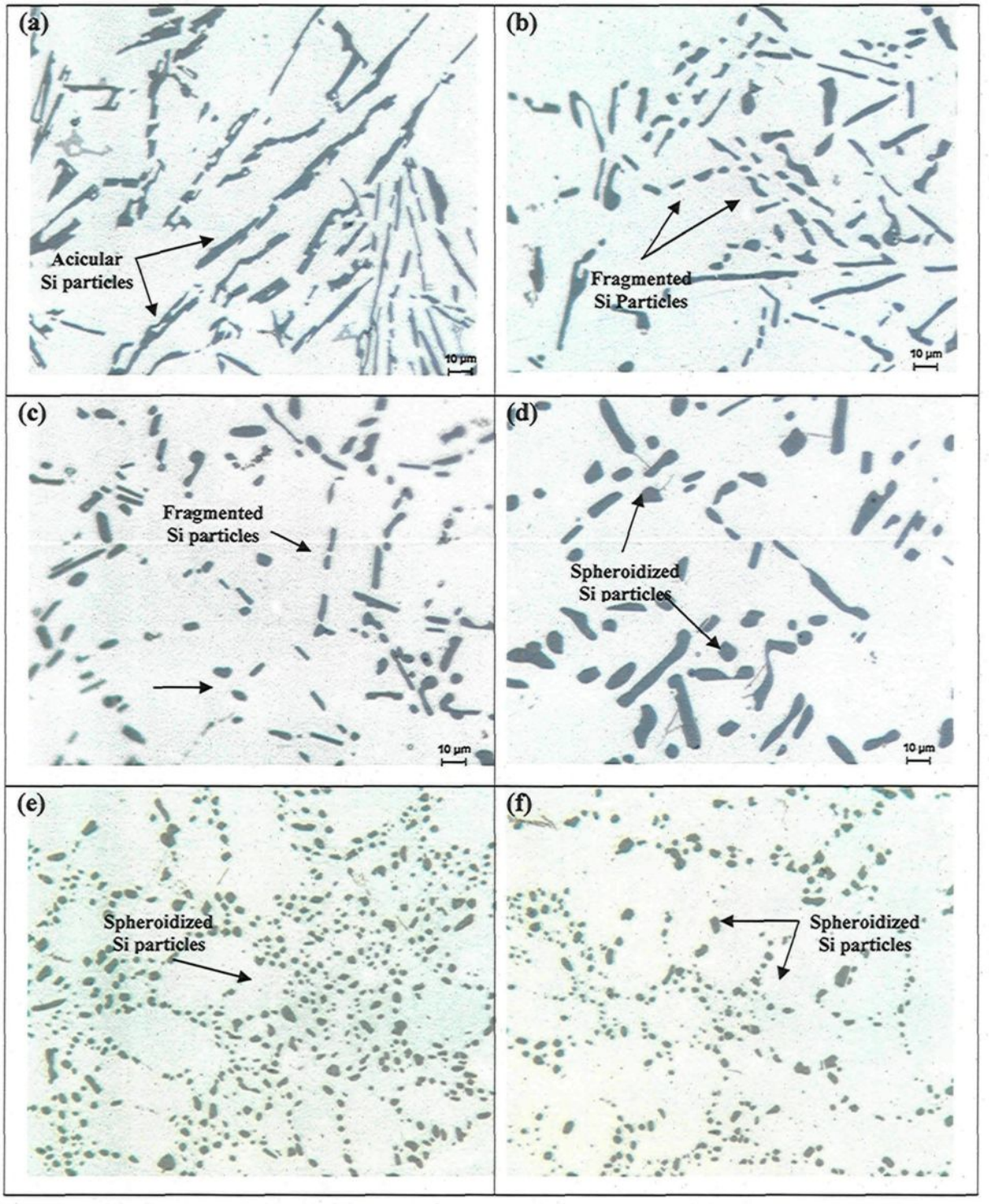

Figure 4.4. Optical micrographs of (a-d) non-modified 356 alloy: (a) as-cast, (b) SHT-0.5hr in FB, (c) SHT-1hr in FB, (d) SHT-5hrs in CF; and (e-f) modified 356 alloy: (e) SHT-12hrs in FB, (f) SHT-12hrs in CF.

These factors are dependent on the diffusivity of Si in the aluminum matrix. Figure 4.4 shows that the Si flake-like or acicular particles in the non-modified 356 alloy are fragmented into finer particles within 0.5h and 1h of solution treatment in a fluidized bed versus 5h in a convection furnace. The mechanism of Si fragmentation in fluidized beds is related to the generation of high thermal stresses at the eutectic Si/Al interface rather than to a thermal mismatch between the eutectic Si and the primary Al. The thermal stresses generated by the high heating rate in the FB impose an elastic strain on the Si particles. The brittle fracture of the Si particles begins when this thermal strain is higher than the fracture strain of the same particles. [12, 135, 173] Figures 4.4 (e) and (f) show the fibrous form of Si particles for the modified 356 alloy after 12 h of solution heat treatment in both the FB and the CF, at which point the fluidized bed-treated sample shows more spheroidized Si particles than that corresponding to the convection furnace.

The modification has a strong effect on the spheroidization and the coarsening kinetics of Si particles; the CF produces slower fragmentation and spheroidization kinetics of the eutectic Si. The rate of spheroidization is extremely rapid in modified alloys; the spheroidization process of silicon through solution heat treatment takes places in two stages: dissolution/separation of the eutectic branches and spheroidization of the separated branches. In the first stage, the Si particles are separated into segments at the corners of thin growth steps, but retain their flake-like morphology. In the second stage, the broken segments spheroidize and the aspect ratio decreases. The dissolution stage has the greatest effect on the time required to complete spheroidization and is strongly affected by the morphology of the Si particles: the smaller the flake length, the greater the spheroidization.

[174, 175] Any process which promotes eutectic branching, whether modification or a higher cooling rate, will speed up the progress of separation and spheroidization. Modification by addition of impurities tends to refine the eutectic Si greatly, to promote twin branching, to raise the energy state with its inhomogeneity, and consequently to promote the kinetics of the spheroidization of the eutectic silicon.

4.2.2. Grain Size and Porosity Measurements

The average grain sizes for the as-cast and heat treated samples are given in Figure 4.5. From the results provided in Figures 4.5 and 4.6, it can be seen that the grain size of the as-cast 356 alloy is smaller than that of the 319 alloy sample, although both the alloys in their initial condition have the same residual titanium content of 0.12 wt%. This difference in grain size can be related to the presence of copper in the 319 alloys which hinders the process of grain refinement, as reported by Gruzleski. [170] On the other hand, the results indicate that the presence of copper in the grain-refined 319 alloy samples does not hinder the grain refining at a higher Ti content of 0.22 wt% than it does at the initial content. It can be noted that the grain size of 319 alloy samples was refined from 1317 μm to 291 μm by the addition of grain refiners. It has been reported by Qiu *et al.* [176] and Marcantonio *et al.* [177] that, during the grain refinement of Al-Si based casting alloys when the Si content exceeds ~2 wt%, a coarsening of the grains starts to occur and the extent of the poisoning effect intensifies with increasing Si content. The addition of other elements, such as Mg, or Sr, and so forth, has also been reported to counteract the poisoning effect of silicon in an effective manner. Gloria [178] reported that after the addition of 0.005wt% boron

to alloy 356, the grain size remained constant at 400 μm. On the other hand, the results obtained for alloy 356 from this study show that the addition of 0.006 wt% boron to the alloy refined the grains by more than 50%, from 442.7 μm to 202.4 μm. Figure 4.5 also shows how the grain size displayed by 356 and 319 alloys ia affected by the application of high heating rates when using an FB at solution heat treatment times of 12 h and 24 h, respectively. It should be noted that the high heating rate of an FB results in a larger grain size than is obtained with a CF. Large grain sizes are related to faster growth velocities, and small grain sizes correspond to slower growth velocities. [178] The driving force for the recrystallization of eutectic grains is the thermal stress which is directly proportional to the heating rate.

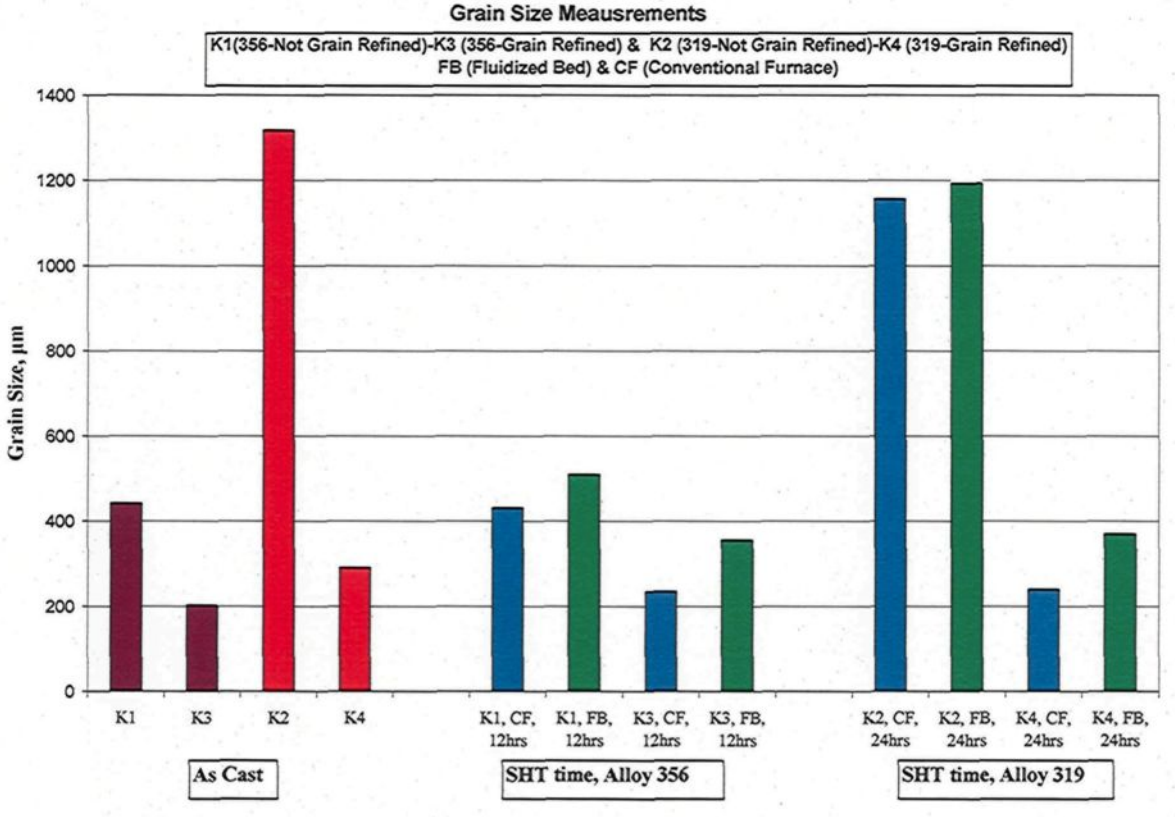

Figure 4.5. Grain size measurements for alloys 356 and 319.

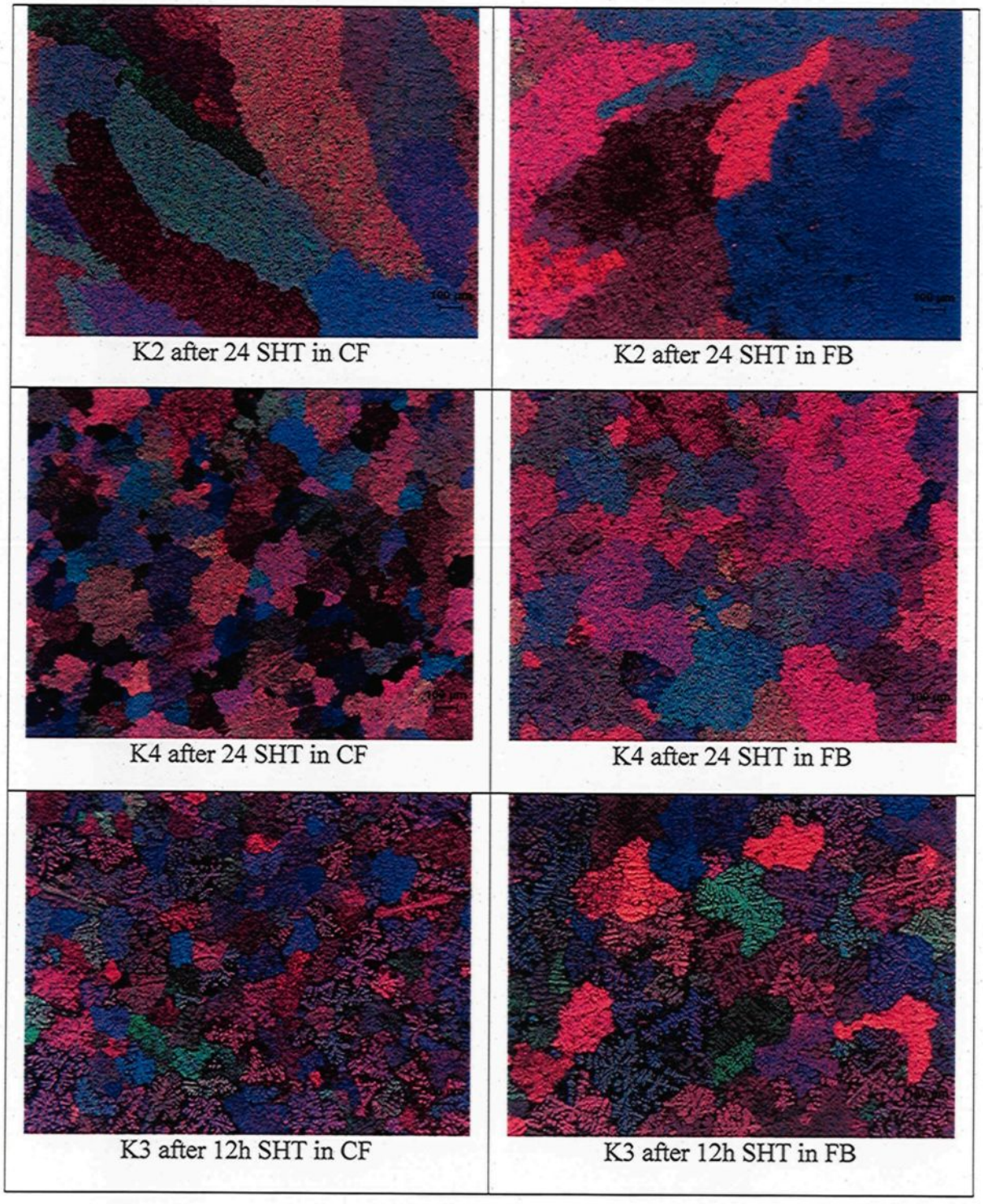

Figure 4.6. Optical micrographs showing the grain size of B319.2 and A356.2 alloy samples in the present study.

Porosity is the most common defect found in Al-Si castings and is considered to be the main cause for the rejection of such castings, since it often results in poor mechanical properties. The formation of porosity in solidifying Al-Si castings can be related to the shrinkage process during solidification, incorrect feeding, and the development of hydrogen gas. [179] Table 4.3 shows the porosity measurements for as-cast alloys 356 and 319 in non-modified and modified conditions. It should be noted here that in all of the cases, the liquid metal was continuously degassed prior to casting in order to minimize the effects of gas- and inclusion-related porosity. The Sr-modified 356 and 319 alloys (*i.e.* K3 and K4 alloys) are characterized by a higher percentage of surface porosity level than the unmodified 356 and 319 alloys (*i.e.* K1 and K2 alloys) alloys as may be seen from Table 4.3. It is worthy of note that the percentage surface porosity is, in fact, a multiple of the pore density and the average pore size. Thus, the increase in percent porosity observed in the Sr-modified alloys may be due to an increase in pore density and/or pore size.

The increased porosity of the Sr-modified alloys can cause a reduction in the mechanical properties in contrast with the unmodified alloys, even though the eutectic Si has been modified. As mentioned previously in the literature review, grain refining has several advantages, including the redistribution and reduction of porosity. Grain refinement of a casting may alter the amount and the morphology of pores in a casting; in many cases, there is also an overall reduction in the amount of porosity in alloys containing small or moderate amounts of gas. [140, 180, 181] The combined addition of grain refiner and modifier to the K3, K4 alloys causes no significant variation observable in the percentage surface porosity, as shown in Table 4.3. For the average values of pore area and pore length, the

modified and grain-refined 356 and 319 alloys are characterized by finer and more widely distributed porosity than is the case for the unmodified alloys. Grain refinment in Al-Si casting alloys improves the mass feeding characteristics during solidification, resulting in a reduction in shrinkage porosity and the promotion of an improved porosity dispersion. [180] Table 4.3 shows that the pore size and area percent porosity for alloy 319 are higher than those for alloy 356. The increase in porosity may be related to the presence of Cu in Al-Si cast alloys, where copper leads to an increase in volumetric shrinkage during solidification due to the accumulation of high levels of Cu in the eutectic liquid. [182]

Table 4.3. Porosity measurements for alloys 356 and 319 in as-cast condition.

Alloy Code	Condition	Average Porosity Measurements					
		Area, μm^2		Length, µm		Area %	
		Av.	SD.	Av.	SD.	Av.	SD.
K1 (356 non-modified)	As-Cast	8.83	31.2	2.5	4.45	0.043	0.052
K3 (356 modified)	As-Cast	2.89	16.9	1.68	2.32	0.065	0.059
K2 (319 non-modified)	As-Cast	35.2	85.7	6.7	8.82	0.064	0.058
K4 (319 modified)	As-Cast	16.2	39.2	4.26	4.44	0.114	0.285

4.2.3. Copper-Rich Intermetallics

In order to investigate the effects of solution heat treatment on the performance and quality of B319.2 alloys, the surface fraction of the undissolved copper phase was measured for various heat treatment conditions. The characteristics of Cu-intermetallic phases observed in alloys K2 and K4 were examined using an optical microscope linked to

a Clemex image analysis system. For each solution heat treatment time condition, 15 fields were examined for each of the corresponding 319 alloy samples at 500X magnification; a given average value of the undissolved copper phase was recorded as well as the standard mean deviation. The surface fraction of the undissolved copper phase was measured at various solution heat treatment times, namely 0.5 h, 1 h, 5 h and 8 h, for non-modified and modified B319.2 type alloys.

Copper intermetallic phases may occur as a mixture of both block-like and eutectic $CuAl_2$ forms which are either partially or completely soluble. The $CuAl_2$ and Mg_2Si phases are formed in the B319.2 alloys after solidification; however, quantitative measurements were carried out for the $CuAl_2$ phase only, since the undissolved Mg_2Si phase, which appears darker than the Al-matrix because of its smaller average atomic number, could be identified easily. Figure 4.7 shows the effects of solution heat treatment time on the amounts of undissolved $CuAl_2$ phase for modified and non-modified B319.2 alloys using both a CF and an FB. In general, it may be observed that the amount of undissolved $CuAl_2$ phase decreases after solution heat treatment compared to the as-cast condition. These phases dissolve during solution treatment by diffusing into the metal matrix thus forming a supersaturated solid solution after quenching. It can also be observed that the FB causes higher dissolution of the $CuAl_2$ phase after 0.5h solution heat treatment than does the CF as a result of the effects of the high heating rate prevailing in an FB. About 53.7% and 36.8% of the total $CuAl_2$ phase dissolved in the matrix after 0.5 h solution heat treatment in an FB and a CF, respectively, for non-modified B319.2 alloys compared to the as-cast condition. The modified B319.2 alloys show greater amounts of undissolved $CuAl_2$ than non-modified

alloys due to the segregation of the Cu phases in the modified condition thereby reducing the dissolution of the $CuAl_2$ phase in the matrix.

The surface fraction of the percentage of the undissolved $CuAl_2$ phase was observed to decrease with an increase in the solution time of up to 5 h, as illustrated in Figure 4.7. It will be observed that the dissolution rate of $CuAl_2$ phases is relatively slow after 1h of solution heat treatment in an FB compared to a CF which shows a higher dissolution rate between 0.5 h and 1 h of solution heat treatment time. Even after prolonged solution heat treatment of up to 8 h duration, the surface fraction percentage of the undissolved $CuAl_2$ phase does not show any significant difference between alloys heat treated in either a CF or an FB. The high heating rate in an FB significantly affects the amount of $CuAl_2$ phase dissolution in that better dissolution of the Cu-phase is obtained after a short solution heat treatment time of 0.5 h. For longer solution heat treatment times of 1 h up to 8 h, there is no observably significant effect of the high heating rate of the FB on the dissolution rate of $CuAl_2$, where the solutionizing time is now the main factor affecting the dissolution. In comparison, the slow heating rate in a CF provides a better dissolution rate of $CuAl_2$ after longer solution heat treatments of 1 h-5 h.

The quality performance of the alloys investigated is affected by the amount of undissolved $CuAl_2$ which may result in a decrease in the quality values of the alloys investigated after solution heat treatment and aging procedures. The main strengthening phase in the B319.2 alloys investigated in the present study is the Q-$Al_5Cu_2Mg_8Si_6$ phase. With respect to this phase, it has been reported that solution heat treatment of 319 alloys using an FB results in complete dissolution of the phase in the Al matrix within 45 minutes.

[137] In the present study, also, the Q-phase was not observed in the solution heat-treated alloy samples. Thus, it is reasonable to say that the performance/quality of the alloys will be controlled by the amount of undissolved $CuAl_2$ remaining after solution heat treatment, which may result in a decrease in the quality values of the heat-treated alloys. It may be noted from Figure 4.7 that the $CuAl_2$ hardening phase is not completely dissolved in the aluminum matrix of the solution heat treated B319.2 alloys using either CF or FB techniques even after 8h of solution heat treatment.

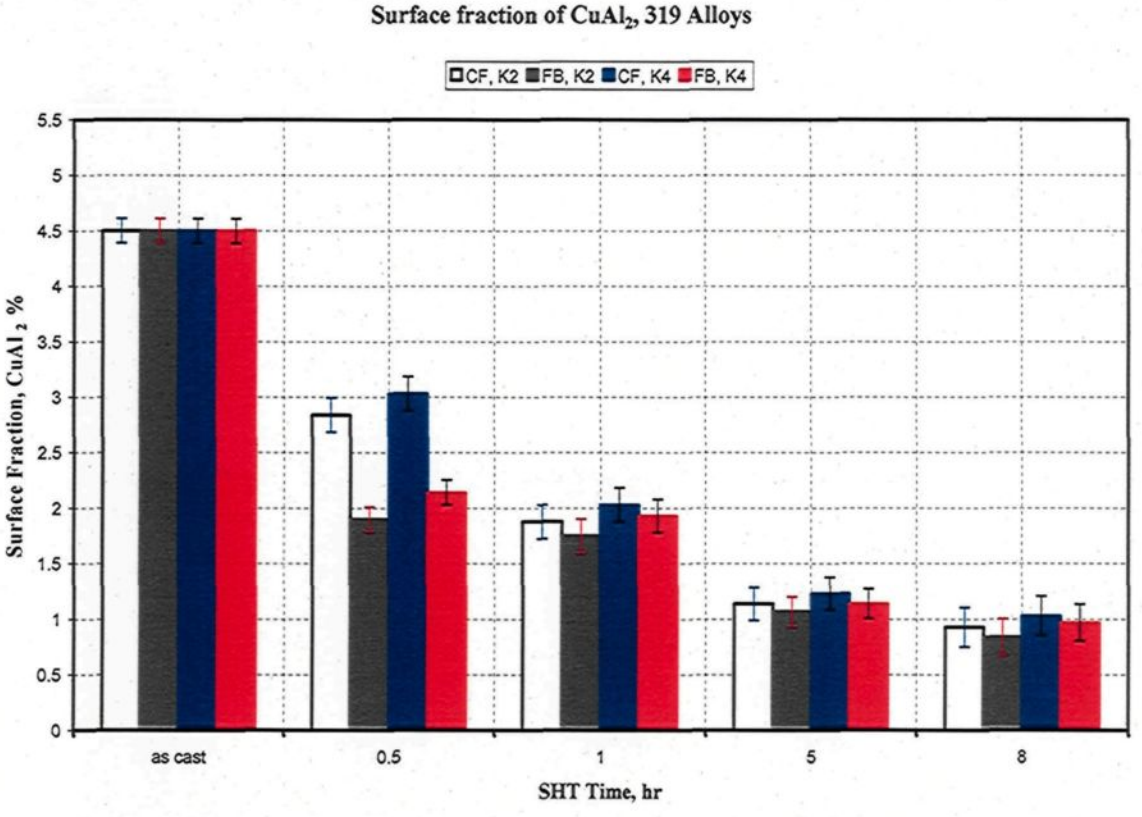

Figure 4.7. Surface fraction (%) of undissolved $CuAl_2$ intermetallic phase as a function of solution heat treatment time.

Figure 4.8 shows the FEGSEM micrographs of the non-modified B319.2 and A356.2 alloys after 0.5 h solution heat treatment using both a CF and an FB. For B319.2 alloys which have been heat treated using an FB, the presence of the undissolved Mg_2Si phase may be observed in the matrix regions, appearing darker than the Al matrix, as shown in Figure 4.8 (a). This amount of undissolved Mg_2Si may be related to the fact that the high heating rate in an FB does not provide sufficient time to dissolve as much as possible all of the hardening intermetallics ($CuAl_2$, $Al_5Mg_8Cu_2Si_6$ and Mg_2Si) present in the B319.2 alloy matrix during the solution heat treatment. Thus, the presence of undissolved amounts of $CuAl_2$ and Mg_2Si in the matrix of heat-treated samples using an FB, as well as the Fe-intermetallics may affect the quality and ductility values of the 319 alloys investigated. In the case of the A356.2 alloys, however, since Mg_2Si is the main intermetallic phase present in the alloy, one would observe the complete dissolution of Mg_2Si in the matrix. These observations are supported by the microstructures of Figures 4.8(c) and (e) which show that solution heat treatment of B319.2 and A356.2 alloys using a CF and an FB, respectively, results in the complete dissolution of Mg_2Si in the matrix. The black spots in matrix (a) in Figure 4.8 correspond to undissolved Mg_2Si while the bright spots correspond to Al_2Cu precipitates; the clusters of white particles in the matrix of Figure 4.8(c) correspond to fragmented Si particles, while the very fine light grey spots observed in the inset in Figure 4.8(e) correspond to Mg_2Si precipitates. Consequently, the quality of A356.2-type alloys may be more responsive to the fluidized sand bed as compared to the B319.2 alloys. In this context, the mechanical performance and quality of alloys investigated will also be discussed in this chapter.

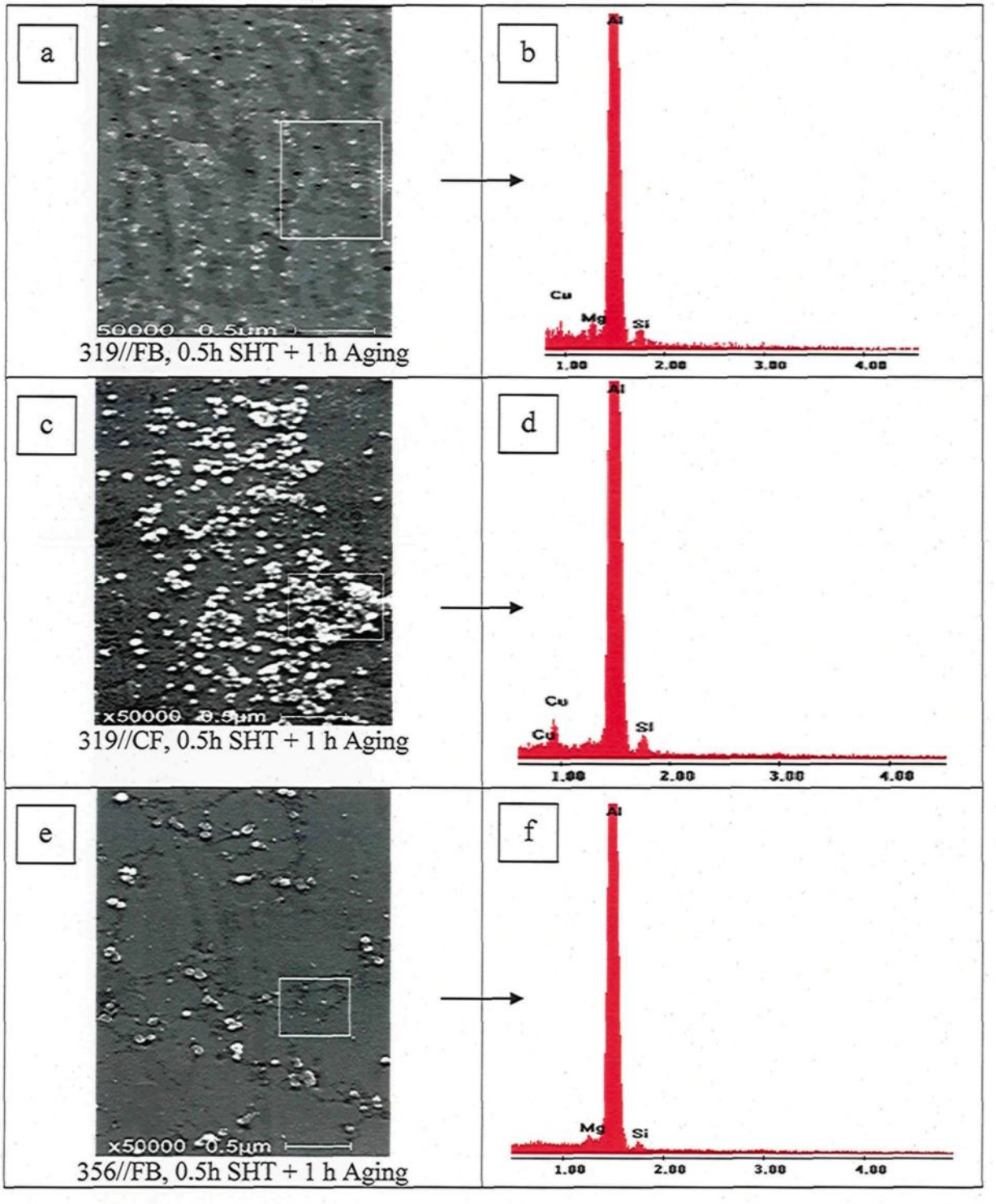

Figure 4.8. FEGSEM micrographs of 319 and 356 alloys after 0.5 h SHT and 1 h of aging. Note that the black spots observed in matrix (a) correspond to undissolved Mg_2Si while the bright spots correspond to Al_2Cu precipitates.

4.2.4. Hardening Precipitates

The present subsection will discuss the influence of high heating rate in an FB on the characteristics of hardening precipitates obtained after aging of 319 and 356 casting alloys. The chemical composition of 319 casting alloys constitutes three hardening elements, namely, copper, magnesium, and silicon. Age-hardening of such Al-Si-Cu-Mg alloys results in the precipitation of the Q-phase and its precursors, which play an essential role in the strengthening of this specific alloy system. In addition to the precipitation of the Q-phase ($Al_5Cu_2Mg_8Si_6$), several others, such as θ-Al_2Cu, β-Mg_2Si, S-Al_2CuMg, σ-$Al_5Cu_6Mg_2$ and their precursors, are also expected to precipitate during age-hardening treatment of B319 type Al-Si-Cu-Mg alloys; the Cu-containing precipitates such as Q-phase and θ-Al_2Cu are the main strengthing particles obtained in the T6-tempered B319.2 alloys investigated in this study. The composition of the 356-Al-Si-Mg alloys contains two efficacious hardening elements, namely, magnesium and silicon. The objective of applying aging treatment to these castings is to precipitate the excess Mg and Si out of the supersaturated solid solution in the form of hardening phases containing Mg and Si; Mg_2Si is the main strengthing phase obtained in the T6-tempered 356 casting alloys investigated. The Mg_2Si precipitates could be seen in the matrix of aged samples, and appeared as oval-shaped grey particles; as shown in Figure 4.9, the oval shape being possibly related to scanning beam diameter-related effects of the FESEM used to detect these precipitates.

The size and density of the precipitates formed at specific aging temperatures and times for non-modified A356.2 and B319.2 alloys are shown in Figures 4.9 and 4.10, respectively. The microstructures of both FB and CF aged alloys contain fine precipitates

of Mg_2Si and $Al_5Cu_2Mg_8Si_6$ for the A356.2 and B319.2 alloys, respectively; these phases were identified by their EDX spectra. Solution treatment and aging times were selected based on results reported in an extensive study on the performance of Al-Si cast alloys heat treated using an FB, where the fluidized bed heat treatment of 319 and 356 alloys produces better strength values after solution heat treatment times of up to 5 h and aging times of up to 5 h compared to those heat treated using a conventional furnace.[147]

Figure 4.9 shows FEGSEM images illustrating the characteristics of the Mg_2Si precipitates which were formed after 5 h solution heat treatment and 5 h aging using an FB and a CF. Particles of Mg_2Si were detected from the EDX spectrum shown in Figure 4.9 (c) which indicates the presence of two Mg and Si peaks at a ratio of 2:1, together with the presence of an Al peak which was picked out from the matrix. The EDX spectrum indicates that the gray particles are Mg-Si containing precipitates which denote the presence of Mg_2Si phase, whereas the bright coarse particles are silicon precipitates formed during the aging procedure in the final stage of phase transformation. The precipitation of silicon in the Al-Si-Mg alloys was reported by Murayama *et al.* [117] and Gupta *et al.*, [118] where it was observed that silicon precipitates form during the aging cycle in the final stage of the phase transformation process. The microstructures reveal the Mg_2Si as uniformly distributed spherically-shaped particles; such spherical Mg_2Si particles were also observed in other studies. [136, 146]

It is possible to show that the fluidized bed produces a large number of finely distributed Mg_2Si particles compared to the convection furnace; this difference in particle density clearly implies the higher precipitation kinetics of aging in an FB. The lower

number of Mg_2Si particles after applying T6 temper using a CF may be related to the long solution heat treatment at the low heating rate which consequently reduces the concentration of defects such as dislocations; it should be noted that such defects act as suitable sites for Mg_2Si nucleation. From these observations, it is apparent that the nucleation rate of Mg_2Si is greater when aged using the FB in which it is much more affected by the high heating rate than in the CF even if for a long aging time.

Figure 4.10 presents SEM images showing the microstructure of 319 alloys aged using an FB *versus* a CF. The precipitation hardening of B319.2, or Al-Si-Cu-0.3%Mg, alloys is a complicated process because of the variety of phases which are expected to precipitate during aging. The precipitates that may be formed are β-Mg_2Si, θ-$CuAl_2$ and Q-$Al_5Cu_2Mg_8Si_6$. Figures 4.10 (a) and (b) illustrate that applying a heat treatment of 5 h solution treatment followed by 5h of aging using an FB results in the precipitation of finer and a greater amount of precipitates in the metal matrix than when using a CF. This difference in precipitation rate may be related to the stability of the GP zones or the clusters of Cu-Mg-Si during the heating-up stage before isothermal aging using an FB. The stability of these zones/clusters is the result of the high heating rate of the FB which does not provide sufficient time for the dissolution of the GP zones. It has been reported that there is a direct relationship between the heating rate and the radius of the clusters during aging treatment. The high heating rate in a fluidized bed leads to the formation of more stable clusters, or GP zones, during the heating-up stage prior to reaching the aging temperature. These clusters can act as suitable sites for the heterogeneous nucleation of further precipitates. [147]

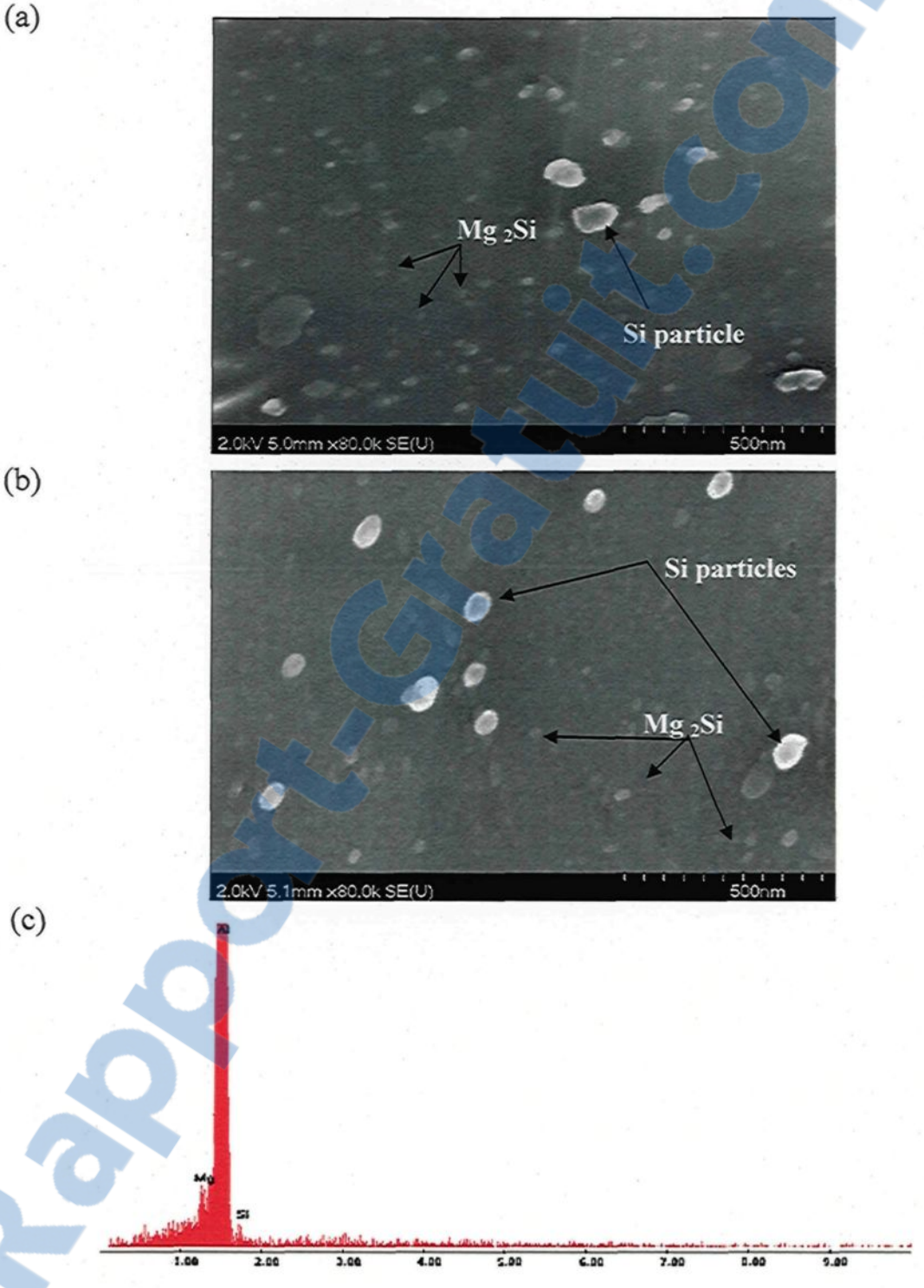

Figure 4.9. FEGSEM micrographs of 356 alloy after 5 h SHT and 5 h aging in (a) FB, (b) CF, and (c) EDX spectrum corresponding to (a).

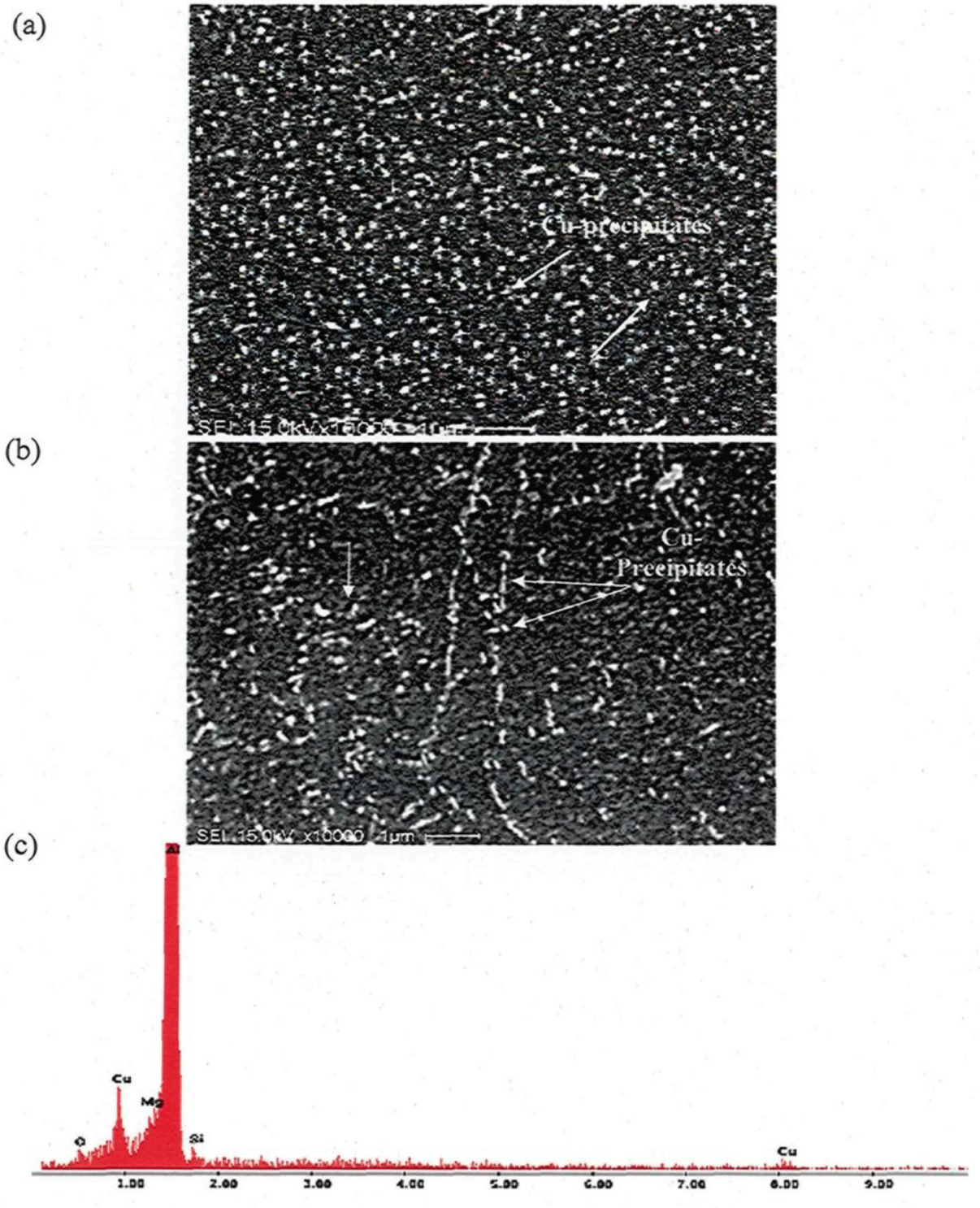

Figure 4.10. SEM micrographs of 319 alloy after 5 h SHT and 5 h aging in (a) an FB, (b) a CF, and (c) EDX spectrum corresponding to (a).

The EDX spectrum presented in Figure 4.10 (c) shows the composition of the phases precipitated during the aging treatment of the 319 alloys, revealing that the precipitates contain Cu, Mg, and Si in addition to Al. The precipitates shown are most probably those of the Q-$Al_5Cu_2Mg_8Si_6$ phase, although other phases such as $CuAl_2$ and Mg_2Si may coexist in the matrix. The main objective for using SEM techniques in this study was to provide an overview of the density and distribution of the precipitates under the effects of the high heating rate in an FB.

4.3. TENSILE PROPERTIES

Tensile properties, UTS, YS and $\%E_f$, were obtained for evaluating the influence of metallurgical parameters on the mechanical performance and quality indices of T6-tempered B319.2 and A356.2-types casting alloys. These parameters include solutionizing time, aging time, melt treatment and heating rate using two different heat treatment techniques, namely FB and CF. The FB technique may speed up the heating rate, thus reducing the time required to arrive at the selected solutionizing and aging temperatures. In addition to saving heat treatment time using an FB, which is very useful from an economical point of view, the high heating rate in an FB has a significant effect on the density and uniformity of hardening precipitates as well as the eutectic silicon characteristics as discussed previously in the subsection on microstructure characterization. This subsection will aim at elucidating the microstructure-tensile property relationships obtained for FB and CF heat-treated casting alloys.

4.3.1. Al-Si-Mg Alloys

Figures 4.11 and 4.12 display the UTS and YS values of non-modified and modified 356 alloys, respectively, for as-cast and all heat-treated conditions. As may be seen, both UTS and YS values increase with an increase in aging time for all solution heat treatment conditions/times studied. The continuous increase in the strength values with the progress of aging time up to 12 h in both CF- and FB-treated samples may be attributed to the natural aging step applied at room temperature for 24 h before carrying out artificial aging at 155°C. This natural aging step leads to the formation of a high density of GP zones which act as nucleation sites for the Mg_2Si precipitates that form in the subsequent aging step.[55, 183]

It should be noted that the fluidized bed produces better strength results than the conventional furnace after aging at 155°C for short aging times of 0.5 h and 1 h, as well as for the longer aging time of 5 h. The fluidized sand bed shows a significant increase in strength results through prolonged solution heat treatment times of up to 8 h; such results can be explained by the high heating rate of the fluidized bed which activates the rate of precipitate formation giving rise to a high density of precipitates. It has been reported [55] that the dislocation concentration in the matrix affects the aging kinetics of Mg_2Si precipitation; the slow heating rate in a CF annihilates the dislocations through recovery, thereby reducing their density prior to reaching the aging temperature. The dislocations are known to be potential sites for Mg_2Si precipitates which would lead to a pronounced improvement in mechanical performance following artificial aging procedures. [55, 56]

From Figures 4.11 and 4.12, it will be noted that both the UTS and the YS of 356 alloys which have been heat treated using an FB increase by 27-36% compared to the as-cast alloy within 30 minutes of solution heat treatment and after 30 minutes of aging. In addition, the strength results show that using the fluidized bed for a solution heat treatment of 0.5h followed by aging for 0.5-1 h would provide similar strength values, or even slightly better ones, compared to those obtained after long solution heat treatment times of 5 and 8 h followed by aging for 0.5-1 h using the conventional furnace. A fluidized sand bed thus provides improved strength results while also saving on the heat treatment time and energy consumption required for the heat treatment procedure since only 0.5-1 h of solution treatment is required in a fluidized bed for achieving optimum strength values (*cf.* 8 h with a CF).

The fluidized sand bed also provides higher strength values than a CF does after an aging time of up to 5 h. This difference in strength values can be explained by the formation and stability of GP zones in the initial stage of aging as well as by the rapid rate of aging kinetics in an FB which results in a greater nucleation rate of Mg_2Si particles. However, the difference in strength values between FB- and CF-treated samples loses its significance after 8 h and 12 h aging for all solution treatment time cycles, particularly so for the 8 h and 12 h solution treatment times; these observations may be related either to the dissolution of meta-stable phases or to the faster coarsening rate of the Mg_2Si precipitates after 8 h of aging in the fluidized bed. [135] With regard to the yield strength, it will be observed that the YS values were more responsive to artificial aging as demonstrated by a nearly vertical rise in YS after 5 h of aging, as compared to the UTS values. This response

is related to the tendency of the yield strength to be influenced more by the microstructural condition of the alloy, and less affected by the soundness of the casting compared to the ultimate tensile strength. [77]

In general, the aging behavior of the 356 casting observed when aging at 155°C is related to the precipitation of the various precursors of the Mg_2Si phase in the metal matrix according to the aging time applied. The early increase in the strength of the alloy is related to the formation of individual clusters of Mg and Si, as well as to co-clusters of the same hardening elements, and to the GP zones. The peak-strength obtained at 12 h is related to the formation of the coherent β"-precipitate which is considered to be the main causative source of strength in the Al-Si-Mg alloys. [184, 185]

Figures 4.12 and 4.13(b) indicate that the modified alloys produce better strength and elongation results, respectively, than the non-modified ones; the nucleation rate of Mg_2Si particles is greater in the modified alloys than it is in the unmodified ones. [35, 49, 55] The acicular morphology of the Si platelets in the eutectic, as shown in Figure 4.4(a), promotes the development of stress raisers at the edge tips in the softer phase, leading to low ductility in the unmodified alloy. This is thought to occur by a simple void formation mechanism at the needle edges of the eutectic Si particles, leading rapidly to crack formation by void coalescence. The modification of the alloy through the addition of Sr leads to the development of a spheroidized eutectic structure, as shown in Figure 4.4(e, f). The Si phase in the eutectic develops into a globular structure and improves the mechanical properties considerably by virtue of an even distribution of the stress around these hard particles; this geometrical change also leads to the disappearance of stress raisers. The

addition of Ti and Sr enhances the favorable effects of both elements in the microstructure, thereby leading to a general improvement in the tensile properties compared to the untreated base alloy.

Figure 4.13 shows the variation in elongation for 356 non-modified and modified alloys, obtained after continuous aging over the same range of solution heat treatment times. As shown in the figure, the elongation values are improved upon going from the as-cast condition to the solution heat-treated one for all solution times studied, at an early stage of aging, namely, 0.5 h. It is also seen that the FB treatment produces better elongation results than the CF treatment over all the aging times imposed. The difference in elongation results between FB- and CF-treated samples is more significant at solution treatment times of 5 h and 12 h. The improvement in the elongation values of the modified alloys is related to the fragmentation and spheroidization of the acicular Si particles and Fe intermetallics through Sr-modification and through the high heating rate prevailing in the fluidized bed. This high heating rate activates the process of the thermal modification of eutectic Si and Fe intermetallics. [147] It may be observed from the plot that the elongation values of alloys aged in an FB increase initially for the first 30 minutes of aging for all the solution treatment times studied, and then they decrease steadily. The decrease in elongation values may be related to the precipitation of Mg_2Si, which hinders the dislocation motion during tensile testing thereby reducing the ductility.

From the point of view of microstructure, the eutectic structure of Al-Si alloys consists of Si particles, as a second phase, embedded in the Al matrix, implying that particle size has a significant influence on the fracture strain. A theoretical analysis by

Saigal *et al.* [186] showed that the stress or strain required to break a particle varied inversely with the particle size, which would signify that the void nucleation strain is higher for fine particles; failure takes place when the void grows to a critical size. Since the failure strain is inversely proportional to void growth rate, it may be suggested that this growth rate is lower in the modified alloys than it is in the unmodified ones. Thus, an increase in the void growth strain should be expected, which would, in turn, increase the fracture strain. The fine fibrous Si morphology of the modified alloys would thus influence the strain sustained to fracture by increasing the void nucleation and void strain simultaneously.

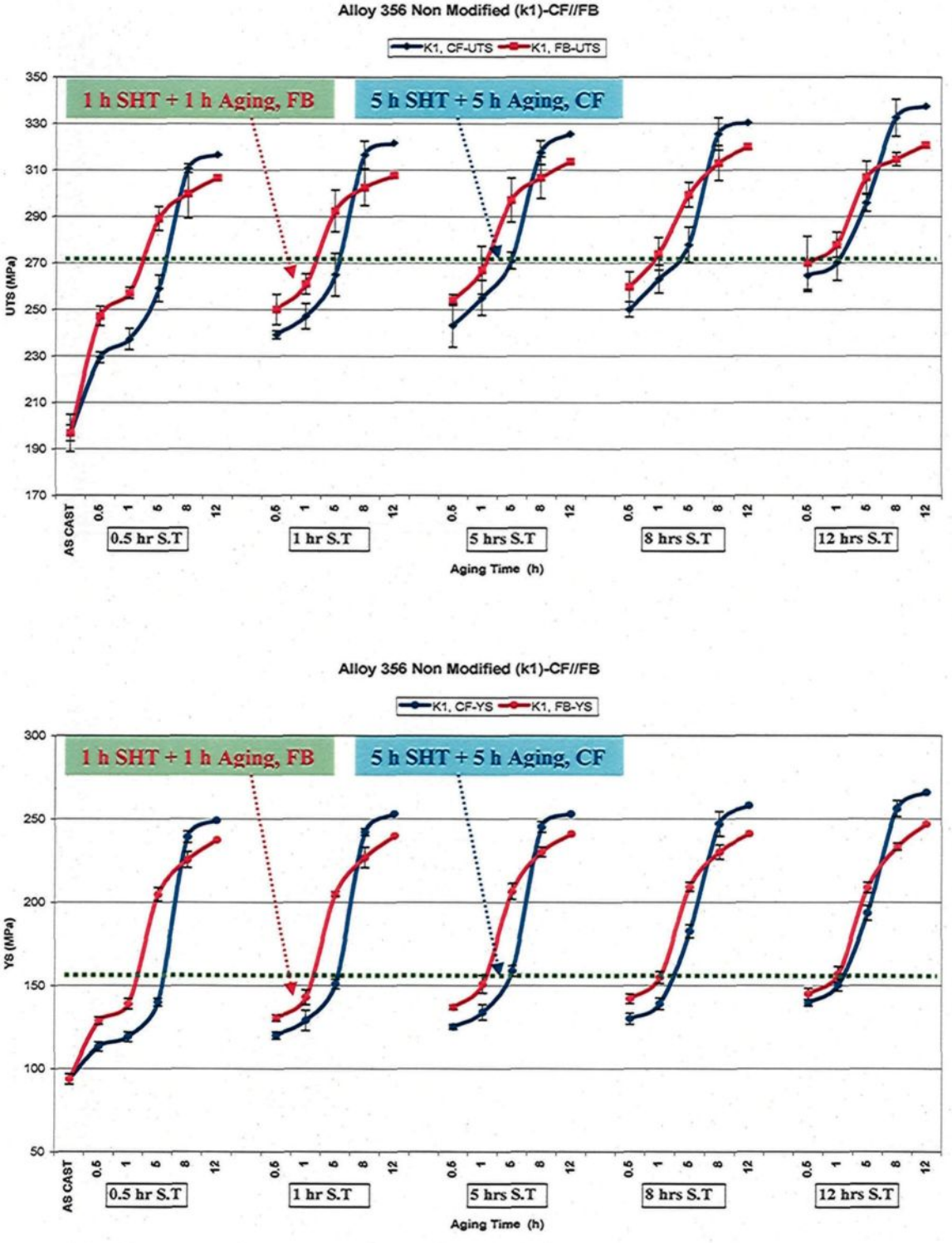

Figure 4.11. Average UTS and YS values for non-modified 356 alloys.

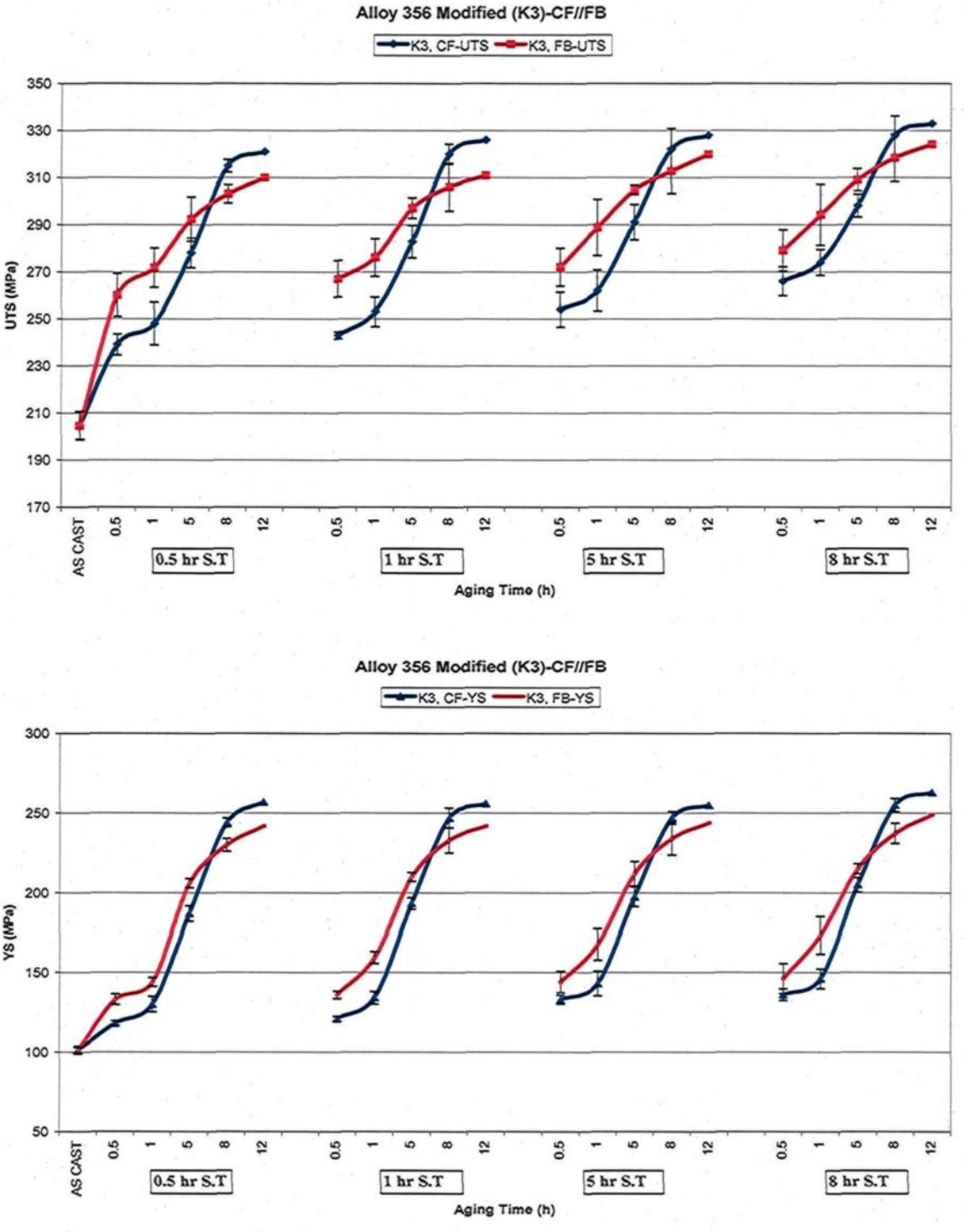

Figure 4.12. Average UTS and YS values for modified 356 alloys.

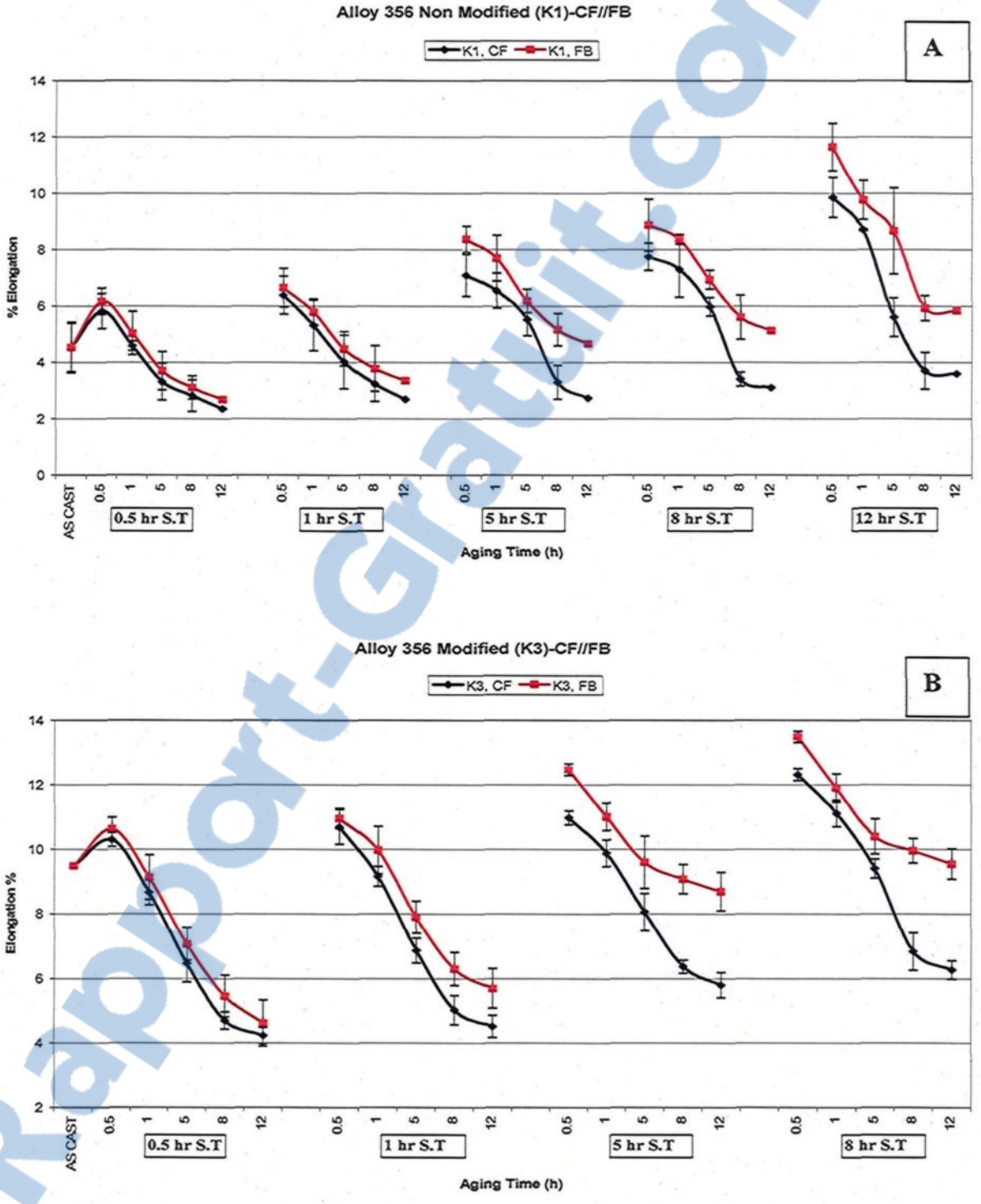

Figure 4.13. Average values of percentage elongation (%El) for 356 alloys: (a) non-modified K1 alloy, and (b) modified K3 alloy.

4.3.2. Al-Si-Cu-Mg Alloys

In general, an improvement in the mechanical properties of Cu- and Mg-containing aluminum alloys is attributed to the formation of the age-hardening compounds Al_2Cu and Mg_2Si, respectively, which precipitate from the solid solution during aging. The degree of strengthening depends on the copper and magnesium content, and an increase in strength due to higher copper and magnesium levels is always accompanied by a corresponding decrease in ductility. The application of an aging treatment to these alloys causes an entire range of precipitates to form according to the temperature and time applied.

Figures 4.14 and 4.15 illustrate the variation in the ultimate tensile strength and yield strength values of non-modified and modified 319 alloys, respectively, as a function of various solution heat treatment time cycles, from 0.5 h up to 24 h. The fluidized bed heat treatment produces better strength values after 0.5 h, 1 h and 5 h aging than those obtained by using the conventional convection furnace for solution heat treatment times of up to 8 h. This difference in strength values is related to the high precipitation rate of $Al_5Cu_2Mg_8Si_6$ and $CuAl_2$ phase particles in the FB-treated samples as opposed to the CF-treated ones, as also to the dissolution of GP zones during the heating-up period to the isothermal aging temperature in the conventional convection furnace. [147]

It may be observed that the optimum strength values for the heat-treated samples using a CF are obtained after 8hrs of aging, followed by a slight decrease in strength as a result of overaging, whereas with the FB treatment, a continuous increase in these values is observed up to 12 h of aging. This upward trend in strength values may be related to the stability of the GP zones and/or of the intermediate precipitates in the early stages of aging

when using a fluidized bed. [145, 147] The peak strength attained after 8hrs aging in a CF or 12 h aging in an FB may be related to the presence of hardening phases such as θ'-$CuAl_2$ + Q'-($Al_4Cu_2Mg_8Si_5$). [187, 188] The strength values obtained after 1 h solution heat treatment + 1 h of aging using a fluidized bed show similar or slightly better values compared to the ones obtained after long solution treatment times, namely, 8 h, 12 h, and 24 h, followed by 1 h of aging using a conventional furnace. In general, the fluidized bed technique provides higher strength values than a convection furnace does for solution heat treatment times of up to 8hrs; beyond that, no noticeable difference is observed between the two techniques.

From both sets of strength results, it will be observed that the UTS and YS of 319 alloys which have been heat treated using an FB increase by 20-34% compared to the as-cast alloys after 30 minutes solution heat treatment and 30 minutes aging. On the other hand, the UTS and YS results of 319 alloys which have been heat treated using a CF tend to increase by only 6-8% compared to the as-cast alloys within the same short period of time. The high heating rate of the FB has a significant influence on the heat treatment characteristics of 319 alloys resulting in higher strength values after short heat treatment times. The high rates of heat transfer upon increasing the heat treatment temperature makes it possible to optimize and reduce treatment cycle times.

In regard to the general aging behavior of the B319.2 alloys investigated, the increased strength when applying aging treatment at 180°C for up to 12 h is related to the precipitation of the GP zones followed by the formation of coherent and semi-coherent precipitates. These precipitation sequences result in an increase in the strength of the castings up to the point of attaining the maximum level of strength at peak-aging, which

occurs at 8 h using a CF and at 12 h using an FB. At 180°C, for an aging time beyond 8 h, the decrease in the strength values of the 319 castings is attributed to the loss of coherency strain surrounding the precipitates. The disappearance of the coherency strain accompanies the formation of the incoherent equilibrium precipitates such as the plate-shaped β, the platelike θ, and the rod-shaped Q phases. The formation of these equilibrium phases results in a reduction in the strength values of the alloys, as may be seen in Figures 4.14 and 4.15.

Figures 4.15 and 4.16 indicate that the modified and grain-refined alloys produce better strength and elongation results than the non-modified ones by ~ 20 MPa and 0.6 %, respectively. This observation indicates that the combined addition of grain refiner (Al-5%Ti-1%B) and modifier (Al-10%Sr) to the base alloy refines the α-Al grains, and modifies the eutectic plate-like silicon into finer, spheroidized particles which, together with the fine eutectic-like Al_2Cu particles present in the interdendritic region result in improved mechanical properties. Higher strength and ductility values of modified alloys may be attributed to two significant factors which minimize the occurrence of voids and limit cracks raisers. The first is achieved by developing microstructures capable of avoiding stress amplification factors, namely, the absence of such stress raisers as acicular eutectic Si and angular primary Si particles. The second factor responsible for retarding void coalescence and crack propagation through the cross-section of a tensile specimen is the grain size of the α-Al present. As the grain size decreases, secondary phases and porosity become more widely dispersed, and as a result, a fine grain size results in an improvement of the mechanical properties of the alloys. [6, 24, 164, 170] Figure 4.16 shows the elongation values for the non-modified and modified 319 base alloys after T6 heat treatment for

continuous aging cycles over the same range of solution heat treatment times. As can be seen from this plot, elongation values are improved on going from the as-cast to the solution heat-treated condition for various solution time durations followed by aging for 0.5 h. The improvement of elongation values in the modified alloy may be related to the fragmentation and spheroidization of the Si particles and Fe intermetallics obtained through Sr-modification and the high heating rate prevailing in the fluidized bed as discussed previously. Figure 4.16 also shows that no noticeable difference in elongation values over aging time is obtained using either technique, except that the FB-treated samples show slightly better results than the CF-treated samples after 0.5 h aging. The elongation values decrease thereafter, with further aging time; the loss of ductility may be related to the strengthening effect associated with the precipitation of the Q'-$Al_4Cu_2Mg_8Si_5$ phase.

It may be seen from the tensile results that B319.2 casting alloy is significantly stronger but less ductile as compared to A356.2 alloy; the noticeable difference in strength and ductility values between the alloys investigated may be related to the higher Cu and Mg contents of the B319.2 alloys which are the main source of the increased strength and the decreased ductility of these castings when compared to the same properties in the A356 alloys after being subjected to the same aging treatments. With respect to the ductility results of the alloys investigated, the presence of a higher Fe content in the B319.2 casting alloys as compared to the A356.2 alloys, *i.e.* 0.4186 and 0.075 wt%, respectively, results in the formation of a greater volume fraction of undissolved Fe-intermetallics which have detrimental effects on the alloy properties, and reduce their elongation values.

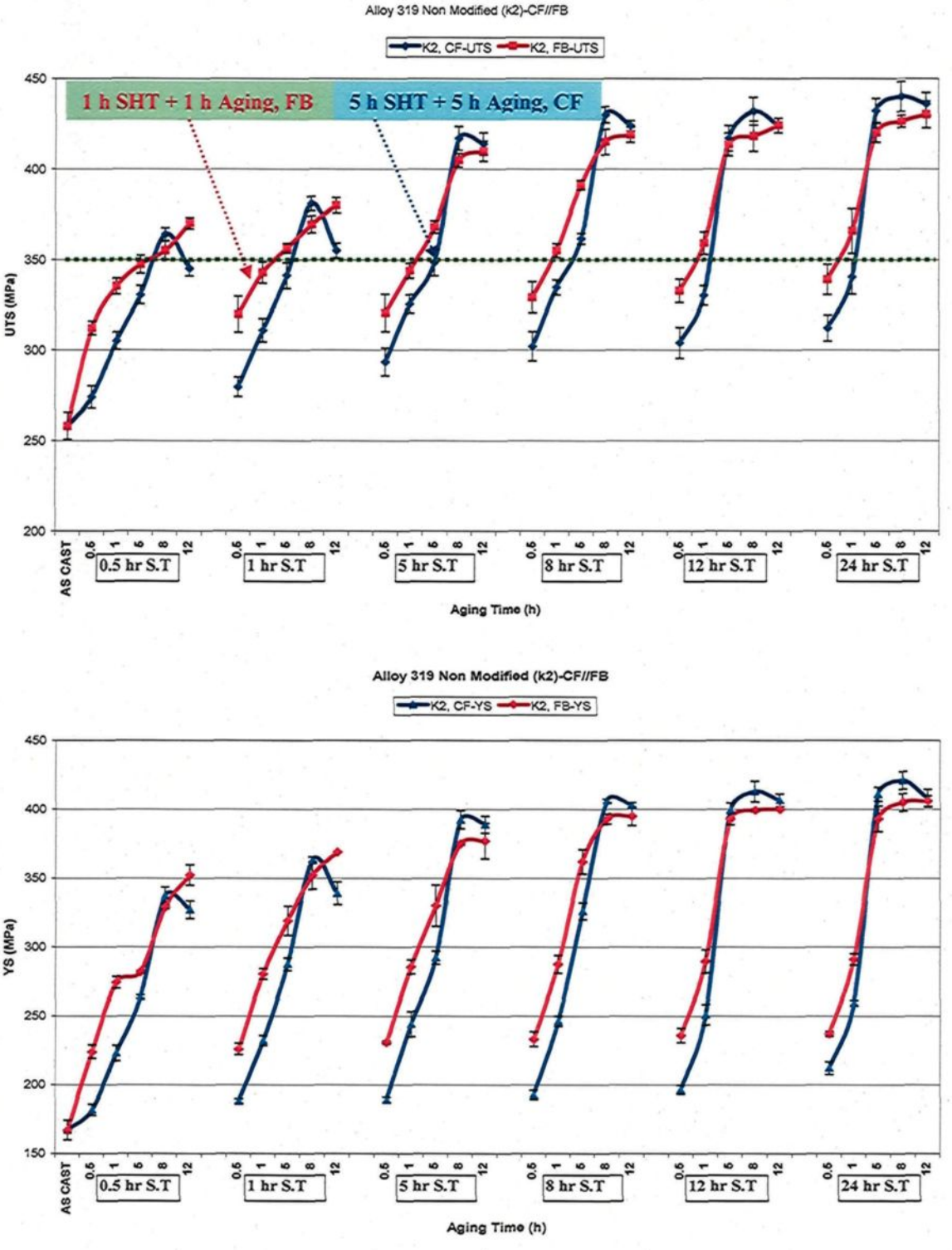

Figure 4.14. Average UTS and YS values for non-modified 319 alloys.

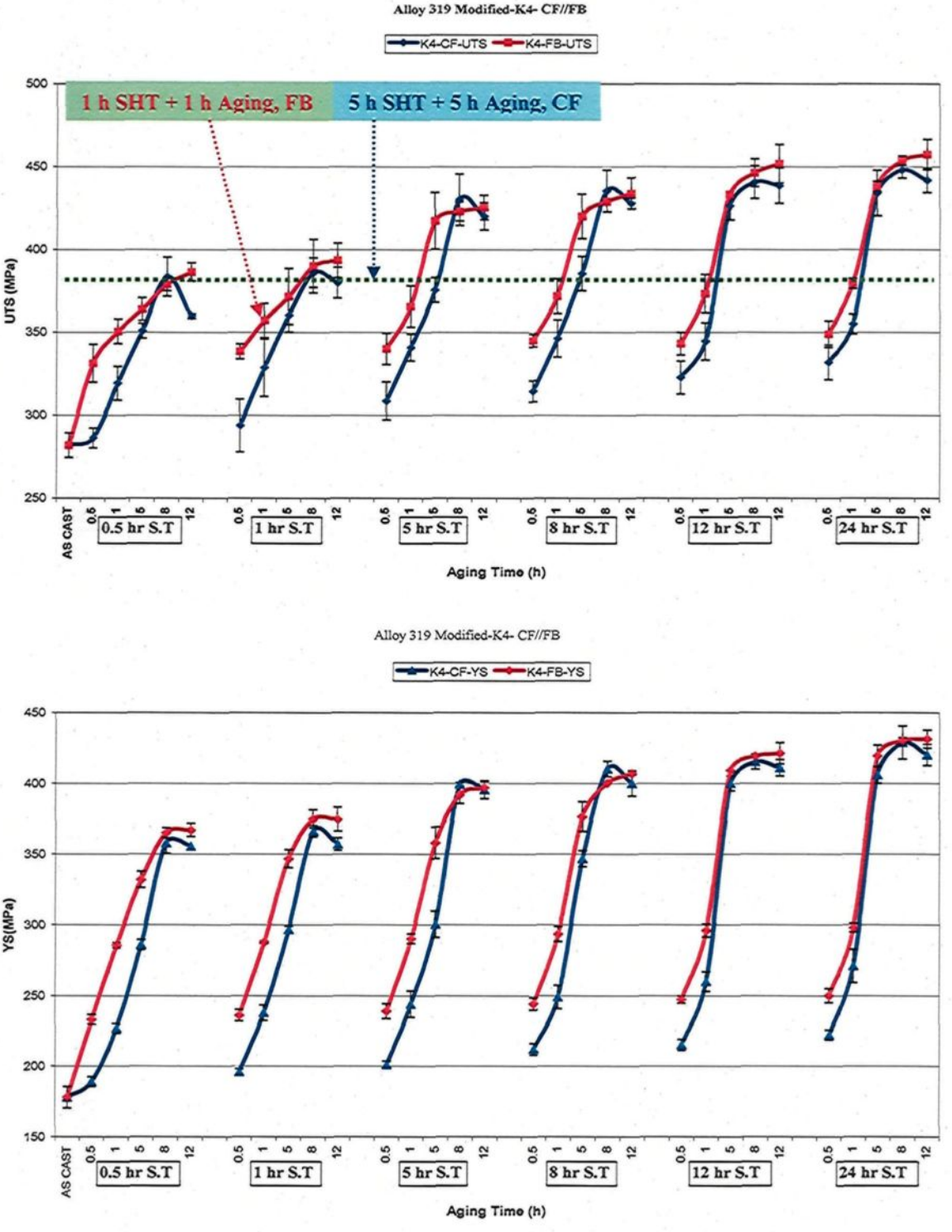

Figure 4.15. Average UTS and YS values for modified 319 alloys.

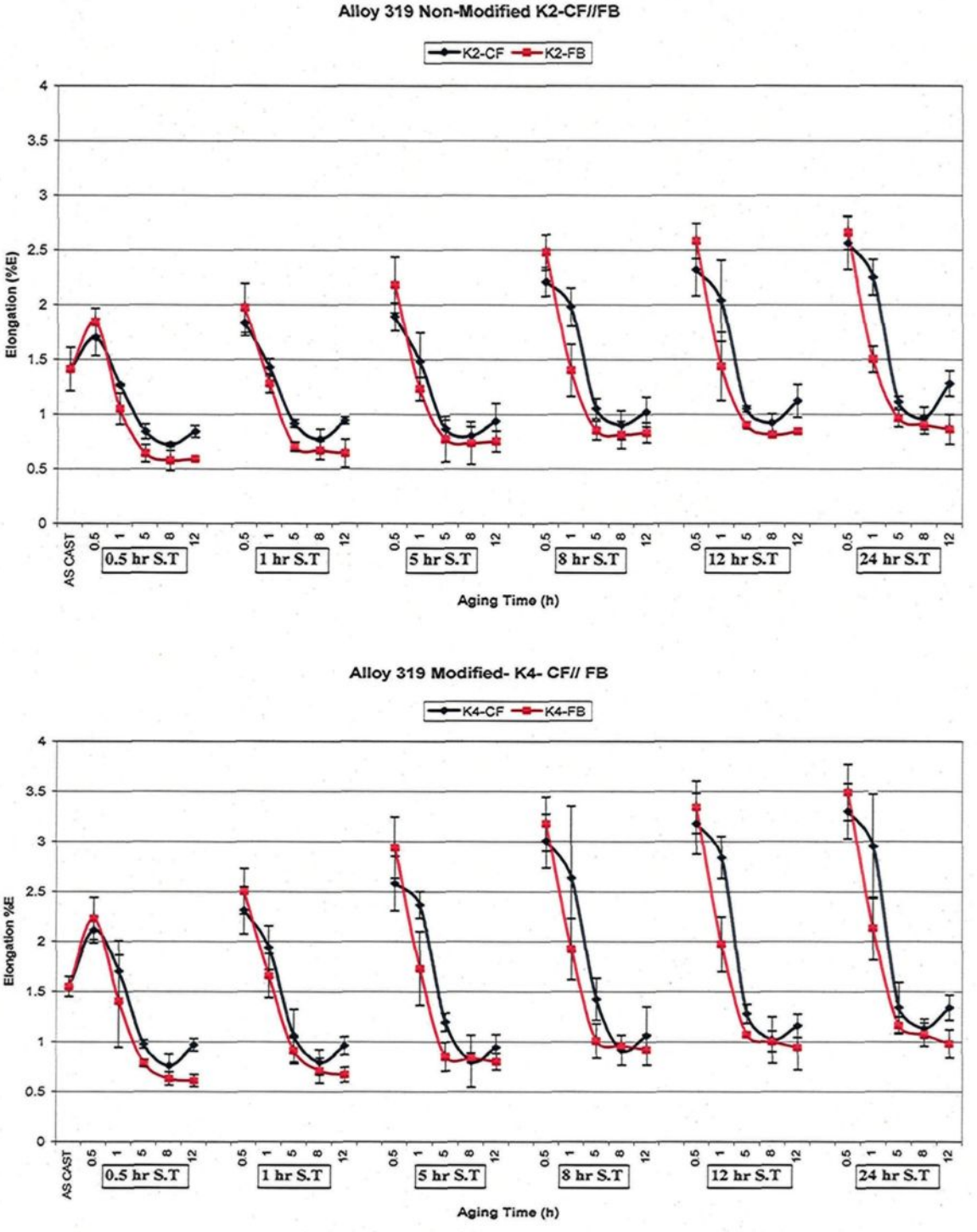

Figure 4.16. Average values of percentage elongation (%El) for 319 alloys: (a) non-modified K2 alloy, and (b) modified K4 alloy.

4.4. ANALYSIS OF QUALITY CHARTS

In the present study, an attempt was made to elucidate the effects of FB versus CF heat treatment techniques as well as melt treatment and heat treatment parameters on the quality performance of A356.2 and B319.2 casting alloys using quality index charts. Such quality charts have often been used in conjunction with heat treatment studies of aluminum alloys, to make it possible to determine the optimum heat treatment conditions needed for obtaining specific properties in a cast component. The evaluation of the results will be carried out using the quality charts based on two models of quality indices, namely, those of Drouzy *et al.* and Cáceres. [155, 156, 157, 158] Accordingly, all the pertinent results will be presented using two types of charts, based on the tensile properties available for each point located in these charts. Generating these specific charts would provide a factual logic-based evaluation of the effects which various parameters may have on the tensile properties and quality indices of the castings under study. The effects of the heating rate corresponding to each heat treatment technique on the quality of the alloys investigated will be studied during a T6 heat treatment applied for several solution heat treatment time cycles.

4.4.1. Al-Si-Mg Alloys

Two models of quality charts were selected for evaluating the influence of metallurgical parameters on the quality indices of non-modified and modified A356 casting alloys. These charts are provided in Figures 4.17 and 4.18. Equations 5 and 6 were used to generate *iso-Q* lines and *iso-yield strength* lines, respectively, in the quality charts shown in Figure 4.17. Equations 10 and 11 were used to generate *iso-flow* lines and *iso-q* lines,

respectively, in the quality charts shown in Figure 4.18; the *Q*-values presented in these charts were determined by applying Equation 13.

Figures 4.17(a) and (b) show the effects of modification and aging parameters on the quality of A356 alloys after 0.5 h and 8 h solution heat treatment in a fluidized bed versus a convection furnace. From the quality maps shown in Figure 4.17, generated using equations (5) and (6), it may be observed that the modified 356 alloys show an improvement in quality values by 50 MPa over the non-modified alloy for all aging times. The main purpose of Sr addition to Al-Si-Mg alloys is to change the morphology of eutectic silicon from an acicular form into a fibrous one resulting in improved ductility and strength with high quality values. In addition to the effect of Sr, the fluidized sand bed has a significant effect on Si particle size, reducing it to more than half after 0.5 h of solution heat treatment as has been soundly discussed in an extensive study. [147] Figure 4.17 (a) shows the positive effects of using a fluidized bed for heat treatment with regard to the UTS and the quality values of the modified and non-modified alloys investigated, for which the quality values produced by a fluidized bed are better than those obtained by a convection furnace through aging times of up to 5 h. Also, it should be noted from the preceding that the quality values produced after only 1 hr of aging using a fluidized bed are better than those obtained after 5 h aging in a convection furnace for non-modified and modified alloys. Figure 4.17 (b) shows that the fluidized bed heat treatment is more effective than that of a convection furnace for producing high quality values through all aging time periods of up to 12 h after a solution heat treatment time of 5 h. The high

heating rate in a fluidized bed activates the precipitation rate and produces more precipitates after a short aging time, as shown previously in Figure 4.9.

Figure 4.18 shows the effects of solution heat treatment time on the quality and mechanical properties of a T6 tempered 356-type non-modified alloy. The quality charts in Figure 4.18 were generated using Equations 10, 11, and 13. The main objectives of the solution heat treatment procedure are to dissolve most of the hardening elements in solid solution such as Mg_2Si and to change the morphology of acicular eutectic silicon to fragmented and spheroidized particles. The solution heat treatment is applied at specific temperatures for specific periods of time to provide a chance for the fragmentation and dissolution of undissolved phases, namely Fe-intermetallics, and to achieve a homogeneous structure for improving the ductility and the quality of Al-Si cast alloys. [189, 190] It may be noted that the increase in solution heat treatment times of up to 8 h and 12 h provides an improvement in the quality values for modified and non-modified alloys, respectively, as shown in Figures 4.17 and 4.18. The effects of solution heat treatment time on the strength values of T6 tempered alloys is not significant, considering that the strength values display no major changes as the quality performance does upon increasing the solution heat treatment time periods. The solution heat treated samples using a fluidized bed show better strength and quality results after aging times of up to 5 h over all solution heat treatment times as compared to heat treated alloys using a convection furnace.

With regard to the effects of aging time, it will be noted that there is no significant change in the quality behavior over all the aging times studied. Aging behavior at 155°C for up to 12 h is quasi-parallel to the *iso-Q* lines, as will be observed in the quality charts

shown in Figures 4.17 and 4.18. This behavior illustrates that aging time up to peak-strength does not affect the quality index values of the 356 castings. Such an observation is related to the fact that increasing the aging time up to 12 h results in a continuous increase in the strength of the casting at the expense of its ductility, although the increase compensates for the reduction in ductility in accordance with Equation 5. Thus, the net effect of this aging treatment ultimately leads to non-significant changes in the quality index values. It has been reported that the quality index is not greatly dependent on the tempering conditions compared to the strength values which depend on the aging parameters. [167] The UTS and YS values increase with an increase in aging time over all the solution heat treatment times studied for the non-modified and modified alloys. As it has been mentioned before, this continuous increase in strength values throughout aging times of up to 12 h in both CFs and FBs may be attributed to the natural aging step applied at room temperature for 24 h before artificial aging at 150°C. This 24 h natural aging step leads to the formation of a high density of GP zones which act as nucleation sites for the resulting Mg_2Si precipitates.

With regard to the quality charts for the 356 alloys shown in Figures 4.17 and 4.18, it may be observed that both models of quality indices reveal similar behavior in the strength and quality of the alloys investigated with respect to a specific application. The difference between the charts in both figures is the accuracy in calculating the yield strength. As may be seen in Figure 4.17, it may be concluded from the quality charts generated using Equations (5) and (6) that the calculated yield strength values differ by a specific percentage of error, 1-15%, as compared to the actual yield strength values

obtained from tensile testing results. On the other hand, the calculated yield strength in the quality charts shown in Figure 4.18 provides better accuracy values (ranging from 90 to 99%). This difference in yield strength values in Figure 4.18 may be related to the deviation of the strength coefficient value of the material, the K-value, at each point corresponding to a different set of heat treatment parameters from the average K-value for the same alloy. The quality charts shown in Figure 4.18 were generated using Equations (11) and (13) with an average K-value of 465 MPa, where the standard deviation for 356 alloys is $\pm$ 23 MPa.

The quality charts are provided in order to select and recommend the optimum conditions required for specific mechanical and quality properties. It will be noted that the high heating rate in fluidized beds has a positive effect on the improvement of strength and quality values in addition to the positive effect of the other metallurgical parameters such as melt treatment (modification) and solution heat treatment for specific periods of time. With regard to the quality performance of the 356 alloy after aging times of up to 8 h, Figures 4.17 and 4.18 show that the quality results of the 356 alloy are more responsive to the FB heat treatment technique than to that of a CF. It may be observed that the fluidized beds provide an improvement in the quality values of the 356 alloys by 25-30 MPa after aging times of up to 5 h, as compared to the conventional furnace.

With regard to the influence of solutionizing time, it may be noted from the quality charts that a prolonged solution heat treatment time is observed to increase the strength and the quality index values of both modified and non-modified alloys significantly as shown in Figure 4.18. The improvements occurring in the strength and quality of the modified and non-modified 356 casting alloys when increasing solutionizing times is related to the

changes in the microstructural features, namely the homogenization of the cast structure; the changes in the volume fraction percentage, size and morphology of the intermetallic phases; and the changes in the size and morphology of the eutectic Si particles. As outlined in section 4.2.1, increasing the duration of solutionizing time up to 12 h was seen to produce advantageous changes in the size and morphology of the eutectic Si particles for both modified and non-modified 356 castings; this will be clear from the optical micrographs shown in Figures 4.4(a) through (f) for the 356 alloys, which reveal that the size of the Si particles increases whereas their aspect ratio decreases upon increasing the solution heat treatment time for both modified and non-modified 356 alloys.

The addition of strontium to 356 alloys, *i.e.* the K3 alloys, has been observed to affect the response of these castings to solution heat treatment. The principal action of strontium in this particular case is revealed in its effect on the length of time required to attain certain mechanical properties and quality index values in the alloys under study since most of the solutionizing time is spent in modifying the eutectic silicon particles. The effects of Sr-modification as well as the high heating rate of the FB in the current case are technologically significant from the economic point of view because of the need to reduce the required time for heat treatments. The effects of Sr-modification on the quality values response to solution heat treatment tend to decrease when the solutionizing time increases up to 8 h, as will be clear from Figure 4.17 (b). Figure 4.18 (b) illustrates that increasing the solutionizing times from 5 h to 12 h results in a continuous narrowing of the gap between the quality index values of the unmodified 356 castings for each heat treatment technique.

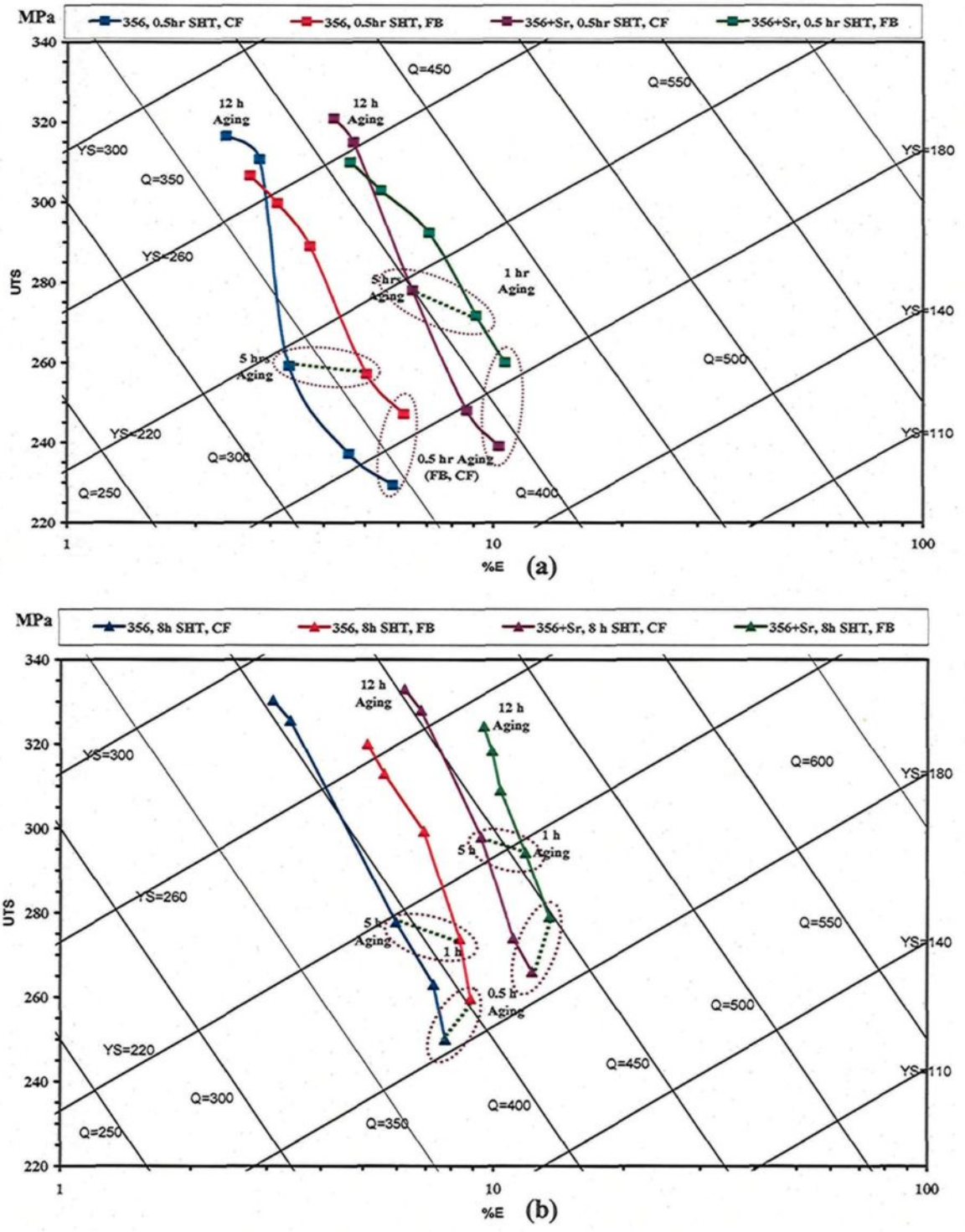

Figure 4.17. Quality charts generated using Equations 5 and 6, showing the effects of modification and aging time on the quality and UTS of T6-tempered 356-type alloys solution heat treated for (a) 0.5h, and (b) 8 h.

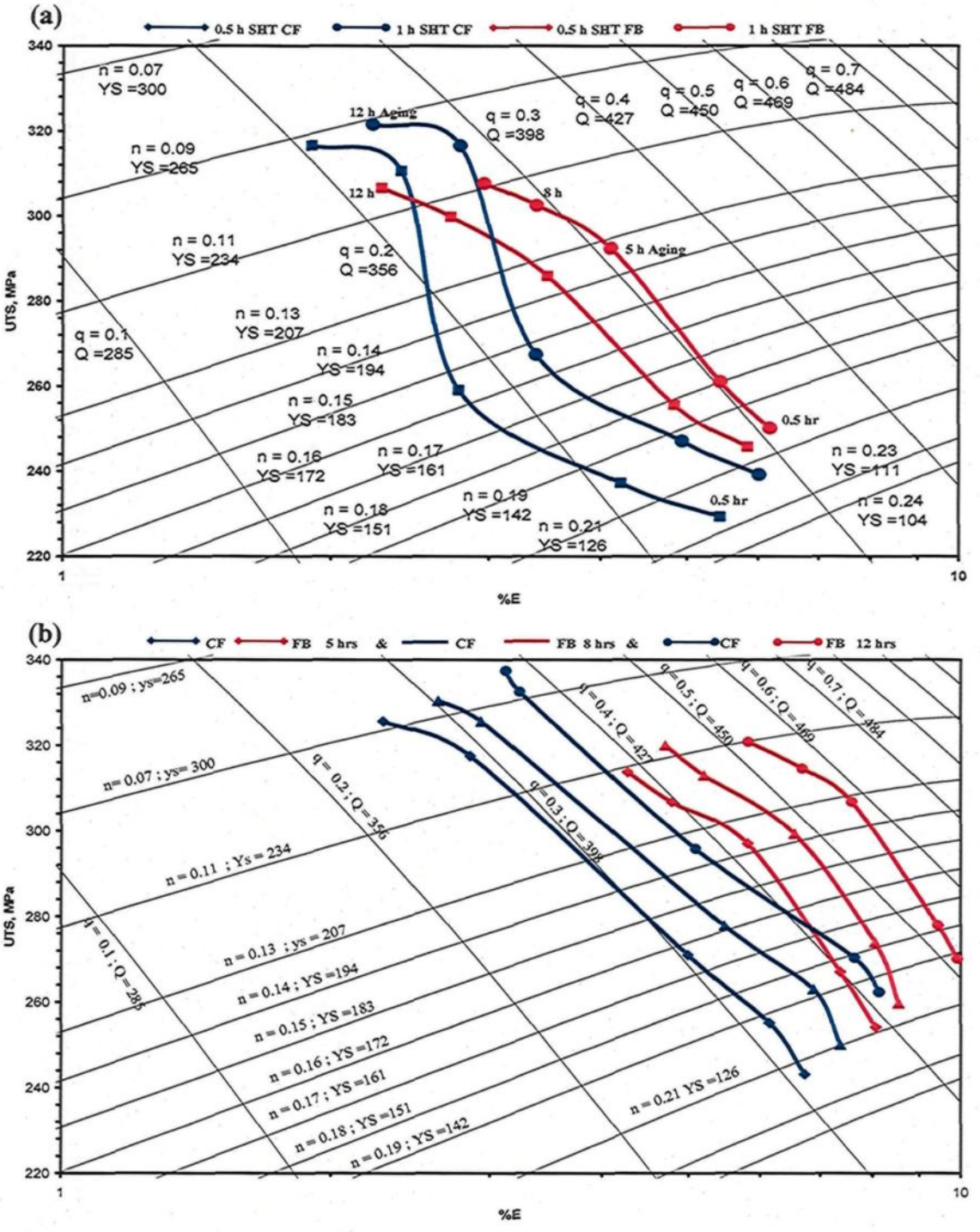

Figure 4.18. Quality charts generated using Equations 11 through 13, showing the effects of solution heat treatment time: (a) 0.5h and 1h, and (b) 5h, 8h and 12h on the quality and UTS of T6 tempered 356 non-modified alloys heat treated using CF and FB techniques.

4.4.2. Al-Si-Cu-Mg Alloys

The present subsection will discuss the influence of heat treatment parameters and melt treatment on the quality index values of the B319.2 casting alloys. The presence of copper in 319-type Al-Si cast alloys contributes to an increase in strength and hardness values although at the expense of ductility. The application of an aging treatment to these alloys causes an entire variety of precipitates to form according to the temperature and time applied. These different types of hardening phases result in a wide variation in strength coefficient values, K, of the heat treated materials depending on the T6 temper parameters. Such a variation in K values has a significant effect on the accuracy of calculated yield strength values obtained from the quality charts compared to the yield strength values obtained from tensile testing. So that, the K values are re-calculated for each heat treatment condition taking the average K value to be used in the quality index values calculations. As in the case of the 356 alloys, improvements in the mechanical performance and quality of such 319 alloys may be obtained by applying Sr-modification (melt treatment) and the application of a high heating rate using a fluidized bed for the relevant heat treatment procedures.

Figures 4.19 through 4.21 show the effects of solution heat treatment time and modification on the strength and quality of T6 tempered 319-type alloys using a fluidized bed *vs.* a convection furnace. The fluidized bed heat treatment produces better quality values than those obtained by using a convection furnace after 0.5 h aging and solution heat treatment for specific times of up to 8 h for modified and non-modified conditions. The quality was greatly affected by the solution heat treatment time and modification, in that the

quality values were significantly improved through increasing the solution heat treatment time by up to 8 h, and as a result of the effect of Sr-modification which transforms the morphology of acicular Si into a fibrous type. For the same solution heat treatment time, the quality values of B319.2 alloys heat-treated in an FB are less than for those obtained using a CF after 1h aging and after long aging times. The FB heat-treated samples show better quality and ductility values, after only a short aging time of 0.5 h, than do those obtained in a CF for the same solution heat treatment times.

The low response of quality values of B319.2 alloys to an FB heat treatment, as compared to 356 alloys, after solution heat treatment times > 0.5 h and aging times from 5 h to 12 h may be related to the high percentage of Fe in the alloy, namely 0.418 wt%, which would form Fe-intermetallics which are know to be detrimental to the alloy properties. These Fe-intermetallics are hardly dissolved even after prolonged solution heat treatment times and/or at high heating rates using the FB heat treatment technique. In addition, as illustrated in Figures 4.7 and 4.8(a), the undissolved $CuAl_2$ and Mg_2Si intermetallics would also reduce the ductility and quality performance of the alloys investigated. The heat-treated samples using a fluidized bed after 1 h of aging provide better quality values compared to the values obtained after a long aging time, namely 5 h, using a conventional furnace for the same solution heat treatment time cycles of up to 8 h. For T6 tempered B319.2 alloys, the fluidized bed technique shows higher strength values than a convection furnace does at solution heat treatment time cycles of up to 8 h; beyond that there is no noticeable difference in strength and quality values between both techniques, whether FB or CF.

With regard to the aging behavior of the B319.2 alloy, Figures 4.19, 4.20 and 4.21 show that increasing the aging time up to peak-strength, i.e., 8 h in a CF and 12 h in an FB, respectively, results in an increase in the alloy strength with a decrease in its quality values for the same solution heat treatment time. However, the aging behavior of the A356.2 alloy is quasi-parallel to the *iso-Q* lines as was described earlier and could be observed in the quality charts shown in Figures 4.17 and 4.18. The aging behavior shows that increasing the aging time does not affect the quality index values of the A356.2 castings which had been heat treated in a CF and an FB. This quality behavior of B319.2 alloys with respect to aging time may be related to the various types of hardening precipitates which affect the K-values required to generate the quality charts; the K-values are affected significantly by the different heat treatment conditions applied to the 319 alloys investigated. In regard to quality, therefore, it may be concluded that the quality values of heat-treated samples of B319.2 alloys are less responsive to an FB than A356.2 alloys after long aging times, namely 5 h and up to 12 h, for all solution heat treatment time cycles.

The precipitation sequences in B319.2 alloys result in an increase in the strength of the castings up to the point of attaining the maximum level of strength at peak aging, which occurs at 8 h and at 12 h using the CF and FB heat treatment techniques, respectively. At aging time beyond 8 h in a CF, a decrease in the strength with an increase in quality index values of the 319 castings is observed, as may be seen in Figures 4.19 through 4.21. This decrease in strength values may be attributed to the loss of coherency strain surrounding the precipitates; the disappearance of the coherency strain accompanies the formation of the incoherent equilibrium precipitates. The increase in the quality at the expense of strength,

for aging times of 8 h and up to 12 h, may be related to the increase in elongation values which has a significant effect on the Q-values as compared to the decrease in strength values for this specific heat treatment condition using a CF, as may be seen from Equation 13.

The aging curves in the case of aging in a CF display curvilinear forms, in the 5-12 h region, as shown in Figures 4.19 and 4.20. This specific form of the aging curves is a result of the overaging conditions which occur upon increasing the aging time for durations longer than the specified peak-aging times. The aging behavior of FB heat-treated 319 alloys is observed to be quasi-parallel to the iso-Q lines in the same region, for solution heat treatment times of up to 24 h as may be seen from Figures 4.19 through 4.21. This behavior illustrates that aging time up to peak strength does not affect the quality index values of the 319 castings. Such an observation is related to the fact that increasing the aging time up to 12 h in an FB results in a continuous increase in the strength of the casting at the expense of its ductility, although the increase compensates for the reduction in ductility in accordance with Equation 13. Thus, the net effect of this aging treatment ultimately leads to non-significant changes in the quality index values.

With respect to the quality values of B319.2 castings after solution heat treatment time conditions of up to 8 h, the Q-index values are reduced by ~45% and ~30% when aging in an FB and a CF, respectively, for aging times ranging from 0.5 h to 12 h as may be seen in Figures 4.19 and 4.20. On the other hand, the 356 castings show no significant change in quality through all the aging times using either a CF or an FB for the heat treatment.

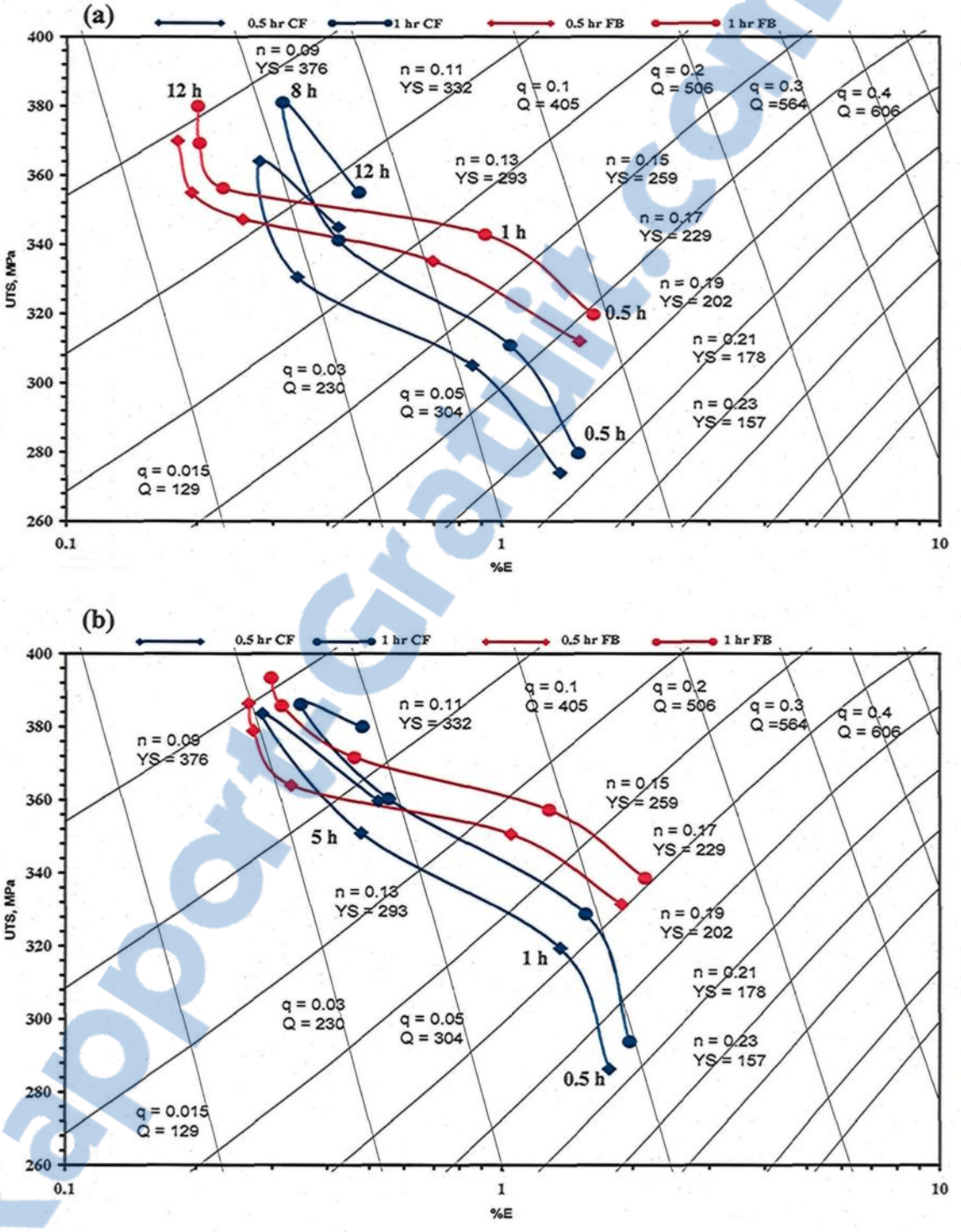

Figure 4.19. Quality charts based on Equations 11 through 13 showing the effects of solution heat treatment time: 0.5h and 1h, and modification on the quality and UTS of (a) non-modified, and (b) modified 319-type alloys.

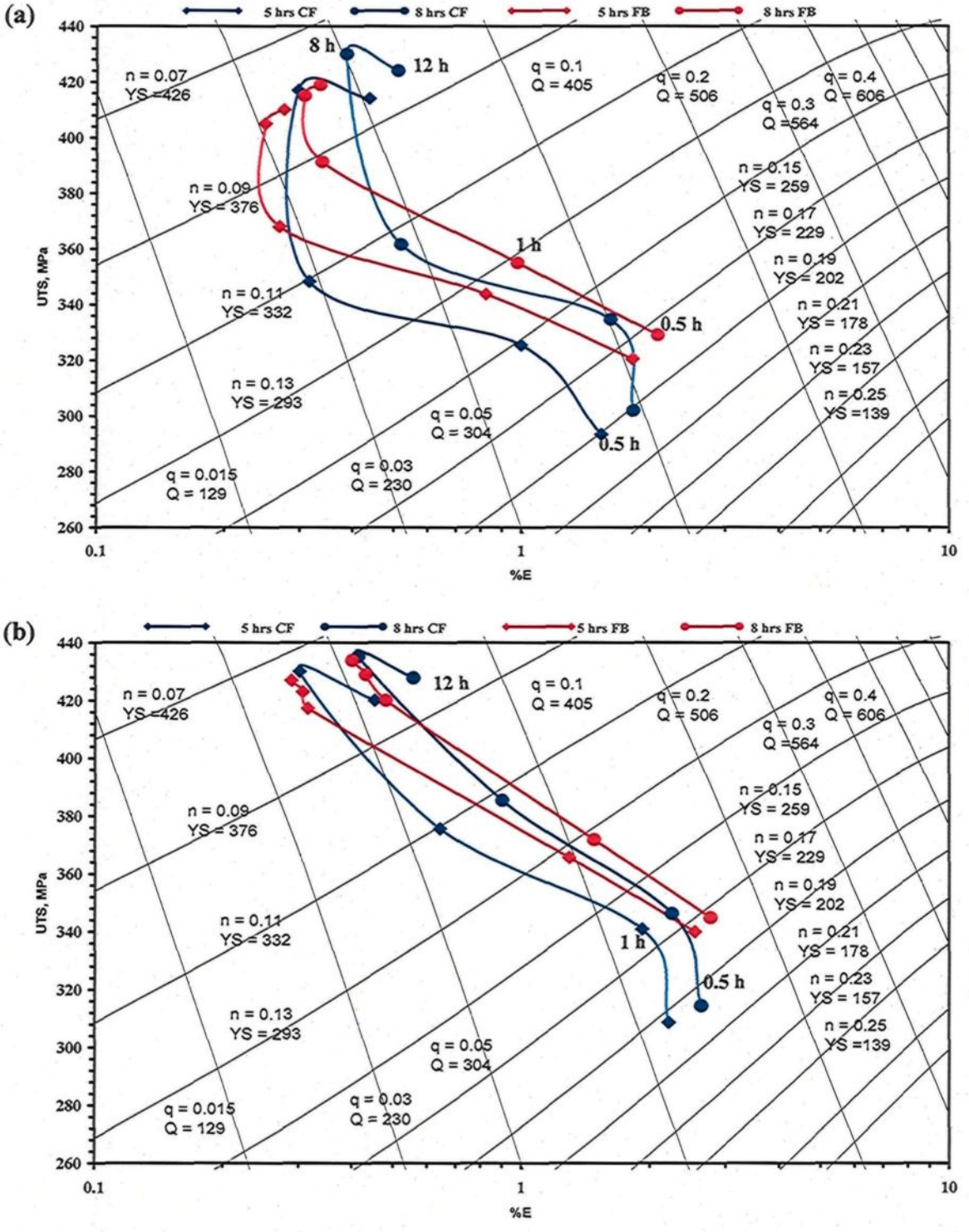

Figure 4.20. Quality charts based on Equations 11 through 13 showing the effects of solution heat treatment time: 5h and 8h, and modification on the quality and UTS of (a) non-modified, and (b) modified 319-type alloys.

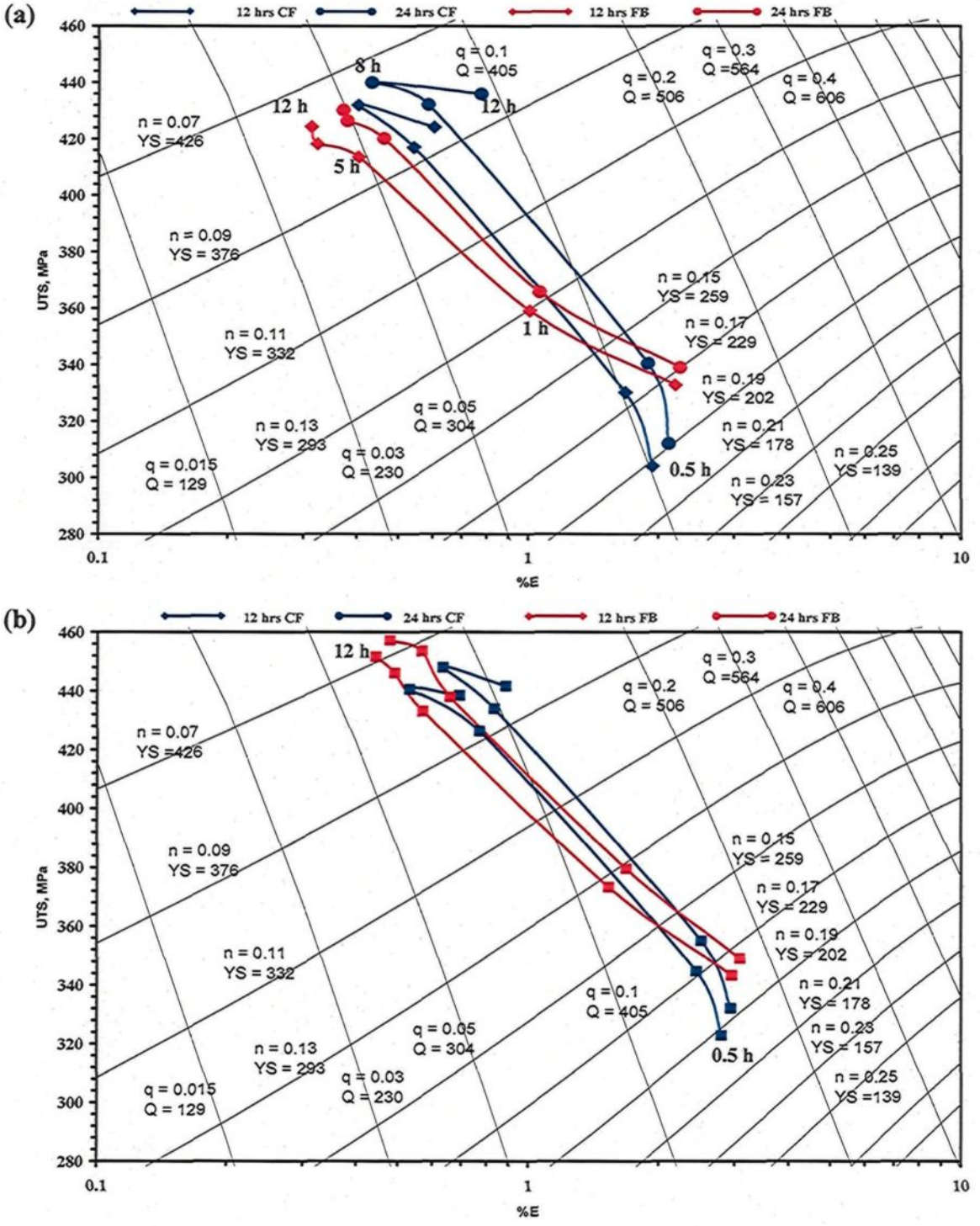

Figure 4.21. Quality charts based on Equations 11 through 13 showing the effects of solution heat treatment time: 12h and 24h, and modification on the quality and UTS of (a) non-modified, and (b) modified 319-type alloys.

4.4.3. Selection of Metallurgical Parameters Using Quality Index Maps

The quality index is considered to be an efficient tool for selecting the best alloy conditions required for a particular engineering consideration. An example is shown in Figures 4.22 and 4.23 which show the effects of solution treatment/aging time combinations and the heat treatment technique used on the quality index values obtained for non-modified and modified B319.2 and A356.2 alloy samples (in terms of their UTS and %El properties), identified by the eight points labeled A through H on the chart shown in Figure 4.22. Only *iso-Q* lines have been plotted on the charts.

Figures 4.22 and 4.23 illustrate the way in which solution treatment/aging time combinations, Sr-modification and the heat treatment techniques applied may have an effect on the quality index values obtained for non-modified and modified B319.2 and A356.2 alloy samples in terms of their UTS and %El properties. It should be noted that only *iso-Q* lines were plotted on the charts. It may be observed that the Q-values of the B319.2 and A356.2 alloys show improvement upon modification. It was reported by Jacob [152] that Sr modification enhances the strength and ductility, as well as the quality of Al-Si alloys. Regarding the quality charts in Figure 4.23, the effects of Sr-modification in addition to the high heating rate of the fluidized bed play a vital role in improving the quality performance of the alloys studied. For both B319.2 and A356.2 alloys, whether modified or non-modified, the Q-values obtained after1hr of solution treatment + 1hr of aging using an FB are nearly the same or better than those obtained after 5hrs of solution treatment + 5hrs aging using a CF. This observation clearly indicates the advantage of using the fluidized bed heat treatment technique in view of the fact that the high heating

rates associated with it help considerably in reducing the total heat treatment time needed for improving the quality of a product compared to the much longer times needed with a conventional convection furnace to achieve the same results. Based on the required tensile properties, the quality requirements and the cost, several metallurgical parameters may be selected from among these, namely the alloys investigated, heat treatment times and heat treatment techniques, as the most suitable parameters for a specific engineering application.

Solution heat treatment and aging at higher heating rates using the FB technique introduces a technologically useful strategy in that by applying a rapid aging treatment to these particular alloy systems, it becomes possible to achieve a noticeable reduction in the aging time required to reach peak-strength. This time reduction in relation to industrial applications has several benefits including lower energy consumption, longer lifetime for the heating furnaces, greater productivity, lower labor costs, and a number of other analogous advantages.

The quality index values as well as the strength results will be re-plotted in different formats such as main effect plots, interaction plots, contour plots and matrix plots by applying statistical analysis as will be presented in the next subsection. This type of analysis was applied, for several metallurgical parameters, to confirm the original analyses and interpretations made using the quality charts regarding the response and/or performance of the alloys investigated with respect to heat treatments using FB *vs.* CF techniques.

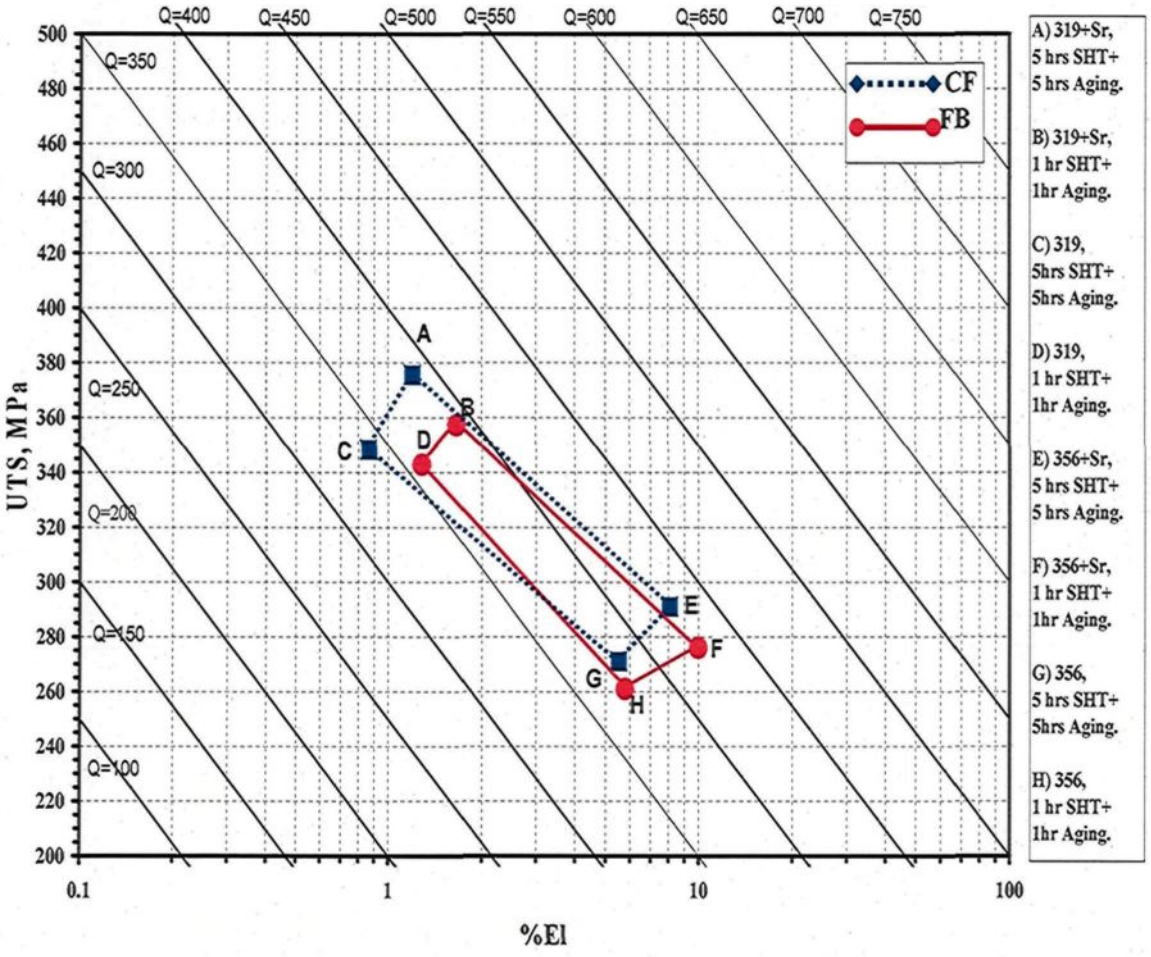

Figure 4.22. Quality index of T6-tempered Al-Si-Cu/Mg alloy systems using FB vs. CF techniques.

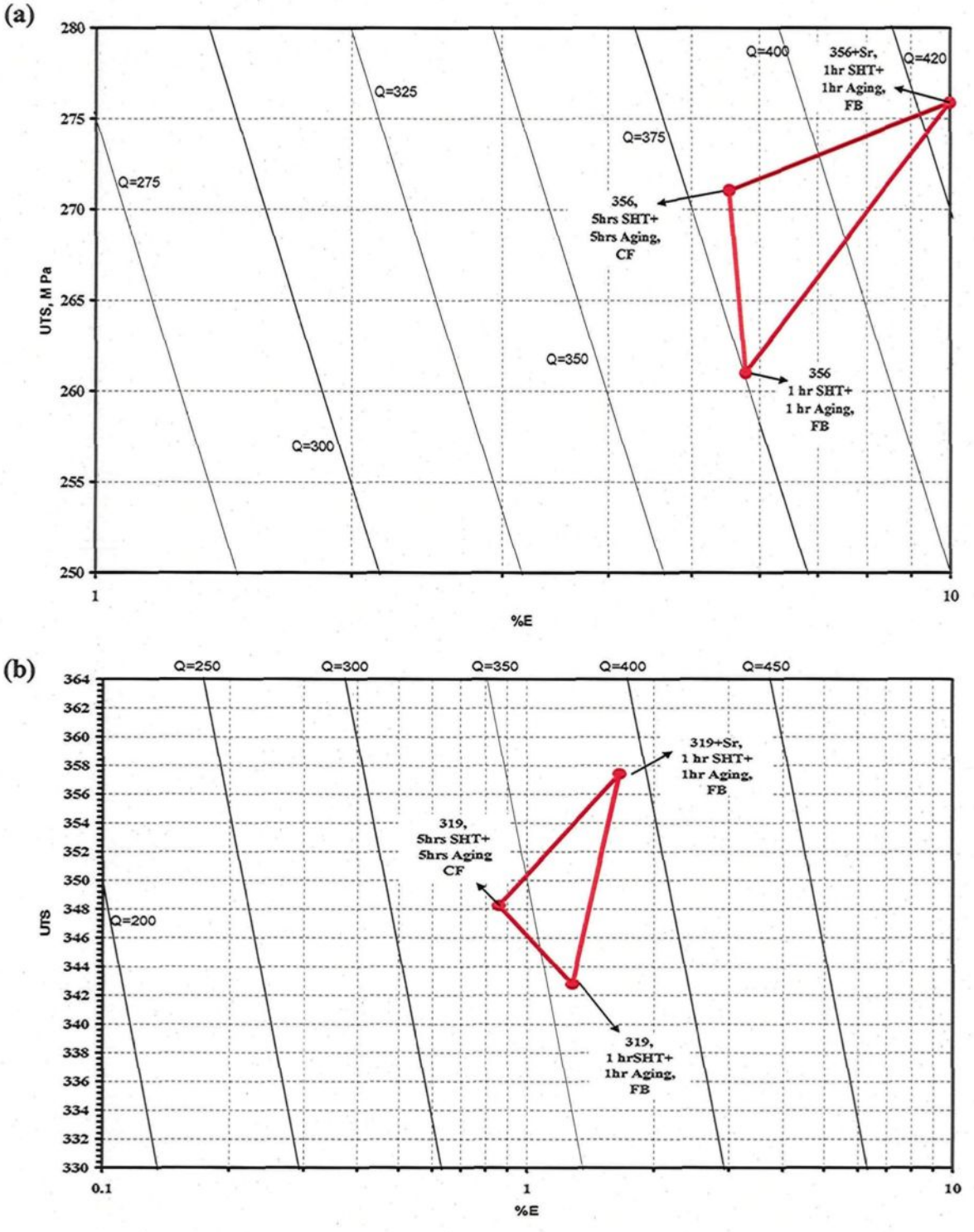

Figure 4.23. Comparison of UTS and quality values of T6-tempered (a) 356 and (b) 319 castings for specific metallurgical conditions, using the quality charts generated by Equation 5.

4.5. STATISTICAL ANALYSIS

Selection of an alloy with certain specific properties is extremely laborious and time-consuming, particularly since classical methods have not always led to the development of a quantitative relationship between the mechanical properties of alloys on the one hand, and their composition or heat-treatment parameters on the other. Therefore, if two or more variables are alternated or interchanged amongst themselves, it could become difficult to quantify the effect that any interaction between different variables would have on mechanical performance and quality. Experiments were made to determine the effect of the independent variable (factor) on the dependent variable (response), while the relationship between them was illustrated using a regression model involving experimental data.

Statistical design of experiments (DOE) is widely used as an efficient experimentation technique which has been applied to produce high quality products, to facilitate the economical operation of a number of procedures, and to ensure the stable and reliable progress of these same procedures. [17, 191] Studies involving the application of DOE methods have been made for more than four decades, and the advance of DOE applications has been assisted by developments in the field of computer science. Mohamed *et al.* [192] and Ganguly *et al.* [193] used the statistical design of experiments to study and control the properties and behavior of Al-Si alloys. Major *et al.* [194] applied fractional factorial design to evaluate the microstructure of the Al-Mg_2Si system in order to optimize alloy composition.

Statistical design of experiments (regression analysis), as a method, has been put into use in the current study to examine and control the properties and behavior of A356.2 and B319.2 alloys and to develop regression equations between the response variable and the factor varied. These equations may be analyzed quantitatively to acquire an understanding of the effects of the variables and their interactions on the quality index of the alloys under investigation. Furthermore, within the variation range of the variables studied, these mathematical equations may be used to predict the performance and/or select the metallurgical parameters of alloys investigated which, after the requisite heat treatment, would have the desired properties required for specific engineering applications. The presence of strong interaction coefficients, as evidenced by non-linearity in the equations, justifies the adoption of an appropriate higher order design.

A current and well-established system will be selected to examine the relevance of this mathematical technique by correlating the results generated in this section with those obtained experimentally by the conventional methods described in subsection 4.4. Four parameters were selected as independent variables and tested at two levels in order to carry out the factorial design. Table 4.4 represents the independent variables, factors, and response variables studied together with the codes used to obtain the final regression equations.

Table 4.4. Independent variables, response variables, and their codes.

Independent variable	Code	Response variable	Code
Modification effect, wt%	X_1	Quality index (Q), MPa	Y
Solution heat treatment time, h	X_2		
Aging time, h	X_3		
Heating rates, HT techniques*	X_4		

* Heat treatment techniques represent conventional furnace (CF) and fluidize bed (FB) parameters.

The data pertaining to the quality index value, Q, were analyzed using Minitab software Version 15 to obtain the regression models, the main effects plot, and the interaction plot, which describe the relationship between the independent variables studied and the mechanical properties of the alloys investigated, as represented by Equation 14 shown below:

$$Y = b0 + b1X1 + b2X2 + b3X3 + b4X4 + \ldots \qquad \textit{Equation 14}$$

where Y is the response variable (YS, UTS, %El, or Q); b0, b1, b2, *etc.* are constants representing the effects of the respective factors; X1, X2, X3 and X4 are the coded values of the factors pertaining to modification effect, solution heat treatment time, aging time, and heat treatment technique, respectively. In general, positive values of the coefficient signify an increase in the property due to a concomitant increase in the individual parameters and their interactions, whereas the magnitude of the coefficients signifies the extent of the influence of individual parameters, or their interactions, on the response variable. For example, positive and higher values of b1 in Equation 14 would signify (i) an increase in the response variable Y, and (ii) a greater effect of the factor X1 on Y, in

comparison to the other factors X2, X3, etc. Similarly, lower values of the coefficients would suggest that the action of associated individual parameters, or their interactions, is non-significant for a given response variable. By processing the data, regression Equations 15 and 16 were developed for Q values of A356 and B319 alloys, respectively, and the variation of a number of different factors, as follows:

$$\mathbf{Y}\ (\text{A356 alloy}) = 291.5 + 22^{*} X_1 + 7.23^{*} X_2 + 6.15^{*} X_3 + 24.4^{*} X_4 \qquad \textit{Equation 15}$$

$$\mathbf{Y}\ (\text{B319 alloy}) = 291.6 + 12.6^{*} X_1 + 10.62^{*} X_2 - 21.7 X_3 + 7.61^{*} X_4 \qquad \textit{Equation 16}$$

Figure 4.24 (a) and (b) shows the residual plots of Q values obtained by regression analysis for alloys 356 and 319, respectively. The R^2 values for Equations 15 and 16 are 98.61% and 95.32%, respectively; these values may be used for representing the degrees of accuracy as well as estimating how well the model accounts for variations in the data set. For example, when the R^2 value equals 0.95, this means that 95% of the variation is accounted for by the model and 5% is accounted for either by variables which are assumed to be constant or by the inability of the data to be modeled by a quadratic equation. The R^2 value for prediction is an estimate of how well the model will predict the response of new data which falls within the bounds of the set variable ranges.

For the purposes of this study, it is recommended that the value of R^2 should be maximized. From these linear equations, one can easily notice that the response Y (Q values of A356 alloys) is affected significantly by the heat treatment technique, followed by modification and then by solution treatment time and lastly, by aging time. However, the response Y (Q values of B319 alloys) is greatly affected by the modification factor and

solution heat treatment time followed by a great negative effect of heat treatment technique. The results obtained from these equations are in satisfactory agreement with the quality index charts of A356 and B319 alloys.

Comparing the regression models for the alloys investigated, it may be noted that the quality performance of A356 casting alloys is more responsive to variation in heating rates during heat treatment using different techniques, as compared to the B319 alloys, showing an impact factor of heating rate parameter of 24.4 *versus* 7.61 for B319 castings. It may be suggested that the quality performance of B319 alloys is sensitive to some factor, or group of factors, which do not lie within the scope of the statistical analysis study. The most significant factor is the high volume fraction of undissolved phases Fe-intermetallics and Si-Fe-Cu-Mg containing intermetallics which are not significantly affected by the heating rate (temperature and time) of the applied heat treatment as discussed earlier in subsection 4.2.3.

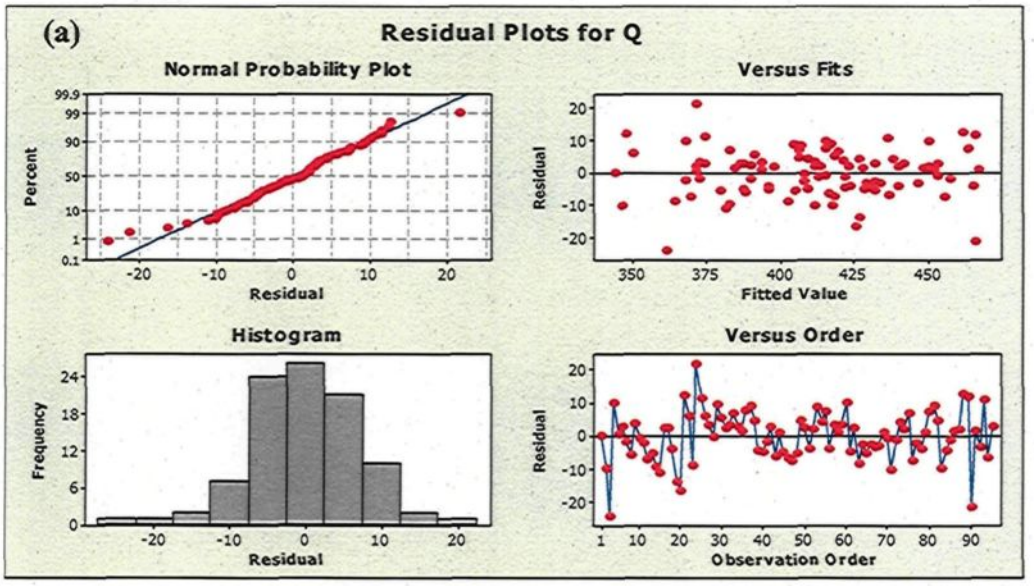

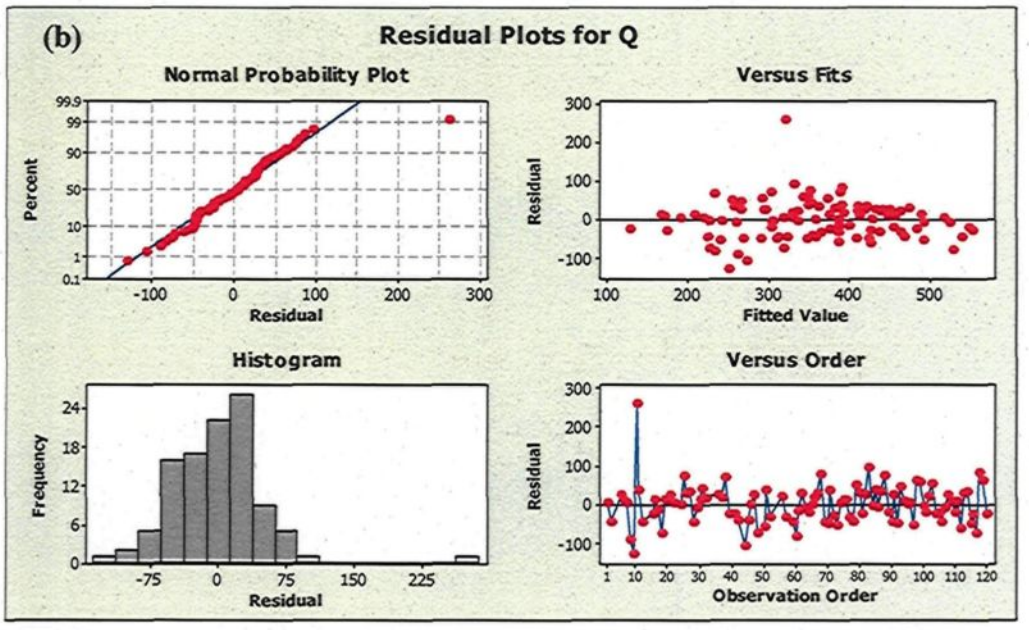

Figure 4.24. Residual plots of Q-regression values obtained for (a) 356 and (b) 319 alloys.

The main effects are assessed by an analysis of the level of average response of the raw data. This analysis is carried out by averaging the raw data at each level of each parameter and plotting the values in graph form. The average responses of the raw data make it possible to analyze the trend of the performance characteristic with respect to the variation in the factor under study. Figures 4.25 and 4.26 show the main effects of all the four variables which affect the quality index values of A356.2 and B319.2 alloys, respectively. The average values of each independent variable are compared within that variable in order to observe its impact on the quality index. The more horizontal the line, the less impact the independent variables have on the property. The presence of optimal testing conditions with regard to these control variables can be easily determined from the relevant graphs. As is evident from Figure 4.25, there is a significant change in the quality

values of A356.2 alloys when the levels of solution heat treatment time and modification are changed from low levels to mid or high levels, compared to the quality values of B319.2 alloys for the same parameters, as shown from Figure 4.26.

It may be concluded from this observation that solution temperature at 530°C for 5 h is enough to complete the dissolution of the hardened Mg_2Si phase in A356.2 alloys. Solution temperature at 495°C for 5 h, however, is not sufficient for the complete dissolution of the hardened precipitated phases, *e.g.* $AlCu_2$ and Mg_2Si, in B319.2 alloys. It may also be noted that the quality values of A356.2 alloys display a significant response to the fluidized bed heat treatment technique, as shown in Figure 4.25, compared to the quality values of B319.2 alloys, as observed in Figure 4.26. It will be observed that the quality values of the A356.2 alloys are slightly affected by the aging time, while the quality values of B319.2 alloys display a significant decrease with increasing the aging times up to 8 h. These results obtained by statistical analysis are corroborated by the results obtained by the quality charts in this study.

In order to examine the dual interaction effect of the individual factors, including all of its levels, on the response Q-value, the detailed interaction plots for quality index values of A356.2 and B319.2 alloys are provided in Figures 4.27 and 4.28, respectively. It may be observed, from the interaction plot for the Q-value of A356.2 alloys, that the fluidized bed heat treatment technique, coded by the digit 2, provides better quality values compared to the convection furnace which is coded by the digit 1. With regard to the interaction plot of the quality response using the technique factor, the fluidized bed technique shows better quality values in interaction with the other factors, namely aging times of up to 5 h and

solution heat treatment times of up to 8 h, for modified A356.2 alloys which are coded by the digit 3. Figure 4.27 shows that the mean quality values are greatly affected by the modification factor due to the significant effects of Sr which had been added to change the acicular eutectic silicon to a fibrous form thereby improving the ductility and quality values.

Liao *et al.* [195] observed that strontium enhances strength and ductility as well as the quality of the alloys investigated. Also, it was observed that the mean quality values were not significantly affected by the aging time factor which matches the results obtained through the main effects plot. With regard to the interaction plot of quality response to the heat treatment technique factor shown in Figure 4.28, the quality of A356.2 alloys, as compared to B319.2 alloys, shows them to be more responsive to FB than to CF heat treatment techniques.

The variation in quality values due to the variation of factors may be better understood by showing surface and contour plots, thereby representing the effects of each of the factors at different levels of variation. These plots, shown in Figures 4.29 and 4.30, made it possible to predict the response for quality values of A356.2 and B319.2 alloys which are based on the regression equations. Figures 4.29(a) and 4.30(a) portray the 3-D response plots, while Figures 4.29(b) and 4.30(b) represent the corresponding 2-D contours for the variables studied. These plots can facilitate predicting the way in which the response reacts to changes in the modification, aging time, and heat treatment technique. As shown in Figure 4.29(a), the surface plot indicates that the highest Q values of A356.2 alloys are obtained when modification levels are high and the heat treatment technique used is a

fluidized bed. Nevertheless, the influence of the modification factor is better than that of the heat treatment techniques, indicating that the former has a better *release-sustaining factor* for the Q values than the latter as may be also seen in Figures 4.29(a) and 4.25. With reference to the Minitab program, the term *release-sustaining factor* refers to the continuing influence of a specific factor on the response variable. In addition, it is possible to acquire a general idea of Q values at various levels of the relevant factors.

The same conclusions may be deduced by the corresponding contour plot, shown in Figure 4.29(b), illustrating the significant positive effect of modification factor on the quality values of A356.2 alloys. Figure 4.30(a) reveals that the Q values of B319.2 alloys are not greatly affected by the FB heat treatment technique. The corresponding 2-D contour plot, shown in Figure 4.30(b), further clarifies the fact that the mean quality values decrease through aging times of up to 8h in a CF and up to 12 h in an FB; the contour plot matches the results obtained by quality charts as well as the interaction plot for B319.2 alloys.

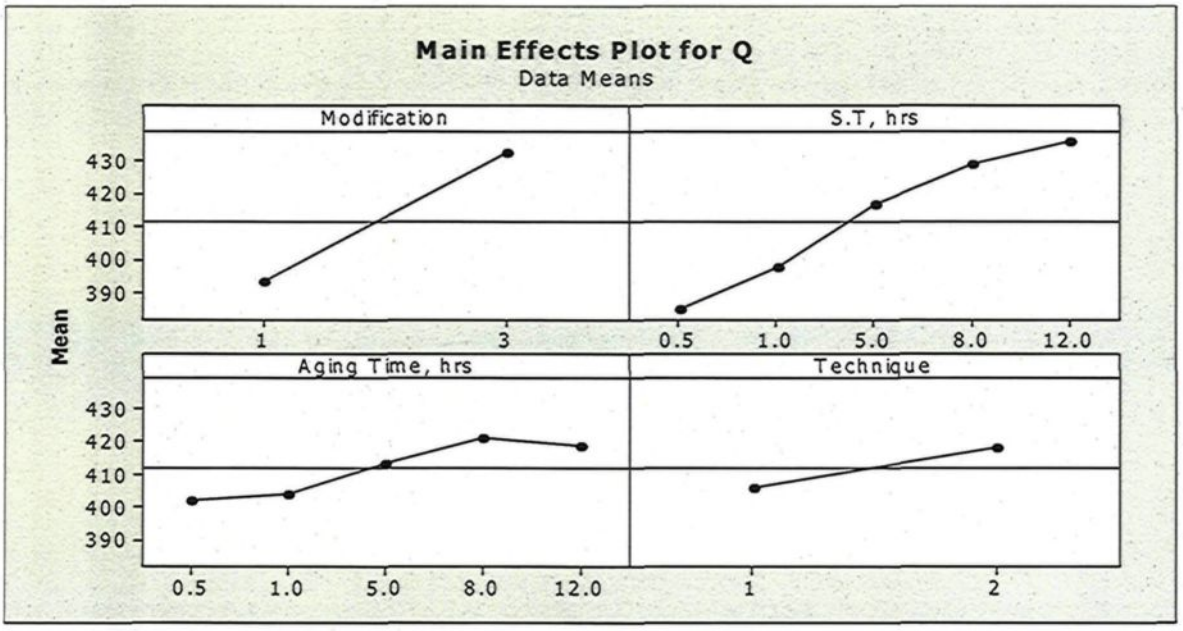

Figure 4.25. Main effects plot of various factors affecting the quality values of A356 alloys.

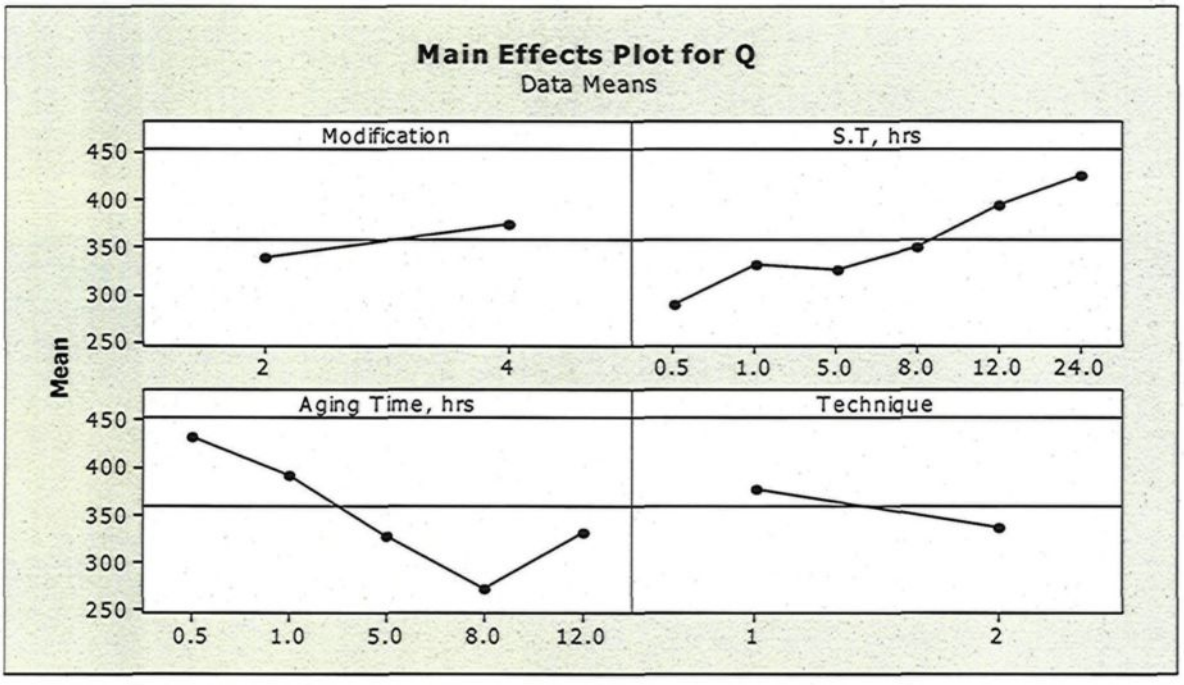

Figure 4.26. Main effects plot of various factors affecting the quality values of B319 alloys.

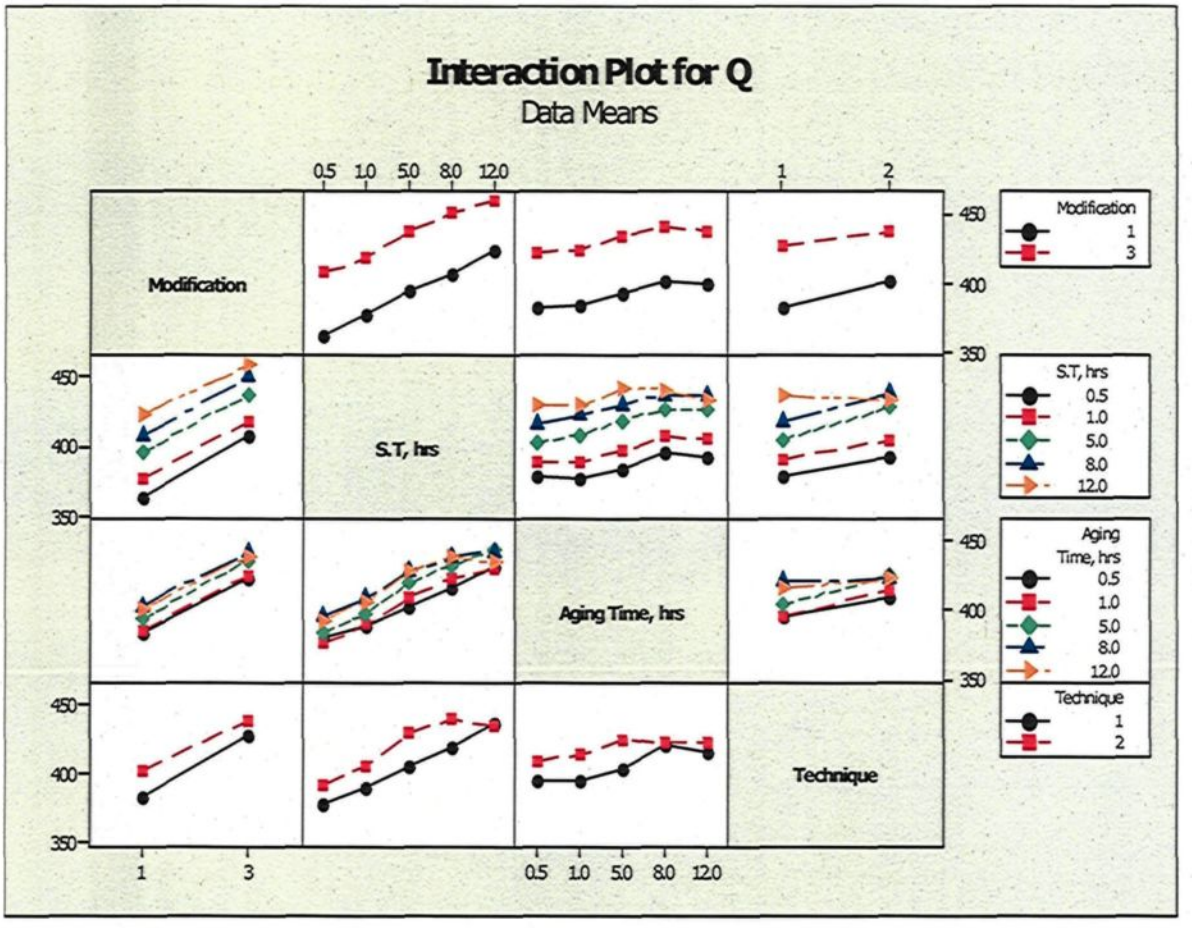

Figure 4.27. Statistical analyses showing the interaction plot for mean Q values of A356-type alloys.

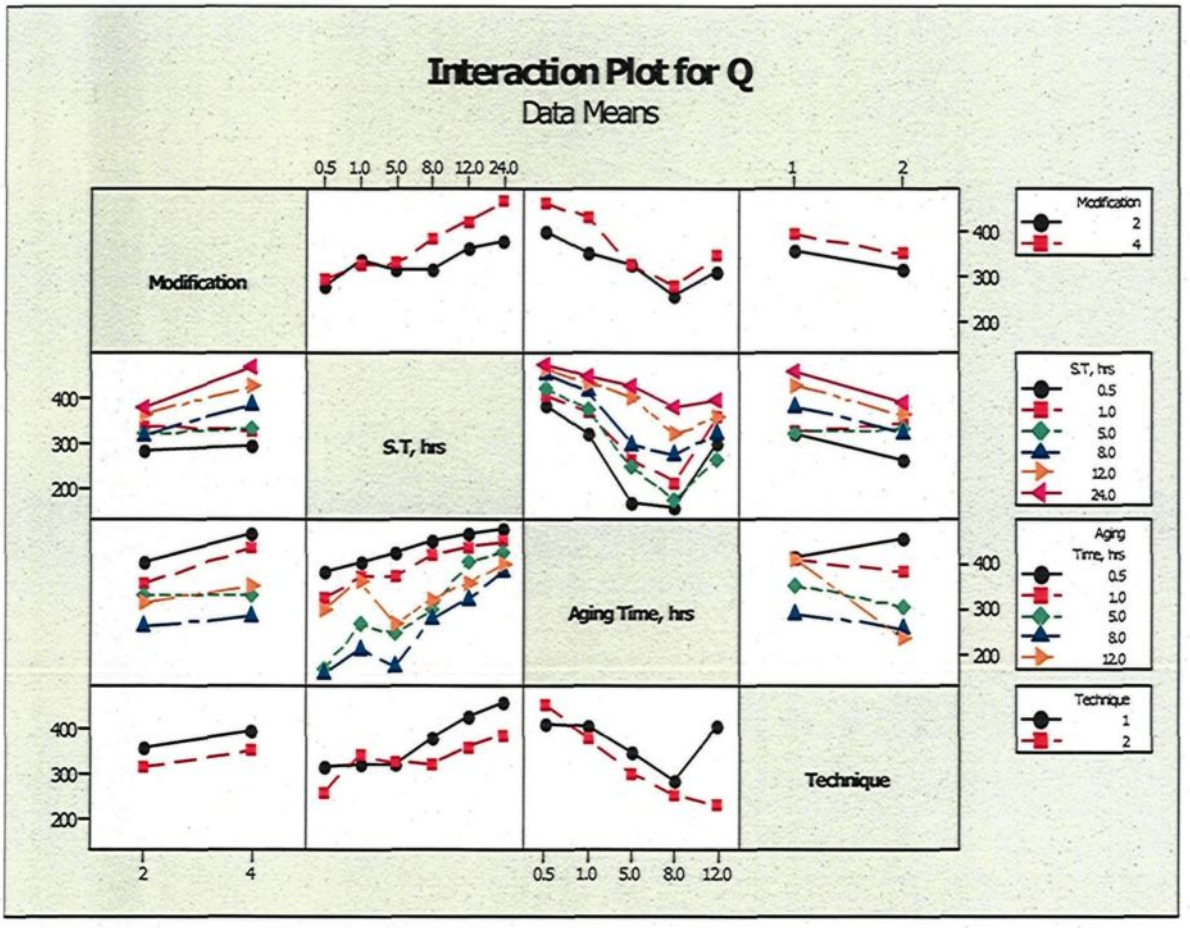

Figure 4.28. Statistical analyses showing the interaction plot for mean Q values of B319-type alloys.

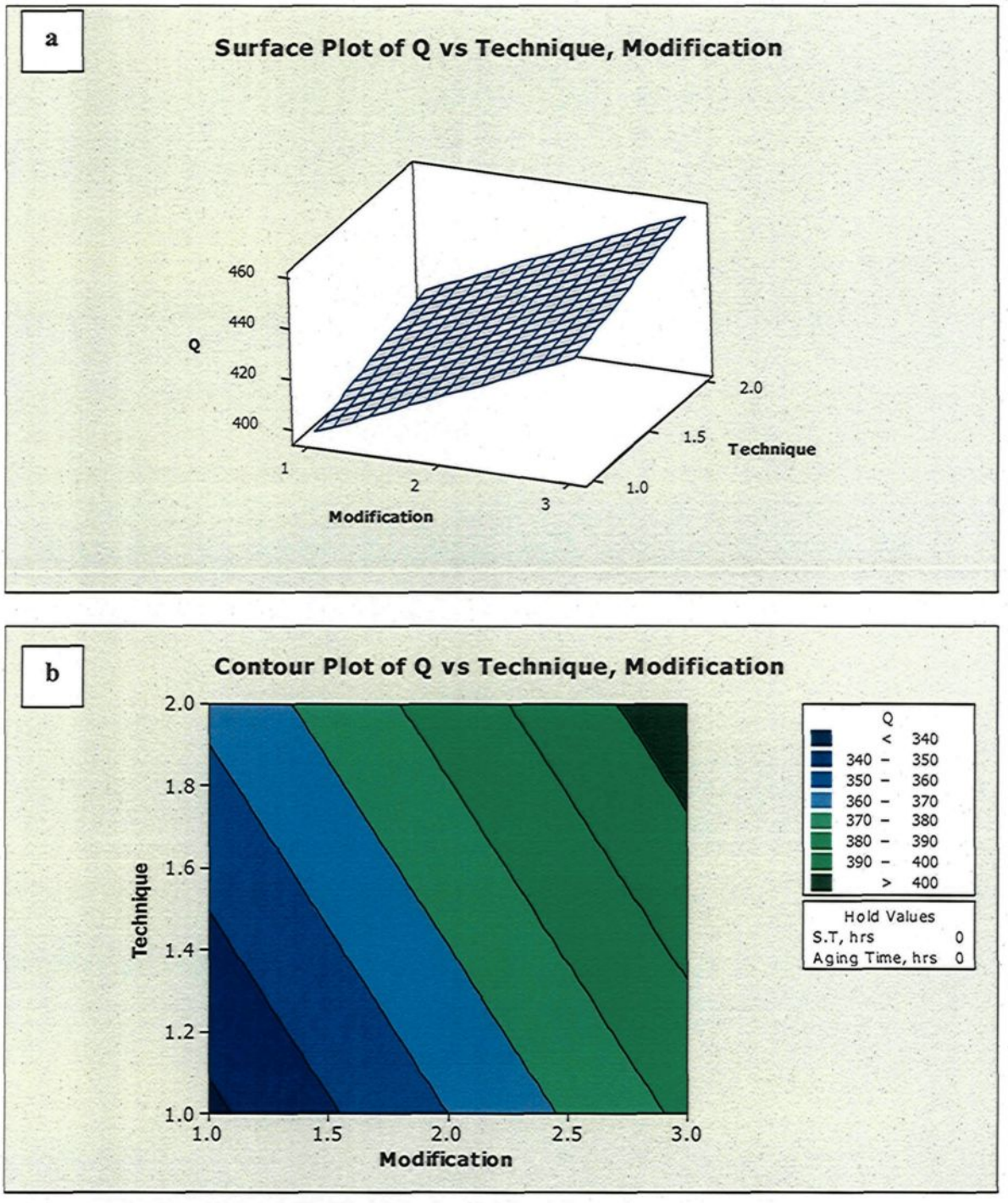

Figure 4.29. (a) Response surface plot showing the influence of modification and heat treatment technique on the quality values of A356.2 alloys; and (b) the corresponding contour plot.

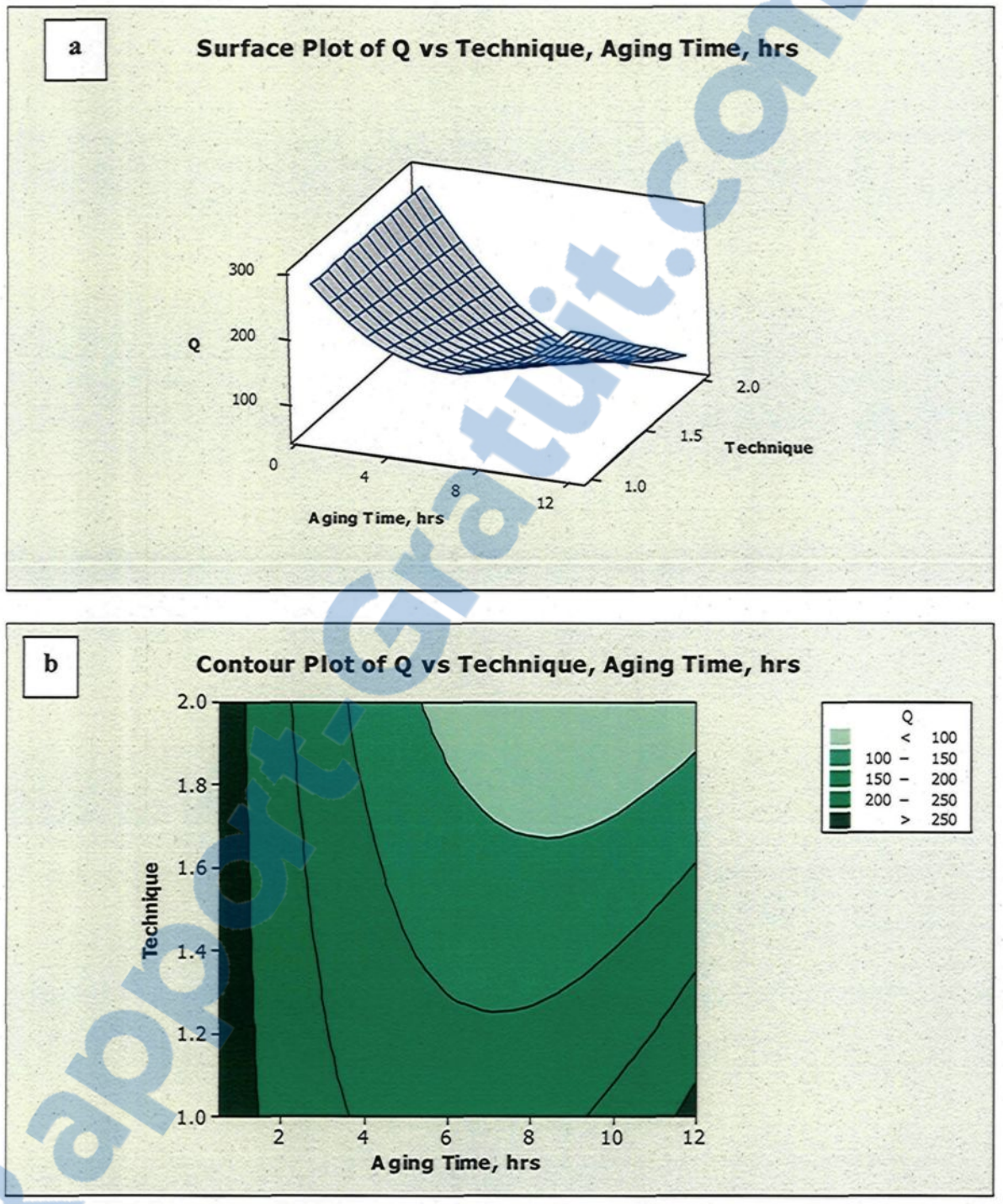

Figure 4.30. (a) Response surface plot showing the influence of aging time and heat treatment technique on the quality values of B319.2 alloys; and (b) the corresponding contour plot.

4.6. FB-HIGH HEATING RATE AND AGING CHARACTERISTICS

As was discussed earlier, the essential role of the FB heat treatment technique involves reducing the total heat treatment time as well as obtaining higher strength values than would be available with the use of a conventional furnace; this overall effect is related to the high heating rate which usually characterizes a fluidized bed. This rate which develops in an FB is associated with the higher heat transfer rate of the sand-bed heat-treatment medium. Heating rate is known to have a considerable effect on aging characteristics, where a high heating rate activates the precipitation rate of the hardening phases in both 356 and 319 aged alloys. The amount of precipitates obtained in alloy samples aged in a fluidized sand bed is significantly higher than it is for samples aged in a conventional convection furnace. Fluidized bed-treated samples show higher strength values than CF-treated ones, especially at earlier aging times of 0.5 h and 1 h; this difference may be related to the stability of solute clusters, or GP zones, which tend to form after quenching, and continue to do so up to the isothermal aging step. The effects of the high heating rate in FBs on the stability of these clusters may be explained from the point of view of thermodynamics and kinetics.

The stability of a solute cluster is highly affected by its radius at a given temperature since the cluster particles are too small in size. The relationship between the radius of the clusters and temperature is defined thermodynamically by the Gibbs-Thompson equation as follows:

$$T = \frac{2\gamma\Omega}{kr \ln S} \qquad \textit{Equation 17}$$

where γ is the interfacial energy, Ω is the atomic volume, k is the Boltzmann constant, r is the cluster radius, and S is the concentration of solute in equilibrium with small particles of radius, r, relative to the equilibrium concentration of solute atoms. [196, 197]

The radius of the solute clusters changes with the progress of time at a given temperature; the kinetics of this change is defined as the Ostwald ripening effect. The changes occurring in the cluster radius over time are given by the following equation:

$$\frac{dr}{dt} = \frac{kDX_p}{r\left(\frac{1}{r_m} - \frac{1}{r}\right)} \qquad \textit{Equation 18}$$

where D is the diffusion rate of solute atoms, X_p is the equilibrium concentration of solute atoms, and r_m is the mean radius of solute clusters. [198]

The effect of the heating rate on this radius for stable clusters can be obtained by taking the differential of Equation 17 by time and substituting for Equation 18 as follows:

$$\frac{dT}{dt} = \frac{2\gamma\Omega}{k \ln S} \times \frac{1}{dr/dt}$$

$$\frac{dT}{dt} = \frac{2\gamma\Omega r}{k^2 D X_p \ln S} \times \frac{1}{(1/r_m - 1/r)}$$

The last equation may be re-written in another form as indicated in Equation 4. From this last equation, it will be noted that there is a direct relation between the heating rate and the radius of the clusters. As the heating rate increases, the radius of the clusters formed will increase in order to be more stable. The high heating rate in an FB thus leads to the formation of more stable clusters, or GP zones, during the heating up stage to reach the aging temperature. These clusters can act as suitable sites for the heterogeneous nucleation

of further precipitates. The precipitation kinetics of such heterogeneously nucleated precipitates is related to the concentration of defects. It was reported that the slow heating rate in a CF leads to the formation of co-clusters of Si and Mg, not GP zones, in 356 alloys; these co-clusters, however, retard the precipitation kinetics of Mg_2Si during aging.[146, 147]

4.7. CONCLUSIONS

The current study was carried out with a view to investigating the influence of fluidized sand bed heat treatment on the tensile properties and quality indices of T6-tempered Al-7%Si-(Cu/Mg) casting alloys, namely B319 Al-7%Si-3.3%Cu-0.26%Mg and A356 Al-7%Si-0.36%Mg. The variables investigated included solution heat treatment time; aging time; and melt treatment. Quality charts as well as statistical analysis were used as evaluation tools for selecting the optimum conditions to be applied in practice in order to develop high strength and optimum quality in 356 and 319 castings for specific engineering applications. From an analysis of the results obtained through this chapter, the following conclusions may be drawn:

1. With regard to Si particle characteristics, the fluidized bed heat treatment displays smaller Si particle size than the convection furnace through solution heat treatment times of up to 12 hrs for non-modified 356 and 319 alloys. For modified and non-modified 356 and 319 alloys, the smallest Si particle size was obtained after only 0.5 h solution treatment using an FB versus 5 h using a CF. The FB treatment results in more fragmented Si particles due to the effects of the high heating rate associated with the technique.

2. Grain-size results indicate that the presence of copper in the 319 alloy samples does not hinder grain refinment at higher Ti contents of 0.22 wt%; the grain size is refined from 1317 μm to 291 μm by the addition of Al-5%Ti-1%B grain refiner. The results from the grain size measurements for alloy 356, as obtained in this study, show that with an addition of 0.006 wt% boron, the grains are refined by more than 50% compared to the non-grain refined alloy, namely from 443 μm to 202 μm.
3. The fluidized bed (FB) technique is more effective than the conventional convection furnace (CF) technique in terms of the strength values achieved in T6-tempered 319 and 356 alloys for solution heat treatment times up to 8 h; beyond this solution time, no noticeable difference in properties is observed with the two techniques.
4. Fluidized bed heat treatment of 319 and 356 alloys produces better strength values after 0.5 h, 1 h, and 5 h aging than those obtained using the conventional convection furnace. This difference in strength may be related to the high precipitation rate of the hardening phases such as $Al_5Cu_2Mg_8Si_6$, Mg_2Si and $CuAl_2$ in FB-treated alloy samples as opposed to CF-treated samples.
5. The difference in the strength values of 356 alloy samples obtained from the fluidized bed loses significance compared to those obtained from the conventional furnace, at aging times between 8 h and 12 h for all solution treatment times, due to the faster coarsening rate of the Mg_2Si precipitates.
6. For the 319 alloys, FB-treated alloy samples show a continuously increasing trend in the strength values with a delay in overaging of up to 12 h resulting from the

stability of the intermediate precipitates, whereas in CF-treated samples, overaging occurs after 8 h.

7. With regard to the quality charts of 319 alloys, heat treated samples show that increasing the aging time up to peak-strength after 8 h and 12 h in a CF and an FB, respectively, results in an increase in the alloy strength with a decrease in its quality values for the same solution heat treatment time.
8. The quality values of the 356 alloys are more responsive to the fluidized bed technique than 319 alloys through long aging times of up to 5 h; the 319 alloys heat treated in an FB, however, show better quality values than those obtained by a CF after 0.5 h aging time. The low response of 319 alloys to an FB heat treatment may be related to the amount of undissolved Cu intermetallics, namely $CuAl_2$, during solution heat treatment, where the high heating rate in an FB has no significant effect on the dissolution of these intermetallics, except at 0.5 h solution treatment time.
9. An analysis of the quality charts for 319 and 356 alloys reveals that, for the same solution heat treatment time, the FB-treatment provides better quality values after only 0.5 h and 1 h aging times using the fluidized bed versus 5 h aging in the convection furnace.
10. The FB treatment provides similar or slightly better alloy quality after only 1 h of solution heat treatment plus 1 h of aging compared to that obtained after 5 h of solution treatment and 5 h of aging with a CF treatment. A fluidized sand bed thus

provides improved strength results while also saving on the heat treatment time and energy consumption required for the heat treatment procedure.

11. With regard to statistical design of experiments, analysis of the results reveals that modification and heating rate of the heat treatment technique have the greatest positive effects on the quality values of the alloy 356. Analysis of the interaction plot as well as of the main effects plot shows that the quality values of 356 alloys, as compared to 319 alloys, are more responsive to FB than to CF heat treatment techniques.
12. Equations developed on the basis of thermodynamic concepts, indicate that there is a direct relationship between the heating rate and the radius of the clusters during aging treatment. It is proposed that the high heating rate in a fluidized bed would lead to the formation of more stable clusters, or GP zones, during the heating up stage to reach the aging temperature. These clusters could act as suitable sites for the heterogeneous nucleation of further precipitates.

CHAPTER 5

INFLUENCES OF QUENCHING MEDIA, AND AGING ARAMETERS

CHAPTER 5

INFLUENCES OF QUENCHING MEDIA, AND AGING PARAMETERS

5.1. INTRODUCTION

Subsequent to solution heat treatment, castings are quenched using several media with different cooling rates. These cooling rates can be controlled by varying certain quenching parameters (e.g. bath temperature, degree of agitation, etc.). Varying these parameters changes the heat transfer rates and the ability to increase or decrease the cooling rate to achieve certain mechanical properties as well as eliminate distortion and the possibility of cracking.

An immediate outcome of quenching is the formation of a supersaturated solid solution, where in the given cooling rate applied during quenching dictates the resulting vacancy concentration and possible phase formation. Generally, the faster the cooling rate, the higher the potential alloy strength after aging. Water is the preferred quenching medium which exhibits an excellent heat-transfer coefficient. However, water quenching raises concerns regarding the unpredictable nature of the transition from the vapor blanket stage to the boiling stage, resulting in large temperature differences between the surface and the center of the quenched part. Temperature gradients are created along the surface, resulting

in part distortion. Therefore, it is of utmost importance to control the transition from the vapor blanket stage to the boiling stage.

For large cast parts, as well as parts with complicated geometries, large temperature gradients may develop within the part. These gradients manifest as high residual stresses, part distortion and cracking. One possible remedy to reduce distortion it to use a fluidized sand bed (FB) as a quenching medium in order to improve the part's mechanical performance and quality. Water and hot air quenching are used to establish a relevant comparison with FB quenching. It was reported that the change in the cooling rate was more drastic for water quenching, where the cooling rate varied from 0 to -80 Ks^{-1} in less than 8 seconds, as compared to FB quenching, where the cooling rate varied from 0 to -14 Ks^{-1} in 18 seconds; the quenching rate of the CF medium is 1.8 Ks^{-1}.[149, 151]

The aging stage follows quenching, where excess solute atoms in the solid solution precipitate and strengthen the alloy; the degree of precipitation is dependent upon the time/temperature applied to the casting. The T6 aging treatment (i.e. peak aging) is preferred in the case of Al-Si-Mg and Al-Si-Cu-Mg alloys, producing very high levels of strength. However, this is often met with a corresponding reduction in ductility. In some cases, the T7 aging treatment (i.e. overaging) is considered a better alternative. Here, the alloys are aged at temperatures in the range of 200-240°C. The T7 aging treatment aims at reducing residual stress while increasing the performance of the alloy, particularly in high temperature applications. The maximum hardening response occurs when an alloy microstructure contains a combination of GP zones and well-dispersed, semi-coherent, intermediate precipitates. Greater hardening is possible provided an increase in the uniform

dispersion of one or more of these phases is attained. This is possible with the use of multi-temperature aging treatments. In this study, multi-temperature aging cycles (involving T7 and T6 aging conditions), as compared to a standard T6/peak-aging cycle, were applied using both a FB and a CF.

This chapter discusses the influences of the quenching media (water, air and sand) and the age-hardening parameters (multi-temperatures, time) on the tensile properties and quality index values of A356.2 and B319.2 casting alloys heat treated using both a CF and an FB. Details of applied heat treatment cycles are provided in Tables 3.2 and 3.3.

5.2. TENSILE PROPERTIES

The following subsection show and discuss the results regarding the effects of quenching conditions and aging parameters on tensile properties (UTS, YS and elongation) of A356.2 and B319.2 alloys heat treated using FB and CF. Fluidized sand bed is considered as an economical/suitable heat treating technique for aluminum casting alloys. The heat transfer involved in an FB is highly uniform and the heat-transfer coefficient is an order of magnitude greater than that of a convection furnace. For quenching and multi-temperature aging cycles, the FB technique may speed up the heating rate, so as to reach the required temperature during heating/quenching. This has a significant effect on the size, density and uniformity of hardening precipitates, which will, in turn, influence alloy strength and elongation.

5.2.1. Al-Si-Mg Casting Alloys

5.2.1.1. Effects of quenching media (FB, CF, and water)

Figures 5.1 and 5.2 display the effects of FB, CF and water quenching media on the strength of non-modified and Sr-modified T6-aged A356.2 type alloys, respectively. For comparison purposes, the as-cast alloy strength results are also included (see Table 3.2 for process details).

As seen from Figures 5.1 and 5.2, the strength (UTS, YS) values of the CF and FB quenched modified and unmodified T6-aged alloys (C1, C2, C3) are lower than those quenched in water (B1, B2, B3). The high cooling rate from water quenching results in the greatest concentration of vacancies; these vacancies act as nucleation sites for precipitates. Conversely, hot air quenching with a CF provides the lowest strength values due to the low cooling rate and low heat transfer rate. The air quenching-CF technique has been employed for automobile castings such as cylinder blocks which are fitted with cast iron liners, where the slow air-quench is suitable due to the difference in the quench characteristics of iron and aluminum.

Several factors affecting the feasibility of air quenching, such as air flow, air quench temperature and casting configuration. [199] When conventional techniques such as the CF system are used, the materials lose a certain amount of energy on cooling (i.e. being quenched) from the solution to the aging temperature inside the furnace. In contrast, it is possible to heat treat materials immediately in an FB system after processing, without any intermediate cooling or loss of energy. This offers great opportunities for the saving of

energy, space and time rather than improving the tensile properties as compared to a CF and/or water quenching media. [148, 199, 200] With respect to strength results, heat-treated alloys using an FB or a CF for direct quenching-aging (C1, C2 and C3), the strength decreases with increased aging temperature (170, 190 and 210°C). This decrease in strength results is related to over-aging, which occurs after the peak aging point (at 170°C).

The reduction in strength results with a reduced quenching rate is related to the lower hardening Mg_2Si precipitates formed, which, in turn, may be related to the amount of vacancies present. Upon quenching from the solution temperature, vacancies are retained in the Al matrix. The lower the vacancy concentration, the slower the resultant aging process and the higher the related transformation temperature for GP zone formation and precipitation.[148] Thus, it is likely that a lower vacancy concentration or lower fraction of clusters/GP zones/metastable phases gives rise to the observed aging process during FB heat treatment.

With regard to the same aging parameters at 170°C/4 h, the FB-quenched alloys show slightly better strength results (C1-FB condition) than the water-quenched alloys followed by aging using a CF (B1-CF condition). The direct quenching to aging temperature using an FB results in the formation of greater amount of some clusters or GP zones. The density of precipitates responsible for strengthing may be affected by the heterogeneous nucleation sites such as those cluster and/or meta-stable phases. [110] The direct quenching-aging process using an FB has several advantages such as saving heat treatment time as well as obtaining optimum combination of high strength and elongation values. For water-quenched alloys(B1, B2, B3), it can be seen that both UTS and YS values

increase with aging time, up to 12 h. The continuous increase in strength with aging time for both CF- and FB-treated samples can be related to the natural aging applied at room temperature for 24 h before artificial aging. This natural aging step leads to the onset of a high density of clusters or GP zones, which serve as nucleation sites for the Mg_2Si phase which form in the subsequent aging step. [147] It should be noted that the fluidized bed heat-treated samples, water quenched or sand quenched, produce better strength results than the conventional furnace-treated samples for all heat treatment conditions (B, C, D). Such results of water-quenched alloys heat treated using an FB, can be explained by the high heating rate of the fluidized bed which activates the rate of precipitate formation giving rise to a high density of precipitates. The dislocation concentration in the matrix affects the aging kinetics of Mg_2Si precipitation; the slow heating rate in a CF annihilates the dislocations through recovery, thereby reducing their density prior to reaching the aging temperature. The dislocations are known to be potential sites for Mg_2Si precipitates the presence of which would lead to a pronounced improvement in mechanical properties following artificial aging. [147]

For the water quenched alloys subjected to multi-temperature aging conditions (D1, D2, D3), it may be observed that the T6-aging conditions (B1, B2, B3) yield higher strength values than almost all of the multi-temperature aging cycles using both CF and FB. The low strength values for multi-stage aging cycles may be related to the formation of co-clusters of Mg and Si. These elements lead to the nucleation of a coarser dispersion of precipitates after aging at elevated temperature (240°C) resulting in lower significantly response to the following second stage of T6 aging, compared to a single step T6 treatment,

as well as high ductility. [117, 185] In general, the fluidized bed heat treated alloys (water quenching, followed by two aging steps) demonstrate slightly better strength values than those heat-treated with a CF. It was reported by Polmear *et al.* [201] that the maximum strengthening by age hardening is achieved for alloys that contain precipitates that are large enough to resist shearing by dislocations, yet too finely spaced to be bypassed. The maximum response to hardening occurs for a microstructure that contains a combination of GP zones/co-clusters (24 h pre-aging at room temperature after quenching) and relatively widely-dispersed, semi-coherent, intermediate phases.[202] This combination of different precipitates can be achieved by applying multi-stage aging treatments to get a compromise between high strength and high ductility. The modified alloys demonstrate a better level of strength than the unmodified alloys, for all heat treatment conditions (B, C and D).

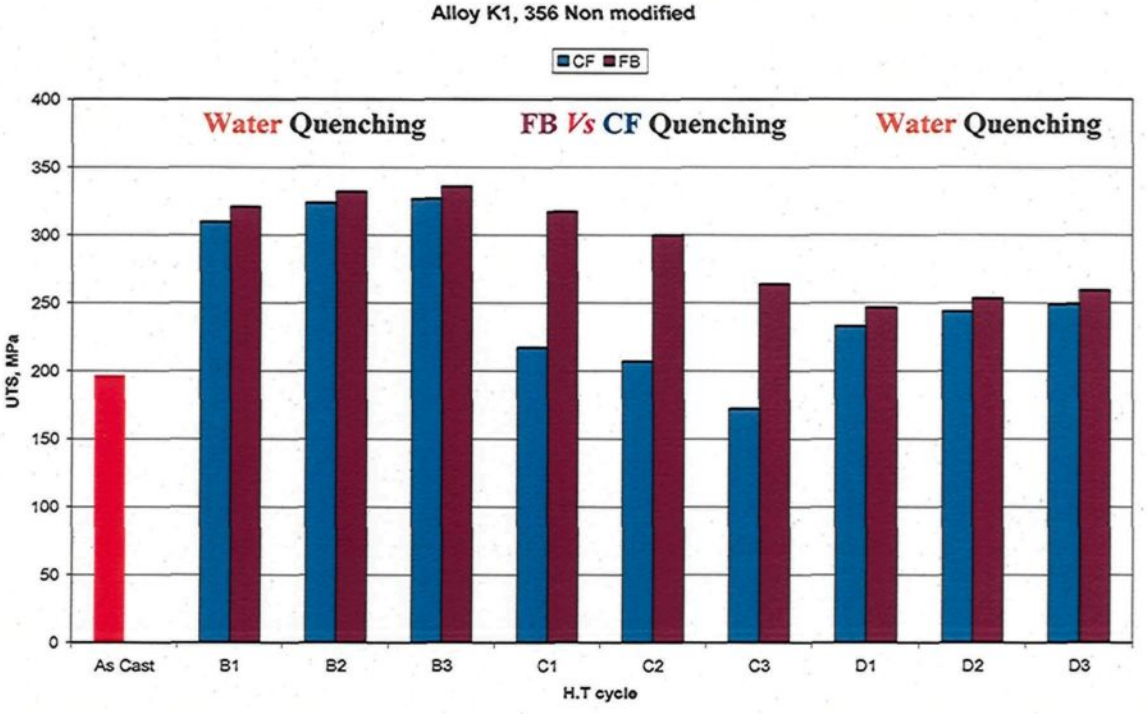

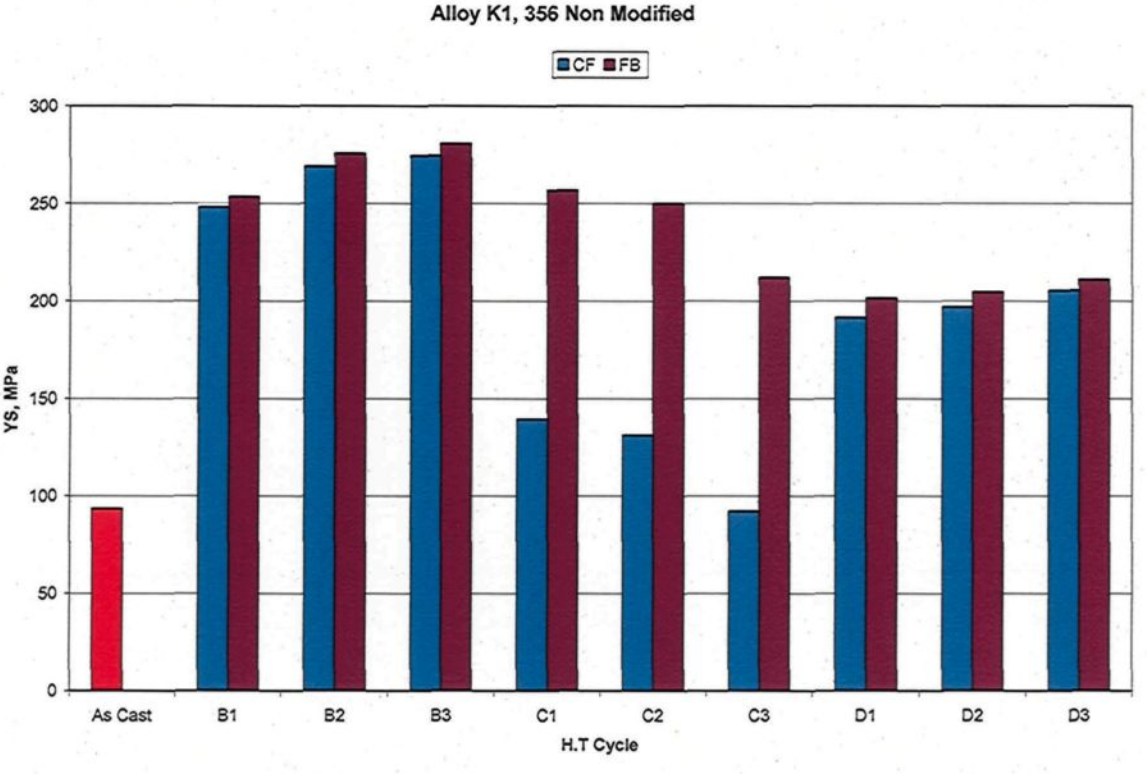

Figure 5.1. Average UTS and YS values for non-modified A356 alloys.

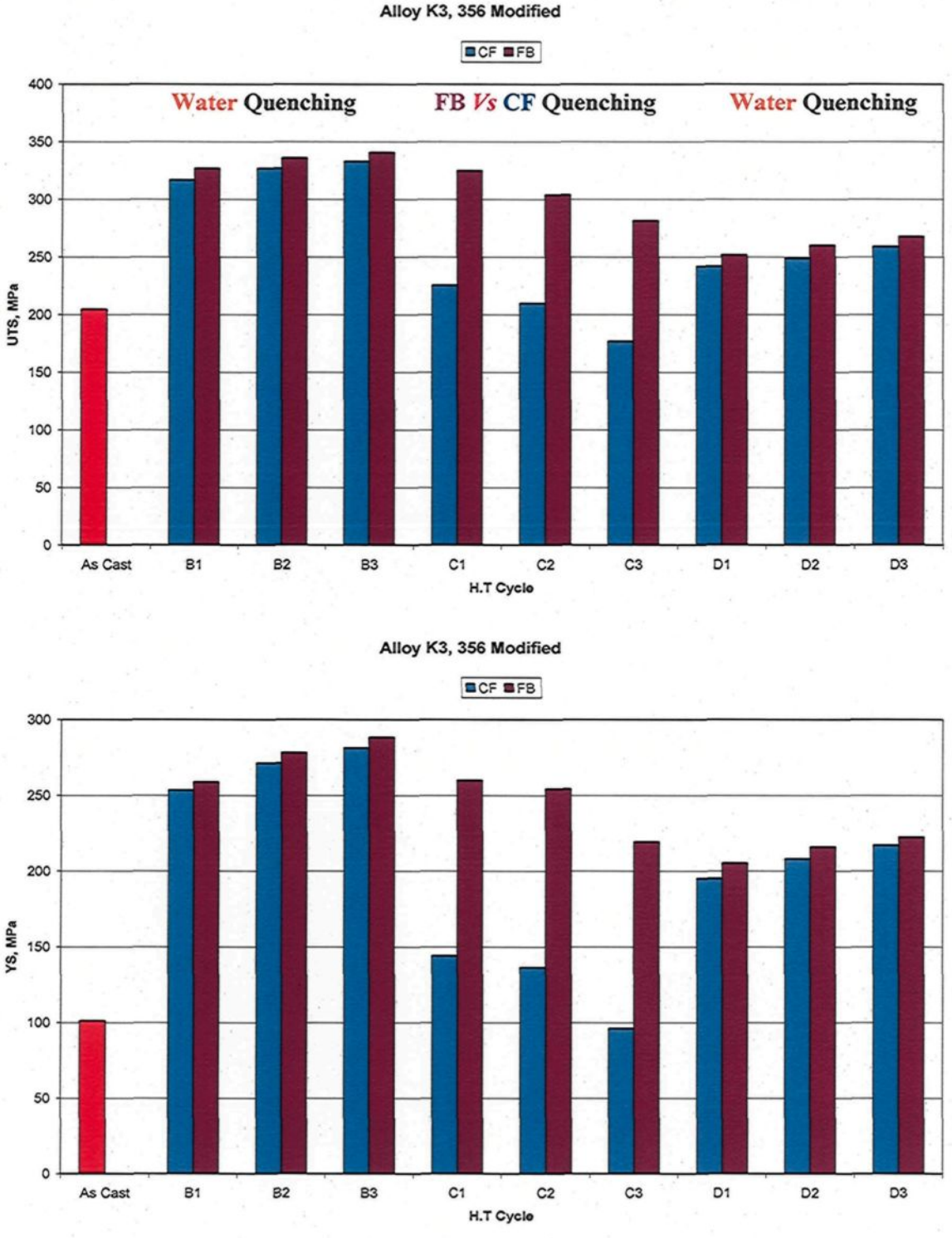

Figure 5.2. Average UTS and YS values for modified A356 alloys.

Figure 5.3 shows the variation in elongation for A356 non-modified and modified alloys, obtained after continuous aging and multi-temperature aging, for quenching carried out in water, air and sand. As shown in Figure 5.3, the elongation values obtained by multi-temperature treatments of group D are higher than those obtained by the T6 treatments of group B, for both FB and CF. The elongation of modified and non-modified A356 alloys is greater when the alloys are FB-quenched, as compared to when they are water-quenched. For water-quenched alloys, it was seen that the FB treatment produced better elongation results than the CF treatment for all aging times imposed for B and D heat treatment conditions. The high heating rate of the FB results in faster fragmentation and spheroidization of the Si particles, as well as the distribution and dissolution of micro-constituents in the matrix, thereby increasing the ductility. [136] The highest values of elongation were obtained with the air quenching/T6-aging cycles of group C using a CF, which is to be expected due to the lowest strength values exhibited by these alloy samples. The improvement in the elongation of the modified alloys is related to the fragmentation and spheroidization of the acicular Si particles and iron intermetallics through Sr-modification and the high heating rate prevailing in the fluidized bed. This high heating rate activates the process of the thermal modification of eutectic Si and Fe intermetallics. [147] The decrease in elongation values, with increasing aging time, for water-quenched alloys, may be related to the precipitation of Mg_2Si, which hinders the dislocation motion during tensile testing, thereby reducing the ductility.

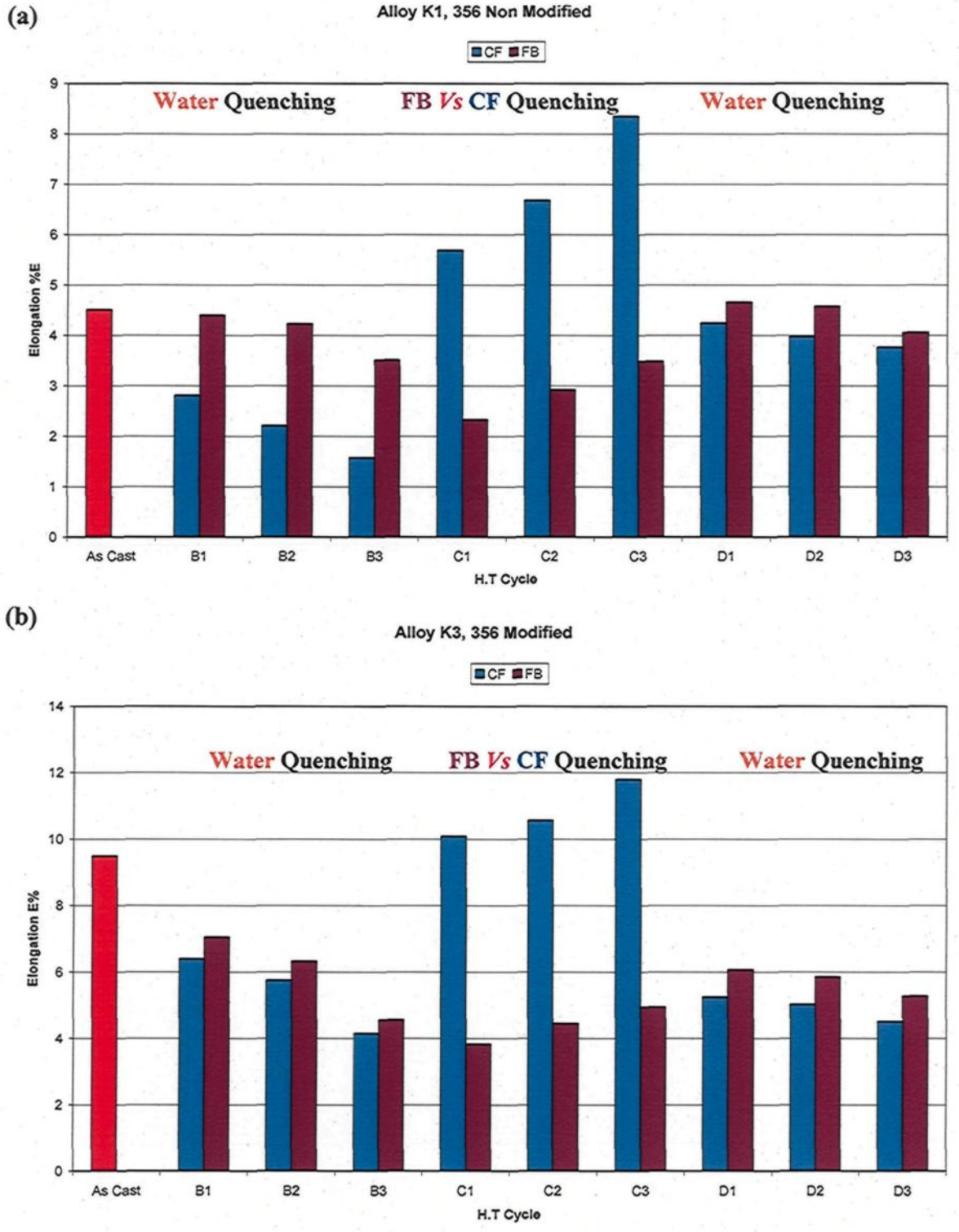

Figure 5.3. Average percentage elongation (El %) values for A356 alloys: (a) non-modified K1 alloy, and (b) modified K3 alloy.

5.2.1.2. Multi-temperature aging treatments (FB Vs CF)

The T6 treatment is usually preferred when heat treating Al-Si-(Mg/Cu) castings; this standard treatment produces the highest strength achievable with, however, a corresponding reduction in ductility. In some cases the T7 treatment is considered a better alternative, where this treatment leads to artificially overaging the alloy at high temperatures in the range of 200°C-240°C. The T7-overaging produces reduction of residual stresses, increased performance, as well as stabilization of the alloy, particularly in applications which involve exposure of the casting to elevated temperatures and thermal fatigue. The multi-temperature aging cycles in this work were divided in two categories starting with T7 temper (230, 249 and 270°C) and followed directly by a T6 (180°C) treatment, for various times. The current subsection will discuss the effects of T7/T6-type multi temperature aging treatments on the tensile properties of the A356.2-base alloys (K1 and K3). The aging temperatures/times applied to these alloys are shown in Table 3.3. The application of multi-temperature aging treatments aims at producing strength levels comparable to those obtained from a T6 temper, yet with increased ductility, equal to or greater than that attained from a T7 temper. The aging treatment is to precipitate an excess amount of Mg and Si out of the supersaturated solid solution in the form of hardening phases containing Mg and Si. According to the temperature and time applied to the A356.2 castings, the decomposition of the supersaturated solid solution may involve the formation of independent clusters of Si and Mg, followed by co-clusters of both Si and Mg, coherent needlelike GP zones, coherent needle-shaped β'', coherent rod-shaped β'', and the incoherent plate-shaped β-Mg_2Si phase. [115, 116, 117]

Figures 5.4 and 5.5 compare the tensile strength and elongation values, respectively, obtained with the T6 continuous aging treatment (180°C/8 h) with those obtained from the multi-temperature aging treatments. From Figure 5.4, it is seen that the T6 treatment yields higher strength values than nearly all of the multi-temperature aging cycles. This decrease in strength may be attributed to an increase in the inter-particle spacing between precipitates, which makes dislocation bowing much easier. [203] The multi-temperature aging cycles produce an increase in strength values with increasing T6-aging times (namely 2, 4 and 8 hours, at 180°C), as compared to a T7 temper alone (i.e. with no subsequent T6 aging stage). At the temperature of second aging stage (180°C), the T7-treated alloy microstructure may have been refined by, the T6 treatment, into a fine dispersion of semi-coherent clusters of Mg_2Si strengthening phase. [117, 118] The difference in strength values at 2 h in the second T6 aging step, and that obtained at 8 h, may be that the incoherent precipitates appearing after 2 h and disappearing later due to the dissolution of the precipitates and homogenization of the matrix. However, as diffusion/precipitation processes are affected by the aging temperature, the precipitates appear in the aluminum matrix only after an extended aging time. [117, 118, 196] In general, the strength values of heat treated alloys decrease with increase in T7 temperature of the multi-temperature aging treatment, due to overaging. The decrease in the strength of the 356 alloy, accompanying the overaging, is related to the loss of the coherency strain surrounding the precipitates through the formation of incoherent, stable β-Mg_2Si phases. In addition this the loss of coherency, the longer aging time results in the coarsening of the large precipitates at the expense of the small ones. This coarsening effect produces a lower density of the widely

dispersed, coarse precipitates. These changes in the precipitates the features reduce the resistance to dislocation motion through the metal matrix and lead to a deformable soft matrix. Figure 5.4 shows that the FB heat-treated alloys produce higher strengths, as compared to those obtained by CF, for all heat treatment cycles. Such results can be explained by the high heating rate of the FB which activates the rate of precipitate formation, giving rise to a high precipitates density. It was reported that the FB produces a large number of finely distributed Mg_2Si particles, compared to the CF. This difference in particle density explains the higher precipitation kinetics of aging in an FB. [204] Additionally, the dislocation concentration in the matrix affects the aging kinetics of Mg_2Si precipitation. The slow heating rate in a CF annihilates the dislocations during recovery, thereby reducing their density prior to reaching the aging temperature.[55, 56, 204]

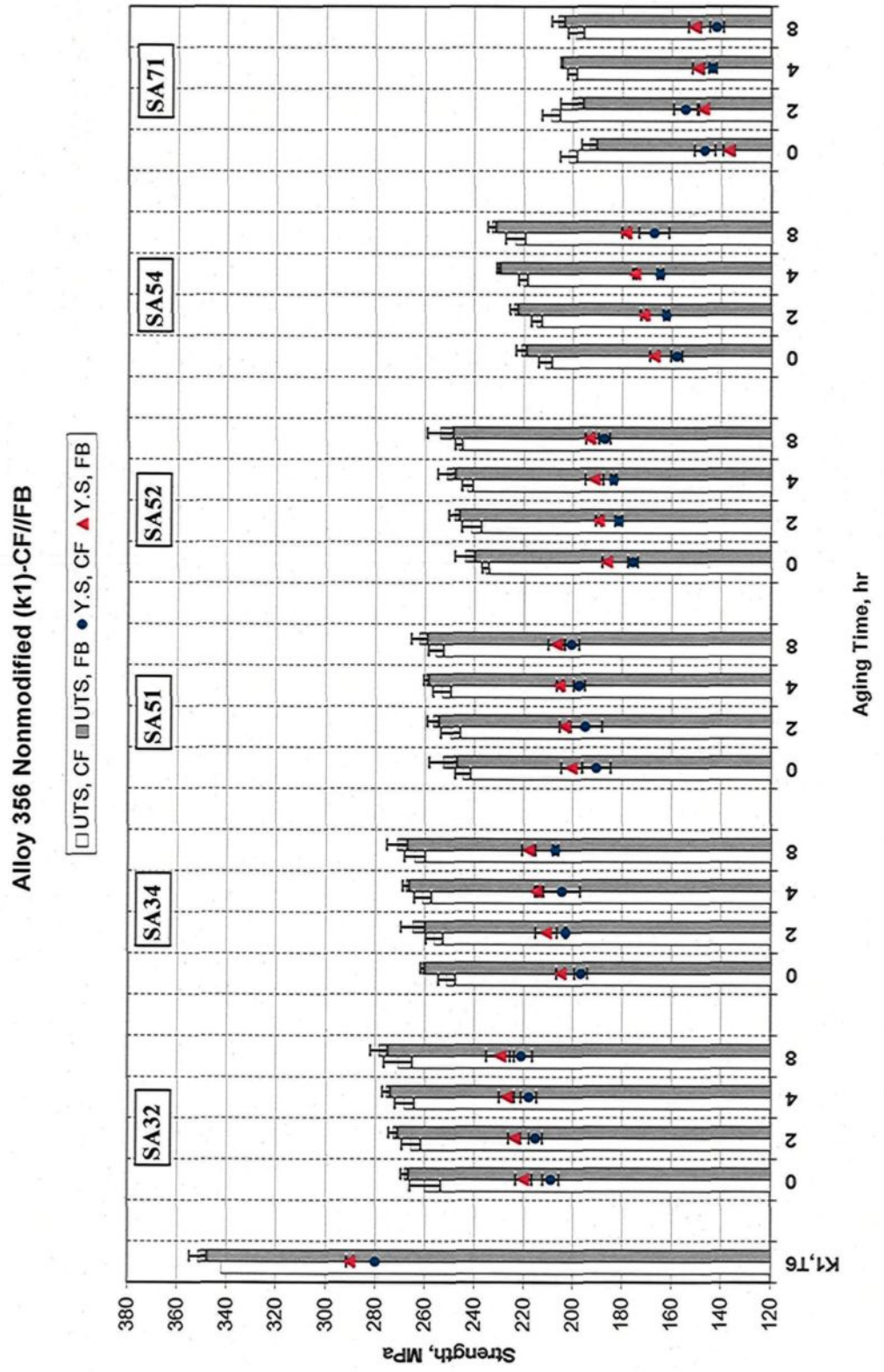

(a)

Figure 5.4

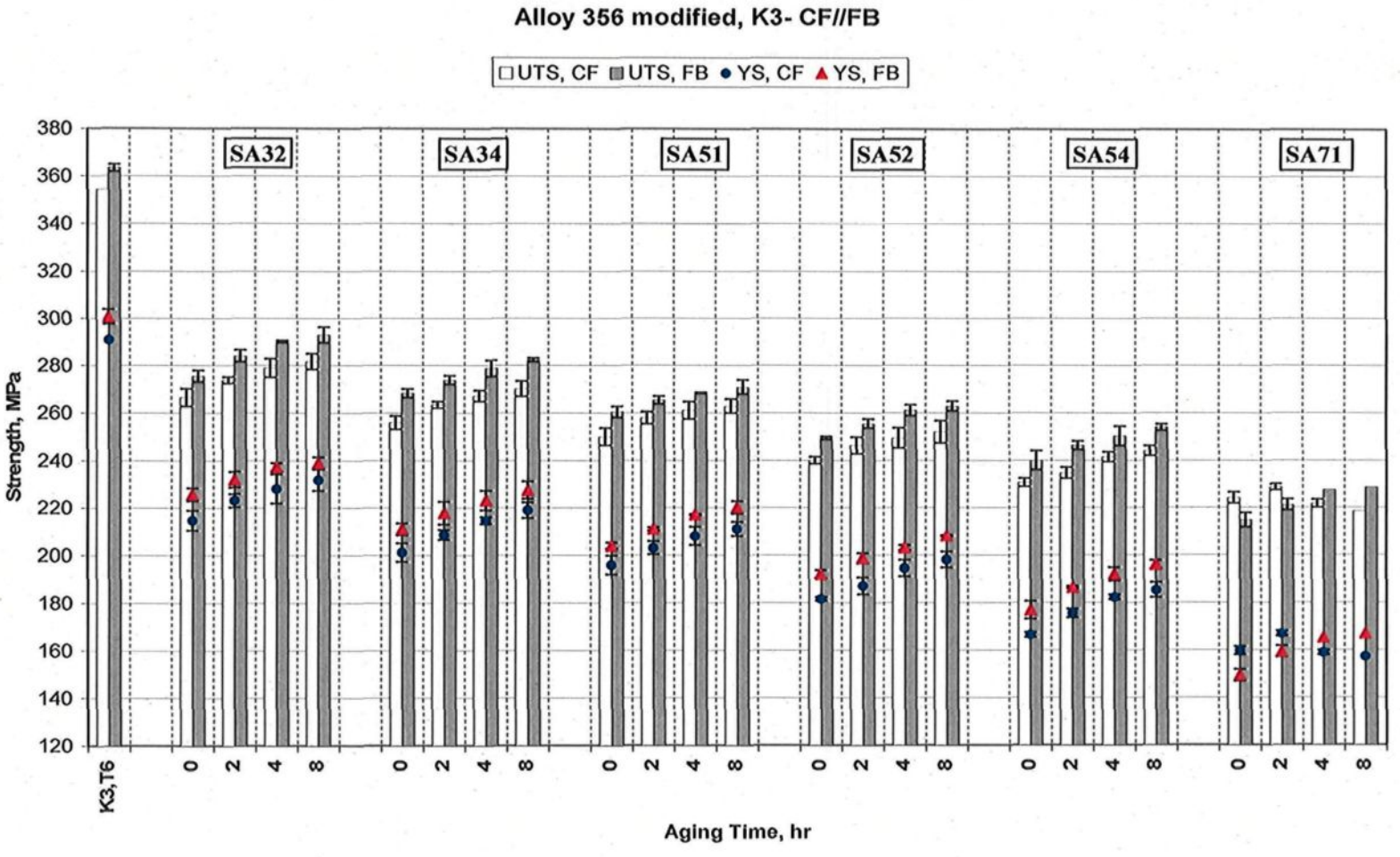

(b)

Figure 5.4. Average UTS and YS values for A356 alloys: (a) non-modified K1 alloy, and (b) modified K3 alloy.

There is a direct relationship between the heating rate and the radius of the clusters during aging treatment. [147, 204] The high heating rate in the FB leads to the formation of more stable clusters, or GP zones, during the heating up stage to reach the aging temperature. These clusters can act as suitable sites for the heterogeneous nucleation of further precipitates. [147] As Figure 5.4 demonstrates, the modified A356 alloys essentially behave in the same way as the mechanical behavior of unmodified alloys except for that fact that they exhibit higher strength values than the unmodified alloys for all heat treatment cycles studied.

Likewise, as Figure 5.5 shows, the modified A356 alloys demonstrate higher elongation values than the unmodified ones; this is attributed to the effect of Sr on the Si particles morphology. From a comparison of elongation values obtained from the T6 continuous aging and the multi-temperature aging treatments, it may be seen that the ductility is improved after the multi-temperature treatments. This behavior is to be expected since the corresponding strength values are lower, compared to the T6-treated samples. As was explained earlier, the noticeable reduction in the strength values of the 356 alloys, upon increasing the aging temperature and/or applying the first stage of aging at high temperatures (T7), is related to the formation of coarser precipitates with a lower density in the matrix, and displaying large inter-particle spacing. These changes facilitate dislocation motion and results in softening effects, thus producing increased ductility, as compared to T6-single stage aging. The second stage of the aging (T6-aging) is applied to the T7 heat treated alloys to improve the strength results, achieving a compromise between strength and elongation values and affecting the quality of the alloys.

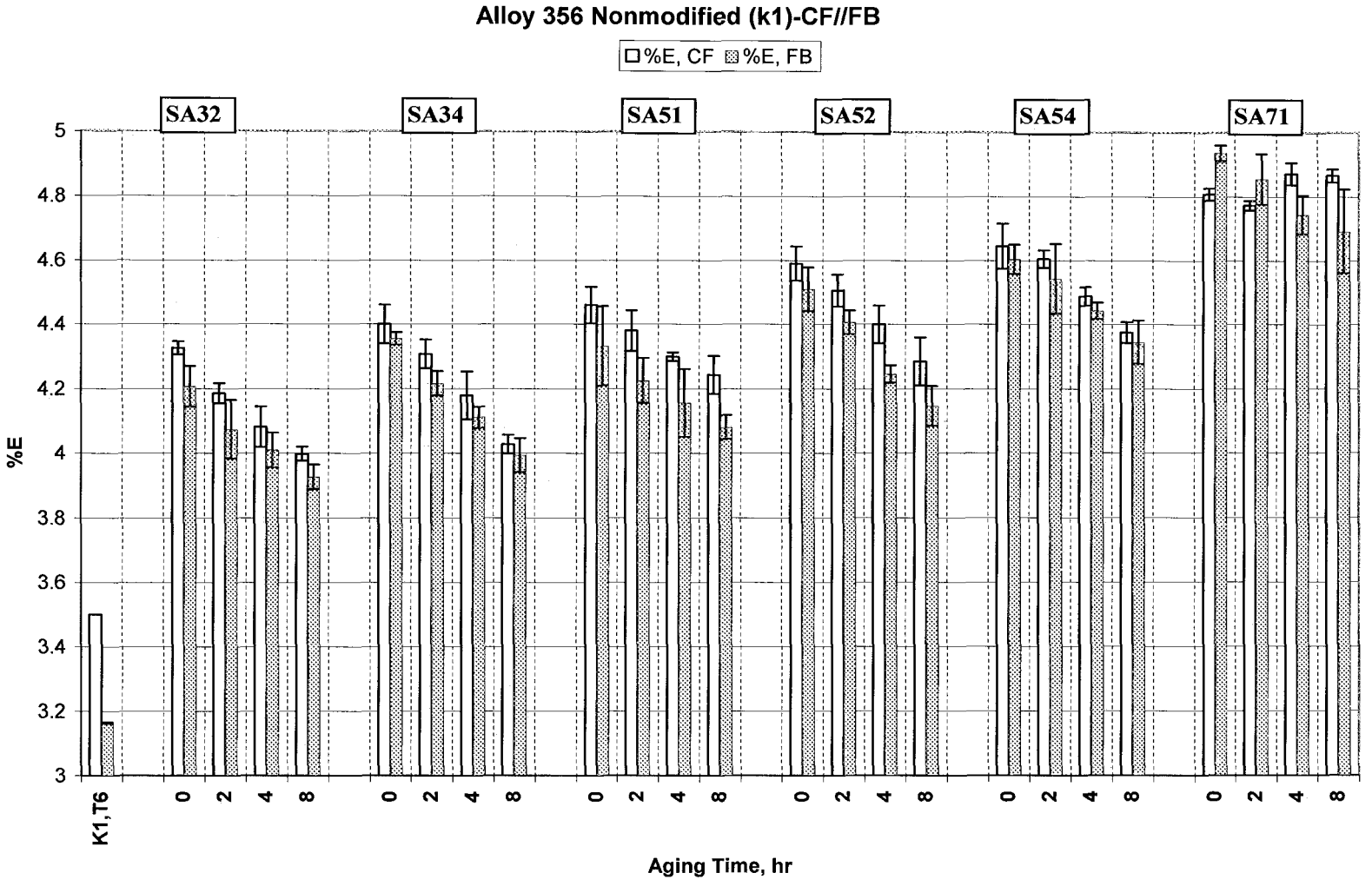

(a) Figure 5.5

193

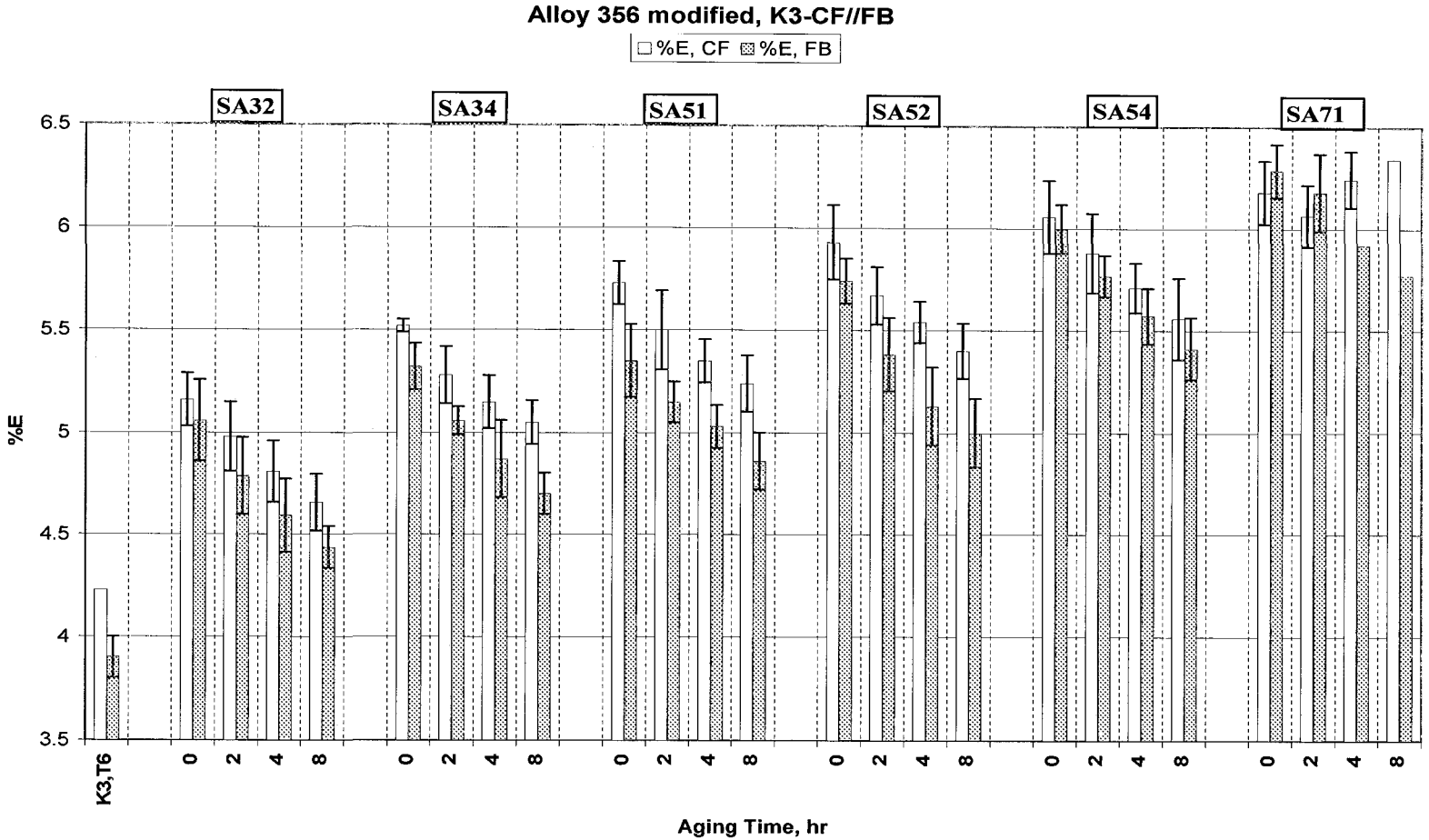

(b)

Figure 5.5. Average values of percentage elongation (El %) for A356 alloys: (a) non-modified K1 alloy, and (b) modified K3 alloy.

194

For the tensile results of unmodified A356 alloys, the multi-temperature heat treatment cycle corresponding to SA32 (see Table 3.3), viz., 230°C/180°C for 2h/8h using an FB shows a UTS of 278.3 MPa and elongation of 3.9% versus 351 MPa UTS and 3.1% elongation values obtained by applying a single-stage T6 aging treatment using an FB. According to the required mechanical properties for specific engineering applications, suitable heat treatment parameters may be selected for these particular alloys. Since the cost of heat treatment play a major role in the selection of type and route for heat-treating an alloy, the T6 treatment using an FB remains the most economical temper in terms of strength for the A356.2 alloy studied.

5.2.2. Al-Si-Cu-Mg Casting Alloys

5.2.2.1. Effects of quenching media

Figures 5.6 and 5.7 illustrate the effects of quenching media (water, air, sand) on the strength of non-modified and modified B319.2 T6-treated alloys. For water-quenched alloys (i.e. B and D heat treatment cycles), the fluidized bed heat treatment produces better strength values compared to those obtained with a conventional furnace, for all aging times. The difference in strength values is related to the high precipitates density of Cu-containing phase particles (i.e. $Al_5Cu_2Mg_8Si_6$ and $CuAl_2$ phase particles) in the FB-treated samples, as opposed to the CF-treated ones, as well as the dissolution of clusters or GP zones during the heating-up period to the isothermal aging temperature in the conventional convection furnace. [147, 204] In this work, the optimum strength values for CF heat-treated samples were obtained after 8 h of aging, (followed by a slight decrease in strength from

overaging), whereas with the FB treatment, a continuous increase in these values was noted. This is related to the stability of the clusters/GP zones and intermediate precipitates in the early stages of aging when using an FB. The peak strength attained after 8 h aging in a CF or 12 h aging in an FB may be related to the presence of hardening Cu-phase precipitates, [147] proposed by others as corresponding to θ-$CuAl_2$ + Q-$Al_4Cu_2Mg_8Si_5$. [187, 188] The FB heat-treated samples display better results than the CF heat treated samples, for all quenching media and heat treatment conditions. The high heating rate in an FB leads to the formation of more stable clusters, or GP zones, during the heating-up stage to reach the aging temperature; these clusters act as suitable sites for the nucleation of further precipitates, where the precipitation kinetics are related to the concentration of defects.

It was reported that the slow heating rate in a CF leads to the formation of co-clusters of Si and Mg, not GP zones, in 356 alloys; these co-clusters, however, retard the precipitation kinetics of Mg_2Si during aging. [146] In general, the strength values of water quenched 319 alloys (conditions B2 and B3) treated to T6 temper using CF and FB are higher than sand- and air-quenched samples (conditions C2 and C3) using both FB and CF, respectively. The high cooling rate due to water quenching, results in a high concentration of vacancies which act as nucleation sites for precipitates during aging stage. The density of precipitates is controlled through these heterogeneous nucleation sites.

Figure 5.6. Average UTS and YS values for non-modified B319 alloys.

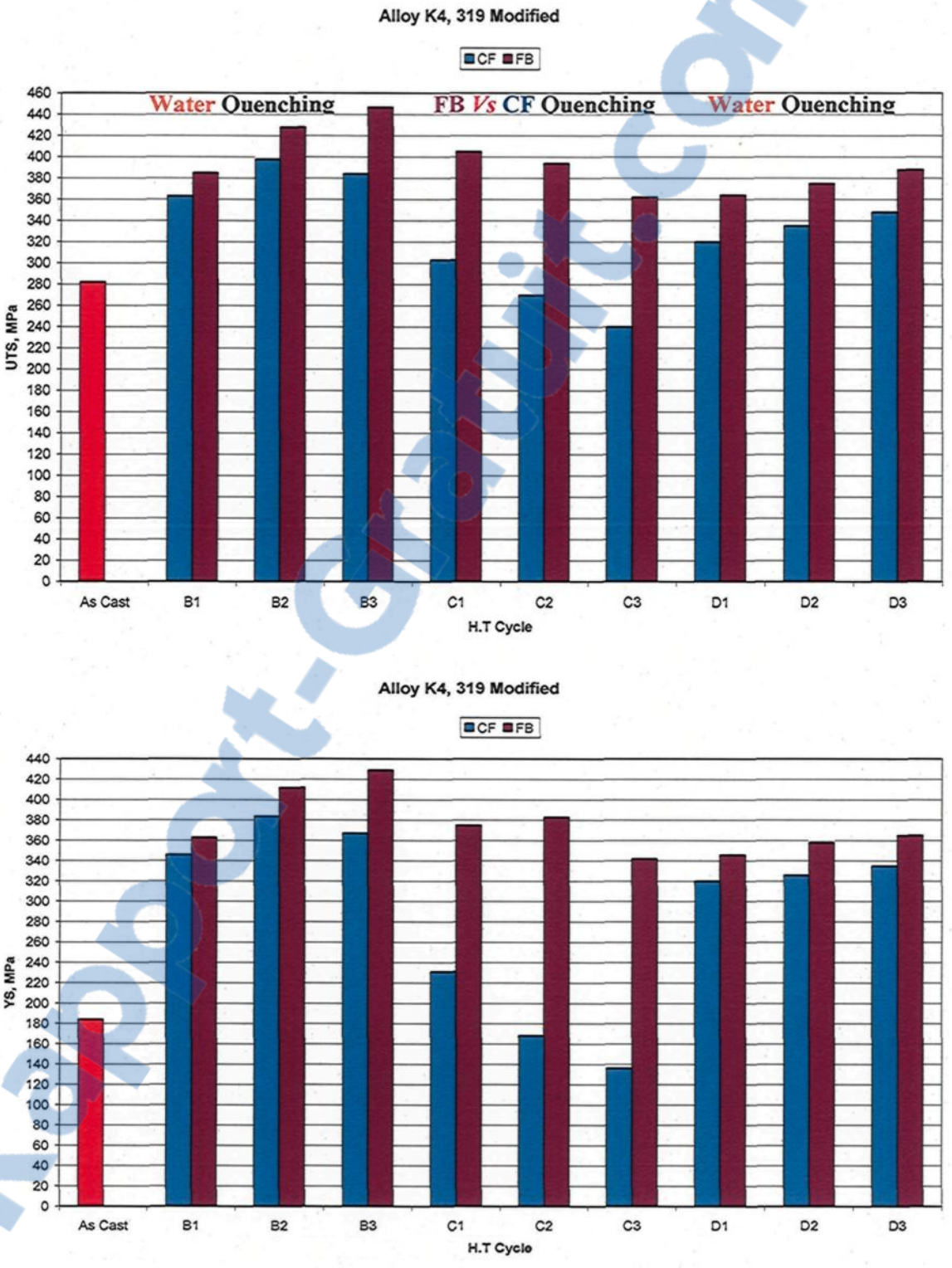

Figure 5.7. Average UTS and YS values for modified B319 alloys.

Comparing the fluidized sand bed and water as quenching media, for the same T6 conditions (B1, C1) at 170°C/4 h, the strength values of FB-quenched samples (C1; FB condition) are higher than those quenched in water, and followed by aging in an FB or CF. The direct quenching-aging treatment process using an FB results in the formation of greater numbers of clusters/GP zones which hinder the dislocation motion and consequently increase the strength values. [150, 151] The increase in YS when quenching is done in an FB versus in water is attributed to the formation of clusters and/or metastable phases that may be formed due to the slower cooling rate of FB quenching, while the low UTS exhibited by FB quenched-aged samples can be related to their relatively low elongation (C1; FB condition) compared to that exhibited by the water-quenched samples (B1-FB/CF). Both UTS and elongation values depends on the ease of dislocation mobility whatever the type of obstacles present in the matrix (clusters and/or Co-Clusters) formed due to the low cooling rate of the FB quenching medium (sand). The YS values depend on the size, density and distribution of precipitates formed in the final stage of the aging treatment process. [130, 132, 147, 150, 151] It may be noted from strength results that the 319 alloys are more responsive to the fluidized bed quenching, as compared to water quenching, than the 356 alloys. The relatively low cooling rate involved in FB quenching results in the formation of greater number of clusters and/or GP zones which by role act as nucleating sites for the hardening precipitates formed during aging with a high heating rate using the same fluidized quenching bed (direct quenching-aging). So that, for the same heat treatment conditions, the direct quenching-aging treatment applied to the 319 alloys using an FB results in marginally higher UTS and YS values than water quenched alloys treated

to T6 temper using either an FB or a CF. It was reported that a greater amount of GP zones are formed by applying T4 temper to Al-Si-Cu-Mg (354) alloys in the case of FB quenching; whereas no GP zones or other meta-stable phases are formed in FB quenched Al-Si-Mg (357) alloys as predicted by the CCT (continuous cooling transformation) and TTT (time-temperature transformation) diagrams. [130, 132, 150, 151] The formation of GP zones and/or meta-stable phases plays a vital role in the subsequent aging properties of the alloy and significantly affects the tensile properties of T6 treated alloys. Another study applying FB quenching on Al-Si-Cu-Mg alloys [151] reported that there is no significant differences in UTS and YS values are observed between FB and water quenched alloys. On the contrary, the tensile results shown in Figures 5.6 and 5.7 demonstrate that the strength of FB-quenched B319.2 alloys is higher than those quenched in water. Regarding the strength of heat-treated alloys using an FB or a CF for direct quenching-aging treatment (C1, C2, C3), the values decrease with increased aging temperature (170°C, 190°C, 210°C). This decrease in strength results is related to overaging. Overaging occurs after the peak strength aging temperature (190°C) is reached, using either CF or FB for direct quenching-aging treatment.

For the water quenched alloys subjected to multi-temperature aging conditions (D1, D2, D3), it may be observed that the T6 treatment cycles (groups B and C) yield higher strength values than almost all of the multi temperature aging cycles using both CF and FB. For multi-temperature treatment cycles, the FB-treated samples show better strength results than those obtained with the CF, where the high heating rate of the FB results in the formation of a high density of stable GP zones that act as nucleation sites for precipitates.

Also the formation of clusters resulting from the 24-hr delay at room temperature after quenching may promote the formation of existing precipitates. [91, 205, 206] The significant response of B319.2 alloys to FB multi-temperature aging heat treatment cycles, compared to that of A356.2 alloys, may be related to the formation of several types of precipitates such as Cu-containing phases and Mg_2Si, with different sizes during multi-stage aging in the B319.2 alloys. Maximum strengthening by age hardening will be achieved for alloys that contain large precipitates to resist shearing by dislocations and yet are too finely spaced to be by-passed. The maximum response to hardening occurs in a microstructure containing a combination of co-clusters/GP zones (after 24 hours pre-aging at room temperature after quenching) and relatively widely dispersed, semi-coherent, intermediate phases. [203, 204, 205, 206] This combination of different precipitates may be achieved by applying multi-temperature aging treatments to get a compromise between high strength and high ductility.

The modified B319.2 alloys show the same mechanical behavior as the unmodified ones for all heat treatment cycles, as shown in Figure 5.7. The modified alloys show slightly better strength results than the unmodified alloys for all heat treatment conditions (B, C, D).

Figure 5.8 illustrates the variation in elongation values of Al-Si-Cu-Mg alloys, obtained with different heat treatment cycles, and using both CF and FB. Elongations for the FB quenched-aged samples were lower than those quenched in water. In general, the CF heat treatment cycles show better ductility than those employing the FB. This is expected for 319 alloys containing Mg due to maximum strengths achieved with FB heat

treatment. The greatest elongation values were obtained with the air quenching-aging, T6 cycles (group C) using a CF, given that these samples also exhibit the lowest strength values. The improvement in ductility for the modified alloy may be related to the fragmentation and spheroidization of the Si particles and Fe intermetallics obtained through modification and the high heating rate prevailing in the FB as discussed previously. For water-quenched alloys, heat treated using both CF and FB, Figure 5.8 shows that no noticeable difference in elongation values with aging time is obtained using either technique; however, CF-treated samples show slightly better results than FB-treated samples, for all aging times. Elongation decreases with further aging time; this loss of ductility is related to the strengthening effect associated with the precipitation of the Mg_2Si and Cu-containing phases. It may be noted that the multi aging cycles (D1, D2, D3) produce either better or similar elongation values, compared to T6 temper cycles (B1, B2, B3) for either FB or CF. The main objective of multi-temperature aging cycles is to achieve a compromise of high strength and elongation, required for a specific engineering applications.

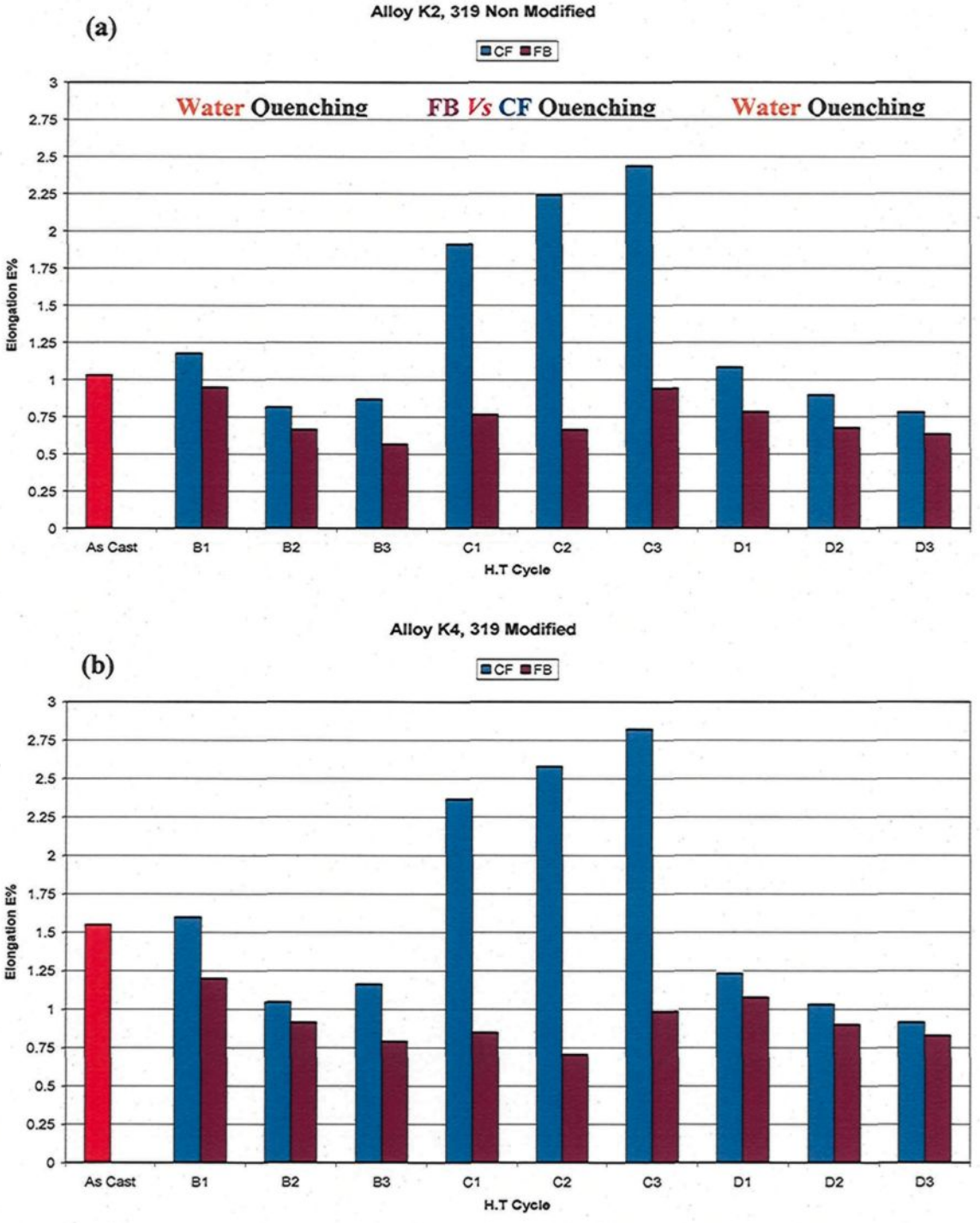

Figure 5.8. Average values of elongation percentage (E%) for 319 alloys (a) non-modified K2 alloy, and (b) modified K4 alloy.

5.2.2.2. T7/T6-type multi-temperature aging treatments (FB Vs CF)

The chemical composition of B319.2 casting alloys contains three hardening elements, namely, copper, magnesium, and silicon. The addition of Mg greatly enhances the artificial aging response of the 319 alloys. Age-hardening treatment of Al-Si-Cu-Mg alloys, results in the precipitation of the quaternary *Q*-phase and its precursors, which play an essential role in the strengthening of this specific alloy system. In addition to the precipitation of the *Q*-phases, several others, such as θ-Al_2Cu, β-Mg_2Si, *S*-Al_2CuMg, σ-$Al_5Cu_6Mg_2$ and their precursors, are also expected to precipitate during age-hardening treatment of B319.2 (Al-Si-Cu-Mg) alloys. [94, 207] As previously mentioned, T7/T6-type multi-temperature aging treatments permit the precipitation of uniformly dispersed, semi-coherent, intermediate precipitates, with the aim of producing strength levels equal to those of the T6 temper but with a ductility equal to or greater than that of the T7 temper. In this work, the multi-temperature aging cycles were divided in two categories, starting with T7 temper (230, 249, 270°C) and followed directly by T6 temper (180°C) treatments for various times. The current section will discuss the effects of these multi-temperature aging treatments on the tensile properties of the B319.2-base alloys (K2 and K4). The aging temperatures and times applied to the alloys are shown in Table 3.3.

Figures 5.9 and 5.10 compare the tensile strength and elongation values, respectively, obtained with the T6 continuous aging treatment (8 h at 180°C) with those obtained from the T7/T6 multi-temperature aging treatments. It may observed that the T6 treatment yields higher strength values than almost all of the multi-temperature aging cycles, with the exception of treatment cycles SA32, SA34 (consisting of aging at 230°C

for 2h and 4h, respectively, followed by aging at 180°C for 8 h). With the use of these heat treatment cycles, the strength values attained are almost identical to those obtained after T6 treatment (397.3 MPa for the T7/T6-type multi-temperature aging treatment versus 400 MPa for the T6) as shown in Figure 5.9. It can be noted from the strength results that even at prolonged aging times (8 h), the strength values of FB-treated multi-temperature aged alloys are still high for heat treatment cycles up to SA54 (aging at 249°C/4 h, followed by aging at 180°C). On the other hand, the strength values of CF-treated multi-temperature aged alloys show signs of overaging after 4 h of aging at 180°C for multi-temperature aging/heat treatment cycles applied up to SA54. The continuous increase in these values may be noted, related to the stability of the GP zones and of the intermediate precipitates in the early stages of aging when using a fluidized bed. The peak strength attained after 4 h aging in a CF or 8 h aging in an FB may be related to the presence of hardening elements such as θ-$CuAl_2$ + Q-$Al_4Cu_2Mg_8Si_5$. [147] The high heating rate in an FB leads to the formation of more stable clusters, or GP zones, during the heating-up stage to reach the aging temperature. These clusters can act as suitable sites for the heterogeneous nucleation of further precipitates. The precipitation kinetics of such heterogeneously nucleated precipitates is related to the concentration of defects.

For the heat treatment cycle SA71 which consists of aging at higher temperature of 270°C for 1h followed by aging at 180°C, the strength values of heat-treated 319 alloys show overaging at an earlier T6 aging time of 2 h using an FB and at zero T6 aging time (*viz.*, directly after T7 aging) using a CF (Figures 5.9 and 5.10). Such a decrease in strength and increase in the ductility of the alloy is related to the softening which occurs as a result

of the over-aging conditions at which the equilibrium precipitates form, leading to the loss of coherency strain between the precipitates and the matrix. In addition, over-aging also result in the continuous growth of large precipitates at the expense of the smaller ones, ultimately leading to coarse precipitates with less density in the metal matrix having large inter-particle spacing. All these changes which accompany over-aging contribute to a decrease in the strength of the castings. It may be noted that the modified 319 alloys have the same mechanical behavior as unmodified ones except that the strength values of modified alloys are higher than those obtained by unmodified alloys for all heat treatment cycles. In general, the fluidized sand bed heat treated alloys show higher strength values than those obtained by heat treatment using the CF for all heat treatment cycles; this is confirming the significant effect of an FB technique for applying T7/T6 multi-temperature aging treatment cycles of B319.2 alloys as well as A356.2 alloys.

Regarding the strength results of B319.2 cast alloys, when compared to A356.2 castings, it may be noted that these alloys were more responsive to T7/T6 multi-temperature aging treatment cycles using an FB (namely SA32 and SA34 cycles), showing the same or slightly better strength as those obtained when applying T6 standard treatment (Figures 5.9 and 5.10). The aging behavior observed when applying the second (T6) aging step at 180°C is related to the precipitation of the Cu- and Mg-containing phases in the metal matrix. The size of these precipitates varies according to the aging time applied to the castings.

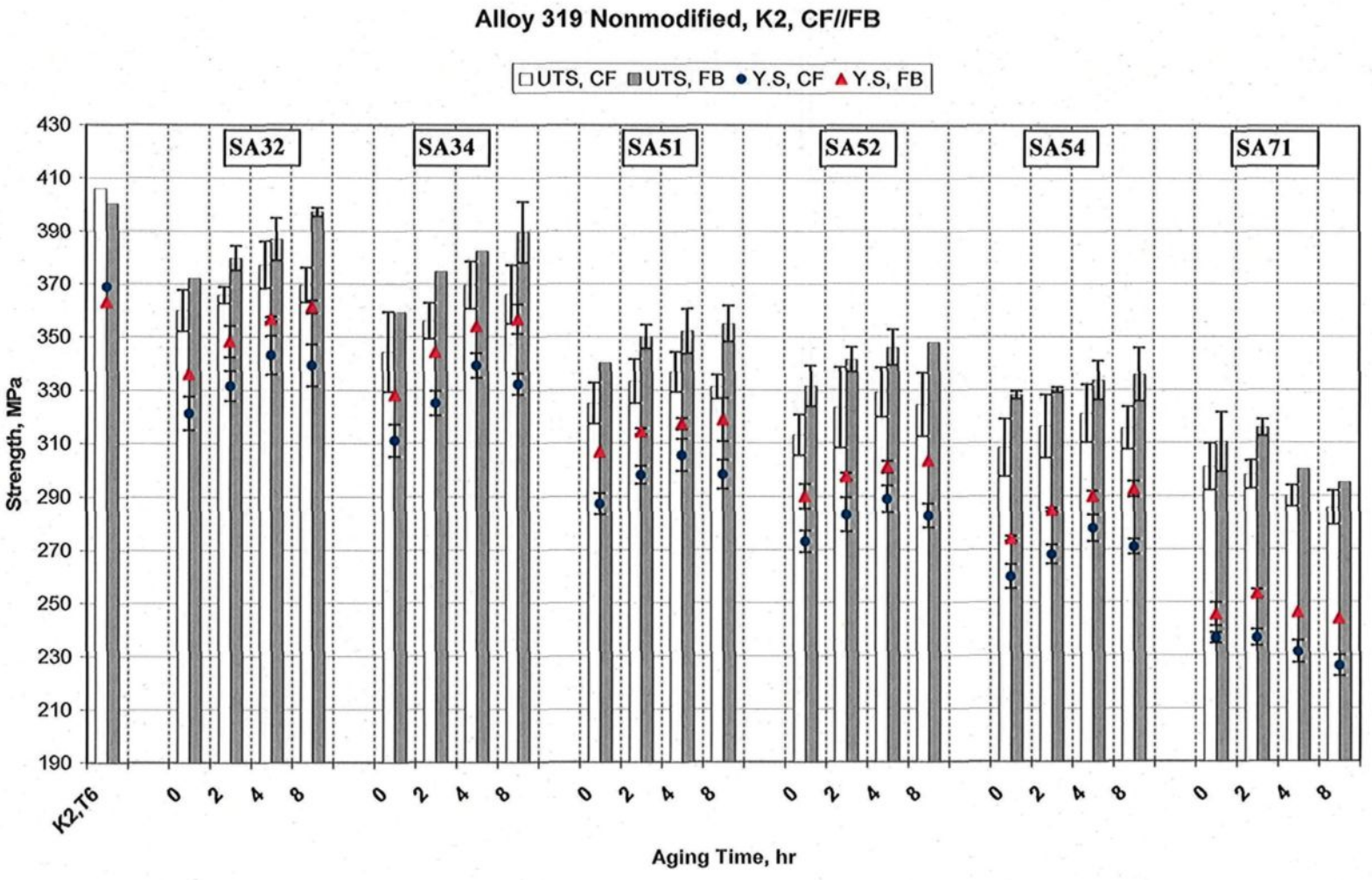
Alloy 319 Nonmodified, K2, CF//FB
UTS, CF
UTS, FB
Y.S, CF
Y.S, FB
SA32
SA34
SA51
SA52
SA54
SA71
Strength, MPa
430
410
390
370
350
330
310
290
270
250
230
210
190
K2,T6
0
2
4
8
Aging Time, hr

(a)

Figure 5.9

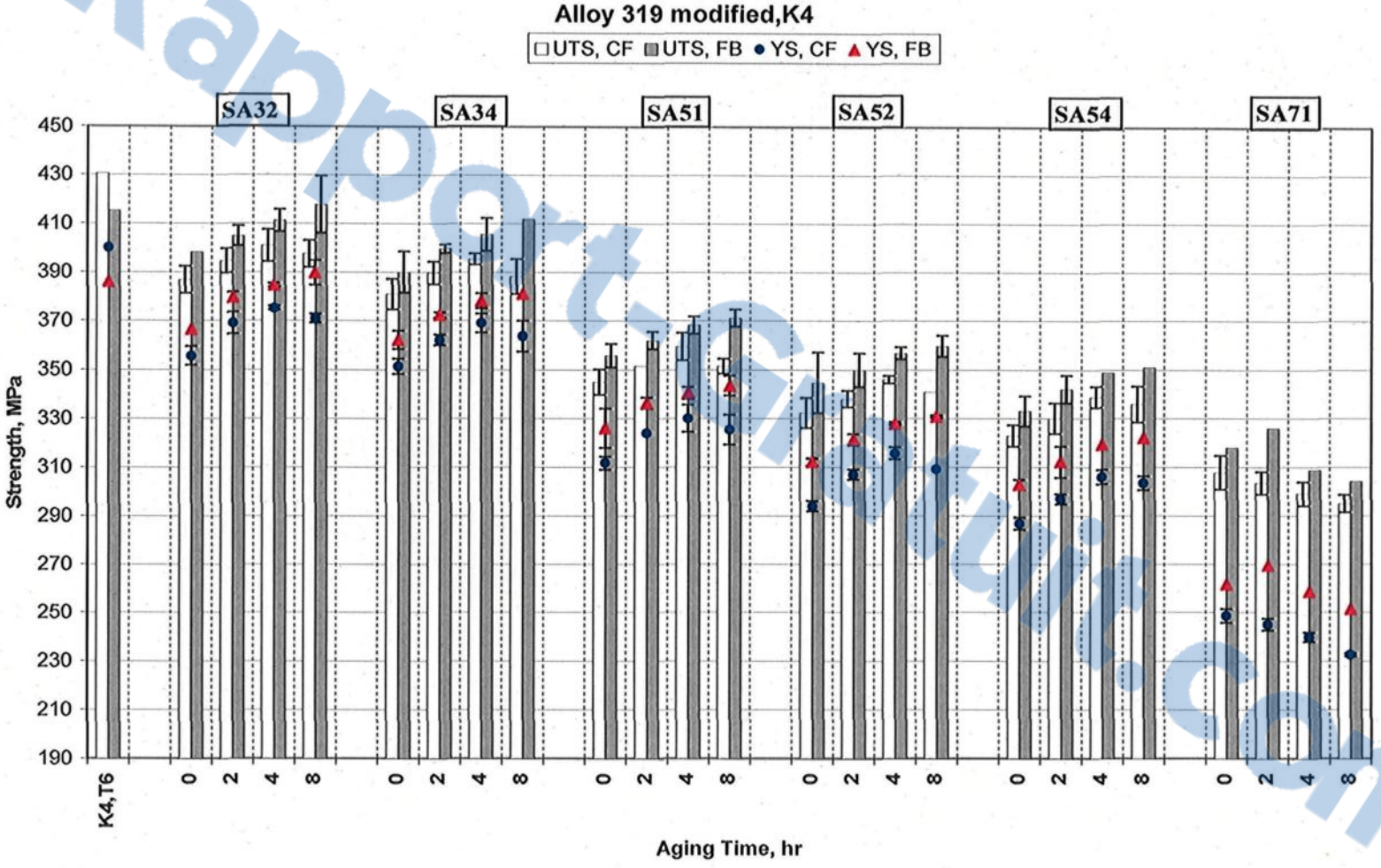

(b)

Figure 5.9. Average UTS and YS values for A356 alloys: (a) non-modified K1 alloy, and (b) modified K3 alloy.

208

The increased strength observed in the early stages of aging is related to the redistribution of the excess solute atoms which thus form clusters of Cu-containing phases. Chakrabarti and Laughlin, [83] Yao et al., [206] and Wolverton [207] have reported these to be the coherent, metastable, rod-shaped Q-phase.

From Figures 5.9 and 5.10, it may be noted that increasing the aging temperature, from 230°C (SA32) to 270°C (SA71), results in reducing the time required to reach peak-aging, observed at 8 h and 2 h using, respectively, using an FB. This specific form of the aging curves is a result of the overaging, occurring with increasing aging temperature and/or time. Applying an aging temperature of 270°C results in an increase in alloy strength, where the aging time required to reach peak strength, in this case, was 2 h. This aging treatment is related to the high rate of atomic diffusion accompanying high heating rate (high temperature, low time) and the direct precipitation of the coherent and semi-coherent phases, which are the main causative source of peak-strength. Aging at 270°C is expected to be higher than the solvus temperatures for the precipitates and zones which usually form during the early stages of aging. Consequently, the time spent in the precipitation and dissolution of these precipitates at lower aging temperatures will be reduced when increasing the aging temperature to 270°C. Any further increase in the aging time results in a further decrease in the alloy strength and an expected increase in elongation values.

Figure 5.10 shows the elongation values obtained for the B319.2 alloys when subjected to the T6 and T7/T6 multi-temperature aging treatments. It may be seen that the percentage elongation values obtained from the multi-temperature treatments are closely

similar to the T6 treatment values. Although the treatment cycles SA52, SA54 and SA71 produce better elongation values as compared to T6 treatment. Overall, taking into consideration both strength results and elongation values, the multi-temperature aging treatments may be considered to be more advantageous for the B319.2 (Al-Si-Cu-Mg) cast alloys. According to the tensile properties obtained in this study, the treatment cycles SA32 and SA34 may be selected for B319.2 alloys used for particular engineering applications that require a compromise of high strength and ductility values as compared to the standard T6 temper treatment. As shown in Figure 5.10, the modified 319 alloys show higher elongation values than the unmodified ones which is related to the effect of Sr on the morphology of Si particles. The improved elongation following the multi-temperature treatments are to be expected as the corresponding strength values are lower compared to those of the T6-treated samples. The noticeable reduction in the strength values of the 319 alloys, upon increasing the aging temperature and/or applying first stage of aging at high temperatures (T7), is related to the formation of coarser precipitates with lesser density in the matrix having large inter-particle spacing (the objective of T7-first stage aging). These changes facilitate dislocation motion and results in softening effects producing higher ductility values as compared to T6-single stage aging. The second stage of T6-aging is applied to the T7-temper heat treated alloys to improve the strength results, thus achieving a compromise between strength and elongation values and affecting the quality of alloys.

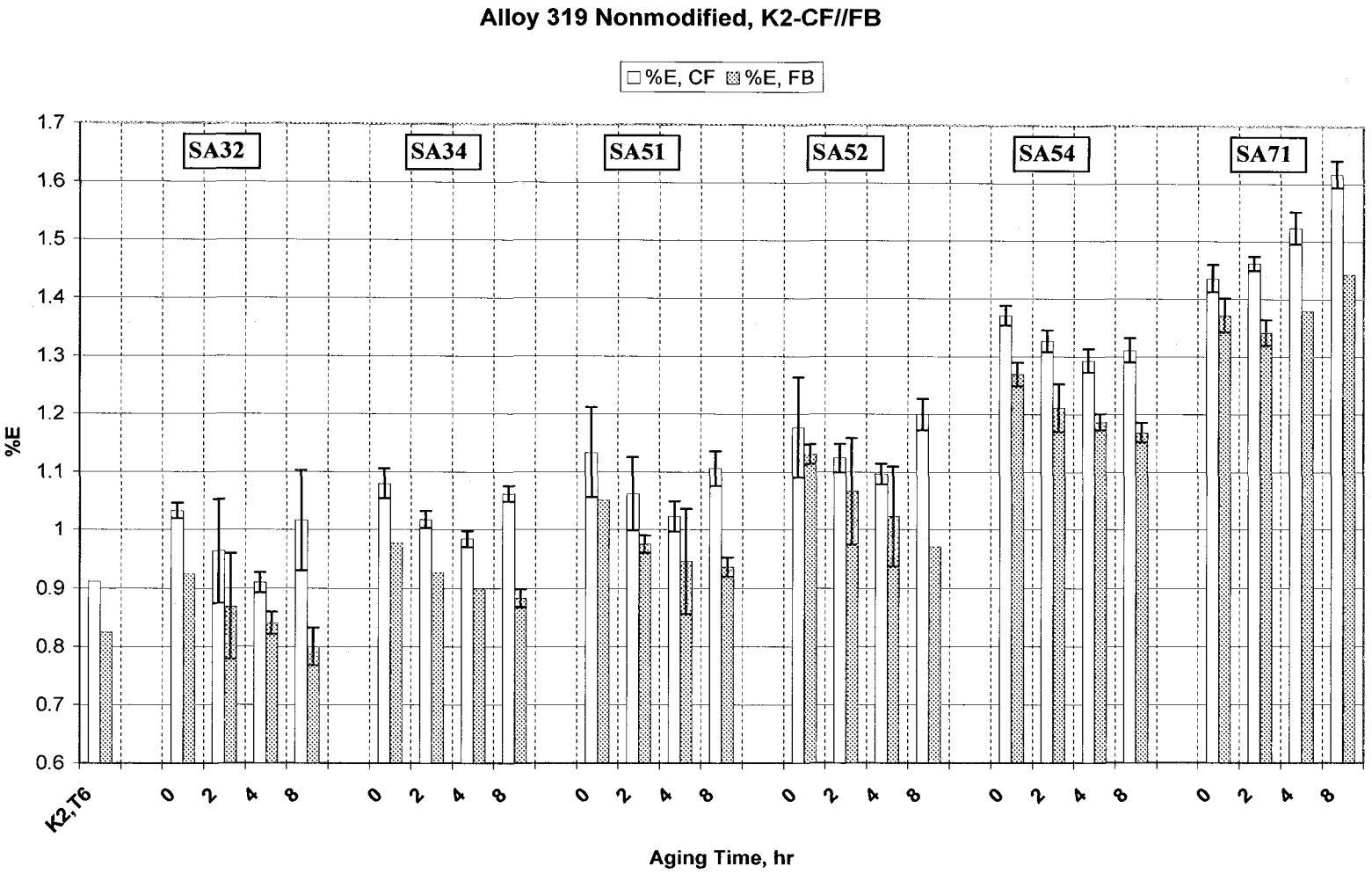
Alloy 319 Nonmodified, K2-CF//FB
□%E, CF ▨%E, FB
%E
1.7
1.6
1.5
1.4
1.3
1.2
1.1
1
0.9
0.8
0.7
0.6
SA32
SA34
SA51
SA52
SA54
SA71
K2,T6
0 2 4 8 0 2 4 8 0 2 4 8 0 2 4 8 0 2 4 8 0 2 4 8
Aging Time, hr

(a)

Figure 5.10

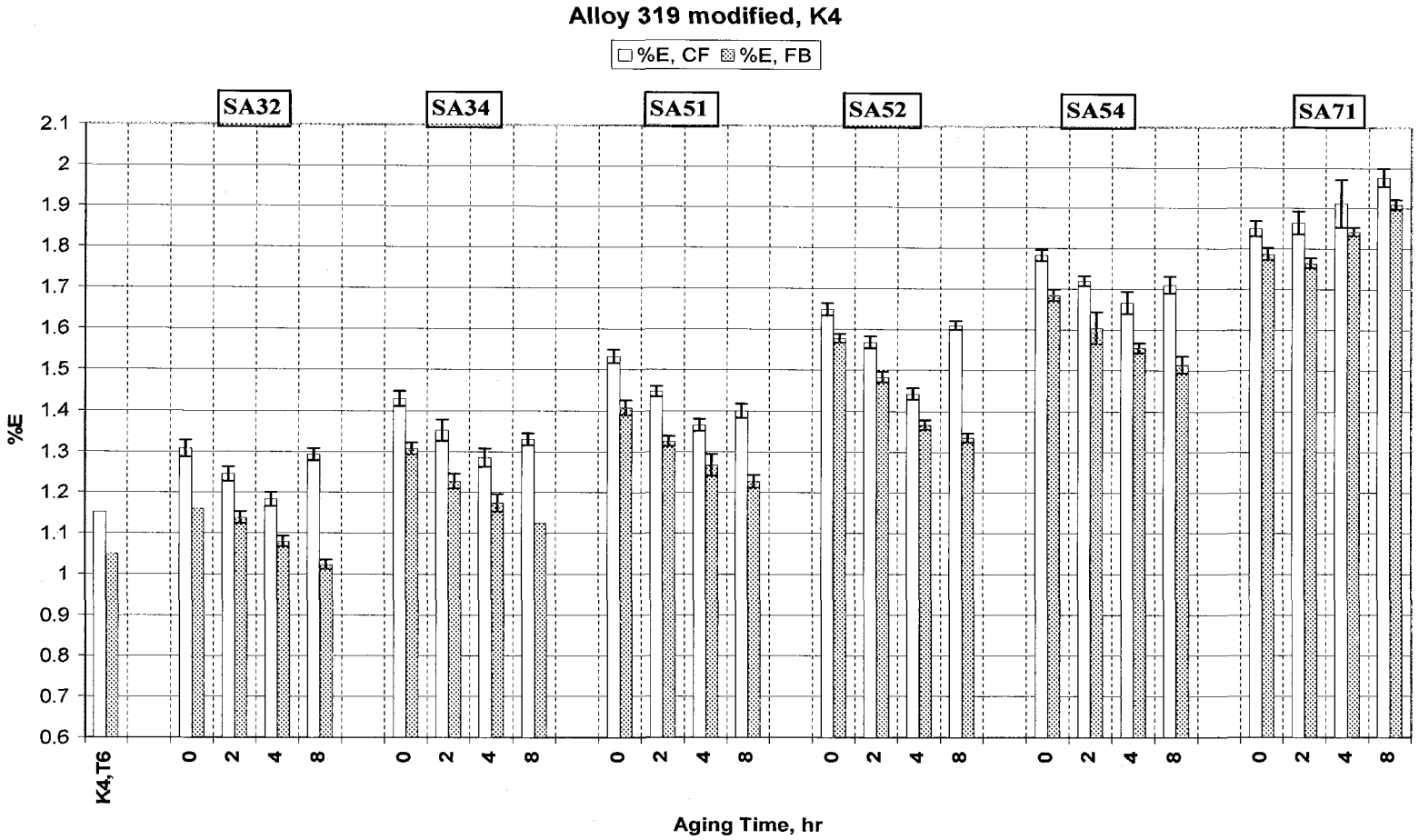

(b)

Figure 5.10. Average values of percentage elongation (El %) for B319.2 alloys: (a) non-modified K2 alloy, and (b) modified K4 alloy.

212

5.3. QUALITY INDICES

Quality indices represents a significant tool for evaluating, selecting and predicting the most appropriate metallurgical conditions to be applied to Al-Si-(Mg/Cu) casting alloys with a view to obtaining specific properties. Accordingly, all pertinent results will be presented using two types of charts, based on the type of alloys investigated: (i) charts for 356 alloys based on Drouzy's approach, and (ii) charts for 319 alloys based on Casers' approach. Generating these charts provides a logical evaluation of the effects various parameters may have on the tensile properties and quality indices of the castings in question. The results in each case were re-plotted using scatter-plots and contour plots to confirm the original analyses and interpretations made using the quality charts. These parameters include the effects of quenching media and multi-temperature aging cycles on the quality performance of A356.2 and B319.2 cast alloys heat-treated using FB and CF heat treatment techniques.

5.3.1. Al-Si-Mg Casting Alloys

Figures 5.11 compares the effects of modification, quenching media and aging parameters on the quality of A356 alloys after a solution heat treatment at 530°C/5h, carried out in a fluidized bed versus a convection furnace. From the quality maps shown in Figure 5.11 (b) generated using Equations (5) and (6), it may be observed that the modified 356 alloys show an improvement in quality values by 45 MPa over the non-modified alloy, for all heat treatment cycles. The main purpose of Sr addition to Al-Si-Mg alloys is to change the morphology of the eutectic silicon from an acicular form into a fibrous one

resulting in improved ductility and strength with high quality values. The addition of the appropriate amount of Sr improves the mechanical properties, specifically, the ductility and the quality index of Al-Si casting alloys. Closset and Gruzleski [112] studied the influence of Sr-level on the quality index of A356-T6 casting alloys which had been subjected to three cooling rates. They observed that the strontium range of 0.005%-0.015% is the optimum amount which may be added to A356 alloys to improve their mechanical properties and quality index values. The mechanism of eutectic silicon modification is based on two concepts: (i) the restricted nucleation and (ii) the restricted growth mechanisms of eutectic silicon particles in the presence of a modifying agent. [51, 208] Lu and Hellawell [209] proposed that the modifying agent is adsorbed at the silicon-liquid interface and results in growth twins and branching of silicon particles. In addition to Sr, the fluidized sand bed has a significant effect on Si particle size, reducing it by more than half after 0.5-5h of solution heat treatment times as discussed in section 4.2.1.

For water-quenched alloys treated to T6 temper (B1, B2, B3 conditions), the quality values exhibited by FB-aged samples are 50 MPa greater than those obtained by a CF, for all aging times, Figure 5.11 (a). The high heating rate in an FB activates the precipitation rate, producing more precipitates after a short aging time, resulting in higher strength and quality values. This difference in quality values between the CF- and FB-aged samples is reduced to 15 MPa due to the significant effect of modification, compared to the effect of high heating rate in an FB, Figure 5.11 (b). Figure 5.11 (a) shows that the water quenched alloys treated to T6 temper using an FB (B1, B2, B3 conditions) produce better quality values than those obtained by FB and CF quenched-aged alloys (C1, C2, C3). For

the same aging parameter conditions (aging at 170°C/4h), the FB quenched-aged alloys (C1-FB condition) show nearly the same or better quality values than those obtained by water-quenched/CF-aged alloys (B1-CF condition), as shown in Figure 5.11 (a). With regard to the water-quenched samples, the aging behavior of 356 alloys treated to T6 temper is quasi-parallel to the *iso-Q* lines as may be observed in the quality charts of Figure 5.11 for the B series. These charts also show that increasing the aging time does not affect the quality index values of the 356 castings which had been heat treated in a CF and an FB. This type of aging behavior may be related to the continuous increase in the strength of the alloy at the expense of its ductility; the reduction in ductility compensates for the increase in strength according to Equation 5, so that the Q values essentially remain the same. In general, It should be noted that using water as quenching medium results in a marked improvement in strength and quality values due to the faster cooling rate achieved by using water as opposed to hot air using a CF. However, the FB quenched-aged samples ensure a reduction of residual stresses, as well as better strength and good quality, compared to alloy samples quenched with water or air.

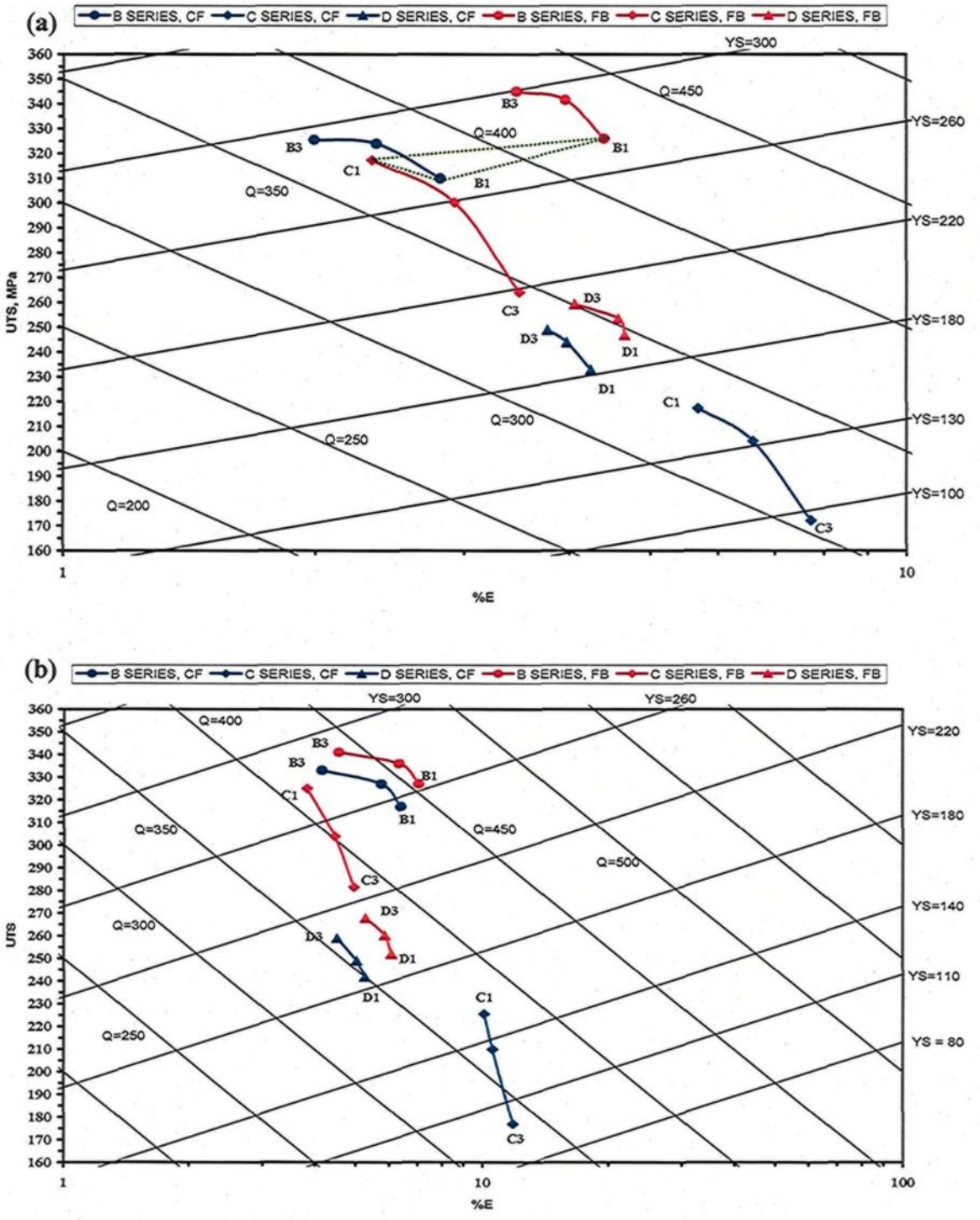

Figure 5.11. Quality charts using Equations (5) and (6) showing the effects of quenching media and modification on the quality and UTS of 356 alloys: (a) non-modified K1 alloy, and (b) modified K3 alloy.

For sand and air quenched-aged alloys, the modified 356 alloys show a noticeable decrease in quality values with an increase in the aging temperature from 170°C to 210°C (C1, C3 conditions). The decrease in quality values is not significant, however, for non-modified 356 alloys; this is related to the fact that increasing the aging temperature up to 210°C results in a continuous decrease in the strength with a continuous increase in ductility. The net effect of this aging treatment thus produces a non-significant decrease in the quality index values of non-modified 356 alloys. For the same heat treatment cycles (C-conditions), the FB quenched-aged alloys produce better quality and strength results than CF quenched-aged alloys; the hot air quenched-aged alloys using a CF show the lowest quality and strength values due to the lowest cooling and heat transfer rates associated with the hot air quenching medium. The slowest cooling rate obtained in a CF quenching medium allows formation of coarser precipitates with lesser density in the matrix displaying large inter-particle spacing resulting in softening effects and reducing the quality values in this case (C1, C2, C3; CF conditions), where the decrease in strength values is more significant than the increase in ductility.

For water-quenched alloys treated to multi-temperature aging cycles, the FB heat-treated samples show higher quality values than those heat-treated using a CF. The combinations of different precipitates which may occur from multi-stage aging treatments would result in a compromise between strength and ductility, and thus affect the quality. The water-quenched alloys treated to T6-temper conditions (B1, B2, B3) show better quality values than those treated to multi temperature aging cycles, namely D1, D2 and D3. This difference in quality values may be related to the significant increases in UTS values

for T6-tempered alloys at the expense of the higher elongation values for multi-temperature aged alloys. It should be noted that the quality values are affected by both UTS and %El values as shown in Equation 5.

Figure 5.12 shows the effects of multi-temperature aging treatments on the quality of A356.2 casting alloys; two heat treatment cycles, namely SA34 and SA54, were selected to be discussed due to the common use of applied T7 temperatures (230°C/4h, 249°C/4 h) in industrial automotive applications. These treatments aim at producing strength levels equal to those of the commonly used T6 temper but a high ductility which is equal to or greater than that of the T7 temper. It can be noted from Figure 5.12 that the modified alloys show better quality values than the non-modified ones heat treated using both CF and FB. The heat treated alloys using an FB show better strength and quality results than those treated using a CF for the selected T7/T6 multi-aging cycles. Regarding to the aging behavior at 180°C for up to 12 h, the quality levels are quasi-parallel to the *iso-Q* lines, as will be observed in the quality chart shown in Figures 5.12 for selected heat treatment cycles. This behavior illustrates that aging time up to peak-strength does not affect the quality index values of the 356 castings. Such an observation is related to the fact that increasing the aging time up to 12 h results in a continuous increase in the strength of the casting at the expense of its ductility, although the increase compensates for the reduction in ductility in accordance with Equation 5. Thus, the net effect of this aging treatment ultimately leads to non-significant changes in the quality index values.

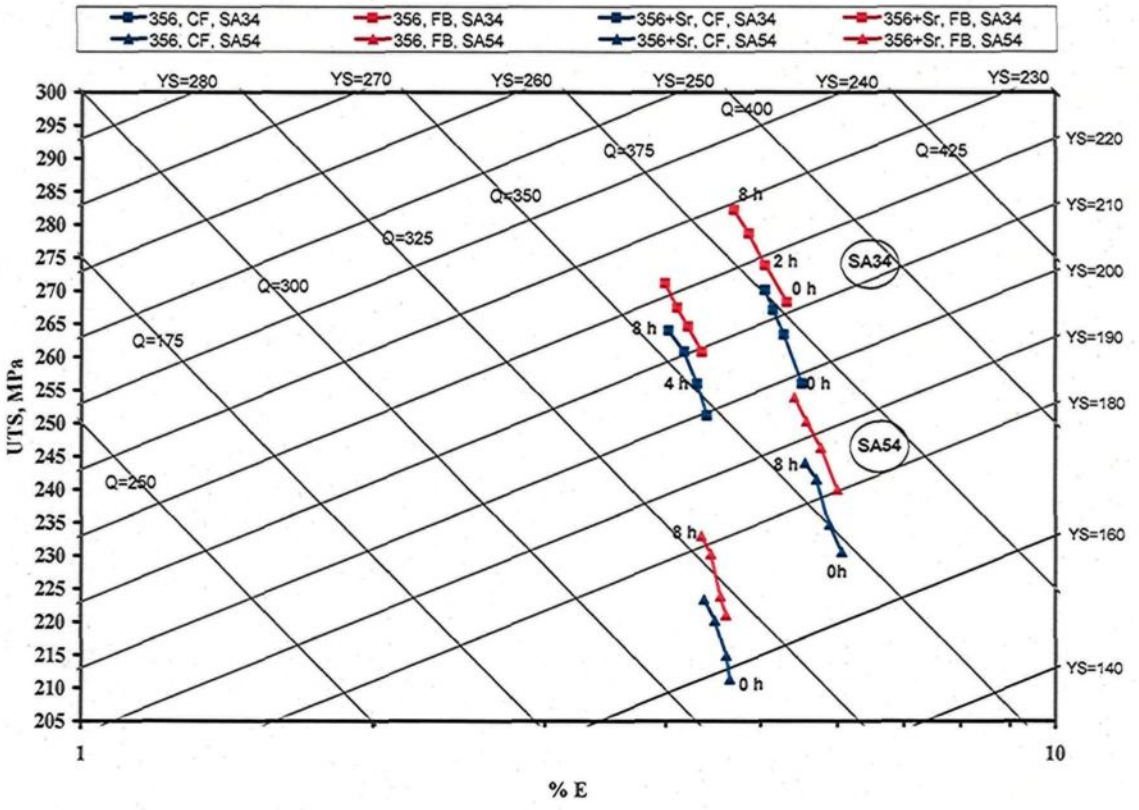

Figure 5.12. Quality charts using Equations (5) and (6) showing the effects of multi-temperature aging cycles and modification on the quality of 356 alloys.

Increasing the aging temperature from 230°C for the SA34 heat treatment cycle to 249°C for the SA54 heat treatment cycle, respectively, results in shifting the aging curve of the 356 casting alloys towards the bottom left-hand corner of the quality chart. This shift in the aging curve indicates that lower level of strength and quality index for the 356 alloy were obtained when increasing the aging temperature. As was explained earlier, the noticeable reduction in the strength and quality index values of 356 alloys when increasing the T7 temperature may be related to the formation of coarse precipitates with lesser density in the matrix at high temperature. The coarse precipitates formed with wide interspacing

facilitate the motion of dislocations through these precipitates resulting in a ductility increase and a strength decrease. In the case of the SA54 heat treatment, carried out at the high temperature of 249 °C, the decrease in strength values, compared to the increase in elongation, affects the net quality values so that they are ~25 MPa lower than those obtained using the SA34 heat treatment, performed at a lower temperature of 230 °C.

5.3.2. Al-Si-Cu-Mg Casting Alloys

The tensile results of B319 alloys, heat-treated using different quenching media, were reused to generate the quality charts shown in Figure 5.13. This figure illustrates the influences of quenching media and aging parameters (i.e., temperature and time) on the quality values of 319 alloys. The strength of these alloys is improved via the formation of Cu- and Mg-containing hardening phase, such as θ-$CuAl_2$ and/or Q-Al5Mg8Cu2Si6 and β-Mg_2Si. These phases can alter the strength coefficient or K values required to generate the quality charts of the heat-treated materials subjected to the range of T6 temper parameters investigated. Such a variation will affect the accuracy of calculated yield strengths calculated from the quality charts, compared to those obtained from tensile testing.

In general, water quenched alloys (B cycles) demonstrate better quality values than those FB-quenched alloys (C conditions; FB). For the same aging parameters, with an FB, at 170 °C/4 h (B1, C1), the water quenched alloys show higher quality values (50-60 MPa) than the FB quenched ones. The difference in quality values may be related to the negative effect of FB quenching on the ductility of 319 alloys, where the FB-quenched alloys (C1 condition) provide higher strength values, at the expense of its ductility, compared to the

water quenched alloys (B1 condition). Compared to the effect on quality due to the increase in strength, the reduction in elongation values of the FB-quenched alloys has a marked effect on the net quality value of 319. For water-quenched/T6-aged alloys (B1, B2, B3 conditions), there is no significant difference in the quality values of FB and CF heat-treated alloys, except that the FB heat treatment produces higher quality values (~15-20 MPa) than the CF for aging times of up to 4 hrs as shown in Figure 5.13. The FB heat-treated samples show higher quality and ductility values, after 4 hours of aging, than the CF treated samples, for the same heat treatment time. As for 319 alloys, after 8 and 12 hours of aging, the quality values are not as responsive to a FB as to a CF. The quality values of FB heat-treated 319 alloys are nearly the same as the CF-treated alloys. For FB samples aged for 8-12 hours (B2 and B3 conditions), the portion of the aging curves up to peak-aging is parallel to the iso-Q lines, implying that, for this range of aging time, the quality index values of the alloy do not display any significant change. However, the CF-aged samples show an increase in quality values with increased aging time.

The FB shows a marked difference in strength values of heat-treated alloys, compared to those treated in a CF, for aging times of up to 12 hours. This difference in strength is related to the high precipitation density of Cu-containing phases/particles in FBs, as opposed to CFs.

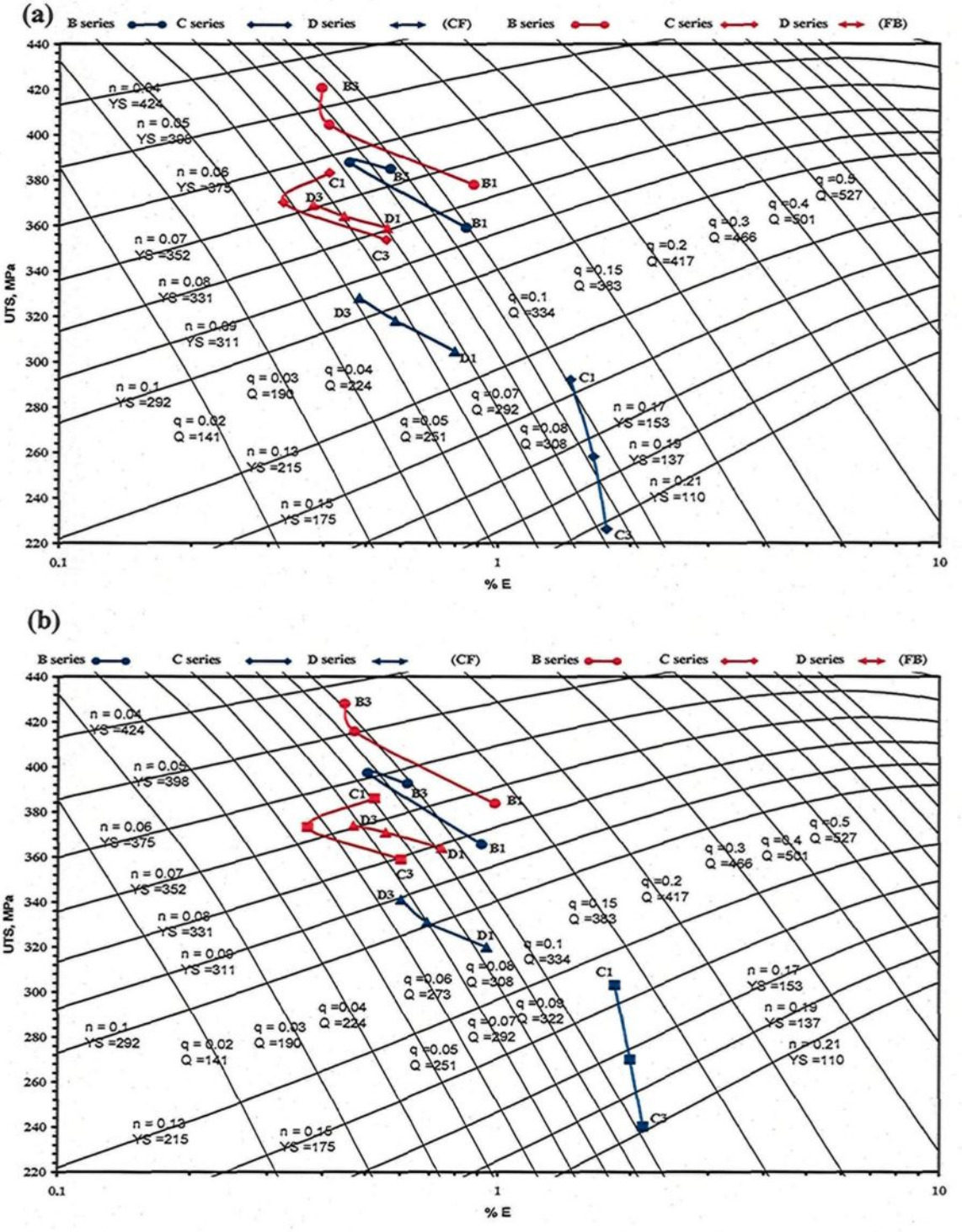

Figure 5.13. Quality charts using Equations (4-6) showing the effects of quenching media and modification on the quality and UTS of 319 alloys (a) non-modified K2 alloy, and (b) modified K4 alloy.

The CF quenched-aged alloys show the lowest strength values; however, they also show better quality values than FB quenched-aged alloys. Compared to water-quenched alloys, the CF air-quenched ones show nearly the same or better quality values. The increase in quality values of air quenched alloys is related to the highest elongation values, compared to water and FB-quenched alloys (Figure 5.8). The significant increase in elongation values of air-quenched alloys has a positive effect, compared to the reduction in strength, on the net quality values (Figure 5.13). Thus, a specific heat treatment technique (CF or FB) and/or quenching medium (water, or air/CF or sand/FB) can be selected for the heat treatment of B319.2 alloys, depending on the strength and/or quality values required for particular engineering applications at specific heat treatment conditions. The CF quenching-aging technique may be selected for heat treatment of B319.2 alloys used for engineering applications that require highest elongation and quality values at the expense of strength while the water and FB quenching media may be suitable for applications that require a compromise of high strength and good quality values. The FB quenched-aged samples insure a reduction of residual stresses as well as better strength and good quality as compared to those quenched using water or air as the medium. For air quenched-aged alloys using a CF (C-cycles), it may be noted from Figure 5.13 that increasing the aging temperature from 170°C to 210°C results in a reduction in the quality values by 25 MPa; this reduction is related to the significant decrease in strength values (60 MPa) and the slight increase in elongation values.

For water-quenched alloys treated to multi-temperature aging cycles (D conditions), FB heat-treated samples show better strength results than those heat treated

using a CF. There is no significant difference, however, in the quality values obtained by either technique. The difference in strength values may be related to the formation of various types of precipitates during the several aging temperature stages applied. Regarding to the aging behavior of 319 alloys, the quality values decrease with increasing the aging time for multi-temperature aging heat treatment cycles (D conditions) using a CF and an FB. This reduction is expected due to the increase in strength values at the expense of the elongation values. As compared to the 356 alloys, the quality values of 319 alloys are more responsive to aging parameters where the aging behavior is not quazi-parallel to the iso-Q lines for all heat treatment cycles.

In addition to the heat treatment parameters, Sr-modification has an effect on the quality index values obtained for B319.2 alloy samples in terms of their UTS and %El properties as shown in Figure 5.13 (b). The improvement observed in the mechanical properties and quality of such 319 alloys may be obtained by applying Sr-modification through melt treatment, and using a high heating rate in the fluidized bed for the relevant heat treatment procedures. The modified 319 alloys show better quality values (15-20 MPa) as compared to the non-modified ones for all heat treatment cycles. It should be noted that Sr modification enhances the strength and ductility, as well as the quality of Al-Si-(Cu-Mg) alloys for all heat treatment cycles. [147, 204]

Figure 5.14 illustrates the quality of B319.2 alloys subjected to two T7/T6 multi temperature aging cycles, namely SA34 and SA54. It may be noted from the aging behavior of B319.2 alloys, that the quality performance of these alloys are not responsive to the fluidized bed technique for the applied multi temperature aging cycles as compared

to the A356 alloys; there is no significant difference between the quality values of heat treated alloys using a CF and an FB. The aging behavior of B319.2 alloys shows that the quality values decrease with an increase in time of T6 second step aging form 0 h up to 8 h; such an observation is related to the continuous increase in strength at the expense of elongation values. The continuous increase in strength values with increasing aging time is related to the precipitation of the Cu- and Mg-containing phases in the metal matrix. The features of these precipitates vary according to the aging time applied to the casting alloys. A further increase in aging time at 180 °C results in the formation of coherent transition phases which contribute to increasing the hardening level of these alloys. The FB heat treated alloys show better strength results than those heat treated using a CF; the over-aging conditions was reached when applying aging treatment cycles at 180 °C/4h using a CF. Such a decrease in strength and increase in the ductility of the alloy is related to the softening conditions and the loss of the coherency strain between the precipitates and the matrix. In addition, the over-aging result in the growth of the large precipitates at the expense of the smaller ones, ultimately leading to coarser precipitates with less density in the metal matrix having large inter-particle spacing. All the changes mentioned which accompany the over-aging condition contribute to a decrease in the alloy strength. Overaging was not reached when using FB heat treatments, for up to 8 h, upon which the maximum strength level was observed. This was attributed to the formation and stability of both coherent and semi-coherent precipitates. Regarding to the applied heat treatment cycles (SA34 and SA54) and techniques (FB and CF), there is no significant difference in the quality values of heat treated B319.2 alloys. The significant difference in the quality

values of alloys is attributed to the effect of Sr-modification parameter, where the modified 319 alloys show better quality values than the unmodified ones for all heat treatment cycles (Figure 5.14).

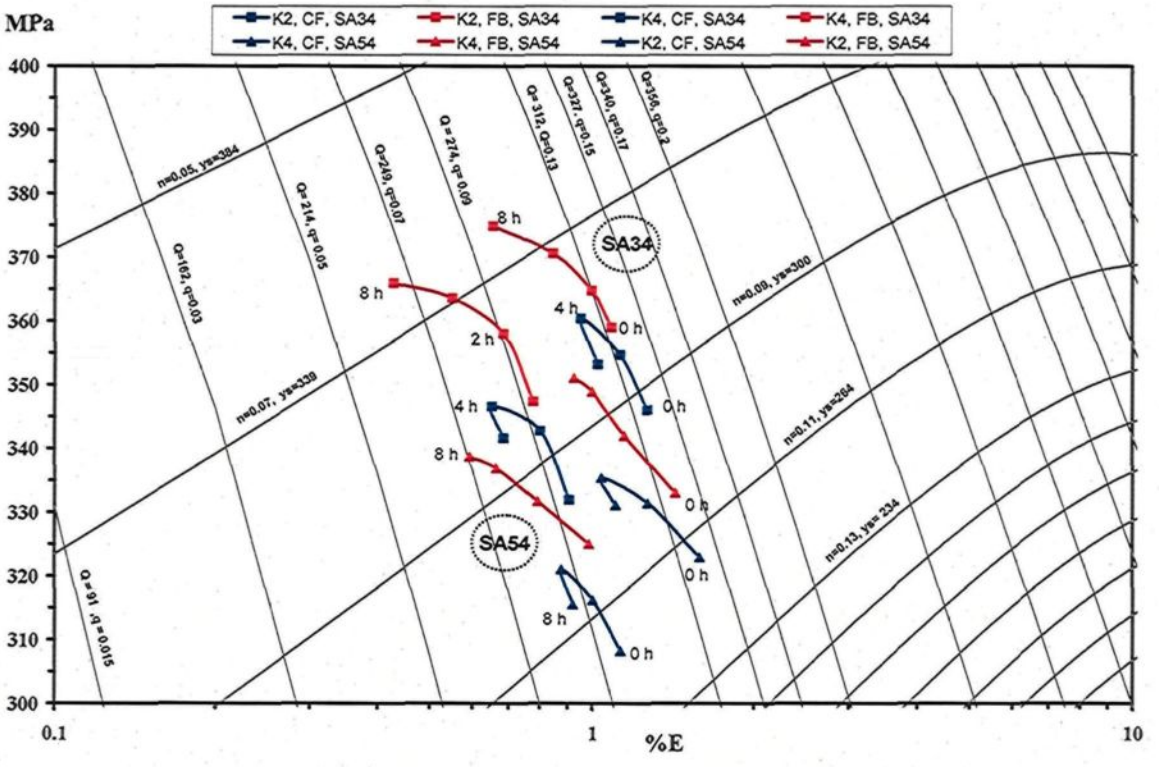

Figure 5.14. Quality charts using Equations (5) and (6) showing the effects of multi-temperature aging cycles and modification on the quality of 319 alloys.

5.3.3. Statistical Analysis for Quality Results of Al-Si-(Cu/Mg) Casting Alloys

An improvement in the performance of Al-Si-Cu/Mg alloys and an understanding of its relationship to heat treatment parameters may be accomplished by applying statistical techniques using the design of experiments (DOE) approach. Statistical design of experiments (regression analysis), as a method, has been put into use to develop regression

equations between the response variables and the independent variables or factors. The data pertaining to the quality index value, Q, were analyzed using Minitab software (version 15) to obtain the regression models, the main effects plot, and the interaction plots which describe the relationship between the independent variables studied and the mechanical properties of the alloys investigated. Table 5.1 represents the independent variables, or factors, and response variables studied together with the codes used to obtain the final regression equations.

Table 5.1. Independent variables, response variables, and their codes.

Independent variable	Code	Response variable	Code
Modification effect, wt%	X_1	Quality index (Q), Mpa	Y
Quenching medium*	X_2		
Heat treatment technique**	X_3		
Aging temperature, T ^{0}C	X_4		
Aging time, h	X_5		

*Quenching medium represents water, air (CF) and sand (FB).
** Heat treatment techniques represent conventional furnace (CF) and fluidized bed (FB).

By processing the data, regression Equations 8 and 9 were developed for Q values of A356 and B319 alloys, respectively, indicating the variation of a number of different factors, as follows:

$$Y\ (A356\ alloy) = 268.2 + 25.1^* X_1 + 1.65^* X_2 + 8.3^* X_3 + 0.233^* X_4 - 1.04^* X_5 \quad \textit{Equation 19}$$

$$Y\ (B319\ alloy) = 287.2 + 21.4^* X_1 + 38.4^* X_2 - 52^* X_3 - 0.251^* X_4 + 3.16^* X_5 \quad \textit{Equation 20}$$

where Y is the response variable (YS, UTS, %El, or Q); b_0, b_1, b_2, *etc.* are constants representing the effects of the respective factors X_1, X_2, X_3 and X_4 which are the codes for the factors representing modification effect, quenching medium, heat treatment technique, aging temperature and aging time, respectively. The R^2 values for Equations 19 and 20 are 97.41% and 95.21%, respectively. In general, positive values of the coefficient signify an increase in the property due to a concomitant increase in the individual parameters and their interactions, whereas the magnitude of the coefficients signifies the extent of the influence of these individual parameters, or their interactions, on the response variable. For example, positive and higher values of b_1 in Equations 19 and 20 would signify (i) an increase in the response variable Y, and (ii) a greater effect of the factor X1 on Y, in comparison to the other factors X_2, X_3, *etc.* Similarly, lower values of the coefficients would suggest that the action of associated individual parameters, or their interactions, is non-significant for a given response variable.

From these linear equations, it may easily be noticed that the response Y (Q values of A356 alloys) is affected significantly by the modification factor followed by heat treatment technique and then by quenching medium. The response Y (Q values of B319 alloys), however, is greatly affected by the quenching medium factor followed by a significant negative effect of heat treatment technique, where the 319 alloys are found to be less responsive to FB heat treatment technique as compared to 356 alloys. The results obtained from these equations are in satisfactory agreement with the quality index charts of A356 and B319 alloys. It can be noted that the mean quality values of B319 alloys are more quench sensitive than A356 alloys due to the formation of a greater percent of GP

zones in Al-Si-Cu-Mg alloys. These GP zones act as heterogeneous nucleation sites for precipitation and so enhance the aging process.

The matrix plots are assessed by level of average response analysis of the raw data. This analysis is carried out by averaging the raw data at each level of each parameter and plotting the values in graph form. The level average responses of the raw data make it possible to analyze the trend of the performance characteristic with respect to the variation in the factor under study. Figures 5.15 and 5.16 show the main effects of all variables which affect the tensile results as well as the quality index values of A356 and B319 alloys, respectively. The average values of each independent variable are compared within that variable in order to observe its impact on the quality index. The more horizontal the line, the less impact the independent variables have on the property. The presence of optimal testing conditions with regard to these control variables can be easily determined from the relevant graphs. As is evident from Figure 5.15, there is a significant change in the quality values of A356 alloys when the levels of modification are changed from low levels to high levels, compared to the quality values of B319 alloys for the same parameters, as shown in Figure 5.16.

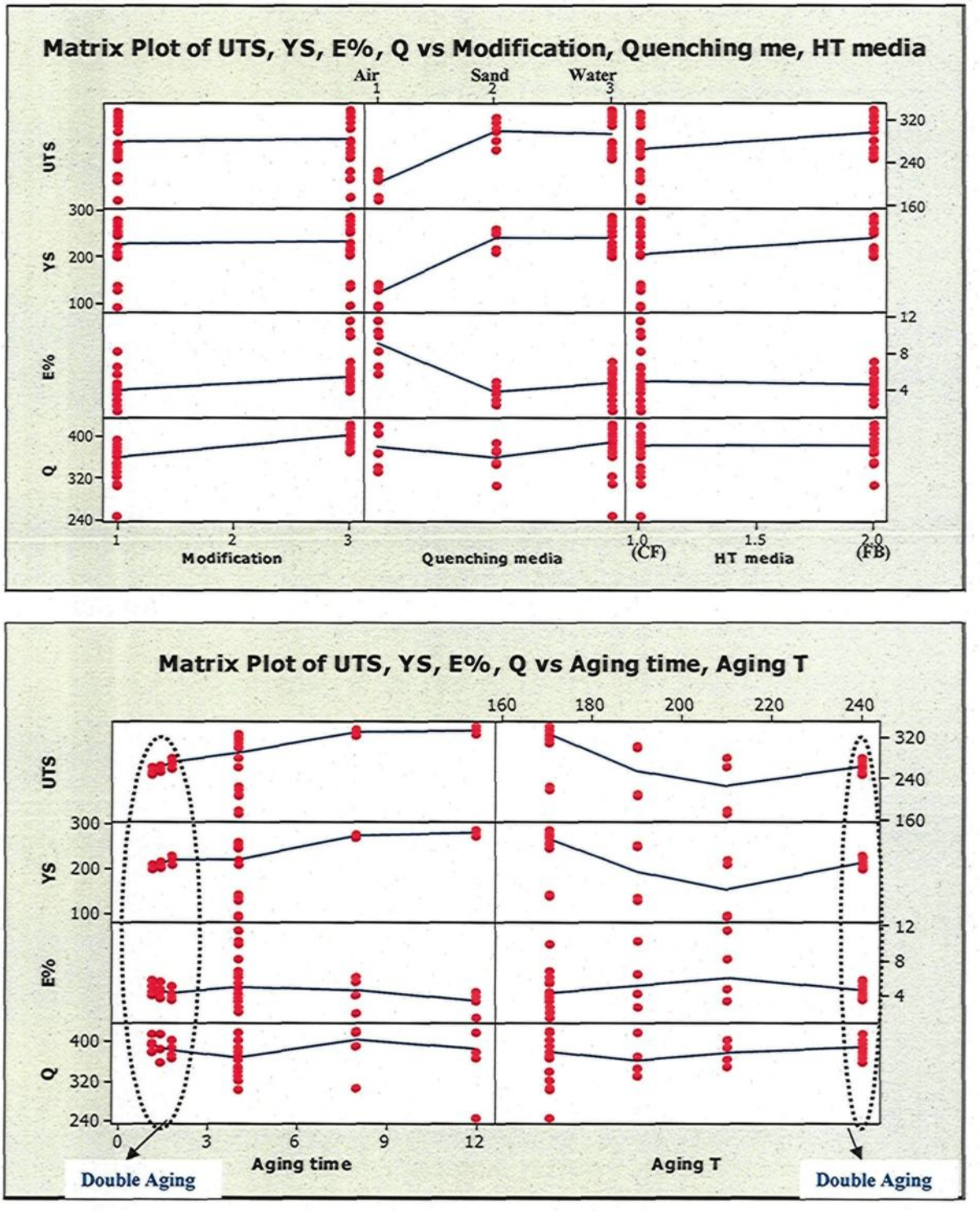

Figure 5.15. Matrix plots of various factors affecting the tensile and quality values of A356 alloys.

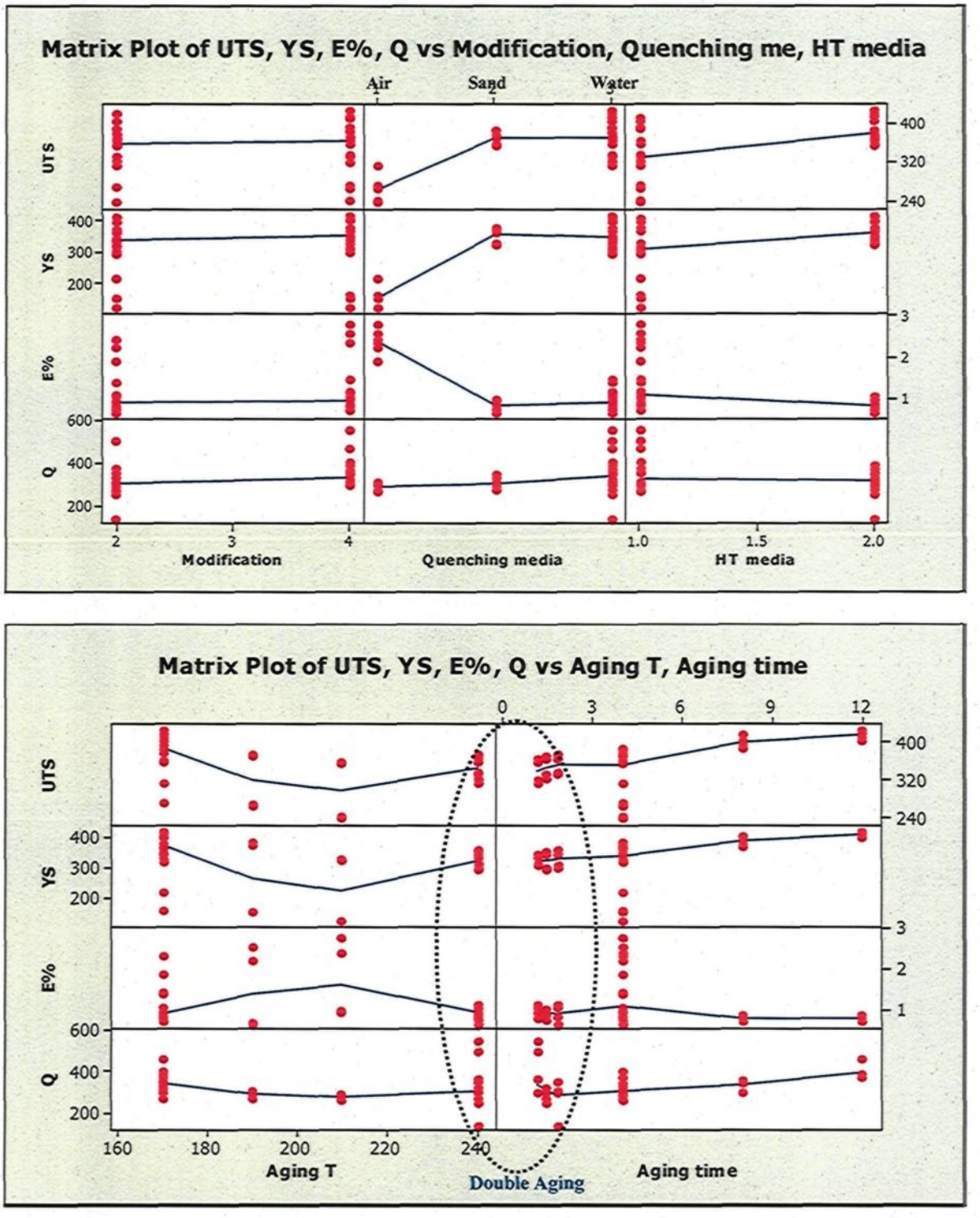

Figure 5.16. Matrix plots of various factors affecting the tensile and quality values of B319 alloys.

Regarding the heat treatment technique factor, it may be noted that the strength values of both A356 and B319.2 alloys are significantly responsive to the fluidized bed heat treatment technique. The average quality values of A356 alloys display a non significant response to the fluidized bed heat treatment technique (Figure 5.15), compared to the quality values of B319 alloys which display a negative response to an FB heat treatment technique (Figure 5.16). The FB-quenched alloys display almost the same or slightly better mean strength results and lower mean quality values compared to water quenched alloys (Figures 5.15 and 5.16).

Regarding the aging parameters, the matrix plots illustrate the effects of the aging temperatures and aging times applied for all heat treatment cycles on the strength and quality index values of the 356 and 319 castings. As may be seen, increasing the aging temperatures up to 210 °C results in a decrease in the strength values and an expected increase in elongation values of the two alloys, and a slight increase (for 356 alloys) or a slight decrease (for 319 alloys) in their quality values. This trend is changed after applying the multi-temperature aging cycles at 240 °C, followed by 180 °C for 356 and 319 alloys, for all aging times, whereby the strength and quality values are increased. These observations are in agreement with the evaluations made from the quality charts presented for 356 and 319 alloys. For the multi-temperature aging cycles, applying T6 treatment after T7 temper results in an improvement in the strength as well as quality values due to the formation of fine and more density precipitates in addition to those, coarse and lesser density precipitates, formed during the T7 first stage temper. The 356 and 319 casting

alloys show a continuous increase in strength and quality index values with increasing the aging time as shown in Figures 5.15 and 5.16.

The matrix plots as well as interaction plots shown in Figures 5.17 and 5.18 likewise correlate the properties of the 356 and 319 alloys with the studied parameters of multi temperature aging cycles, namely aging T1 (T7), aging time1 (T7) and aging time2 (T6), in addition to the heat treatment technique and modification factors. These plots show that increasing the aging temperature of the T7 stage results in a decrease in the mean strength and quality values whereas increasing the aging time of the second aging stage (T6) results in an increase in the strength values and a decrease in the quality values. As before, the matrix plots support the observations made from the quality charts presented in Figures 5.12 and 5.14. According to the tensile results and/or quality values presented in these matrix plots, specific aging parameters (temperature and time) could be selected for multi temperature aging heat treatment cycles required for particular industrial applications. The matrix plots also show that the modification factor is still the most significant factors affecting the performance of alloys investigated. It may be seen that the fluidized bed heat treatment technique affects significantly on the strength values as compared to the quality index values. Figure 5.18 show the interaction plots for the dual effects of independent variables on the quality values of 356 and 319 alloys; the modified alloys show better quality values obtained for all other independent variables.

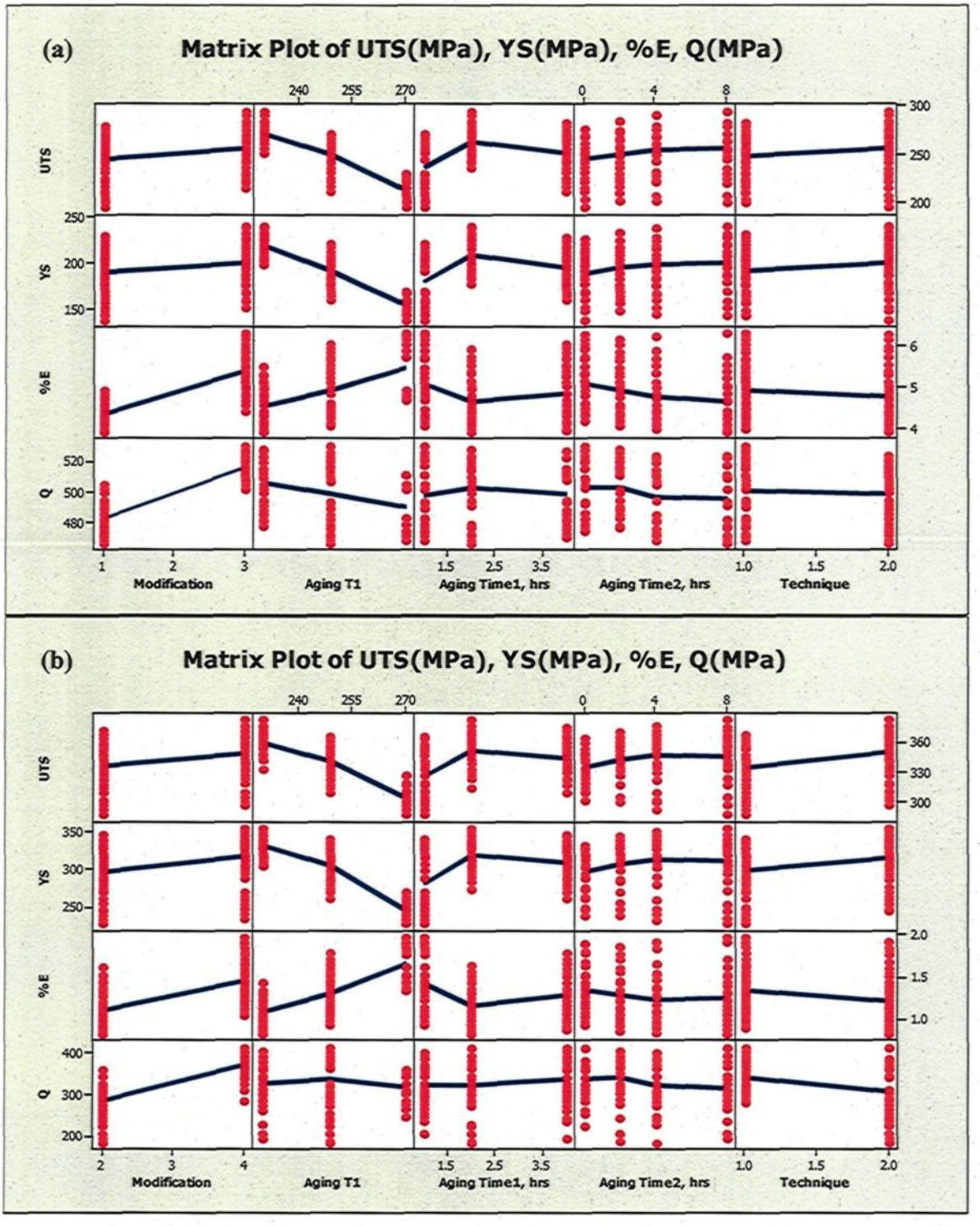

Figure 5.17. Matrix plots of various factors affecting the tensile and quality values of (a) A356.2 and (b) B319 alloys.

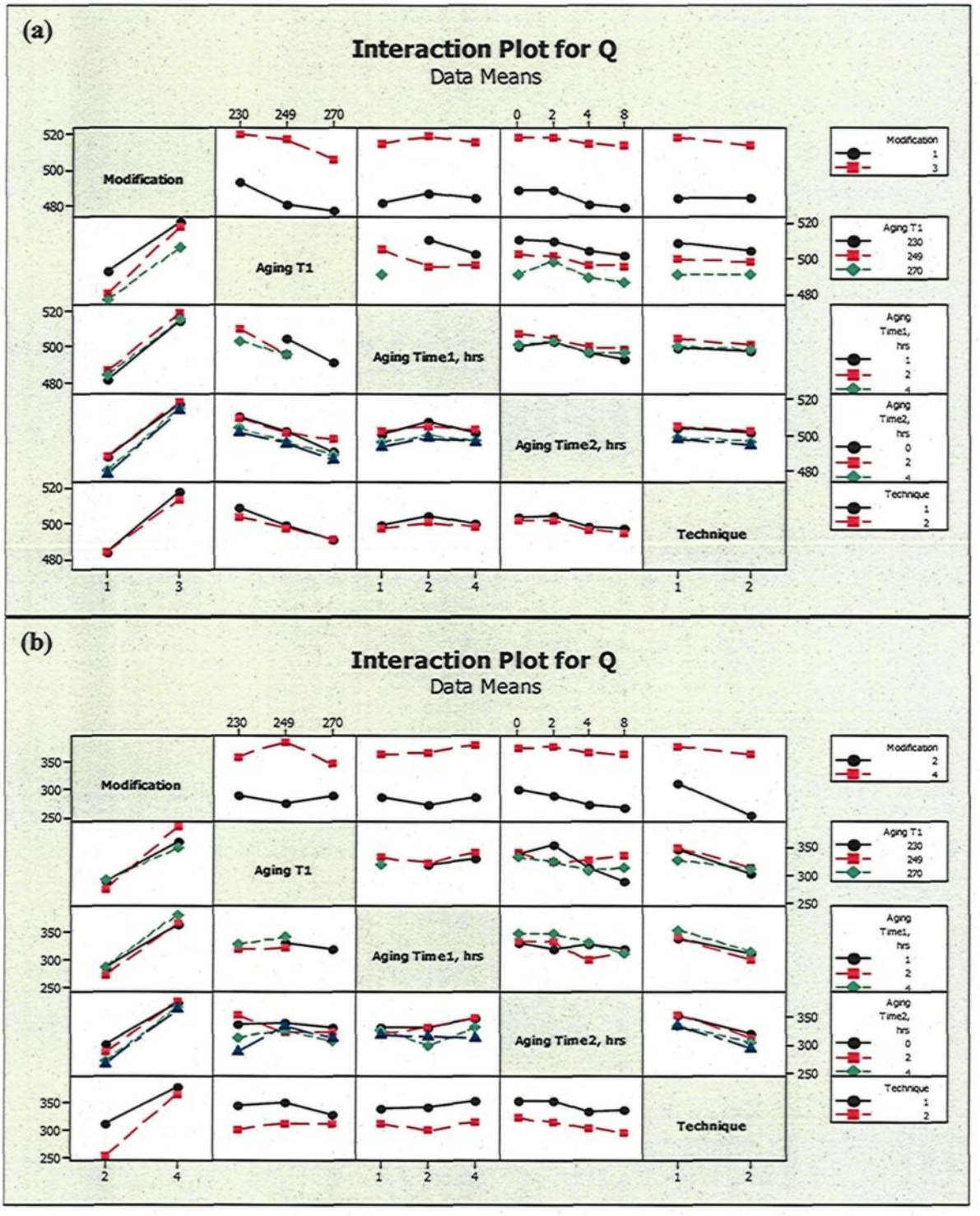

Figure 5.18. Statistical analyses showing the interaction plot for mean Q values of (a) A356-type alloys and (b) B319.2-type alloys.

With respect to the dual effects of the T7 aging temperature of the first stage with each of the other variables, an aging temperature of 230 °C is the most suitable parameter, applied for 356 alloys, resulting in the highest quality values with all other independent variables, namely modification, aging time and heat treatment technique. For 319 alloys, the most significant variables affecting the quality values are the modification and heat treatment technique factors; the modified alloys heat treated in a CF show better quality values for all other independent variables. As mentioned earlier, the quality values of 319 alloys are not responsive to an FB heat treatment technique due to the presence of several undissolved Cu and Fe containing intermetallics that are not affected by the high heating rate of the FB. [204]

The quality results of 356 and 319 alloys, subjected to multi-temperature aging cycles, were re-plotted in the form of contour plots, as shown in Figures 5.19 and 5.20. These plots re-illustrate clearly the dual effects of the most significant parameters, shown in Figure 5.18, on the mean quality values of alloys investigated. It may be noted from Figure 5.19(a) that increasing the aging temperature of the T7 first stage results in a significant decrease in quality values. This reduction is expected and may be related to the significant decrease in strength values of 356 alloys. For the 319 alloys, there is no significant change in quality values with increase in the aging temperature of T7 stage. These contour plots confirmed the significant role of the modification factor in improving the quality values of the alloys investigated; the highest quality values may be obtained by applying T7 first stage at 230°C for the modified 356 alloys as shown in Figure 5.19 (a).

Figure 5.20 shows the dual effects of T7/T6 aging parameters (T7 temperature and T6 time) on the quality performance of 356 and 319 alloys. For 356 alloys, it may be seen that the highest quality values, of ~505-510 MPa, may be obtained by applying T7/T6 multi-aging cycles at temperatures of 230/180 °C for T6 aging times of up to 4 hours. For 319 alloys, the contour area for quality values in the range of 310 to 320 MPa is significant at 249/180 °C for T6 aging times period of 4 to 8 hours; the highest quality values, i.e., more than 330 MPa, may be obtained by applying multi-aging cycles in the temperature range of 230-250 °C for the T7 stage, followed by the T6 stage for an aging time of 1 h as may be deduced from the contour plot shown in Figure 5.20 (b).The contour plots, matrix plots and interaction plots can be used as significant tools for determining and/or selecting the suitable heat treatment parameters of multi-temperature aging cycles that could be applied to the 356 and 319 alloys for obtaining the optimum quality and/or strength values required for particular engineering applications. Multi-stage heat treatments have been used to clarify transformation mechanisms and to provide a basis for obtaining improved properties. Generally, the second stage of aging at reduced temperature (T6) results in the evolution of the pre-existing precipitates formed during the primary ageing stage at a higher temperature (T7), in addition to the nucleation of new precipitates characteristic of the second ageing temperature. The temperatures and times of both first and second ageing stages can be manipulated in order to promote the formation of the desired kind of precipitates. The increase in strength values after applying the second aging stage at low temperature is related to the presence of small, hard precipitate particles which, in addition to the large particles formed at T7 resist the movement of dislocations. [201, 210]

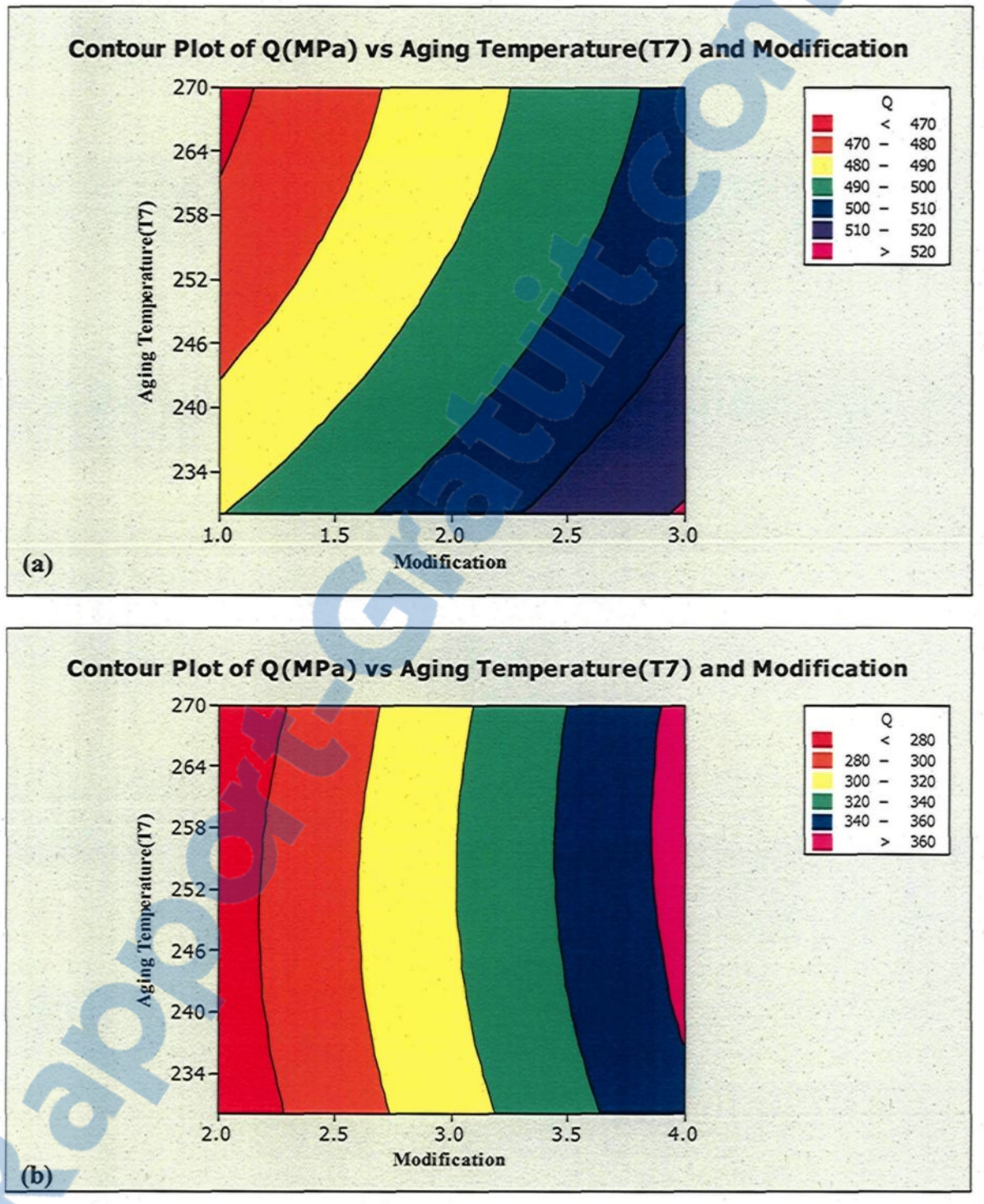

Figure 5.19. Contour plots showing the influence of aging temperature (T7) and modification factors on the quality values of (a) A356.2 alloys and (b) B319.2 alloys.

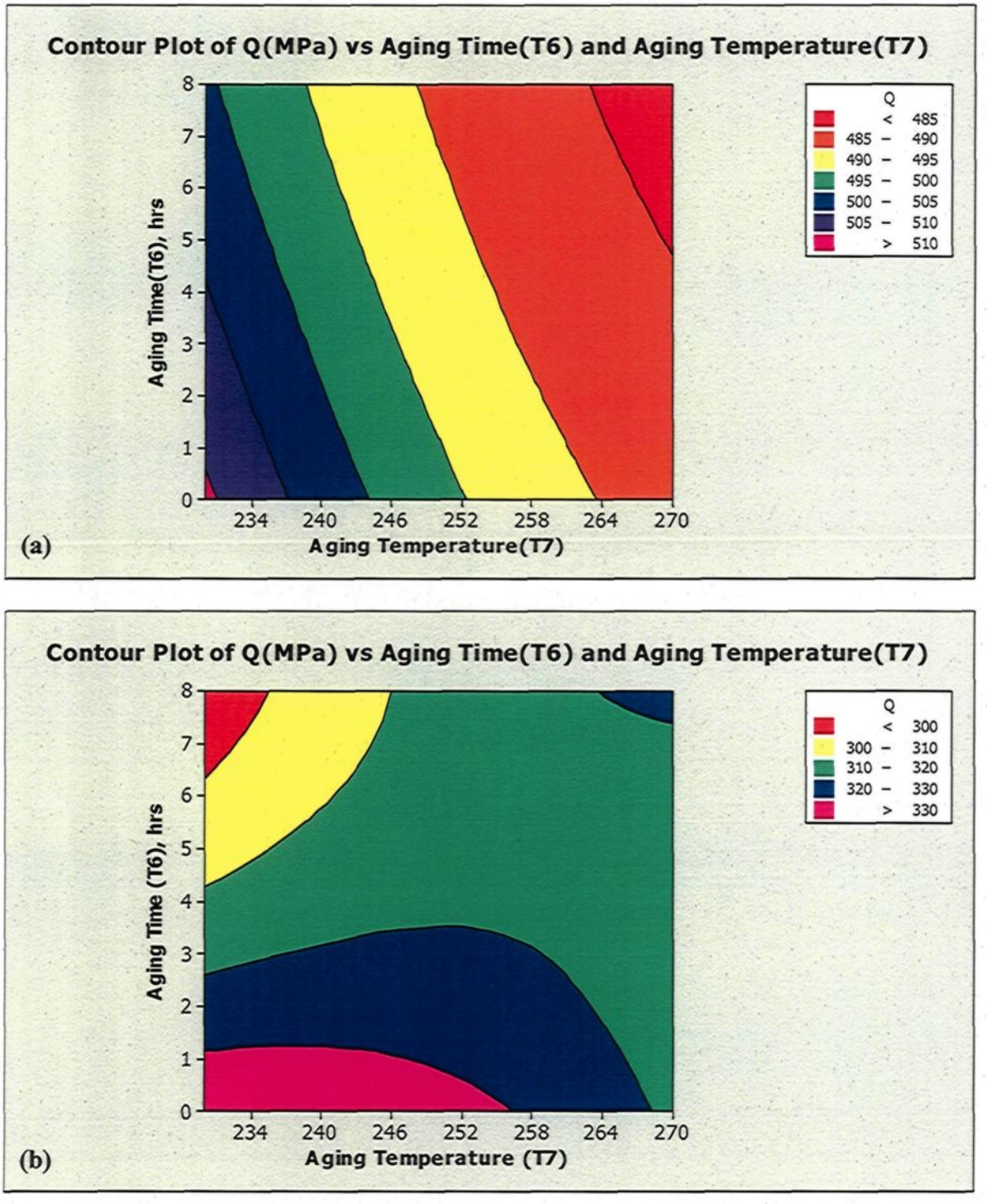

Figure 5.20. Contour plots showing the influence of aging time (T6) and aging temperature (T7) factors on the quality values of (a) A356.2 alloys and (b) B319.2 alloys.

Figure 5.21 shows the size and density of the hardening precipitates of T6-tempered A356.2 alloys under the effect of quenching-aging media in an FB versus hot forced air in a CF. The scanning electron microscope (SEM) was used to identify the precipitates observed in the 356 alloy samples which were subjected to direct quenching-aging treatment at 170 °C/4 hours (C1 condition) using an FB versus a CF. The strengthing of the 356 alloys during aging results from the precipitation of the β-Mg_2Si phase. The EDX spectrum shown in Figure 5.21 (c) illustrates the fact that the gray particles are Mg-Si containing phases which indicate the presence of β-Mg_2Si precipitates.

Based on the analysis made using the SEM, it was observed that the precipitation density and the distribution of Mg_2Si particles is high in the FB quenched alloys compared to the air-quenched ones. This difference in precipitate density may be related to the slow cooling rate associated with air quenching, which would lead to a low vacancy concentration, and thus affect the formation of clusters/GP zones during the early stages of aging. These clusters or GP zones affect the precipitate size and distribution. The CF quenched-aged alloys show coarser precipitates, compared to FB quenched-aged alloys. This indicates that the coarsening rate of the Mg2Si particles formed in aged alloys subsequent to CF quenching is greater than that formed in FB-quenched 356 alloys. Coarsening rate also depends on the vacancy concentration in the matrix: the greater vacancy concentration, the greater coarsening rate of precipitates. [59, 61]

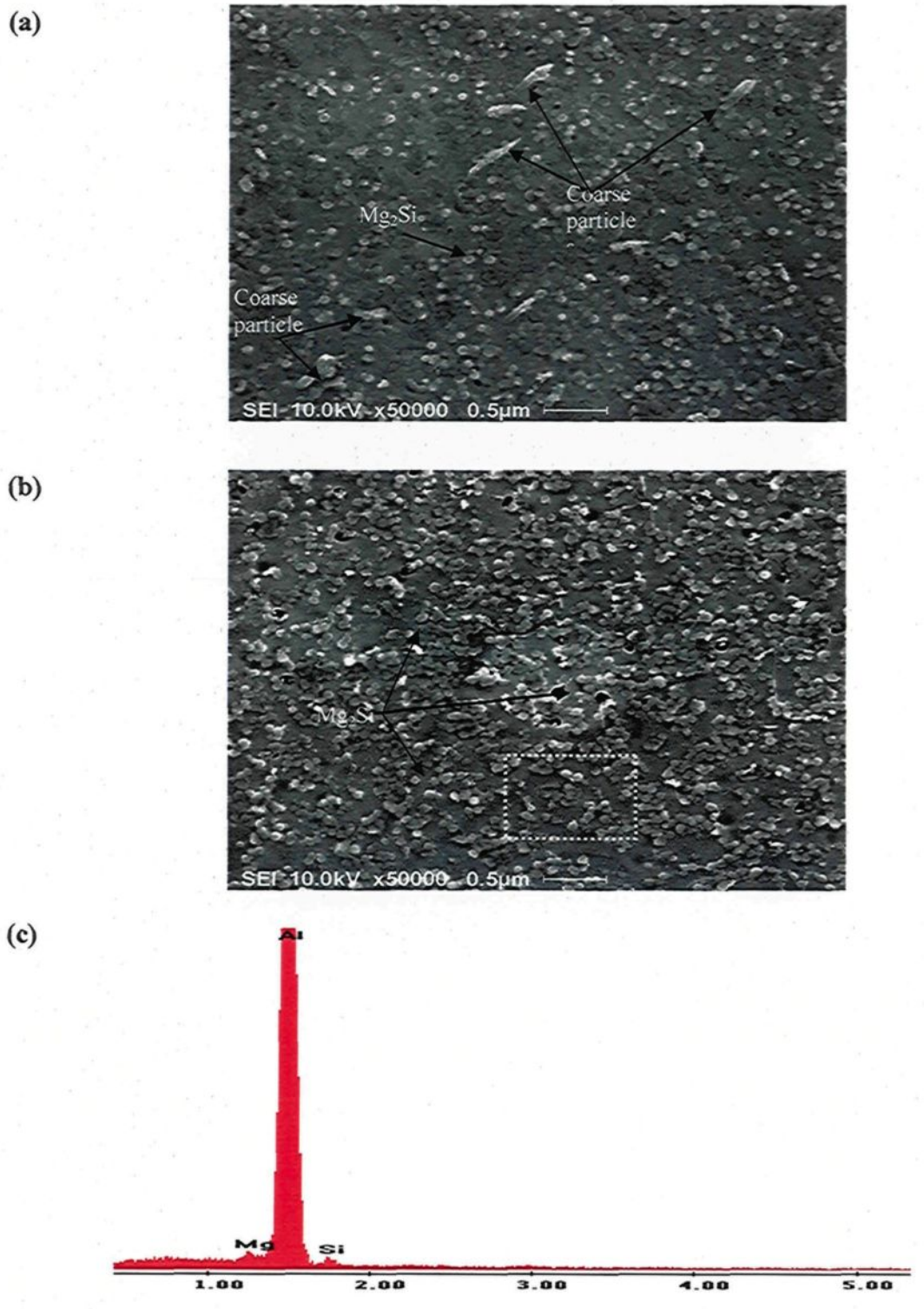

Figure 5.21. SEM images of T6 tempered A356.2 alloy quenched-aged in (a) a CF, (b) an FB, and (c) EDX spectrum of Mg_2Si for an FB quenched sample.

Figure 5.22 shows a comparison of the effect of FB quenching versus air quenching on the precipitation density of Cu-containing phase particles in 319 non-modified alloys. That these precipitates were Cu-containing phase was detected using EDX analysis. The EDX spectrum presented in Figure 5.22 (C) shows that these precipitates contain Cu, Mg, and Si in addition to Al, which may indicate the presence/co-existence of the *Q*-$Al_5Cu_2Mg_8Si_6$, *θ*-Al_2Cu, *β*-Mg_2Si and *S*-Al_2CuMg particles in the matrix. All these types of precipitates cannot be identified precisely using the EDX in conjunction with the SEM technique because of their tiny size. In this study, the main purpose of using the SEM technique was to provide an overview of the size and density of the precipitates under various quenching-aging media/conditions applied to the castings.

From these micrographs shown in Figure 5.22 (a, b), it is evident that the FB-quenched alloys show finer and denser Cu-containing precipitates as compared to those obtained with the hot air quenching medium in a CF. The FB quenching medium also provides a more uniform distribution of the precipitates in the Al matrix. This difference in precipitates size and density between the two quenching-aging techniques explains the significant difference in strength results of the 319 and 356 alloys subjected to direct quenching-aging treatment at 170°C/4h. It should be noted that the finer and denser precipitates formed at lower aging temperatures or shorter aging times have small inter-particle spacing. This type of precipitates provides a strong resistance to dislocation motion and the occurrence of Orowan looping becomes difficult leading to a hardening of the materials and an increase in the overall strength.

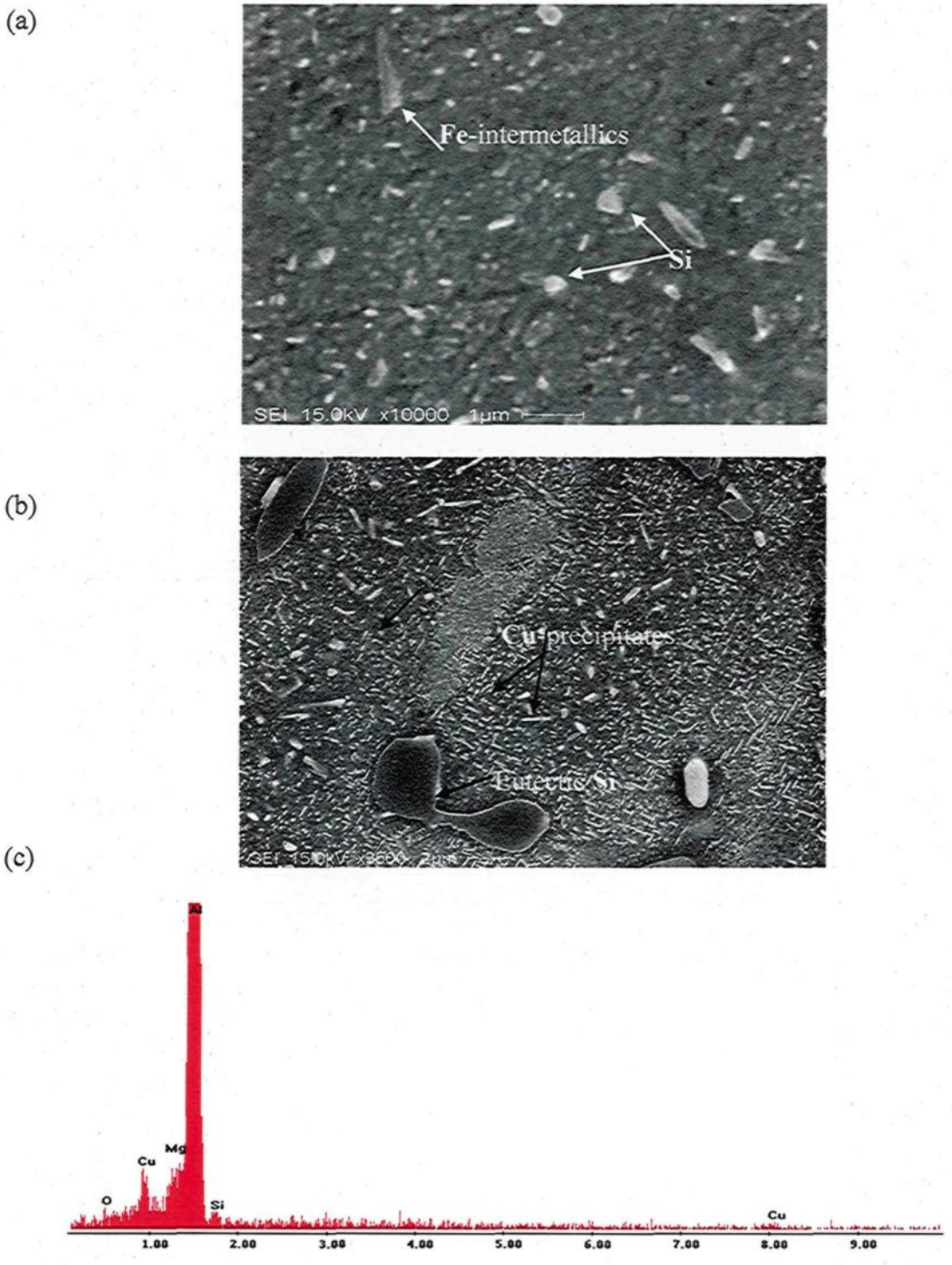

Figure 5.22. FEGSEM micrographs of T6 tempered 319 alloy quenched-aged in (a) a CF, (b) an FB, and (c) EDX spectrum of Cu precipitates for an FB quenched sample.

5.4. CONCLUSIONS

The influences of quenching media and multi temperature aging cycles on the tensile properties and quality indices of A356 and B319 casting alloys were investigated and the results presented in this chapter. Accordingly, the following conclusions may be drawn from these investigations:

1. In general, both UTS and YS values of T6 tempered A356 and B319 alloys are greater when quenched in water as compared to those quenched in FB and CF. For the same aging conditions (170°C/4h), the FB quenched-aged 319 and 356 alloys (C1 condition) show better strength values than those quenched in water (B1 condition).
2. The direct quenching-aging treatment of alloys (A356 and B319) in an FB yields greater UTS and YS values compared to CF-quenched alloys. In contrast, elongation values of alloys quenched in FB-quenched alloys (sand quenching) are lower than those quenched in a CF (hot air quenching).
3. The fluidized bed technique is more effective than the convection furnace with respect to strength and quality values of water-quenched 319 and 356 alloys after aging times of 4 and 4-8 hrs, respectively. Beyond these heat treatment times, there is no noticeable difference in quality values between the two techniques.
4. For water quenched alloys, the aging cycles, D1, D2 and D3, yield lower strength and better elongation values than almost all of the T6 treatment conditions using both CF and FB. The low strength values for multi-temperature aging cycles may

be related to the formation of Mg and Si co-clusters which result in a coarser dispersion of precipitates after aging at elevated temperatures.

5. The strength results obtained after the T6 continuous aging treatment of A356 alloys are not improved by means of multi-temperature aging cycles, indicating that the optimum properties are obtained by T6 aging treatment.
6. The optimum strength properties of B319.2 alloys is obtained by applying T7/T6 type multi-temperature aging cycles, such as at 230 °/2h, followed by 180 °C/8 h (i.e. SA32 condition), as compared to T6 aging treatment.
7. Based on the quality charts developed for alloys under effect of quenching media, the higher quality index values are obtained by water-quenched/FB-aged alloys and CF quenched-aged alloys for 356 and 319 alloys, respectively. The modification factor has the most significant effect on the quality results of alloys investigated for all heat treatment cycles, as compared to other metallurgical parameters.
8. For T7/T6 type multi-temperature aging cycles, the modification factor has the most significant role in improving the quality index values of 356 and 319 alloys. The FB heat-treated alloys have the highest strength values for all heat treatment cycles, as compared to those obtained for CF heat-treated alloys. The FB has no significant effect on the quality values of 319 alloys compared to the CF.
9. With regard to regression models, the mean quality values of B319 alloys are more quenc-sensitive than A 356 alloys due to the formation of a greater percent of clusters/GP zones in Al-Si-Cu-Mg alloys. These clusters or GP zones act as a heterogeneous nucleation sites for precipitation and enhance the aging process.

10. With respect to the interaction plots for multi temperature aging cycles, the most significant factors that have a positive effect on the quality values of 356 alloys are modification and the T7/T6 multi-aging cycle applied at 230°C/2h, followed by aging at 180°C/2 h.
11. Statistical analysis using matrix plots reveals that the T7/T6 multi-temperature cycle of aging at 249°C/4h, followed by aging at 180°C/2 h, is the optimum heat treatment condition that improves the quality values of 319 alloys.
12. The 319 alloys display higher strength levels when compared to the 356 alloys, for all heat treatment cycles, at the expense of ductility, resulting in higher quality values for the 356 alloys when compared to 319 alloys.
13. The FB is a significant heat treatment technique which may be used for solutionizing, quenching and aging. This technique was applied to 356 and 319 alloys in the present study in order to obtain the best possible compromise between alloy strength and quality values.

RECOMMENDATIONS FOR FUTURE WORK

Based on the results obtained from this study it would be interesting and useful for the aluminum industry to conduct further investigations along the following lines:

1. Use of high resolution transmission electron microscopy to investigate the effects of (a) the rapid heating rate associated with the use of the fluidized sand bed, as well as that of (b) the quenching medium following solution heat treatment by monitoring the formation of GP zones. In the context of the latter, it should be kept in mind that the casting would be in direct contact with the heating medium when quenching in hot sand, whereas in case of quenching in a conventional furnace, the casting would be heated by convection.

2. Applying the tensile test data obtained from the fluidized bed heat-treated test bars used in this study to real complex shaped castings in order to adjust the heating, quenching, and aging parameters to achieve superior properties compared to those obtained using traditional heat treatments. This would essentially constitute a form of technology transfer.

REFERENCES

REFRENCES

1. W.S. Miller, L. Zhuang, J. Bottema, A.J. Wittebrood, P. De Smet, A. Haszler and A. Vieregge, "Recent Development in Aluminum Alloys for the Automotive Industry," Materials Science and Engineering A, Vol. 280, 2000, pp. 37-49.

2. C.S. Cole and A.M. Sherman, "Lightweight Materials for Automotive Applications," Materials Characterization, Vol. 35 (1), 1995, pp. 3-9.

3. ASM Handbook Vol. 2, "Properties and Selection: Nonferrous Alloys and Special-Purpose Materials," ASM International, Materials Information Society, U.S.A., 1990.

4. Y.J. Li, S. Brusethaug and A. Olsen, "Influence of Cu on the Mechanical Properties and Precipitation Behavior of AlSi7Mg0.5 Alloy during Aging Treatment," Scripta Materialia, Vol. 54, 2006, pp. 99-103.

5. G. E. Totten and D.S. Mackenzie, "Handbook of Aluminum, Vol. 1: Physical Metallurgy and Processes," Marcel Dekker, NY, U.S.A., 2003.

6. J.E. Hatch, Aluminum: Properties and Physical Metallurgy, American Society for Metals, Metals Park, OH, U.S.A., 1984.

7. J.R. Davis, Aluminum and Aluminum Alloys, ASM Specialty Handbook, ASM International, Materials Park, OH, U.S.A., 1993.

8. J.G. Kaufman and E.L. Rooy, Aluminum Alloy Castings: Properties, Processing, and Applications, ASM International, Materials Park, Ohio, U.S.A., 2004.

9. D. Dingman and G. Handzel, "Short-cycle Solution Heat Treatment in a Modern Fluidized Bed" Industrial Heating, 2003, pp.1–5.

10. R.W. Reynolds, Heat Treatment in Fluidized Bed Furnace, ASM International, Metals Park, Ohio, 1993, p. 51.

11. A.S. Zavarov and S.V. Grachev, "Heat and Chemical Heat Treatment in a Fluidized Bed", Ural Polytechnic Institute, Translated from Metallov, No. 10, October 1987, pp. 36-38

12. C.N. Bergman, "Faster Aluminum Solutionizing Via Fluidized Beds", Heat Treating Progress, Vol. 3, No. 1, 2003, pp. 48-49.

13. J. Van Wert, D. Apelian, C. Bergman, "Fluidized Bed Heat Treating: The Answer to One-Piece Flow as a Commercial Application", AFS International Conference on Structural Aluminum Casting, Vol/No. 2-4, 2003, pp. 383-392.

14. R.W. Reynolson, R. North, A. S. Fitchett and Wantirna, Fluidized Bed Heat treatment Furnace, Patent, USA, No. 5832848, Nov. 10, 1998.

15. C.H. Cáceres, L. Wang, D. Apelian and M. Makhlouf "Alloy Selection for Die Castings Using the Quality Index," AFS Transactions, Vol. 107, 1999, pp. 239-247.

16. N.D. Alexopoulos, "Definition of Quality in Cast Aluminum Alloys and Its Characterization with Appropriate Indices," Journal of Materials Engineering and Performance, Vol. 15 (1), 2006, pp. 59-66.

17. D.C. Montgomery, Design and analysis of experiments, 3rd ed., New York: John Wiley & Sons; 1991, PP. 270-569.

18. D.M. Steinberg, W.G. Hunter, Experimental Design: Review and Comments. Technometrics, 1984; 26(2), pp.71-97.

19. R. Askeland and P. Phule, The science and engineering of materials, 4th edition, Bill Stenquist, USA, 2003, pp. 366, 373, 374.

20. G. Davies, Materials for Automobile Bodies, Butterworth-Heinemann, Oxford, 2003, pp. 61-90.

21. I.N. Fridlyander, V.G. Sister, O.E. Grushko, V.V. Berstenev, L.M. Sheveleva and L.A. Ivanova, "Aluminum Alloys: Promising Materials in the Automotive Industry," Metal Science and Heat Treatment, Vol. 44 (9-10), 2002, pp. 365-370.

22. D. St John, C. Caceres, D. Zhang, Geoff Edwards, John Taylor and Graham Schaffer, "Aluminum Alloys for Cast Automotive Components" Materials in the automotive industry conference, Australia, April 1996.

23. A.T. Spada, "In Search of Light-Weight Components: Automotive's Cast Aluminum Conversion," Engineered Casting Solutions, Vol. 4 (2), 2002, pp. 28-31.

24. M.F. Ashby and D.R. Jones, Engineering Materials1, 2nd edition, Butterworth-Heinemann, Oxford, 1996, pp. 261-270.

25. I.J. Polmear, Metallurgy of the Light Metals, London, New-York: E. Arnold, 1989.

26. L.F. Mondolfo, Aluminum Alloys: Strusture and Properties, London, Boston: Butterworths, 1976.

27. J.A. Taylor, "The Effect of Iron in Al-Si Casting Alloys," Proceeding of the 35th Australian Foundry Institute National Conference, Adelaide, Australia, 31 Oct -3 Nov 2004, pp. 148-157.

28. R. Sharma, Anesh and D.K. Dwivedi, "Influence of silicon (wt.%) and heat treatment on abrasive wear behaviour of cast Al–Si–Mg alloys", Materials Science and Engineering, Vol. A 408, 2005, pp. 274–280.

29. L. Heusler and W. Schneider, "Influence of alloying elements on the thermal analysis results of Al–Si cast alloys", Journal of Light Metals, Vol. 2, 2002, pp. 17–26.

30. A.S. Lee, "A Study on the Economics of Hypereutectic Aluminum-Silicon (Al-Si) Alloy Machining," International Journal of Advanced Manufacturing Technology, Vol. 16, 2000, pp. 700-708.

31. J.L. Jorstad, W.M. Rasmussen and D.L. Zalensas, Aluminum Casting Technology, Second Edition, The American Foundrymen's Society, Inc., Des Plaines, IL, U.S.A., 1993.

32. M. Warmuzek, Aluminum-Silicon Casting Alloys: Atlas of Microfractographs, ASM International, Materials Park, OH, U.S.A., 2004.

33. J.L. Jorstad, "Hypereutectic Al-Si Casting Alloys: 25 Years, What's Next," AFS Transactions, Vol. 104, 1996, pp. 669-671.

34. A. L. Donsa, G. Heiberg, J. Voje , J. S. Melandd, J. O. Løland and A. Prestmo, "On the effect of additions of Cu and Mg on the ductility of AlSi foundry alloys cast with a cooling rate of approximately 3 K/s", Materials Science and Engineering A, Vo. 413–414, 2005, pp. 561–566.

35. P.B. Crosley and L.F. Mondolfo, "The Modification of Aluminum Silicon Alloys,"Modern Castings, Vol. 49, 1966, pp. 89-100.

36. L. Lu, K. Nogita and A.K. Dahle, "Combining Sr and Na Additions in Hypoeutectic Al-Si Foundry Alloys," Materials Science and Engineering A, Vol. 399, 2005, pp. 244-253.

37. J. G. Kaufman, Introduction to aluminum alloys and tempers, Materials Park, Ohio: ASM International, 2000.

38. E. Sjölander, S. Seifeddine, "The Heat Treatment of Al–Si–Cu–Mg Casting Alloys", Journal of Materials Processing Technology, Vol. 210, 2010, pp. 1249–1259.

39. Charlie R. Brooks, Heat Treatment, Structure and Properties of Nonferrous Alloys, Metals Park, Ohio: American Society for Metals, 1982.

40. M.A. Grossmann, Principles of Heat Traetment, Cleveland, Ohio: American Society for Metals, 1964.

41. F. C Campbell, Elements of Metallurgy and Engineering Alloys, Materials Park, Ohio: ASM International, 2008.

42. ASM Handbook Vol. 4, "Heat Treating: Heat Treating of Aluminum Alloys" ASM International, Materials Information Society, U.S.A., 1990, pp. 1861-1887.

43. ASTM standard B917/B917M-2001, "Standard practice for heat treatment of aluminum alloys castings from all processes", PhiladelphiaPA, 2001.

44. R. Li, "Solution Heat Treatment of 354 and 355 Cast Alloys," AFS Transactions, Vol. 104, 1996, pp. 777-783.

45. G.K. Sigworth, J. Howell, O. Rios and M. Kaufman: "Heat Treatment of Natural Aging Aluminum Casting Alloys", International Journal of Cast Metals Research, Vol. 19, 2006, pp. 123-129.

46. S. Shivkumar, S. Ricci, Jr., C. Keller and D. Apelian, "Effect of Solution Treatment Parameters on Tensile Properties of Cast Aluminum Alloys," Journal of Heat Treating, Vol. 8 (1), 1990, pp. 63-70.

47. Metals Handbook, 2nd edition, vol. 1, "Aluminum and Aluminum Alloys", American Society for metals, Metals Park, Ohio, 1998, pp. 417-420.

48. R-X. Li, R-D. Li, Y-H. Zhao and C-X. Li, "Effect of Heat Treatment on Eutectic Silicon Morphology and Mechanical Property of Al-Si-Cu-Mg Cast Alloys," Transactions of Nonferrous Metals Society of China, Vol. 14 (3), 2004, pp. 496-500.

49. G. Chai and L. Bäckerud, "Factors Affecting Modification of Al-Si Alloys by Adding Sr-Containing Master Alloys," AFS Transactions, Vol. 100, 1992, pp. 847-854.

50. S. Hegde and K.N. Prabhu, "Modification of Eutectic Silicon in Al-Si Alloys," Journal of Materials Science, Vol. 43, 2008, pp. 3009-3027.

51. R.W. Smith, "Modification of Aluminum Silicon Alloys," Proceedings of the Conference on Solidification of Metals, Iron and Steel Institute, Brighton, London, U.K., 1967, pp. 224-236.

52. H.J. Li, S. Shivkumar, X.J. Luo and D. Apelian, "Influence of Modification on the Solution Heat-Treatment Response of Cast Al-Si-Mg Alloys," Cast Metals, Vol. 1 (4), 1989, pp. 227-234.

53. F. Paray et J.E. Gruzleski, "Microstructure-mechanical property relationships in a 356 alloy, Part 1: Microstructure", Cast Metals, vol. 7, no. 1, 1994, pp. 29-40.

54. C.W. Meyers, "Solution Heat Treatment in A357 Alloys". AFS Transactions, Vol. 93, 1985, pp. 741-750.

55. D. Apelian, S. Shivkumar and G. Sigworth, "Fundamental Aspects of Heat Treatment of Cast Al-Si-Mg Alloys," AFS Transactions, Vol. 97, 1989, pp. 727-742.

56. D. Emadi, L.V. Whiting, M. Sahoo, J.H. Sokolowski, P. Burke and M. Hart, "Optimal Heat Treatment of A356.2 Alloy," Proceeding of the 132th TMS Annual Conference, Light Metals 2003, The Mineral, Metals & Materials Society, San Diego, USA,2003, pp. 983-989.

57. G.E. Totten and D.S. Mackenzie, "Aluminum Quenching Technology: A Review", Materials Science Forum, 2000, Vol. 331-337, pp. 589-594.

58. K.N. Prabhu and P. Hemanna, "Heat transfer During Quenching of Modified and Unmodified Gravity Die-Cast A357 Cylindrical Bars", Journal of Materials Engineering and Performance, Vol. 15, 2006, pp 311-315.

59. T. Chen, G. Phen and J. C. Huang, "Low Quench Sensitivity of Superplastic 8090 AI-Li Thin Sheets", Metall. Mater. Trans. A, 1996, 27A, 2923–2933.

60. D.S. Mackenzie, "Design of Quench Systems for Aluminum Heat Treating Part1-Quenchant Selection", Industerial Heating, Vol. 73, 2006, pp. 53-57.

61. C. Garcia-Cordovilla and E. Louis Calorimetric, "Studies of Al-Cu Alloys: Quench Sensitivity and Sample Preparation", Metall. Mater. Trans. A, 1984, 15A, 389–391.

62. C.E. Bates, G.E. Totten, Heat Treating, ASTM Metals Handbook, ASM International, Vol. 4, 1991.

63. Zhang Ke-Jian, "Investigation on Two Main Shortcomings of Tap Water as a Quenching Medium", Beijing Huali Fine Chemical Company Ltd, Beijing 102200, China, September 8, 2011.

64. http://www.houghtonintl.com/images/Hougton%20on%20quenching.pdf

65. M H Jacobs, Precipitation Hardening, Interdisciplinary Research Centre in Materials, The University of Birmingham, UK, EAA - European Aluminum Association, 1999, TALAT Lecture 1204.
http://www.eaa.net/eaa/education/TALAT/lectures/1204.pdf

66. S. Zafar, N. Ikram, M.A. Shaikh and K.A Shoaib, "Precipitation Hardening," Journal of Materials Science, Vol. 25 (5), 1990, pp. 2595-2597.

67. E. Hornbogen, "Hundered Years of Precipitation Hardening", Journal of Light Metals Vol. 1, 2001, pp. 127-132.

68. J.F. Nie and B.C. Muddle, "The Form of the Age-Hardening Response in High Strength Aluminium Alloys", Materials Science and Engineering A, Vols. A319–321, 2001, pp. 448–451.

69. J.W. Martin, Precipitaion Hardening, Butterworth-Heinemann, Oxford, Engalnd, 1998, p. 215.

70. T. Gladman, "Precipitation Hardening in Metals," Materials Science and Technology, Vol. 15 (1), 1999, pp. 30-36.

71. R.X. Li, R.D. Li, Y.H. Zhao, L.Z. He, C.X. Li, H.R. Guan and Z.Q. Hu, "Age-Hardening Behavior of Cast Al-Si Base Alloy," Materials Letters, Vol. 58, 2004, pp. 2096-2101.

72. K.T. Kashyap, S. Murali, K.S. Raman and K.S.S. Murthy, "Casting and Heat Treatment Variables of Al-7Si-Mg Alloy," Materials Science and Technology, Vol. 9, 1993, pp. 189-203.

73. S. Murali, K.T. Kashyap, K.S. Raman and K.S.S. Murthy, "Inhibition of Delayed Ageing by Trace Additions in Al-7Si-0.3Mg Cast Alloy", Scripta Metallurgical et Materialia, Vol. 29, 1993, pp. 1421-1426.

74. D. Ovono, I. Guillot and D. Massinon, "The Microstructure and Precipitation Kinetics of a Cast Aluminium Alloy", Scripta Materialia, Vol. 55, 2006, pp. 259–262.

75. W. Reif, J. Dutkiewicz, R. Ciach, S. Yu and J. Krol, "Effect of Ageing on the Evolution of Precipitates in AlSiCuMg Alloys," Materials Science and Engineering A, Vol. A234-236, 1997, pp. 165-168.

76. I.J. Polmear, "Role of Age Hardening in Modern Aluminum Alloys," Proceedings of the Third International Conference on Aluminum Alloys: ICAA3, The Norwegian Institute of Technology, Trondheim, Norway, 1992, pp. 371-384.

77. F.J. Tavitas-Medrano, J.E. Gruzleski, F.H. Samuel, S. Valtierra and H.W. Doty, "Effect of Mg and Sr-modification on the mechanical properties of 319-type aluminum cast alloys subjected to artificial aging", Materials Science and Engineering A, Vol. 480, 2008, pp. 356–364.

78. F.H. Samuel, A.M. Samuel and H.W. Doty, "Factors Controlling the Type and Morphology of Cu-Containing Phases in 319 Al Alloy", AFS Transactions, 1996, Vol. 104, pp. 893-901.

79. L. Backerud, G. Chai and J. Tamminen, "Solidification Characteristics of Aluminum Alloys", vol. 2, Foundry Alloys, AFS/SKANALUMINIUM, Des Plaines, IL, USA, 1990.

80. G. Garcia-Garcia, J. Espinoza-Cuadra and H. Mancha-Molinar, "Copper Content and Cooling Rate Effects over Second Phase Particles Behavior in Industrial Aluminum-Silicon Alloy 319", Materials and Design, Vol. 28, 2007, pp. 428–433.

81. Z. Li, A.M. Samuel, F.H. Samuel, C. Ravindran, S. Valtierra, H.W. Doty, "Factors Affecting Dissolution of Al2Cu Phase in 319 Alloys", AFS Trans, Vol. 2, 2003, pp. 241–54.

82. J. Gauthier, P.R. Louchez, F.H. Samuel, "Heat treatment of 319.2 aluminum automotive alloy, part 1: Solution heat treatment", Cast metals, Vol. 8, 1995, 91-106.

83. D.J. Chakrabartia and David E. Laughlinb, "Phase relations and precipitation in Al–Mg–Si alloys with Cu additions", Progress in Materials Science, Vol. 49, 2004, pp. 389–410.

84. A.M. Samuel, J. Gauthier and F.H. Samuel, "Microstructural Aspects of the Dissolution and Melting of A12Cu Phase in Al-Si Alloys During Solution Heat Treatment", Metallurgical and Materials Transactions A, Vol. 27A, 1996, pp. 1785-1798.

85. Z.Li, A.M. Samuel, F.H. Samuel, C. Ravindran, S. Valtierra and H.W.Doty, " Parameters Controlling The Performance of AA319-Type Alloys, part I. Tensile properties", Materials Science and Engineering A, Vol. A367, 2004, pp. 96-110.

86. C.H. Caceres, I.L. Svensson and J.A. Taylor, "Strength- Ductility Behaviour of Al-Si-Cu-Mg Casting Alloys in T6 Temper", International Journal of Cast Metals Research, Vol. 15, 2003, pp. 531-543.

87. H.J. Sokolowski, X-C. Sun, G. Byczynski, D.O. Northwood, D.E. Penrod, R. Thomas and A. Esseltine, "The Removal of Copper-Phase Segregation and the Subsequent Improvement in Mechanical Properties of Cast 319 Aluminum Alloys by a Two-Stage Solution Heat Treatment," Journal of Materials Processing Technology, Vol. 53, 1995, pp. 385-392.

88. F.H. Samuel, P. Quellet, A.M. Samuel, H.W. Doty, "Effect of Mg and Sr Additions on the Formation of Intermetallics in Al-6 wt pct Si-3.5 wt pct Cu-(0.45) to (0.8) wt pct Fe 319 type alloys", Metallurgical and Transaction A, Vol. 29, 1998, pp. 2871–2884.

89. F.H. Samuel, "Incipient Melting of Al5Mg8Si6Cu2 and Al2Cu Intermetallics in Unmodified and Strontium-Modified Al-Si-Cu-Mg (319) Alloys during Solution Heat Treatment," Journal of Materials Science, Vol. 33, 1998, pp. 2283-2297.

90. N. Crowell and S. Shivkumar, "Solution Treatment Effects in Cast Al-Si-Cu Alloys," AFS Transactions, Vol. 103, 1995, pp. 721-726.

91. G.E. Byczynski, W. Kierkus, D.O. Northwood, D. Penrod, J.H. Sokolowski, W.A. Esseltine, J. Oswald and R. Thomas, "The Effect of Quench Rate on Mechanical Properties of 319 Aluminum Alloy Castings," Materials Science Forum, Vol. 217-222, 1996, pp. 783-788.

92 D.G. Eskin, "Decomposition of Supersaturated Solid Solutions in Al-Cu-Mg-Si Alloys," Journal of Materials Science, Vol. 38, 2003, pp. 279-290.

93. S.K. Son, M. Takeda, M. Mitome, Y. Bando and T. Endo, "Precipitation Behaviour of an Al-Cu Alloy during Isothermal Aging at Low Temperatures," Materials Letters, Vol. 75, 2005, pp. 629-632.

94. C. Cayron, L. Sagalowicz, O. Beffort and P.A. Buffat, "Structural Phase Transition in Al-Cu-Mg-Si Alloys by Transmission Electron Microscopy Study on an Al-4wt%Cu-1wt%Mg-Ag Alloy Reinforced by SiC Particles," Philosophical Magazine A, Vol. 79 (11), 1999, pp. 2833-2851.

95. S.P. Ringer and K. Hono, "Microstructural Evolution and Age Hardening in Aluminum Alloys: Atom Probe Field-Ion Microscopy and Transmission Electron Microscopy Studies," Materials Characterization, Vol. 44, 2000, pp. 101-131.

96. N. Boukhris, S. Lallouche, M.Y. Debili, and M. Draissia, "Microhardness Variation and Related Microstructure in Al–Cu Alloys Prepared by HF Induction Melting and RF Sputtering", the European Physical Journal Applied Physics, Vol. 45, 2009, pp. 30501.

97. Aniruddha Biswas, Donald J. Siegel, C. Wolverton and David N. Seidman, "Precipitates in Al–Cu Alloys Revisited: Atom-probe Tomographic Experiments and First-principles Calculations of Compositional Evolution and Interfacial Segregation", Acta Materialia, Vol. 59, 2011, pp. 6187–6204.

98. P.Ouellet, F.H. Samuel, "Effect of Mg on the ageing behaviour of Al-Si-Cu 319 Type Aluminum casting alloys", Journal of materials science, Vol. 34, 1999, 4671-4697.

99. G. Wang, X. Bian, X. Liu and J. Zhang, "Effect of Mg on Age Hardening and Precipitation Behavior of an AlSiCuMg Cast Alloy," Journal of Materials Science, Vol. 39, 2004, pp. 2535-2537.

100. M. Hafiz, T. Kobayashi, "Mechanical Properties of Modified and Non-Modified Eutectic Al-Si alloys", Journal of Japan Institute of Light Metals, Vol. 44 (1),1994, pp. 28-34.

101. S. Esmaeili, X. Wang, D.J. Lloyd and W.J. Poole, "On the Precipitation-Hardening Behavior of the Al-Mg-Si-Cu Alloy AA6111," Metallurgical and Materials Transactions A, Vol. 34A, 2003, pp. 751-763.

102. L. Lasa and J. M. Rodriguez, "Evolution of the main intermetallic phases in Al-Si-Cu-Mg casting alloys during solution treatment", Journal of Materials Science, Vol. 39, 2004, pp. 1343 – 1355.

103. Annual Book of ASTM Standards, Section 2: Nonferrous Metal Products, Aluminum and Magnesium Alloys, Vol. 02, 2004, B108-03a.

104. E.L. Roy, ASM Handbook, Castings, 9th Edition, ASM International, Materials Park, OH, 1992, Vol. 15, pp. 743-769.

105. S. W. Han, K. Katsumata, S. Kumai, A. Sato, "Effects of solidification Structure and Aging Condition on Cyclic Stress–Strain Response in Al–7% Si–0.4%" Mg Cast Alloys", Materials Science and Engineering: A, Vol. 337, Issues 1-2, 25 November 2002, pp. 170-178.

106. Erhard Ogris, Development of Al-Si-Mg Alloys for Semi-Solid Processing and Silicon Spheroidization Treatment (SST) for Al-Si Cast Alloys, PhD Thesis, Swiss Federal Institute of Technology Zurich, 2002.

107. M. Abdulwahab, I.A. Madugu , S.A. Yaro, S.B. Hassan and A.P.I. Popoola, "Effects of multiple-step thermal ageing treatment on the hardness characteristics of A356.0-type Al–Si–Mg alloy", Materials & Design, Vol. 32, Issue 3, March 2011, pp. 1159-1166.

108. J.A. Taylor, D.H. St-John and M.J. Couper, "Solution Treatment Effects in Al-Si-Mg Casting Alloys: Part II: Solid Solution Chemistry," Aluminum Transactions, Vol. 4-5, 2001, pp. 111-124.

109. M. Tiryakioğlu, J.T. Staley and J. Campbell, "Evaluating Structural Integrity of Cast Al-7%Si-Mg Alloys Via Work Hardening Characteristics: II. A New Quality Index," Materials Science and Engineering A, Vol. 368, 2004, pp. 231-238.

110. S. Shivkumar, S. Ricci, Jr., B. Steenhoff, D. Apelian and G. Sigworth, "An Experimental Study to Optimize the Heat Treatment of A356 Alloy," AFS Transactions, Vol. 97, 1989, pp. 791-810.

111. S. Shivkumar, S. Ricci, Jr. and D. Apelian, "Influence of Solution Parameters and Simplified Supersaturation Treatments on Tensile Properties of A356 Alloy," AFS Transactions, Vol. 98, 1990, pp. 913-992.

112. B. Closset and J. E. Gruzleski, "Structure and Properties of Hypoeutectic Al-Si-Mg Alloys Modified with Pure Strontium", Metallurgical Transaction A, Vol. 13, 1981, pp. 982-945.

113. George Y. Liu, Effect of Ageing Heat Treatment on the Hardness nd Tensile Properties of Aluminum A356.2 asting Alloy, M.Sc Thesis, McMaster University Hamilton, Ontario, 2009.

114. D.L. Zhang and L. Zheng, "The Quench Sensitivity of Cast Al-7 Wt Pct Si-0.4 Wt Pct Mg Alloy," Metallurgical and Materials Transactions A, Vol. 27A, 1996, pp. 3983-3991.

115. M. Murayama, K. Hono, M. Saga and M. Kikuchi, "Atom Probe Studies on the Early Stages of Precipitation in Al-Mg-Si Alloys," Materials Science and Engineering A, Vol. 250, 1998, pp. 127-132.

116. L. Zhen, W.D. Fei, S.B. Kang and H.W. Kim, "Precipitation Behaviour of Al-Mg-Si Alloys with High Silicon Content," Journal of Materials Science, Vol. 32, 1997, pp. 1895-1902.

117. M. Murayama and K. Hono, "Pre-Precipitate Clusters and Precipitation Processes in Al-Mg-Si Alloys," Acta Materialia, Vol. 47 (5), 1999, pp. 1537-1548.

118. A.K. Gupta, D.J. Lloyd and S.A. Court, "Precipitation Hardening in Al-Mg-Si Alloys with and without Excess Si," Materials Science and Engineering A, Vol. 316, 2001, pp. 11-17.

119. Incropera, Frank P. DeWitt, David P, Introduction to Heat Transfer, 4th Edition, New York ; Toronto : J. Wiley, 2002.

120. Jon L. Dossett, Practical heat treating, 2nd Edition, Materials Park, Ohio: ASM International, 2006.

121. S. K. Chaudhury and D. Apelian, "Fluidized-Bed: High Efficiency Heat Treatment of Aluminum Castings", Heat Treating Progress, USA, Sep/Oct 2007, Vol. 7, pp 29-33.

122. ASM Handbook Vol. 4 "Heat Treating: Fluidized Bed Heat Treating Equipment", ASM International, The Materials Information Society, U.S.A., 1990.

123. C.A. Girrell, "Fluidized Bed Heat Treating and its Applications in the Foundry", Modern Casting, Vol. 73, No. 12, 1983, pp. 26-28.

124. D. Kunii and O. Levenspiel, Fluidization Engineering, Second Edition, Butterworth-Heinemann, USA, 1991, pp1-12.

125. P. G. Ramsell, "Fluidised Bed Furnaces Offer Process Flexibility", Metallurgia, Vol. 57, No. 5, 1990, pp. 214, 216.

126. C.A. Girrell "Applications of Fluidized Bed Furnaces in the Foundry", AFS, Vol. 91, 1983, pp. 21-24.

127. E. M. Fainshmidt, "Theory and Practice of Fluidized Bed Heat Treatment of Parts Fabricated From Metals and Alloys", Metal Science and Heat Treatment, Vol. 47, 2005, pp. 83-96.

128. S. K. Chaudhury and D. Apelian, "Fluidized Bed- An Innovative Method for Heat Treating Al Casting", Advanced Casting Research Center, Metal Processing Institute, Report to Material Science and Engineering Program, WPI, Worcester, USA, 2003.

129. J. Keist, "The Development of a Fluidized Bed Process for the Heat Treatment of Aluminum Alloys", Industrial Insight, JOM, Vol. 57, April 2005, pp. 34-39.

130. J. Keist, S. Chaudhury and D. Apelian, "Fluidized Bed Quenching Performance and Its Application for Heat Treating Aluminum Alloys", Heat Treating Society: Proceedings of The 24th Conference, Materials Park, Ohio, ASM International, 2007, pp. 225-230.

131. S. Chaudhury, S. Shankar, D. Apelian, J. Van Wert, "Short Cycle Heat Treating with Flidized Beds: Microstructure Evolution", AFS International Conference on Structural Aluminum Casting, Vol/No. 2-4, 2003, pp. 305-320.

132. J. Keist, D. Dingmann and C. Bergman, "Fluidized Bed Quenching: Reducing Residual Stresses and Distortion", In the Proceedings of the 23rd Heat Treating Society Conference, Pittsburgh, PA, 2005, pp. 263-270.

133. J. Gauthier, F.H. Samuel, "Tensile properties and fracture behaviour of solution heat treated 319.2 Al automotive alloy", AFS Transaction, Vol. 103, 1995, 849-857.

134. D. Apelian and S. K. Chaudhury "Fluidized Bed Heat Treatment of Aluminum Cast Components", Journal de Physique, IV, Vol. 120, 2004, pp. 555-562.

135. J. Keist and C. Bergman, "Short Cycle Heat Treating with Fluidized Beds: Optimizing Mechanical Properties", AFS International Conference on Structural Aluminum Casting, Vol/No. 2-4, 2003, pp. 297-304.

136. S. K. Chaudhury and D. Apelian, " Effects of Rapid Heating on Solutionizing Characteristics of Al- Si- Mg Alloys Using a Fluidized Bed", Metallurgical and Material Transactions A, Vol. 37A, 2006, pp. 763-778.

137. S. K. Chaudhury and D. Apelian, "Effects of Solution Heat Treatment on Microstructure and Mechanical Properties of Al-Si-Cu-Mg (354) Alloy Using a Fluidized Bed Reactor", AFS Transactions, Paper 05-071 (02), 2005, pp. 117-130.

138. D.L. Zhang, L.H. Zheng and D.H. StJohn, "Effect of a Short Solution Treatment Time on Microstructure and Mechanical Properties of Modified Al-7wt.%Si-0.3wt.%Mg Alloy," Journal of Light Metals, Vol. 2, 2002, pp. 27-36.

139. G.K. Sigworth, "Controlling Tensile Strength in Aluminum Castings," Special Communication, 2006.

140. G.K. Sigworth, "The Modification of Al-Si Casting Alloys: Important Practical and Theoretical Aspects," International Journal of Metalcasting, Vol. 2 (2), 2008, pp. 19-40.

141. S.G. Shabestari and F. Shahri, "Influences of Modification, Solidification Conditions and Heat Treatment on the Microstructure and Mechanical Properties of A356 Aluminum Alloy", Journal of Materials Science, Vol. 39, 2004, pp. 2023-2032.

142. J.A. Taylor, D.H. StJohn, J. Barresi and M.J. Couper, "Influence of Mg Content on the Microstructure and Solid Solution Chemistry of Al-7%Si-Mg Casting Alloys During Solution Treatment," Materials Science Forum, Vol. 331-337, 2000, pp. 277-282.

143. L. Druge and V. Pantya, "Heat Treatment Technology-Optimization of Heating with Heat Treatment in Fluidized Bed", Plenum Publishing Corporation, No. 8, 1979, pp 14-16.

144. V.P. Kurbatov and V.I. Murav'ev, "Rapid Heating and Cooling of Aluminum Alloys in a Fluidized Bed", Translated from Metallovedenie I, Termicheskaya, Obra-botka, Metallov, No. 2, 1970, pp. 66-68.

145. S. K. Chaudhury and D. Apelian, "Fludized Bed Heat Treatment of Cast Al-Si-Cu-Mg Alloys", Metallurgical and Material Transactions A, Vol. 37A, 2006, pp. 2295-2311.

146. S.K. Chaudhury, L. Wang and D. Apelian, "Fluidized Bed Reactor Heat Treatment of A356 Alloy: Microstructure Analysis and Mechanical Properties", AFS Transactions, Vol. 14, 2004, pp. 289-304.

147. Kh.A. Ragab, A.M. Samuel, A.M.A. Al-Ahmari, F.H. Samuel and H.W. Doty, "Influence of fluidized sand bed heat treatment on the performance of Al-Si cast alloys", Materials and Design, Vol. 32, 2011, pp. 1177-1193.

148. O. K. Abubakre, U. P. Mamaki and R. A Muriana, "Investigation of the Quenching Properties of Selected Media on 6061Aluminum Alloy", Journal of Minerals & Materials Characterization & Engineering, Vol. 8, No.4, 2009, pp 303-315.

149. L. Pedersen and L. Arnberg, "The Effect of Solution Heat Treatment and Quenching Rates on Mechanical Properties and Microstructures in Al-Si-Mg Foundry Alloys.

150. J. Keist and C. Bergman, "Heat Treating Aluminum Alloys Utilizing Fluidized Bed Quenching", Paper presented at the 2004 TMS Annual Meeting & Exhibition, Charlotte, NC, March, 2004.

151. S.K. Chaudhury and D. Apelian, "Effects of Fluidized Bed Quenching on Heat Treating Characteristics of Cast Al-Si-Mg and Al-Si-Mg-Cu Alloys", International Journal of Cast Metals Research, Vol. 19, No. 6, 2006, pp. 361-369.

152. S. Jacob, "Quality Index in Predicting of Properties of Aluminum Castings-A Review," AFS Transactions, Vol. 108, 2000, pp. 811-818.

153. N.D. Alexopoulos, "Generation of Quality Maps to Support Material Selection by Exploiting the Quality Indices Concept of Cast Aluminum Alloys," Materials and Design, Vol. 28, 2007, pp. 534-543.

154. N.D. Alexopoulos and S.G. Pantelakis, "Quality Assessment of Artificially Aged A357 Aluminum Alloy Cast Ingots by Introducing Approximate Expressions of the Quality Index QD," Metallurgical and Materials Transactions A, Vol. 35A, 2004, pp. 3079-3089.

155. M. Drouzy, S. Jacob and M. Richard, "Interpretation of Tensile Results by Means of Quality Index and Probable Yield Strength," AFS International Cast Metals Journal, Vol. 5, 1980, pp. 43-50.

156. C.H. Cáceres, "Microstructure Design and Heat Treatment Selection for Casting Alloys Using the Quality Index," Journal of Materials Engineering and Performance, Vol. 9 (2), 2000, pp. 215-221.

157. C.H. Cáceres, "Particle Cracking Damage and Quality Index of Al-Si-Mg Casting Alloys," AFS Transactions, Vol. 108, 2000, pp. 709-712.

158. C.H. Cáceres and J. Barresi, "Selection of Temper and Mg Content to Optimize the Quality Index of Al-7Si-Mg Casting Alloys," International Journal of Cast Metals Research, Vol. 12, 2000, pp. 377-384.

159. T. Din, A.K.M.B. Rashid and J. Campbell, "High Strength Aerospace Casting Alloys: Quality Factor Assessment," Materials Science and Technology, Vol. 12, 1996, pp. 269-273.

160. C.H. Cáceres, "A Rationale for the Quality Index of Al-Si-Mg Casting Alloys," International Journal of Cast Metals Research, Vol. 10, 1998, pp. 293-299.

161. C.H. Cáceres, J.H. Sokolowski and P. Gallo, "Effect of Aging and Mg Content on the Quality Index of Two Model Al-Cu-Si-Mg Alloys," Materials Science and Engineering A, Vol. 271, 1999, pp. 53-61.

162. C.H. Cáceres, M. Makhlouf, D. Apelian and L. Wang, "Quality Index Chart for Different Alloys and Temperatures: A Case Study on Aluminum Die-Casting Alloys," Journal of Light Metals, Vol. 1, 2001, pp. 51-59.

163. C.H. Cáceres, I.L. Svensson and J.A. Taylor, "Microstructural Factors and the Mechanical Performance of Al-Si-Mg and Al-Si-Cu-Mg Casting Alloys," Proceeding of the 2nd International Aluminum Casting Technology Symposium, ASM International, Columbus, OH, U.S.A., 7-9 October, 2002, pp. 427-434.

164. G.E. Dieter, Mechanical Metallurgy: Third Edition, McGraw-Hill, New York, 1986.

165. J.R. Davis, Tensile Testing: Second Edition, ASM International, Materials Park, OH, U.S.A., 2004.

166. C.H. Cáceres, "A Phenomenological Approach to the Quality Index of Al-Si-Mg Casting Alloys," International Journal of Cast Metals Research, Vol. 12, 2000, pp. 367-375.

167. C.H. Cáceres, T. Din, A.K.M.B. Rashid and J. Campbell, "Effect of Aging on Quality Index of an Al-Cu Casting Alloy," Materials Science and Technology, Vol. 15 (6), 1999, pp. 711-716.

168. S. Shivkumar, "The Interactive Effects of Sr Modification and Heat Treatment on the Mechanical Properties of Cast Aluminum Alloys," 17th ASM Heat Treating Society Conference Proceedings Including the 1st International Induction Heat Treating Symposium, Vol. 15-18, 1998, pp. 265-269.

169. W.R. Osório, L.R. Garcia, P.R. Goulart and A. Garcia, "Effects of Eutectic Modification and T4 Heat Treatment on Mechanical Properties and Corrosion Resistance of an Al-9wt%Si Casting Alloy," Materials Chemistry and Physics, Vol. 106, 2007, pp. 343-349.

170. J.E. Gruzleski and B.M. Closset, The Treatment of Liquid Aluminum-Silicon Alloys, American Foundrymen's Society, Inc., Des Plaines, IL, U.S.A., 1990.

171 H. Rosenbaum, D. Turnbull, "Metallographic Investigation of Precipitation of Silicon from Aluminum", Acta Metallurgica, 1959, vol. 7, pp. 664-674.

172 J.V. Suchtelen, "Coarsening of Eutectic Structures during and after Unidirectional Growth", Journal of Crystal Growth, 1978, vol. 43, pp. 28-46.

173. I. Kovacevic, "Simulation of spheroidization of elongated Si-particle in Al–Si alloys by the phase-field model", Material Science and Engineering, 2008; Vol. 496A, pp. 345–54.

174. P.Y. Zhu, Q.Y. Liu, "Kinetics of Granulation of Discontinuous Phase in Eutectic Structures", Materials Science and Technology, 1986, vol. 2, pp. 500-507.

175. P. Zhu, Q. Liu, T. Hou, "Spheroidization of Eutectic Silicon in Al-Si Alloys", AFS Transactions, 1985, vol. 93, pp. 609-614.

176. D. Qiu, J.A. Taylor, M-X Zhang and P.M. Kelly, "A Mechanism For the Poisoning Effect of Silicon On The Grain Refinement of Al–Si alloys" Acta Materiala, 2007, Vol. 55, pp. 1447–56.

177. J.A. Marcantonio, L.F. Mondolfo, "Grain Refinement In Aluminum Alloyed With Titanium and Boron", Metallurgical Transaction, 1971, Vol. 2B, pp.465–71.

178. D. Gloria, Control of Grain Refinement of Al-Si Alloys by Thermal Analysis. PhD Thesis, McGill University, Montreal, Canada; 1999.

179. G.K. Sigworth, C. Wang, H. Huang, J.T. Berry, "Porosity Formation in Modified and Unmodified Al–Si Alloy Castings", AFS Transaction, 1994, Vol.102, pp. 245–61.

180. W. LaOrchan, J.E. Gruzleski, "Grain Refinement, Modification and Melt Hydrogen -Their Effects on Microporosity, Shrinkage and Impact Properties in A356 Alloy", AFS Transactions, 1992, vol. 100, pp. 415-424.

181. S. Shivkumar, L. Wang, D. Apelian, "Molten Metal Processing of Advanced Cast Aluminum Alloys", Journal of Metals, 1991, pp. 26-32.

182. G.A. Edwards, G.K. Sigworth, C.H. Cáceres, H.D. StJohn and J.Barresi, "Microporosity formation in Al–Si–Cu–Mg casting alloys", AFS Transaction, 1997, Vol. 105, pp. 809–815.

183. J.F. Hernandez-Paz, F. Paray, J.E. Gruzleski, D.Emadi, "Natural aging and heat treatment of A356 aluminum alloy", AFS Transaction, 2004, Vol. 112, pp. 155–64.

184. C.D. Marioara, S.J. Andersen, J. Jansen and H.W. Zandbergen, "The Influence of Temperature and Storage Time at RT on Nucleation of the β" Phases in a 6082 Al-Mg-Si Alloy," Acta Materialia, Vol. 51, 2003, pp. 789-796.

185. G.A. Edwards, K. Stiller, G.L. Dunlop and M.J. Couper, "The Precipitation Sequence in Al-Mg-Si Alloys," Acta Materialia, Vol. 46 (11), 1998, pp. 3893-3904.

186. A. Saigal, J. Berry, "Study of the Effects of Volume Fraction, Size and Shape of Silicon Particles on Mechanical Properties in Al-Si Alloys Using Finite Element Method", AFS Transactions, 1985, vol. 93, pp. 699-704.

187. F.J. Tavitas-Medrano, A.M.A Mohamed, J.E. Gruzleski, F.H. Samuel, "Precipitation–Hardening in Cast Al–Si–Cu–Mg Alloys", Journal of Material Science, 2009, Vol. 45, pp. 641–51.

188. J.Y. Hawang, R. Banerjee, H.W. Doty, M.J. Kaufman, "The Effect of Mg on the Structure and Properties of Ttype 319 Aluminum Casting Alloys", Acta Materiala, 2009, Vol. 57, pp. 1308–17.

189. S.K. Tang and T. Sritharan, "Morphology of β-AlFeSi Intermetallic in Al-7Si Alloy Castings", Materials Science and Technology, 1998, Vol. 14, pp. 738-742.

190. G.K. Sigworth and C.H. Cáceres, "Quality Issues in Aluminum Net Shape Castings", AFS Transactions, 2004, Vol. 112, pp. 1-15.

191. Berthouex, L. Brown, Statistics for Environmental Engineers, 2nd ed., Lewis Publishers, New York, 2002, pp. 185-276.

192. A.M. Mohamed, F. H. Samuel, A. M. Samuel, H. Doty and S. Valtierr, "Application of Experimental Design to Study and Control Properties and Behavior of Cast Al–10.8Si Eutectic Alloy", International Journal of Cast Metals Research, 2007, Vol. 20, No. 5, pp. 246-253.

193. R. Ganguly, B. Dhindaw, P. Dhar, "Study and Control of Properties and Behaviour of Al-Mg-Si Alloys by Application of Statistical Design of Experiments", Transactions of the Japan Institute of Metals, 1977, vol. 18(7), pp. 511-519.

194. J. Major, A. McLeod, J. Rutter, "Designed Experimentation: Microstructural Optimization of Al AA512 for the PM Process and Its Possible Use as a Structural Diecasting", AFS Transactions, Pittsburgh, PA, USA, 2000, vol. 108, pp. 287-296.

195. H. Liao, Y. Sun and G. Sun, "Correlation Between Mechanical Properties and Amount of Dendritic α-Al Phase in As-Cast Near-Eutectic Al-11.6% Si Alloys Modified with Strontium", Materials Science and Engineering, 2002, Vol. 335A, pp. 62-66.

196. D.A. Porter, K.E. Easterling, M.Y. Sherif, Phase Transformations in Metals and Alloys. Third Edition, CRC Press, USA, 2009, pp. 259, 263, 296.

197. R.E. Smallman, R.J. Bishop, Modern Physical Metallurgy & Materials Engineering. Sixth Edition, Butterworth Heinemann, Oxford, 1999, pp. 272-73.

198. R.E. Smallman, A.H. Ngan, Physical metallurgy and advanced materials. Seventh Edition, Butterworth Heinemann Elsevier, USA, 2007, pp. 404-5.

199. V R. Knobloch, J R. Garrett, "Heat Treatment Systems-Today and Tomorrow", Casting Plant and Technology International, Vol. 18, No. 4, 2002, pp. 10-14.

200. M. Glasser, "Heat Treating Aluminum With Fluidized Bed Quenching", JOM, Aluminum Innovations, Part III, May 1998.

201. I.J. Polmear, "Aluminium Alloys- A Century of Age Hardening", Materials Forum, Vol. 28, 2004.

202. Z. Martinova, D. Damgaliev, M. Hirsh, "The Effect of Room Temperature Pre-Ageing on Tensile and Electrical Properties of Thermo-mechanically Treated Al-Mg-Si Alloy", Journal of Mining and Metallurgy, Vol. 38, 2002, pp. 61-73.

203. D.D. Risanti, M. Yin, P.E.J. Rivera Diazdel Castillo, S. Vau der Zwang, "A Systematic Study of the Effect of Interrupted Ageing Conditions on the Strength and Toughness Development of AA6061", Materials Science and Engineering A, Vol. 523, 2009, pp. 99-111.

204. Kh.A. Ragab, A.M.A. Mohamed, A.M. Samuel, F.H. Samuel and A.M.A. Al-Ahmari, "Effect of Rapid Heating on the Quality Assessment of 356 and 319 Aluminum Cast Alloys Using Fluidized Bed", Accepted in International Journal of Cast Metal Research, 2011.

205. Erhard Hornbogen, "Hundred Years of Precipitation Hardening", Journal of Light Metals, Vol. 1, 2001, pp. 127-132.

206. Ji-Yong Yao, A. Edwards, A. Graham, "Precipitaion and Age-Hardening in Al-Si-Cu-Mg-Fe Casting Alloys", Materials Science Forum, Vol. 217-222, 1996, pp. 777-782.

207. C. Wolverton, "Crystal Structure and Stability of Complex Precipitate Phases in Al-Cu-Mg-(Si) and Al-Zn-Mg Alloys," Acta Materialia, Vol. 49, 2001, pp. 3129-3142.

208. S-Z Lu and A. Hellawell, "The Mechanism of Silicon Modification in Aluminum-Silicon Alloys: Impurity Induced Twinning," Metallurgical Transactions A, Vol. 18A, 1987, pp. 1721-1733.

209. S-Z Lu and A. Hellawell, "Modification and Refinement of Cast Al-Si Alloys," Light Metals, 1995, pp. 989-993.

210. J. Buha, R.N. Lumley, A.G. Crosky and K. Hono, "Secondary precipitation in an Al-Mg-Si-Cu alloy", Acta Materialia, Vol. 55, 2007, pp. 3015-3024.

Appendix

Appendix A

STATISTICAL DESIGN OF EXPERIMENT (REGRESSION ANALYSIS)

INFLUENCES OF MELT AND SOLUTION HEAT TREATMENTS ON ALLOY PERFORMANCE

Table A.1. Response surface regression analysis for quality values of A356.2 alloys.

Term	Coefficient	*P values
Constant	291.528	0.000
Modification	22.030	0.000
SHT, time (hr)	7.234	0.000
Aging time (hr)	6.149	0.000
HT Technique	24.394	0.000

*P values (significance of input parameters) determine whether or not the regression model adequately fits data.

Table A.2. Response surface regression analysis for quality values of B319.2 alloys.

Term	Coefficient	*P values
Constant	291.647	0.000
Modification	12.632	0.493
SHT, time (hr)	10.627	0.005
Aging time (hr)	-21.753	0.003
HT Technique	7.614	0.843

*P values (significance of input parameters) determine whether or not the regression model adequately fits data.

Appendix B

STATISTICAL DESIGN OF EXPERIMENT (REGRESSION ANALYSIS)

INFLUENCES OF QUENCHING MEDIA, AND AGING PARAMETERS

Table B.1. Response surface regression analysis for quality values of A356.2 alloys.

Term	Coefficient	*P values
Constant	268.253	0.000
Modification	25.142	0.000
Quenching media	1.653	0.000
HT Technique	8.324	0.000
Aging T, °C	0.233	0.002
Aging time (hr)	-1.045	0.000

*P values (significance of input parameters) determine whether or not the regression model adequately fits data.

Table B.2. Response surface regression analysis for quality values of B319.2 alloys.

Term	Coefficient	*P values
Constant	287.163	0.000
Modification	21.478	0.234
Quenching media	38.462	0.051
HT Technique	-52.024	0.321
Aging T, °C	-0.251	0.002
Aging time (hr)	3.167	0.024

*P values (significance of input parameters) determine whether or not the regression model adequately fits data.